PB84-240654

Development of Criteria for Extension of Applicability of Low-Emission High-Efficiency Coal Burners
Fourth Annual Report

Energy and Environmental Research Corp.
Irvine, CA

Prepared for

Industrial Environmental Research Lab.
Research Triangle Park, NC

Aug 84

U.S. Department of Commerce
National Technical Information Service
NTIS

PB84-240654

EPA-600/7-84-087
August 1984

DEVELOPMENT OF CRITERIA FOR EXTENSION OF APPLICABILITY OF LOW-EMISSION, HIGH-EFFICIENCY COAL BURNERS

Fourth Annual Report

by

R. Payne
P. L. Case
M. P. Heap
J. Lee
C. N. McKinnon
P. Nelson
D. W. Pershing

Energy and Environmental Research Corporation
18 Mason
Irvine, CA 92714

EPA Contract No. 68-02-2667

EPA Project Officer: Dennis C. Drehmel

Industrial Environmental Research Laboratory
Office of Environmental Engineering & Technology
Research Triangle Park, NC 27711

INDUSTRIAL ENVIRONMENTAL RESEARCH LABORATORY
OFFICE OF RESEARCH AND DEVELOPMENT
U.S. ENVIRONMENTAL PROTECTION AGENCY
RESEARCH TRIANGLE PARK, NC 27711

REPRODUCED BY
NATIONAL TECHNICAL
INFORMATION SERVICE
U.S. DEPARTMENT OF COMMERCE
SPRINGFIELD, VA. 22161

TECHNICAL REPORT DATA

(Please read Instructions on the reverse before completing)

1. REPORT NO. EPA-600/7-84-087

2.

3. RECIPIENT'S ACCESSION NO. PB8 4 240654

4. TITLE AND SUBTITLE
Development of Criteria for Extension of Applicability of Low-emission, High-efficiency Coal Burners: Fourth Annual Report

5. REPORT DATE August 1984

6. PERFORMING ORGANIZATION CODE

7. AUTHOR(S)
R. Payne, P. L. Case, M. P. Heap, J. Lee, C. N. McKimmon, P. Nelson, and D. W. Pershing

8. PERFORMING ORGANIZATION REPORT NO.

9. PERFORMING ORGANIZATION NAME AND ADDRESS
Energy and Environmental Research Corporation
18 Mason
Irvine, California 92714

10. PROGRAM ELEMENT NO.

11. CONTRACT/GRANT NO. 68-02-2667

12. SPONSORING AGENCY NAME AND ADDRESS
EPA, Office of Research and Development
Industrial Environmental Research Laboratory
Research Triangle Park, NC 27711

13. TYPE OF REPORT AND PERIOD COVERED Annual; 10/80 - 10/81

14. SPONSORING AGENCY CODE EPA/600/13

15. SUPPLEMENTARY NOTES IERL-RTP project officer is Dennis C. Drehmel, Mail Drop 4, 919/541-7505. EPA-600/7-81-171c was the third annual report.

16. ABSTRACT

The report summarizes technical progress during the fourth year of effort on EPA contract 68-02-2667. NOx and SOx emission characteristics of two low-NOx distributed-mixing burners were tested with three coals in a large water-tube simulator furnace (50-70 million Btu/hr firing rate). Increasing burner load, burner zone stoichiometry, or overall excess air increased NOx emissions. Staging was limited by increases in CO emissions and problems with flame stability at burner zone stoichiometries below 0.6. The feasibility of using dry sorbents injected directly into the furnace for SO2 emission control was investigated. Sorbent type (Ca(OH)2 vs. CaCO3) and injection location had a small effect on sulfur capture. Fuel sulfur content also affected sulfur capture. Sulfur captures on the order of 40-50 percent were obtained at Ca/S molar ratios of 2.0. Parametric studies of the sulfur capture process were performed in a specially constructed Boiler Simulator Furnace fired at 1.0 million Btu/hr. Under fuel-lean conditions, thermal history exerted controlling influence on sulfur capture. Firing and heat extraction rates strongly influenced sulfur capture due to their effect on thermal history. Sorbent location, burner zone stoichiometry, overall excess air, and tertiary air velocity had secondary effects on capture.

17. KEY WORDS AND DOCUMENT ANALYSIS

a. DESCRIPTORS		b. IDENTIFIERS/OPEN ENDED TERMS	c. COSATI Field/Group	
Pollution	Stoichiometry	Pollution Control	13B	07D
Coal		Stationary Sources	21D	
Burners		Distributed Mixing	13A	
Nitrogen Oxides		Dry Sorbents	07B	
Sulfur Oxides				
Combustion			21B	

18. DISTRIBUTION STATEMENT Release to Public

19. SECURITY CLASS *(This Report)* Unclassified

20. SECURITY CLASS *(This page)* Unclassified

21. NO. OF PAGES 375

22. PRICE

EPA Form 2220-1 (9-73)

NOTICE

This document has been reviewed in accordance with U.S. Environmental Protection Agency policy and approved for publication. Mention of trade names or commercial products does not constitute endorsement or recommendation for use.

ABSTRACT

This report summarizes technical progress during the fourth year of effort on EPA Contract 68-02-2667. The NO_x and SO_x emission characteristics of two low NO_x distributed mixing type burners were tested in a large water-tube simulator furnace at loads from 50 to 70 MBtu/hr with three coals. The effects of burner zone stoichiometry, overall excess air level and burner load on NO_x and CO emissions were determined. Increasing burner zone stoichiometry increased NO_x emissions as did increasing overall excess air. Staging was limited by increases in CO emissions and problems with flame stability at burner zone stoichiometry below about 0.6. Increasing burner load increased NO_x emissions. The feasibility of using dry sorbents injected directly into the furnace for SO_2 emission control was investigated. Both burners were fired in the minimum NO_x mode. Sorbent type [$Ca(OH)_2$ versus $CaCO_3$] had a small effect on sulfur capture, as did sorbent injection location. Fuel sulfur content also affected sulfur capture. Sulfur captures on the order of 40-50 percent at Ca/S molar ratios of 2.0 were obtained.

Bench scale parametric studies of the sulfur capture process were performed in a specially constructed Boiler Simulator Furnace fired at 1.0 MBtu/hr. Under fuel-lean conditions, thermal history exerted controlling influence on sulfur capture. Firing rate and heat extraction rate had strong influences on sulfur capture due to the effect on thermal history. Sorbent location, burner zone stoichiometry, overall excess air and tertiary air velocity had secondary effects on sulfur capture. Sulfur capture under fuel-rich conditions was also investigated. Measurements indicated significant retention of sulfur in the solid phase and a gaseous sulfur species distribution considerably different than that expected from equilibrium calculations. Sorbent injection location and method (with air or nitrogen) affected sulfur capture under fuel-rich conditions. Sulfur capture was best when the sorbent was injected with air into the fuel-rich region downstream of the coal.

This report was submitted in partial fulfillment of Contract 68-02-2667 by Energy and Environmental Research Corporation under the sponsorship of the U.S. Environmental Protection Agency. This report covers the period October 1, 1980, to October 1, 1981. Work is ongoing.

TABLE OF CONTENTS

Section Page

1.0 SUMMARY 1-1

2.0 INTRODUCTION 2-1

3.0 PILOT AND PLANT-SCALE STUDIES OF SO_x CONTROL VIA DRY SORBENT INJECTION: A REVIEW OF EARLIER WORK 3-1

- 3.1 Early Pilot-Scale Studies 3-1
- 3.2 Early Plant-Scale Studies 3-18
- 3.3 Recent Investigations 3-23
- 3.4 Further Studies 3-53

4.0 STEINMÜLLER AND PROTOTYPE BURNER PILOT-SCALE STUDIES 4-1

- 4.1 Steinmüller Burner Tests 4-1
- 4.2 Prototype Burner Tests 4-26
- 4.3 Comparison of Results 4-34

5.0 THE COAL/SULFUR/SORBENT SYSTEM IN PULVERIZED FUEL COMBUSTION: EVOLUTION, OXIDATION AND RETENTION OF SULFUR 5-1

- 5.1 Coal Sulfur Chemistry 5-3
- 5.2 Alkali Sorbents Addition: Interactions of the Coal/Sulfur/Sorbent System 5-30

6.0 EXPERIMENTAL PLAN--BENCH-SCALE STUDIES 6-1

- 6.1 Small-Scale Studies 6-1
- 6.2 Test Plan, Boiler Simulator Furnace 6-2

7.0 EXPERIMENTAL FACILITIES 7-1

- 7.1 Pilot-Scale Facilities 7-1
- 7.2 Small-Scale Facilities 7-1
- 7.3 Boiler Simulator Furnace 7-5

8.0 MEASUREMENT SYSTEMS 8-1

- 8.1 Sample Extraction and Conditioning System 8-1
- 8.2 Gas Sample Analysis 8-2
- 8.3 Solids Analysis 8-14
- 8.4 Temperature Measurement 8-19

Section Page

9.0 GAS-PHASE, PROGRAM-DEFINITION EXPERIMENTS 9-1

9.1 Excess Air Experiments 9-1
9.2 Staged Combustion 9-9
9.3 Sorbent Decomposition 9-13
9.4 Equilibrium Considerations 9-19
9.5 Comparison With Available Models 9-27

10.0 PULVERIZED COAL FIRED EXPERIMENTS 10-1

10.1 Pulverized Coal Fired Experiments, Small Scale Furnaces, Preliminary Results 10-1
10.2 Boiler Simulator Furnace Results 10-7

11.0 CONCLUSION 11-1

11-1 Pilot-Scale Results, NO_x and SO_x Control 11-1
11-2 Bench-Scale Results, Parametric Screening Studies of Sorbent Injection for SO_2 Control 11-5

12.0 REFERENCES 12-1

LIST OF FIGURES

Figure No. Page

2-1 Program Structure for Development of Criteria for Extension of Applicability of Low-Emission/High-Efficiency Coal Burners 2-2

2-2 Program Plan Approach - Combined NO_x / SO_x Control 2-4

3-1 SO_2 Removal Versus Stoichiometry for Pilot-Scale Injection Tests with Dry Sorbent 3-2

3-2 Pilot Plant Experimental Systems 3-4

3-3 Comparison of T(t) Profiles for Three Experimental Studies . . 3-6

3-4 Effect of Residence Time and Temperature on SO_2 Removal at Various Stoichiometric Ratios - SO_2 Gas Injected Into Burner Secondary Air 3-8

3-5 Schematic of T(t) Design Operating Region for Maximum SO_2 Removal 3-10

3-6 Effect of Temperature on Calcination (Ref. 1) 3-12

3-7 Effect of Additive Feed Rate (Ref. 1) 3-13

3-8 Effect of Injecting Various Sodium Minerals on Percent SO_2 Removal (Ref. 2) 3-15

3-9 Effect of Injection Point on SO_2 Removal (Ref. 3) 3-16

3-10 Effect of Excess Combustion Air on SO_2 Removal (Ref. 3) . . . 3-17

3-11 SO_2 Removal vs. Stoichiometry for Reported Plant-Scale Tests of Dry Limestone Injection Process (Ref. 4) 3-19

3-12 Sulfur Balance--Pulverized Coal 3-20

3-13 Field Scale Studies - General Combustion Chamber Flow Pattern 3-21

3-14 Time - Gas Temperature Profile and Limestone Residence Time for TVA Unit 3-22

3-15 SO_2 Emission and Molar Ca/S Ratio (Ref. 5) 3-26

3-16 SO_2 Emission and Ca/S Ratio of the Fuel (Monthly Average Values for Boiler Fuels) (Ref. 5) 3-27

3-17 Installation of the Dry Additive System (Schematic) at the Fortune II Power Plant - West Germany 3-28

3-18 SO_2 Capture with Several Additives (Ref. 5) 3-29

3-19 Emission Reduction with $CaCO_3$ (Ref. 5) 3-31

3-20 Schematic of Various Possibilities of Injection of the Additive for the Steinmüller Staged Mixing Burner 3-33

3-21 Schematic of IFRF Furnace with Staged Mixing Burner and Typical Temperature Levels Measured with a 2.3 MW Coal Flame . 3-34

Figure No. Page

3-22 Typical Results of Desulfurization With Injection of Sorbent at the Periphery of the Flame (Position 3) 3-36

3-23 Effect of Sorbent Injection Location on Desulfurization Rates for Three Different Coals (Ref. 6) 3-37

3-24 Effect of Staging on SO_2 Reduction Rates with Injection of $Ca(OH)_2$; Correlation With Average Residence Time in Burner Quarl When $Ca(OH)_2$ Is Mixed With Coal (Ref. 6) 3-38

3-25 Actual Levels of SO_2 and NO_x Emission With Staged Combustion and With Injection of $Ca(OH)_2$ at the Periphery of the Burner (Position 3) 3-40

3-26 Schematic of First Generation Small Watertube Simulator (SWS) and Support Facilities 3-41

3-27 Sketch of Distributed Mixing Burner 3-43

3-28 The Effect of the Addition of Limestone to the Utah Coal Prior to Pulverization on SO_2 Emissions (Ca/S = 1.0) 3-48

3-29 The Effect of the Addition of Limestone to the Western Kentucky Coal Prior to Pulverization on SO_2 Emissions (Ca/S = 1.0) 3-51

3-30 The Effect of Sorbent on NO_x Emissions (Utah Coal Ca/S = 1) . 3-54

4-1 Schematic of the Steinmüller Staged Mixing Burner 4-2

4-2 Characteristics of the LWS Test Furnace 4-5

4-3 Effect of Staging on Emissions, Utah Coal 4-13

4-4 Effect of Excess Air on Emissions, Utah Coal 4-14

4-5 Effect of Burner Load on Emissions, Utah Coal 4-15

4-6 Effect of Burner Zone Stoichiometry - Indiana Coal 4-17

4-7 Effect of Excess Air, Indiana Coal 4-18

4-8 Effect of Burner Load, Indiana Coal 4-19

4-9 Effect of Coal Type - EPA Prototype 3 Burner 4-20

4-10 Effect of Burner Zone Stoichiometry - Saar Coal 4-21

4-11 Effect of Excess Air, Saar Coal 4-22

4-12 Effect of Burner Load, Saar Coal 4-23

4-13 Schematic of the SO_2 Sampling System 4-25

4-14 Comparison of Sulfur Capture for Two Coals Using Calcium Hydroxide as the Sorbent and the Steinmüller Low NO_x Burner . 4-27

4-15 Comparison of Sulfur Capture with Calcium Hydroxide and Calcium Carbonate with the Steinmüller Burner 4-28

4-16 EPA Prototype DMB with Foster Wheeler Burner Components (Tertiary Ports Not Shown) 4-29

Figure No. Page

4-17 Prototype DMB NO_x Emissions 4-31

4-18 Effect of Sorbent Injection Location - EPA Prototype DMB, Indiana Coal 4-32

4-19 Effect of Sorbent Injection Location - EPA Prototype DMB, Utah Coal 4-33

4-20 Sulfur Balance - EPA Prototype DMB, Limestone Injected Through All Four Tertiary Ports 4-35

4-21 Effect of Burner Zone Stoichiometry on NO_x Emissions ~ Comparison of Data, Steinmüller Burner 4-36

4-22 Effect of Excess Air on NO_x Emissions - Comparison of Data, Steinmüller Burner 4-37

4-23 Effect of Load on NO_x Emissions ~ Comparison of Data, Steinmüller Burner 4-38

4-24 NO_x and CO Emissions for the EPA Prototype DMB Fired in the LWS Furnace 4-41

4-25 Summary of Results Obtained with the Steinmüller Burner in the IFRF Furnace 4-42

4-26 Comparison of Steinmüller and DMB Data - Limestone Injected in Tertiary Ports 4-43

5-1 Conceptual View of Sulfur and Sorbent Transformation During Coal Combustion 5-2

5-2 Sulfur Distribution in Some Typical U.S. Coals 5-9

5-3 Combustion Behavior of a Single Coal Particle 5-10

5-4 Sulfur Evolution Data (Solomon) 5-13

5-5 Elemental Loss During Devolatilization 5-14

5-6 Inherent Sulfur Capture Results 5-26

5-7 Calcium Utilization 5-29

5-8 Possible Transformations and Interactions of Sorbent Particles in a Coal-Fired Furnace 5-31

5-9 Change of Specific Surface Area of Limestone by Calcination and Reaction in Combustion Gases 5-37

5-10 Effect of Calcination Temperature on Particle Physical Characteristics (120 minutes) 5-39

5-11 General Summary of Effect of Calcination Temperature on Particle Physical and Chemical Characteristics 5-40

5-12 Effect of Pore Diameter on Reaction Rate 96 μ Particles . . . 5-42

5-13 Reaction Rate at Constant Sulfation as Affected by the Pore Size of the Calcine, Illustrating Zero, Linear, and Exponential Responses to $1/\overline{D}_p$ 5-43

Figure No. Page

5-14 Reaction Rate vs. $1/\overline{D}_p$; Sulfate Loading = 2×10^{-3} g. moles/g 5-45

5-15 Particle Heat-Up Time for Limestone 5-46

5-16 Typical Particle Heat-Up Characteristics 5-47

5-17 Effect of Gas Temperature on Calcination 5-48

5-18 Relationship Between Effectiveness Factor and Pore Size . . . 5-50

5-19 Pore Volume and Particle Volume as a Function of Conversion in 0.025 cm Particles 5-52

5-20 Relation Between Ratio of Reacted Lime and Sulfur Dioxide Concentration (Joban Limestone) 5-55

5-21 Arrhenius Plot for the Reaction of CaO with SO_2 Showing the Effect of SO_2 Concentration (Joban Limestone) 5-56

5-22 Arrhenium Plots for the Reaction of Sulfur Dioxide with Four Limestones 5-58

5-23 Relation Between SO_2 Concentration at Injection Point and the Reactivity of Lime 5-59

5-24 Arrhenius Plot for the Reaction of CaO with SO_2 Showing the Effect of Gas Temperature at Injection Point 5-60

5-25 Reaction Rate vs. Surface Area 5-61

5-26 Comparison of Initial SO_2 Reaction Rates in a Dispersed-Phase Reactor 5-62

5-27a Reaction Rate of CaO with COS (0.1%) at 500°C; in N_2 and in N_2 with 10% CO 5-64

5-27b Effect of Flow Rate on Reaction Rate at 900°C with 0.1% COS and 10% CO in N_2; with Flow Rates of 1000 SCCM and 2000 SCCM . 5-64

5-27c Effect of Temperature on Reaction Rate with 0.1% COS and 10% CO in N_2 5-64

5-27d Effect of COS Concentration on Reaction Rate at 800°C with 10% CO and the Marked COS Composition in N_2 5-64

5-28 Analysis of the Reaction Order with Respect to COS at 800°C . 5-65

5-29 Extrapolation of Reaction Data to High Temperatures 5-67

5-30 Relative Stability of CaS and $CaSO_4$, Equilibrium Calculations 5-68

6-1 Sample, Sorbent Injection, and H_2S Injection Locations for Propane-Fired Experiments (Series B-1) 6-8

7-1 Bench-Scale Reactor, Coal/Argon Fired 7-2

7-2 Cross-Section Schematic of the Combustor, Convective Furnace 7-3

Figure No. Page

7-3 Schematic of Experimental System for Gas Phase Sulfur Experiments, Argon/Propane Furnace 7-4
7-4 Burner Schematic, Propane/Argon Furnace 7-6
7-5 Gas Additive System 7-7
7-6 Solids Transport System, Propane/Argon Furnace 7-8
7-7 Summary of Design Criteria for Boiler Simulator Furnace . . . 7-13
7-8 BSF - System 1.1 - Batch Pulverized Coal Production System - Version 1.0 7-15
7-9 BSF - System 1.2 (with 2.1) - Coal and Solid Additive System . 7-16
7-10 BSF - Gas Fuel Delivery - Metering System 7-17
7-11 BSF - Air Supply - Metering 7-18
7-12 Distributed Mixing Burner Schematic, B.S.F. (Tertiary Air Ports Not Shown) 7-22
7-13 BSF - Radiant Section, Side Cross Section 7-31
7-14 BSF - Radiant Adiabatic Furnace Module 7-32
7-15 BSF - Post Flame Cavity - Concept 7-34
7-16 BSF - Convective Air Cooled Superheater Module 7-35
7-17 BSF - Furnace Heat Extraction Control System 7-37
7-18 BSF - Data Acquisition System Scheme 7-39
7-19 Boiler Simulator Furnace - Original Configuration 7-45
7-20 Modified Post Flame Cavity - As of August 22, 1981 7-47
7-21 BSF - Downfired Configuration as of Late October, 1981 7-48
7-22 BSF Cross Sectional Flow Area Versus Axial Distance 7-49
8-1 Phase Discrimination Probe 8-3
8-2 Gas Phase Sulfur Species Measurement System 8-4
8-3 Verification of Permeation Tube Drier 8-5
8-4 BSF - Four-Probe Sample and Analytical System 8-6
8-5 Comparison of SO_2 Analysis Methods: NDUV Versus Method 7 . . 8-9
8-6 Sample Conditioning System for H_2S-Bearing Gases 8-11
8-7 H_2S Measurement Verification 8-12
8-8 Typical Gas Chromatogram of First-Stage Sample (Fuel Rich) . . 8-13
8-9 Retention of H_2S in GC System at Start-Up 8-15
8-10 Flow Diagram of GC Sampling System 8-16
8-11 Calibration Curve for Known Sulfur Standards on LECO Analyzer 8-18

Figure No. Page

8-12 Suction Pyrometer Schematic 8-20

9-1 Effects of Sorbent Particle Size on Sulfur Capture, SO_2 as Dopant, <80 Mesh 9-3

9-2 Effects of Sorbent Particle Size on Sulfur Capture, SO_2 as Dopant, <200 Mesh 9-3

9-3 Effect of Ca/S Ratio on Sulfur Capture, ~46,000 Btu/hr, $Ca(OH)_2/Al_2O_3 \cdot 4SiO \cdot H_2O$, 50/50 Mix 9-4

9-4 Effect of Ca/S on SO_2 Capture, 32,000 Btu/hr, P-Coal $Ca(OH)_2$ 9-5

9-5 Effect of Furnace Load on Sulfur Capture 9-6

9-6 Effect of Excess Air on Sulfur Capture, 32,000 Btu/hr $Ca(OH)_2$ 9-7

9-7 Effect of Excess Air on Capture, 48,000 Btu/hr, $Ca(OH)_2$ . . . 9-8

9-8 Effect of Input Sulfur on Sulfur Capture, Low Load (30,000 Btu/hr), $CaCO_3/Al_2O_3 \cdot 4SiO \cdot H_2O$ 50/50 Mix 9-10

9-9 Effect of SO_2 Concentration on Sulfur Capture 4 Percent O_2, Propane at 32,000 Btu/hr, $Ca(OH)_2$ 9-11

9-10 Effect of SO_2 Concentration on Sulfur Capture 9-12

9-11 Effect of Primary Zone Stoichiometry on Sulfur Capture Staged Combustion 9-14

9-12 Effect of Staging on Sulfur Capture 9-15

9-13 Effect of Choke on Sulfur Capture 9-16

9-14 Effect of First Stage Stoichiometry on Sulfur Capture, Sorbent with Second Stage Air 9-17

9-15 Effect of Excess Air on $CaSO_4$ Decomposition 9-18

9-16 Effect of Excess Air on CaS Decomposition 9-20

9-17 Effect of Air Preheat on CaS Decomposition, 50,000 Btu/hr . . 9-21

9-18 Equilibrium Sulfur Species Distribution, Fuel Lean Propane + H_2S + $CaCO_3$, SR = 1.20 9-22

9-19 Equilibrium Calculation for Fuel-Rich Sulfur Species Distribution, Propane + H_2S 9-23

9-20 Equilibrium Calculatons for Fuel Lean Sulfur Species Distribution, Lignite Coal + $CaCO_3$, Ca/S = 1.6, SR = 1.25 . . 9-24

9-21 Equilibrium Calculation for Fuel-Rich Sulfur Species Distribution, Lignite Coal SR_1 =.50 9-25

9-22 Equilibrium Temperature for 50 Percent Condensed Sulfur (CaS or $CaSO_4$) as a Function of Overall Fuel/Air Stoichiometry 9-26

Figure No. Page

9-23 Percent Sulfur Capture, Normalized by SO_2 Concentration as a Function of Calcium-to-Sulfur Ratio. Argon Furnace Fired with Propane and Air 9-28

10-1 Inherent Capture as a Function of Sulfur Content 10-2

10-2 Sulfur Balance, Convective Furnace 10-5

10-3 Effect of Load on Sulfur Capture 10-6

10-4 Furnace Response to SO_2 Pulse, 3 Minute Pulse, Propane Fired 10-8

10-5 Baseline SO_2 Profile Through BSF, Propane + SO_2 Fired . . . 10-9

10-6 Baseline SO_2 Profile Through BSF, Indiana Coal Fired 10-10

10-7 Effect of Cooling and Load on Time/Temperature Profile of BSF 10-11

10-8 Sulfur Capture With 15 Percent Heat Extraction by Probes in Initial Post-Flame Zone. Firing Rate 1 MBtu/hr. Calcium Hydroxide Sorbent 10-12

10-9 Sulfur Capture as a Function of Calcium Additive/Sulfur Ratio with Firing Rate (Load) as a Parameter. Indiana Coal, 2.56 Percent Sulfur, Full Load is 0.95 MBtu/hr, Calcium Hydroxide Sorbent 10-13

10-10 Effect of Flame Shape on Sulfur Capture, 1 x 10^6 Btu/hr, Cold Start, Uncooled, $CaCO_3$ in Tertiary Air, $SR_B = 0.75$, $SR_T = 1.25$ 10-14

10-11 Baseline Drift, Furnace Shakedown Experiments, Base Case Conditions 10-16

10-12 Baseline Drift, High T.A. Velocity Experiments 10-17

10-13 Sulfur Capture/Base Case Conditions 10-21

10-14 Sulfur Capture Through the Furnace, Base Conditions 10-22

10-15 Relative SO_2 Capture for Added $CaCO_3$ and Individual Furnace Sections 10-24

10-16 Correlation of Sulfur Capture - Base Case Conditions 10-25

10-17 Influence of Heat Extraction Rate - Base Case Conditions . . 10-26

10-18 Importance of Heat Extraction with Alternate Sorbent Location 10-28

10-19 Additional Studies on Heat Extraction 10-29

10-20 Effect of Heat Extraction on Zone Capture - Base Case Conditions 10-30

10-21 Effect of Heat Extraction on Zone Capture - Low Load 10-31

10-22 Role of Overall Excess Air 10-32

10-23 Influence of Burner Zone Stoichiometry - Uncooled 10-34

Figure No. Page

10-24 Summary of Burner Zone Stoichiometry Results 10-35

10-25 Effect of Burner Zone Stoichiometry on Zone Capture - Base Case Conditions 10-36

10-26 Role of Sorbent Location 10-37

10-27 Influence of Sorbent Location - Uncooled Condition 10-38

10-28 Influence of Firing Rate 10-40

10-29 Influence of Firing Rate - Alternate Conditions 10-41

10-30 Effect of Firing Rate on Zone Capture 10-42

10-31 Effect of Tertiary Air Velocity - Base Case Conditions . . . 10-43

10-32 Effect of Tertiary Air Velocity on Zone Capture - Base Case Conditions 10-45

10-33 Detail of Boiler Simulator Furnace - External Staging Schematic 10-46

10-34 Impact of External Staging on Thermal Environment, BSF . . . 10-47

10-35 Effect of First Stage Stoichiometry on Sulfur Evolution from Indiana Coal 10-49

10-36 Effect of First Stage Stoichiometry on Sulfur Species Distribution, Cooled 10-50

10-37 Effect of First Stage Stoichiometry on Sulfur Species Distribution - Uncooled 10-51

10-38 Effect of First Stage Stoichiometry on Sulfur Capture and Post Flame Temperature 10-52

10-39 Effect of First Stage Stoichiometry on Individual Sulfur Species Captures 10-54

10-40 Effect of Sorbent Injection Method on Sorbent Utilization . 10-55

10-41 Effect of Sorbent Location on Sulfur Capture. Externally Staged, Cooled 10-56

10-42 Effect of SR_1 on Sorbent Utilization, Sorbent Added With Air at Base of P.F.C. 10-57

10-43 Effect of SR_1 on Sorbent Utilization Low Load, Uncooled . . 10-59

10-44 Effect of SR_1 on Sorbent Utilization for Propane Doped with H_2S (2500 ppm Equivalent Exhaust SO_2) 10-60

10-45 Capture and Retention of Sulfur Under External Staged Conditions for Coal and Propane Doped with H_2S, Sorbent Added with Air at Base of Post Flame Section, Uncooled . . . 10-61

11-1 Effect of Burner Zone Stoichiometry on NO_x Emissions - Comparison of Data, Steinmüller Burner 11-2

11-2 Effect of Excess Air on NO_x Emissions - Comparison of Data, Steinmüller Burner 11-3

Figure No. Page

11-3 Effect of Load on NO_x Emissions - Comparison of Data, Steinmüller Burner 11-4

11-4 Comparison of Steinmüller and DMB Data - Limestone Injected in Tertiary Ports 11-6

11-5 The Effect of Load and Radiant Zone Cooling on Sulfur Capture 11-7

11-6 Effect of Stoichiometry on Sulfur Species Distribution. A, Equilibrium Calculations; B, Propane and H_2S; C, Indiana Coal 11-9

11-7 The Effect of Rich Zone Stoichiometry on Sorbent Utilization and Thermal History, Indiana Coal-Fired 11-10

LIST OF TABLES

Table No. Page

3-1 Pilot-Scale Test Conditions 3-5

3-2 Field-Scale Results 3-24

3-3 Analytical Instrumentation 3-45

3-4 Sorbents Used in Sulfur Capture Tests 3-46

3-5 Summary of Results 3-49

3-6 Coal Composition 3-50

4-1 Nominal Input and Operating Conditions for the Steinmüller Staged Mixing Burner Design 4-3

4-2 LWS Operating Parameters 4-6

4-3a Analysis - Utah Coal 4-8

4-3b Analysis - Indiana Coal 4-9

4-3c Analysis - Saar Coal 4-10

4-4 Pulverized Coal Size Analyses 4-11

5-1 Coal Sulfur Forms 5-5

5-2 Total Sulfur of U.S. Coals 5-7

5-3 Sulfur Content of World Coals (Yurovskii, 1960) 5-8

5-4 Thermal Decomposition of Hydrogen Sulfide 5-17

5-5 Hydrogen Sulfide Oxidation 5-18

5-6 Carbon Disulfide Oxidation at 927°C, 30 torr Pressure 5-20

5-7 Carbonyl Sulfide Oxidation at 997°C, 74 torr Pressure 5-21

5-8 Reactions Involved in SO_3 Production and Depletion in COS and H_2S Flames 5-23

5-9 Sulfur Balances for Gascoyne Lignite (Brown, et al, 1978) . . 5-27

5-10 Physical Characteristics of Several Raw Stones and Their Calcines 5-35

5-11 Specific Surface Area of Calcined Limestone and Hydrated Limes Heated Rapidly 5-36

6-1 Test Matrix--Series A-2--Staged Combustion Screening 6-4

6-2 External Staging Studies Test Matrix 6-6

6-3 Thermal Environment Studies--Propane-Fired 6-7

6-4 Thermal Environment Studies--Coal-Fired 6-10

6-5 Test Matrix for Fuel/Sorbent Studies (Series C) 6-11

7-1 Summary of Data Obtained on Other Research Furnaces 7-10

7-2 Combustion Air Stream Design Capacity, BSF 7-20

Table No. Page

7-3 Design Specifications 7-23

8-1 Instrumentation for Continuous Measurements 8-8

10-1 Inherent Capture Data 10-4

10-2 Series A-1 Test Matrix Combustion Parameter Screening . . . 10-19

1.0 SUMMARY

This is the fourth annual report describing progress on EPA Contract 68-02-2667, "Development of Criteria for Evaluation of Applicability of Low Emission, High Efficiency Coal Burners". The significant accomplishments in this year's effort were:

Pilot-Scale Testing of EPA Prototype DMB and Steinmuller Burners

The emissions characteristics of a 50 x 10^6 Btu/hr (15 MW) coal-fired staged mixing burner developed by the Steinmuller Company of West Germany were investigated using the LWS (Large Watertube Simulator). The effects of burner zone stoichiometry, overall excess air level and burner load on NO_x and CO emissions was determined for three coals; Utah, Indiana and Saar. The effects of the operational parameters on emissions from all three coals was similar: increasing burner zone stoichiometry increased NO_x emissions as did increasing overall excess air. Staging (decreasing burner zone stoichoimetry) was limited by increases in CO emissions and problems with flame stability at burner zone stoichiometry below about 0.6. Increasing burner load increased NO_x emissions from all three coals. The emission characteristics of the EPA prototype Low NO_x Distributed Mixing Burner (DMB) were established in tests conducted under EPA Contract 68-02-3127, again fuel had little effect on NO_x emissions, especially when compared to the effect of operational parameters.

A brief series of experiments to investigate the feasibility of using dry sorbents injected directly into the furnace for SO_2 emission control was conducted. Both the Steinmuller and prototype burners were used, both burners in the minimum NO_x mode; no attempt was made to optimize the burners for SO_2 capture. Sorbent type ($Ca(OH)_2$ vs. $CaCO_3$) had a small effect on sulfur capture in the Steinmuller burner as did sorbent injection location. Fuel sulfur content also affected sulfur capture (higher coal sulfur-higher capture). Sulfur captures on the order of 40-50 percent at Ca/S molar ratios of 2.0 were obtained.

Review of the Dry Sorbent Injection for SO_2 Control Process

A brief review of recent pilot and plant-scale studies of the dry injection process was compiled and is presented in this report, as is a review of the coal/sulfur/sorbent system. The current literature on the effects of operational parameters, fuel and sorbent types and sorbent sulfur chemistry was summarized.

Bench-scale Studies of SO_2 Capture by Dry Sorbent Injection

The major experimental effort during this reporting period was characterization of the SO_2 capture process using bench-scale facilities. The effort included: the development of sampling and analytical systems for the measurement of SO_2 and determination of sulfur capture; the design, construction and testing of an experimental facility, the boiler simulator furnace (BSF) ; and the investigation of the effect of various combustion and operational parameters on sulfur capture in the BSF. The measurement of sulfur species in combustion products containing active sorbents introduces several problems related to sample acquisition. A "phase determination" probe, which minimizes gas-solid contacting after sample extraction, was designed, constructed and tested. Methods for measuring sulfur species concentrations in fuel-rich combustion gases were developed as were methods for solids analysis (including sorbent ash and coal composition and surface areas).

The bench-scale facility constructed for these studies is capable of duplicating the history of the solid particles (coal and sorbent) and the products of combustion in a pulverized coal-fired boiler. The facility consists of three major components:

- A radiant furnace, a horizontal refractory-lined cylinder which simulates the firing zone. Removable cooling tubes provide heat extraction.
- A post-flame cavity which simulates the space between the firing zone and the superheater of a conventional boiler.
- A convective section, cooled by banks of air-cooled stainless steel tubes which simulates the superheater, air heater and economizer.

A parametric screening study of the effect of combustion and operation variables on sulfur capture by sorbents directly injected into the furnace was planned and the first portion of this study completed. The results of program definition experiments were used to specify design criteria for the BSF and parameters for the first set of screening studies. Parameters investigated included: Firing rate, heat extraction rate, sorbent injection location, overall excess air, burner zone stoichiometry and tertiary air velocity. One sorbent, Vicron 45-3, a large grain-size, calcite limestone, and one coal, a medium sulfur (1-2%), bituminous, Indiana coal were used for all of the studies. The studies established that under fuel-lean conditions, thermal history exerts a controlling influence on sulfur capture. Firing rate and heat extraction rate had strong influences on sulfur capture due to the effect on thermal history. Sorbent location, burner zone stoichiometry, overall excess air and tertiary air velocity had secondary effects, which depended to some extent on other variables, on sulfur capture. Sulfur capture under fuel-rich conditions was also investigated. Fuel-rich conditions should favor sulfur capture because of increased gas-phase driving forces (due to less dilution), faster reaction rates between CO and H_2S and greater stability of Ca/S at high temperatures. The experiments did not show an improvement in sulfur capture under fuel-rich conditions. Measurements indicated significant retention of sulfur in the solid phase and a gaseous sulfur species distribution considerably different than equilibrium predictions. Sorbent injection location and method (with air or nitrogen) affected sulfur capture under fuel-rich conditions. Sulfur capture was best when the sorbent was injected with an air carrier into the fuel-rich region downstream of the coal.

Experimental plans for the next year were made and include: Testing of the DMB prototype burner in a smaller scale, hotter pilot test furnace, the MT (Medium Tunnel); investigation of sulfur capture in the fuel-rich region of gas flames (eliminating the char sulfur retention complication) in the BSF: more detailed investigation of the effect of thermal environment on sulfur capture, and investigation of the effect of fuel and sorbent type on sulfur capture.

2.0 INTRODUCTION

This annual report describes the progress on EPA Contract 68-02-2667, "Development of Criteria for Extension of Applicability of Low-Emission, High Efficiency Coal Burners". The program was initiated in October, 1977 and was structured to provide data for a wider design base in the application of the delayed mixing burner (DMB) concept as a means of controlling the emissions of NO_x. In this context the program has the following main objectives:

- Expand the fuel capability of low NO_x burners to include the major types of solid fossil fuels projected for use by the utility industry.
- Explore additional burner concepts and configurations that show potential for improving the emission and thermal performance of pulverized coal burners.
- Determine the effects of multiple burner configurations that are encountered in utility boilers.
- Provide for direct comparison between the experimental burners being developed herein and the current state-of-the-art for commercially available coal burners.
- Provide testing in support of planned application of the burner technology.

In order to meet these objectives the program has been divided into seven tasks as depicted in Figure 2-1. These tasks are designed to provide experimental data relative to the distributed mixing concept. The work moves progressively from bench-scale studies of the basic processes, through single burner studies at a range of pilot scales, to multiple burner configurations and a comparison of DMB emission and operating characteristics against current commercial technology. The base program provides also for technology transfer and review of progress by the industry through an Industry Coordination task.

During the past reporting period the main focus of the program has shifted somewhat, and a renewed attention has been directed towards dry sorbent SO_x

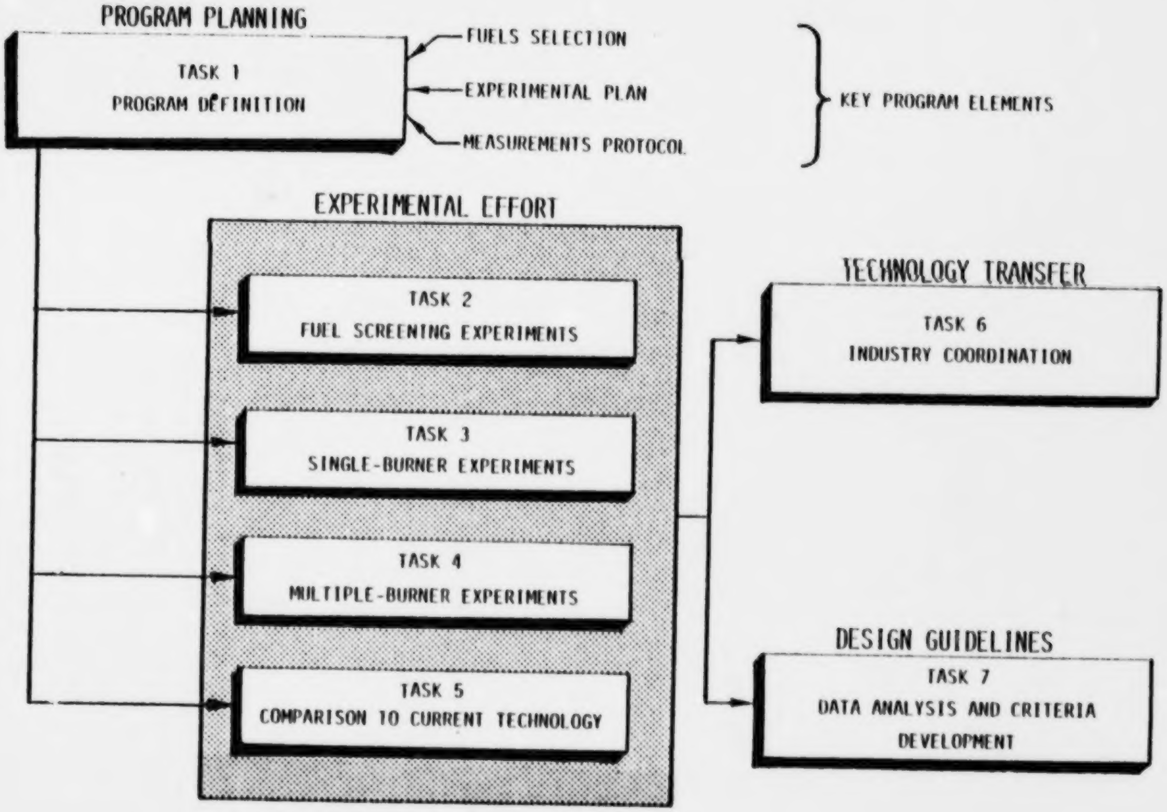
PROGRAM PLANNING
TASK 1
PROGRAM DEFINITION
FUELS SELECTION
EXPERIMENTAL PLAN
MEASUREMENTS PROTOCOL
KEY PROGRAM ELEMENTS
EXPERIMENTAL EFFORT
TASK 2
FUEL SCREENING EXPERIMENTS
TASK 3
SINGLE-BURNER EXPERIMENTS
TASK 4
MULTIPLE-BURNER EXPERIMENTS
TASK 5
COMPARISON TO CURRENT TECHNOLOGY
TECHNOLOGY TRANSFER
TASK 6
INDUSTRY COORDINATION
DESIGN GUIDELINES
TASK 7
DATA ANALYSIS AND CRITERIA DEVELOPMENT

Figure 2-1. Program Structure for Development of Criteria for Extension of Applicability of Low-Emission / High-Efficiency Coal Burners.

control technology. The use of sorbents to control emissions of sulfur oxides is not new and was extensively studied in the late 1960's and early 1970's in a series of development and demonstration projects. Although the pilot plant studies showed promise the results could not be duplicated in full scale systems. This work, together with results from recent pilot scale studies, is reviewed in Section 3. Here some of the more recent data suggests that those burner conditions necessary for the minimization of NO_x are favorable also for enhanced sulfur capture by injected sorbents. This has led to the concept of a combined NO_x/SO_x control strategy and to a need for a definition of the conditions under which the emission of both pollutants can be minimized, without a significant impact on overall combustion system performance. A modified program plan approach for Contract 68-02-2667, which extends the original goals to include SO_x control, is presented in Figure 2-2. The experimental portion of this program provides both for bench scale studies to define optimum conditions for sulfur capture, and for pilot scale studies with real burner systems in order to optimize and evaluate the potential for combined NO_x/SO_x control.

In the present reporting period of the contract, pilot scale studies have been carried out with a reduced scale (50 x 10^6 Btu/hr) version of the Steinmuller Staged Mixing Burner to provide a comparison between DMB performance and current commercial technology. A field prototype version of the DMB burner system has also been extensively tested under EPA Contract 68-02-3127. Both burner tests also provided an opportunity to investigate sorbent injection in unmodified (for SO_x control) systems, and results are presented and discussed in Section 4. While the experimental data indicate some potential for significant SO_x removal under low NO_x conditions the results provide no further understanding of the basic mechanisms involved in sulfur capture, or of those ideal conditions required for process optimization. In Section 5 an overview is presented of the current understanding of those factors which affect the evolution, oxidation and retention of sulfur species in pulverized coal combustion. These considerations provide background for the development of bench scale experimental plans for the study of sulfur removal under low NO_x conditions, which are presented in Section 6.

In the execution of the bench scale studies two different experimental approaches have been taken. The first attempts to remove some of the complexities associated with coal combustion and examines sorbent/sulfur interactions

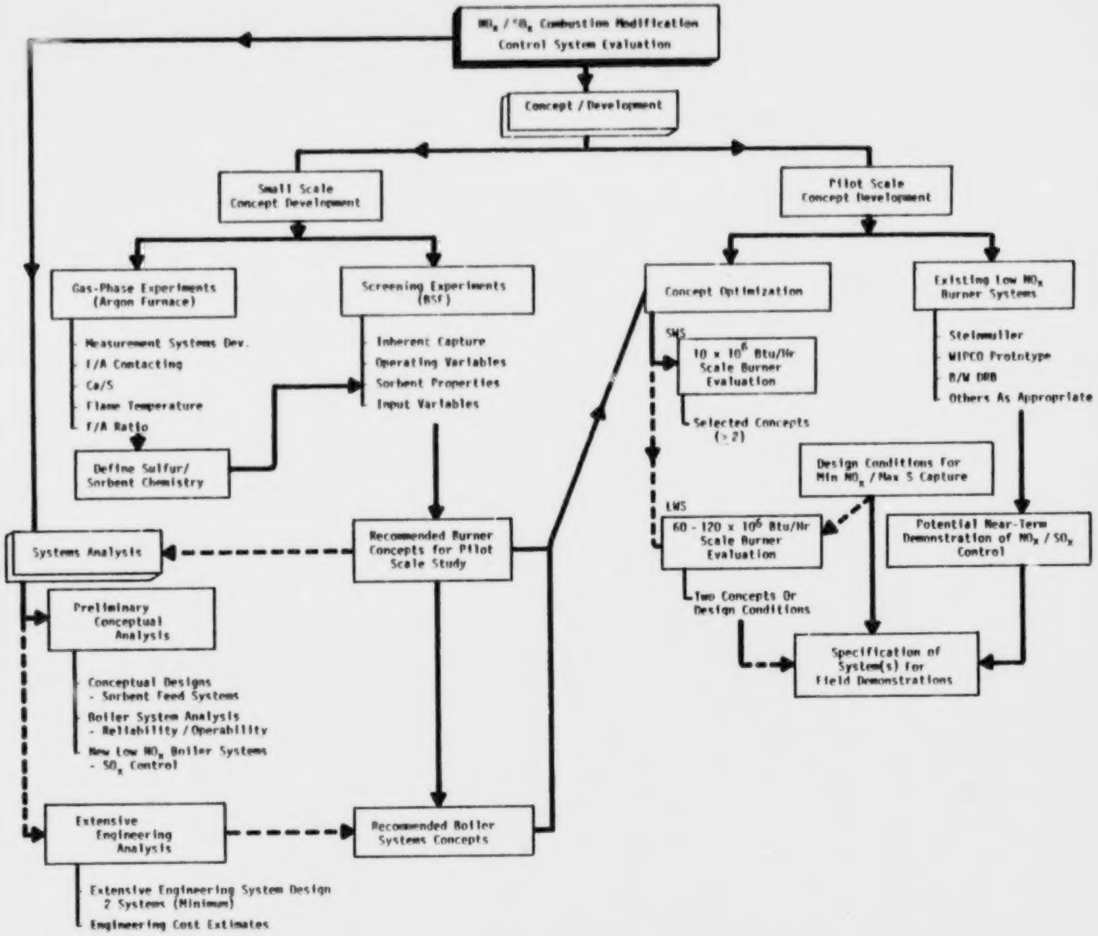
NO$_x$ / SO$_x$ Combustion Modification Control System Evaluation
Concept / Development
Small Scale Concept Development
Pilot Scale Concept Development
Gas-Phase Experiments (Argon Furnace)
- Measurement Systems Dev.
- F/A Contacting
- Ca/S
- Flame Temperature
- F/A Ratio
Define Sulfur/ Sorbent Chemistry
Screening Experiments (BSF)
- Inherent Capture
- Operating Variables
- Sorbent Properties
- Input Variables
Concept Optimization
SWS
10 x 10^6 Btu/Hr Scale Burner Evaluation
Selected Concepts (> 2)
LWS
60 - 120 x 10^6 Btu/Hr Scale Burner Evaluation
Two Concepts Or Design Conditions
Existing Low NO$_x$ Burner Systems
- Steinmuller
- WIPCO Prototype
- B/W DRB
- Others As Appropriate
Design Conditions For Min NO$_x$ / Max S Capture
Potential Near-Term Demonstration of NO$_x$ / SO$_x$ Control
Specification of System(s) For Field Demonstrations
Systems Analysis
Recommended Burner Concepts for Pilot Scale Study
Preliminary Conceptual Analysis
- Conceptual Designs
- Sorbent Feed Systems
- Boiler System Analysis
- Reliability / Operability
- New Low NO$_x$ Boiler Systems
- SO$_x$ Control
Extensive Engineering Analysis
- Extensive Engineering System Design 2 Systems (Minimum)
- Engineering Cost Estimates
Recommended Boiler Systems Concepts

Figure 2-2. Program Plan Approach - Combined NO$_x$ / SO$_x$ Control.

in a totally gaseous phase system. In the second, coal combustion is studied under furnace conditions which simulate the temperature/time history of a complete boiler system, and for which it was necessary to construct a new Boiler Simulator Furnace (BSF) facility. Details of the two experimental facilities are given in Section 7, together with a more detailed description of the BSF operation and preliminary experiences which led to redesign of part of this facility. Experimental results from both phases of the bench-scale experimental program are presented and discussed in Sections 9 and 10. Analytical requirements for this program were extensive and previous experience has shown the need for carefully controlled conditions when sampling for sulfur species in the presence of active sorbents. These requirements necessitated the development of several new sampling and analytical capabilities at EER and these are described in Section 8. Some conclusions (although still of an interim nature) which may be drawn from the results of the work to date are presented in Section 11.

3.0 PILOT AND PLANT-SCALE STUDIES OF SO_x CONTROL VIA DRY SORBENT INJECTION; A REVIEW OF EARLIER WORK

Several studies of SO_2 control through dry sorbent injection have been conducted at pilot and plant-scale; for the purposes of this report, these have been classified into three categories which will be discussed individually:

- Early Pilot-Scale
- Early Plant-Scale
- Recent Investigations

A review of all previous studies in this subject area is beyond the scope of this report. In selecting the studies considered here, every attempt was made to represent the full spectrum of combustion systems, fuels, and experimental techniques.

3.1 Early Pilot-Scale Studies

The objective of this section is to present experimental information obtained under pilot-scale test conditions which indicate the feasibility of in-situ sulfur removal by the dry sorbent technique. A large number of studies have been conducted that could be classified as pilot-scale; a summary of the results of these studies showing the percent SO_2 removal as a function of Ca/S molar ratio (stoichiometry) is presented in Figure 3-1. It is obvious from these results that a wide variation in SO_2 removal is possible, depending on the specific environmental and physical conditions under which the tests were conducted. For stoichiometric ratios of one, the maximum SO_2 removal for limestone was about 50 percent, corresponding to a 50 percent utilization of the sorbent. Note that for Nahcolite, where communition (explosion of the sorbent particles when heated rapidly) may occur, the SO_2 removal (and utilization) is considerably greater. Due to the wide differences in results from these programs, three studies have been selected for detailed review which are representative of those covering the range in SO_2 removal shown in Figure 3-1. The three studies are: 1) Peabody Coal Company (1), which used a pilot-scale stoker to produce coal combustion gases and injected limestone at various

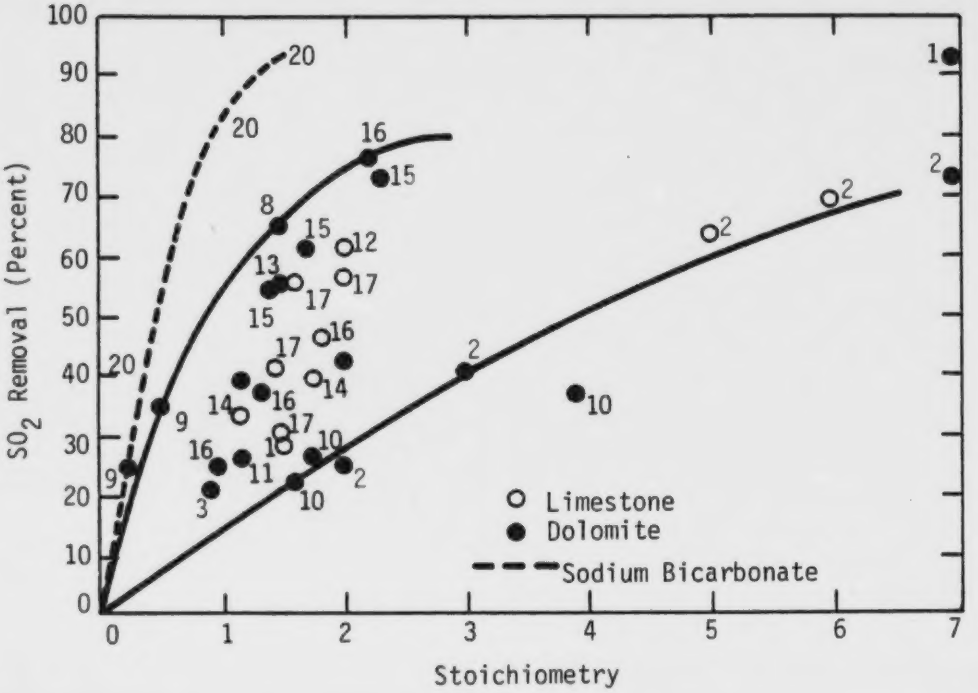

Key Number	Investigator	Fuel	Sorbent
1	TVA	Coal (Sim. Gas)	Limestone
2	TVA	Coal (Sim. Gas)	Dolomite
3	TVA	Coal (Sim. Gas)	Limestone
8	Peabody Coal	Coal	Limestone
9	Peabody Coal	Coal	Dolomite
10	Babcock & Wilcox	Coal	Dolomite
11	Peabody Coal	Coal	Dolomite
12	Peabody Coal	Coal	Limestone
13	Peabody Coal	Coal	Limestone
14	Babcock & Wilcox	Coal	Limestone
15	Poland	Coal	Dolomite
16	Poland	Coal	Dolomite
17	Czechoslovakia	Coal	Limestone
20	Superior Oil Co.	Oil	Sodium Bicarbonate

Figure 3-1. SO$_2$ Removal Versus Stoichiometry for Pilot-Scale Injection Tests with Dry Sorbent.

locations along a flue section; 2) Superior Oil Company (2), which injected sodium bicarbonate into an oil-fired reactor then injected gaseous SO_2 at various temperature locations; and 3) Babcock and Wilcox (3), which used a pilot-scale pulverized coal reactor and injected limestone at various locations along the reactor and convection pass. Schematics of the various experimental systems are shown in Figure 3-2 and typical experimental conditions are summarized in Table 3-1. The above described studies not only cover a broad range in combustion systems, but also span the range of oil, stoker coal, and pulverized coal fuel firing.

Four major variables have been identified for detailed discussion:

1. Gas temperature/time history
2. Particle size effects
3. Sorbent types
4. Oxygen concentration

It is realized that additional parameters such as dispersion, etc., are extremely important; however, no direct measurements have been made of their effect on sulfur capture.

3.1.1 Gas Temperature/Time History

The T(t) characteristics for the three studies are compared in Figure 3-3. In the Peabody experimental rig, the gas temperature/time profile can be changed by varying load; however, the rate of temperature decrease is very low after about 0.75 seconds. For the low load condition, the temperature is about 1400^oF at 1 sec, which corresponds to the minimum temperature for calcination. In contrast, the experimental set-up of Superior Oil, while providing only one temperature/time profile, does have a more rapid overall decay than that of the Peabody system. Babcock and Wilcox inject the sorbent at different locations, thereby obtaining differing T(t) histories without changing the input coal/air conditions.

In the Peabody experiments the combustion products rise about 4 feet from the bed before the sorbent is injected into the gas stream. Samples are then taken at four discrete locations along the duct leading to the stack. In addition to the single sorbent injection location, Peabody can inject the

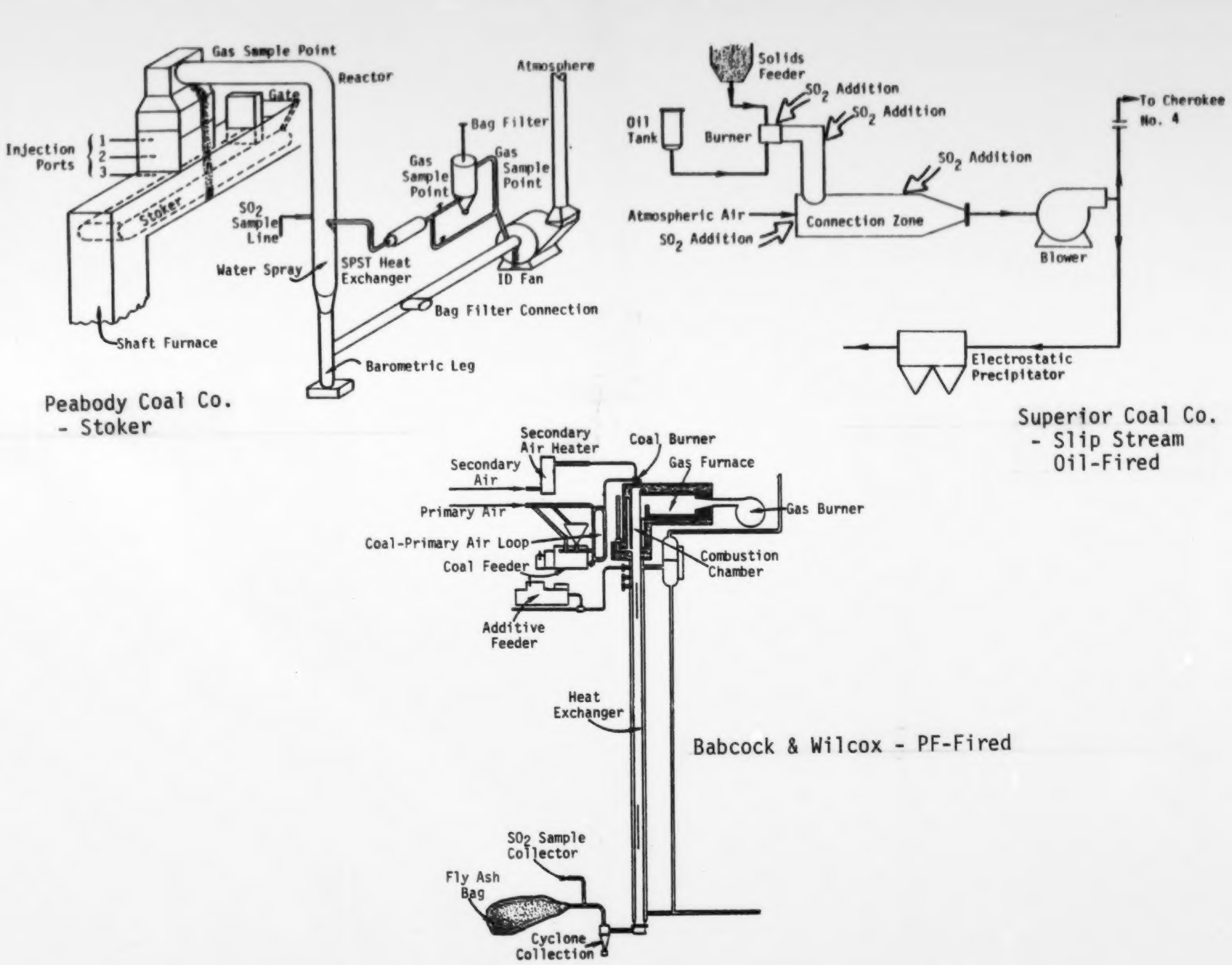
Gas Sample Point
Reactor
Atmosphere
Injection Ports
1
2
3
Gate
Bag Filter
Gas Sample Point
Gas Sample Point
SO_2 Sample Line
Stoker
Water Spray
SPST Heat Exchanger
ID Fan
Bag Filter Connection
Shaft Furnace
Barometric Leg
Solids Feeder
SO_2 Addition
SO_2 Addition
Oil Tank
Burner
To Cherokee No. 4
SO_2 Addition
Atmospheric Air
Connection Zone
SO_2 Addition
Blower
Electrostatic Precipitator
Secondary Air Heater
Coal Burner
Gas Furnace
Secondary Air
Primary Air
Gas Burner
Coal-Primary Air Loop
Coal Feeder
Combustion Chamber
Additive Feeder
Heat Exchanger
SO_2 Sample Collector
Fly Ash Bag
Cyclone Collection

Peabody Coal Co.
- Stoker

Superior Coal Co.
- Slip Stream
Oil-Fired

Babcock & Wilcox - PF-Fired

Figure 3-2. Pilot Plant Experimental Systems.

Table 3-1. Pilot-Scale Test Conditions

Characteristics	Peabody Coal Co.	Superior Oil	Babcock & Wilcox
Reactor			
• Size	Moving Grate Stoker	Oil-Fired Slip Stream	PF-Fired 100,000 Btu/hr
Fuel			
• Type	Coal	Oil	Coal
• Btu/lb	13,500	18,000	12,500
• Percent Sulfur	3.1	---	4.2
• Percent Ash	7.3	---	13
• Mine	Western Kentucky Seam II	---	(Colbert Steam Plant)
Sorbent			
• Injection Method	Nozzle	Nozzles	Nozzles
• Location	Variable	With SO_2 in Reaction Zone	Variable
• Gas Injection	2000 to 2450°F	400 to 2500°F	3000 to 1400°F
• Type	Limestone - Dolomite	Sodium Bicarbonate Soda Ash, Nahcolite	Limestone - Dolomite
• Particle Size	70 percent < 100 mesh	100 percent < 65 mesh	Pulverizer Grade

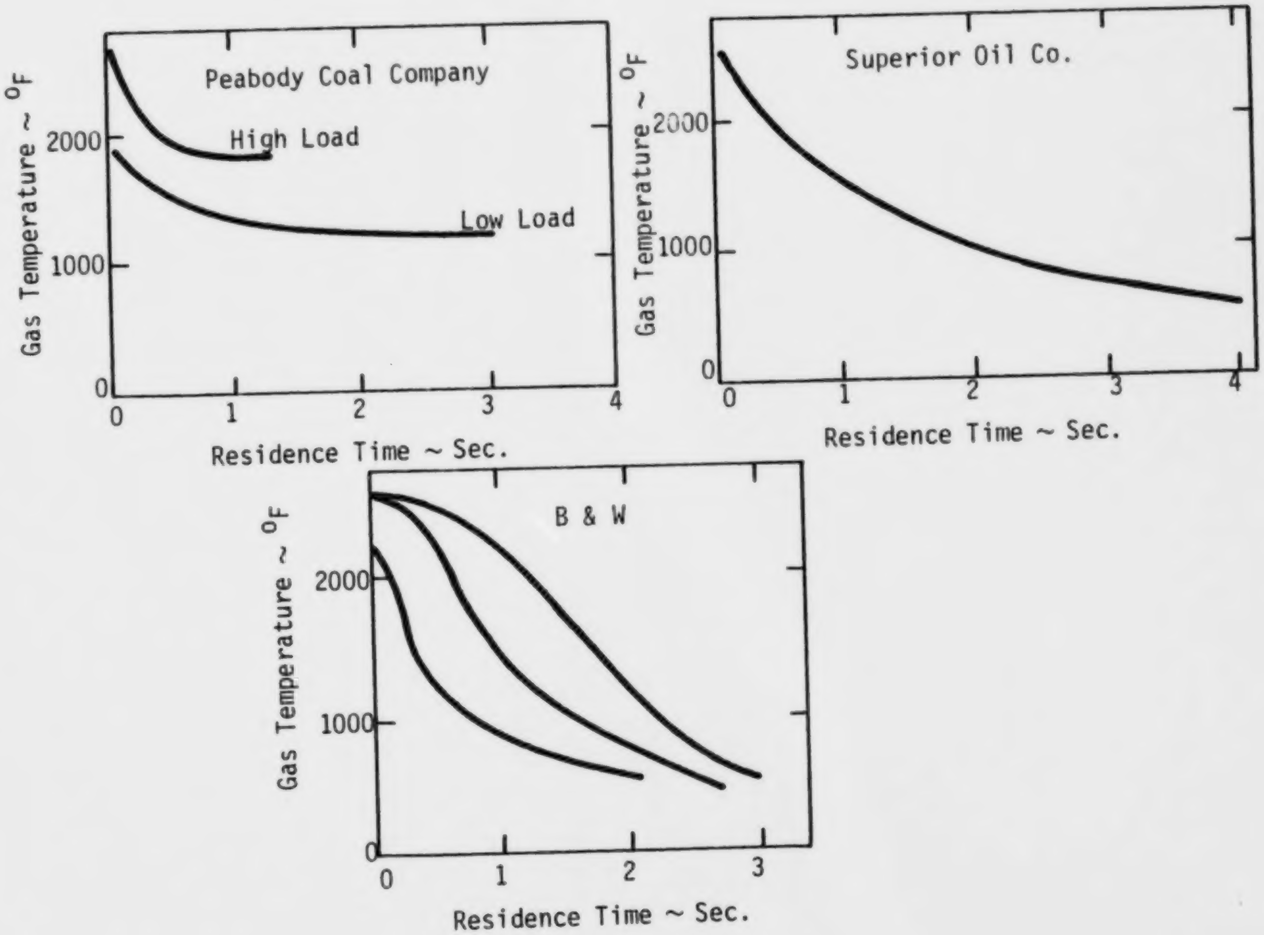

Figure 3-3. Comparison of T(t) Profiles for Three Experimental Studies.

sorbent with the coal so that it is subjected to the high combustion temperatures occurring at the bed surface. At stoichiometric proportions with limestone, 50 percent SO_2 reduction was achieved (depending on particle distribution) corresponding to 50 percent utilization of the sorbent. Maximum SO_2 removal was achieved at injection temperatures in the range of 2000-2450°F and corresponding residence times of 0.5 to 0.75 seconds. Referring again to Figure 3-3, note that this is the region of rapid temperature decrease suggesting that the calcination/sulfation process can be made rapid enough that the processes can be completed before significant overburning occurs. This, of course, will depend on such properties as the chemical characteristics of the sorbent and on particle characteristics. When the limestone was introduced with the coal, significant reduction in SO_2 removal occurred. There is, therefore, an optimum $T(t)$ and T_{max} which maximizes the reaction rates, particle chemistry, and morphology, allowing rapid diffusion of SO_2 into the particle pores and rapid CaO conversion to $CaSO_4$ before particle overburning occurs. Since overburning did occur with aragonite when injected with the coal (assuming that the distribution of the sorbent could be maintained uniform when introduced in this manner) it suggests that very high temperatures cannot be maintained for long periods of time since diffusion of sulfur into the particle may take longer than the particle heat-up time. The data also suggest that a maximum temperature (or range of temperature) may exist which optimizes the reaction rate and pore diffusion rates resulting in minimum residence time for complete conversion. This optimum will, of course, depend on the particle characteristics and will be different for each sorbent.

In the Superior Oil experiments, the sorbent was always injected in the high temperature region near the oil burner where the gas temperatures are about 2500°F, and SO_2 was added to the gas stream either at the same location or at other points downstream. The results presented in Figure 3-4 correspond to conditions where the sorbent (nahcolite) and the SO_2 are injected with the burner secondary air at injection temperatures approaching 2500°F. Regardless of the stochiometry, the SO_2 absorption is almost complete when the gas temperature has been reduced to approximately 1400°F, corresponding to a one-second residence time. Since only one $T(t)$ profile was possible, it is not known whether the low temperature (1400°F) is too low to support any signifi-

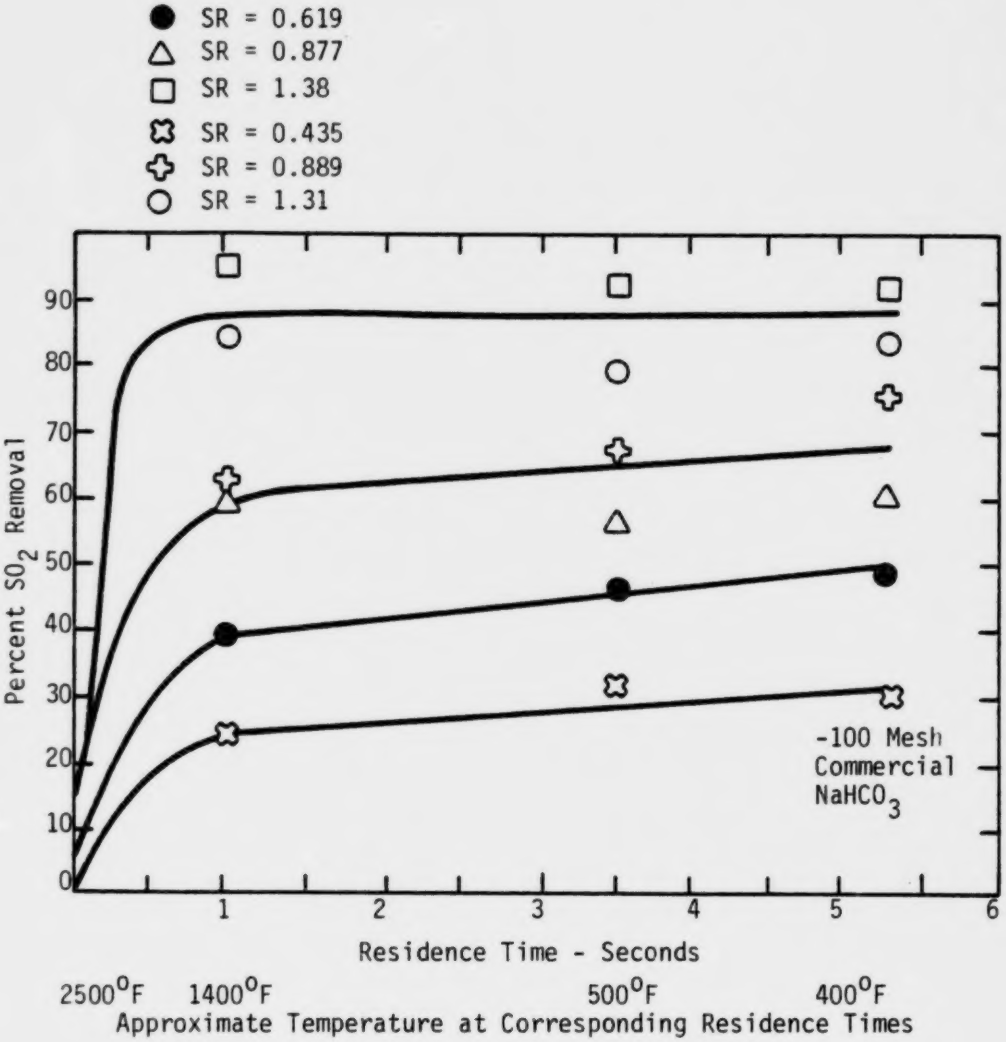

Figure 3-4. Effect of Residence Time and Temperature on SO_2 Removal at Various Stoichiometric Ratios - SO_2 Gas Injected into Burner Secondary Air.

cant reaction or whether sulfation is complete over the entire specific surface area within 1 second. However, these results are surprisingly similar to those obtained in the Peabody studies. The slight increase in residence time required for maximum SO_2 removal may be coincident with the more rapid decrease in temperature for those tests. About 65-70 percent SO_2 is removed with nahcolite at a stoichiometric ratio of one, which corresponds to a 65-70 percent sorbent utilization. This value is greater than that obtainable from the initial BET surface area. Particle size measurements made by Superior support their conclusion that communition occurs with this sorbent during particle heat-up, resulting in a significant increase in total specific surface area. In fact, their measurements show a 40/1 decrease in mean particle size.

Babcock and Wilcox's experimental set-up allowed for injection of the sorbent either with the coal in the circular burner or at five other locations. The injection temperatures can be varied in this manner (with a corresponding loss in residence time) from 3000°F to 1500°F. The T(t) profiles presented in Figure 3-3 show that, under these conditions, which are typical of current boiler designs, the temperature profile is considerably different from those discussed earlier. In comparing the temperature/time characteristics of the three systems, the high temperatures are maintained for longer periods in the B & W system than in the other reactors; additionally, the average temperature over the residence time shown in Figure 3-4 is higher, although the maximum temperature is similar. This represents an extremely low value in comparison with the other studies under these injection conditions, and clearly demonstrates the sensitivity of the overall process to the T(t) and residence time characteristics. For most of the sorbents studied, the maximum SO_2 removal was about 25 percent at stoichiometric conditions.

The major difference in environmental conditions between the three studies (in addition to sorbent type) is the T(t) profile; the maximum temperature was almost identical for each experiment. If all of the data are considered, then it would appear that there is a region of temperature/time history that will result in maximum SO_2 removal efficiencies. This is shown schematically in Figure 3-5. The lower limit ($\sim$1400°F) represents the temperature at which reaction rate is essentially zero. The lower of the two upper limit lines

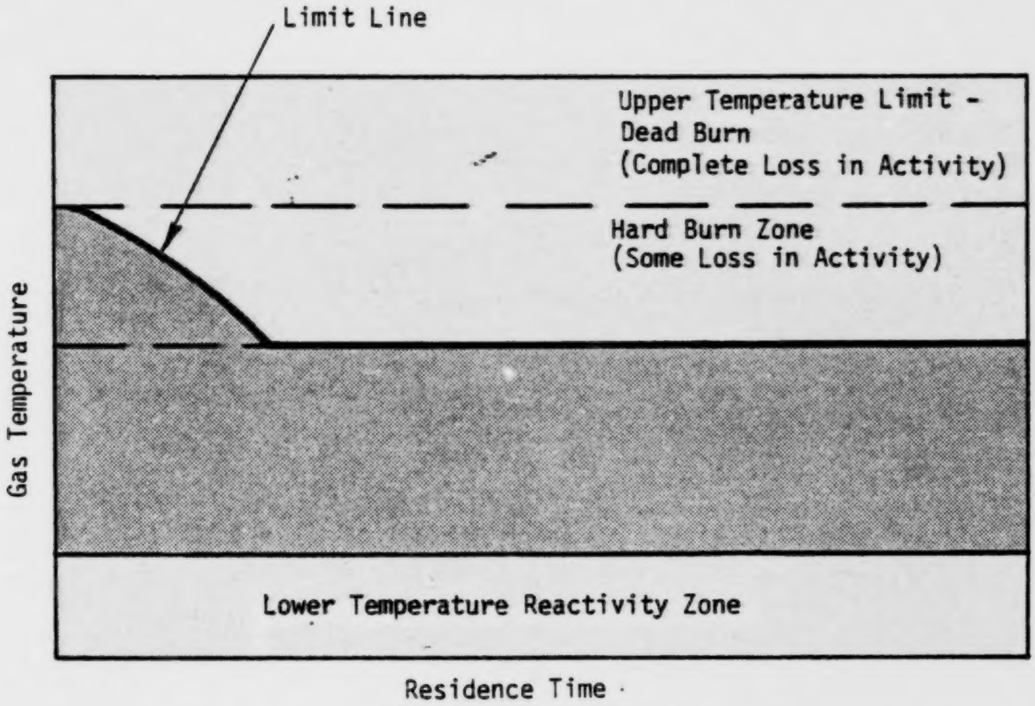
Limit Line
Upper Temperature Limit -
Dead Burn
(Complete Loss in Activity)
Hard Burn Zone
(Some Loss in Activity)
Gas Temperature
Lower Temperature Reactivity Zone
Residence Time

Figure 3-5. Schematic of T(t) Design Operating Region for Maximum SO_2 Removal.

corresponds to the temperature at which overburning is initiated (termed hardburning) and some loss in activity will result (∿2000°F). As the temperature is increased, the degree of hardburning increases with continued loss in activity until deadburning occurs (∿3000°F). When deadburning occurs the surface is essentially deactivated. The small area in the overburning region which is included in the acceptable design region represents the time that the sorbent can withstand the high temperature before significant loss in activity occurs. At the lower temperatures within the shaded area no overburning will occur. To minimize the residence time required for complete conversion, the T(t) profile should correspond to the limit line shown in Figure 3-5, or as close as practically possible. The available data are insufficient for an exact definition of this curve.

3.1.2 Particle Size Effects

The effect of temperature on percent calcination for various particle size cuts was investigated by Peabody, and the results of this investigation are presented in Figure 3-6. The data suggest that, as the temperature is increased above 2000°F, the effect of particle size becomes very small. Consequently, for injection of sorbent into the high temperature zone of the boiler, particle size will not be important for calcination but would become increasingly important when injected near the convective section.

The results from both B & W and Peabody tend to support results obtained in more fundamental studies. Babcock and Wilcox show that for particle sizes in the 40 micron range, particle size had almost no effect on SO_2 removal. Typical results from Peabody are shown in Figure 3-7 and reveal that until the particle sizes were in the 80 micron (140-200 mesh size) range, (corresponding to complete utilization of the sorbent specific surface) particle size had a large effect on SO_2 removal. The nahcolite used in the Superior Oil study underwent communition, therefore, no data are available on particle size effects. The B & W and Peabody results definitely show that small particle sizes are desirable, but there is a lower limit beyond which decreases in diameter have no further beneficial effect on SO_2 removal.

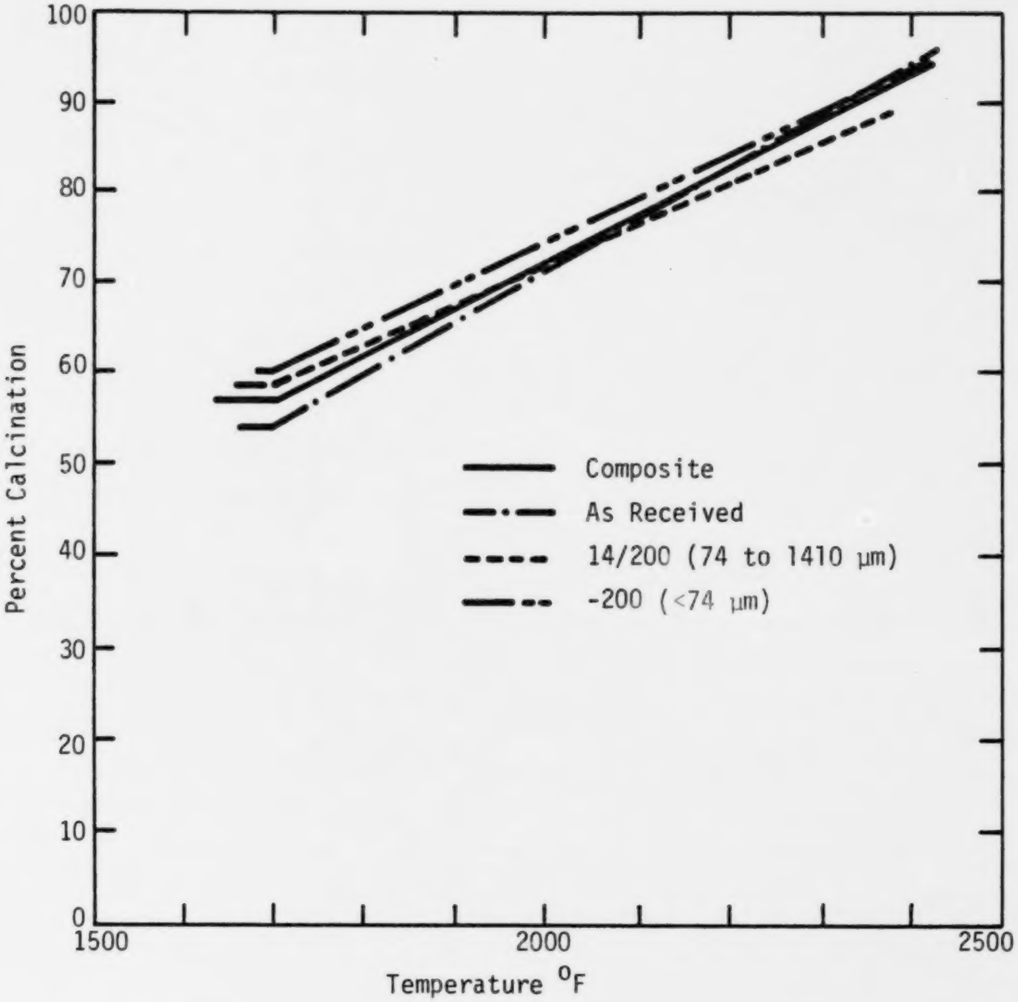

Figure 3-6. Effect of Temperature on Calcination (Ref. 1).

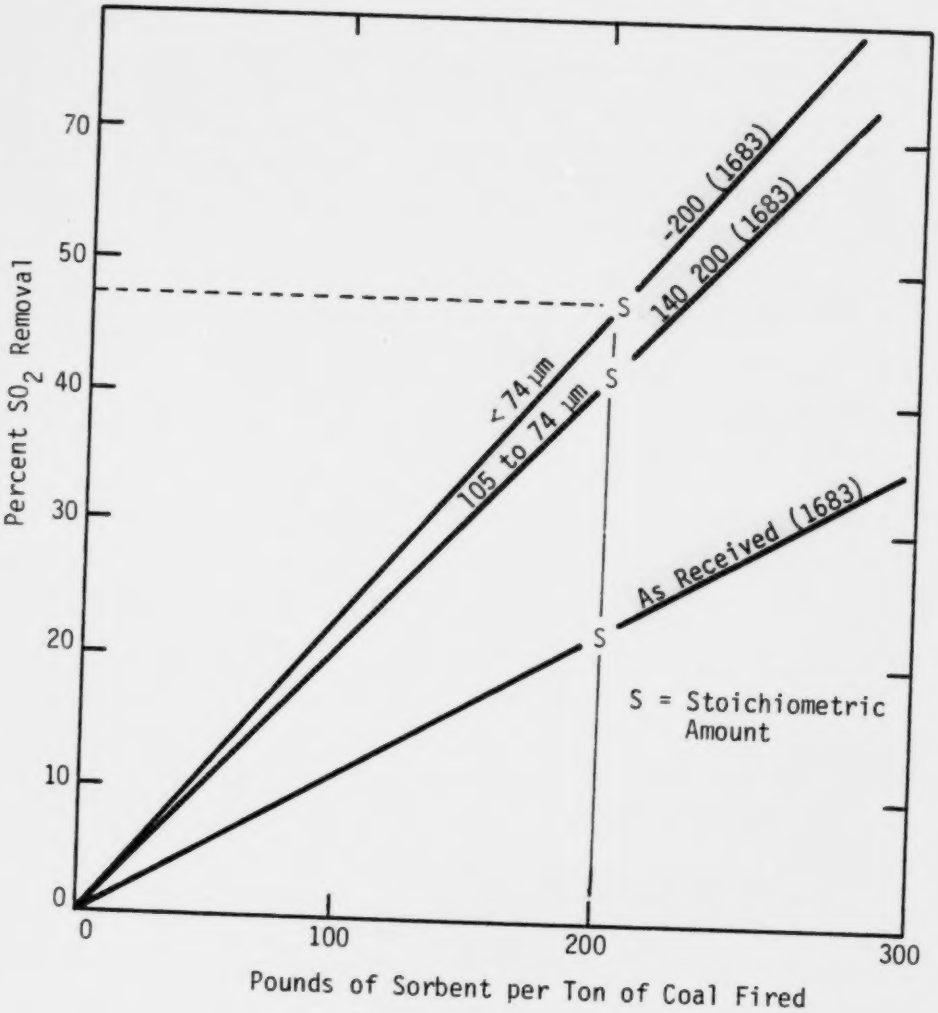

Figure 3-7. Effect of Additive Feed Rate (Ref. 1).

3.1.3 Sorbent Types

All three studies showed the marked effect of sorbent type on the degree of SO_2 removal. For example, at injection temperatures above 2000°F, Peabody found that aragonite was the most effective, removing up to 60 percent of the SO_2, followed by dolomite (20-60 percent), and calcite (20-40 percent). The variations in capture efficiency for these stones appear to be primarily the results of residence time changes and minor variations in Ca/S ratio. Superior Oil Company investigated commercial soda ash and sodium bicarbonate in addition to predecomposed commerical sodium bicarbonate and nahcolite. These results, presented in Figure 3-8, show that commercial soda ash results in extremely low conversion efficiency while predecomposed sodium bicarbonate gives substantially higher results. It appears that only minor variations in chemical properties exist between these two stones so that the differences in SO_x removal efficiencies are probably due more to particle physical characteristics rather than chemical effects. Specific measurements were not made of the particle BET or pore characteristics. The sodium bicarbonate and nahcolite resulted in very high conversion efficiencies which is attributed to increased surface area resulting from communition during rapid heat-up. Superior Oil suggests that the rapid heat-up causes excessive internal stresses in the particle due to H_2O vapor and CO_2 which cannot quickly escape. B & W (Figure 3-9) found that, even under the temperature/time profile wherein significant overburning occurs for limestone, marl achieved about 45 percent SO_2 removal at Ca/S ratios of one. These results strongly suggest that the critical T(t) characteristics will be dependent on the sorbent chemical and physical characteristics.

3.1.4 Oxygen Concentration

The majority of investigators have found that increasing the O_2 concentration results in an increase in SO_2 absortion. For example, the results of B & W, Figure 3-10, show a marked increase in SO_2 removal as the O_2 level in the flue gas varied from about 0.5 to 2 percent. Further increases in O_2 concentration had little effect on SO_2 removal. There is some question regarding these data, however, since the residence time/temperature profile also varies as the excess air is changed so that the results should be treated with

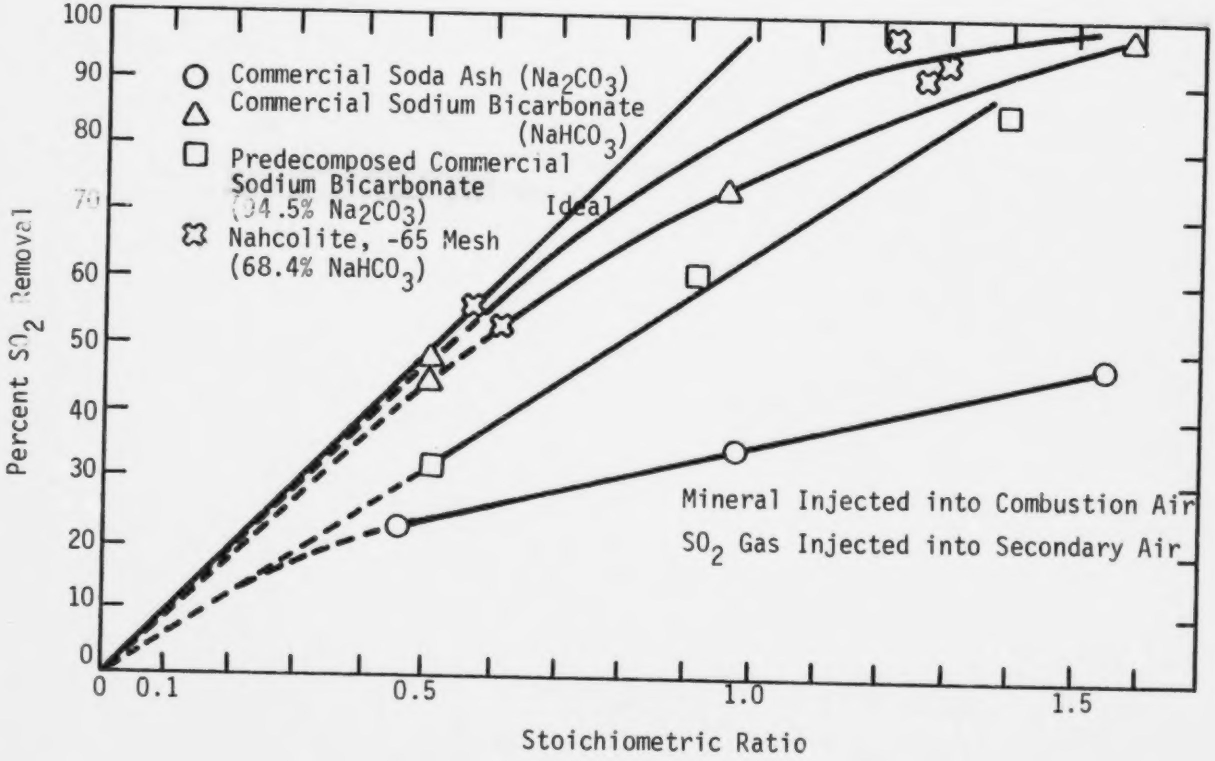

Figure 3-8. Effect of Injecting Various Sodium Minerals on Percent SO_2 Removal (Ref. 2).

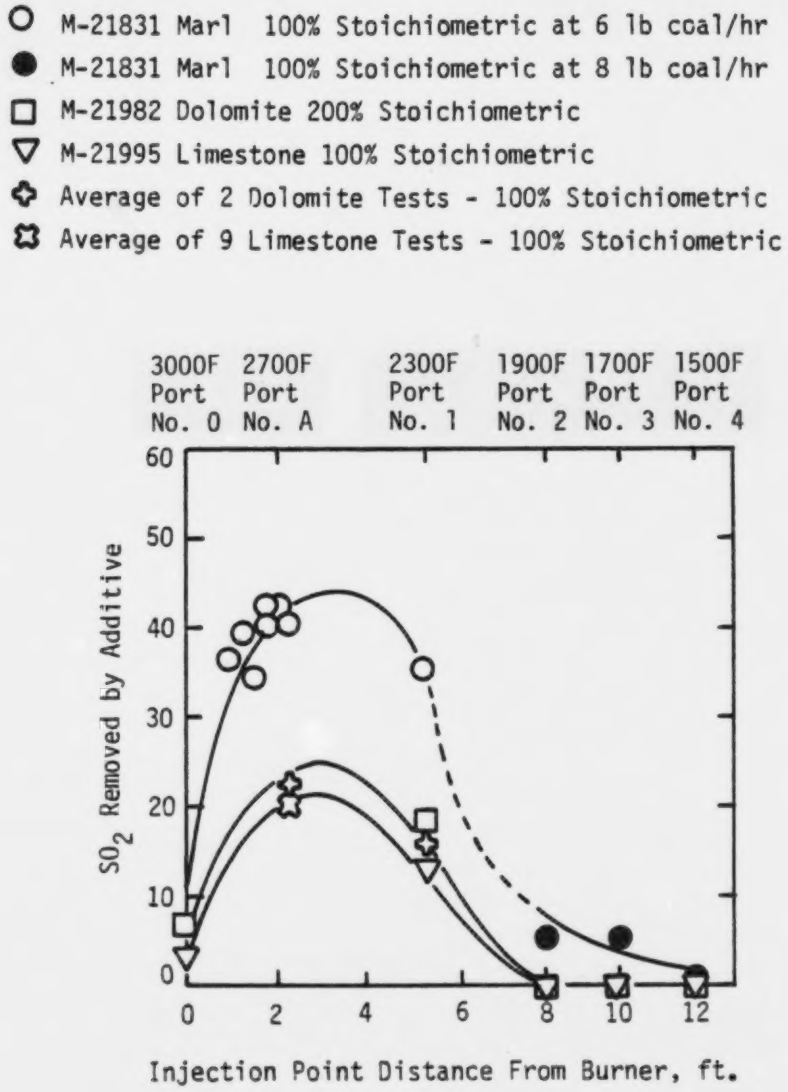

Figure 3-9. Effect of Injection Point on SO_2 Removal (Ref. 3).

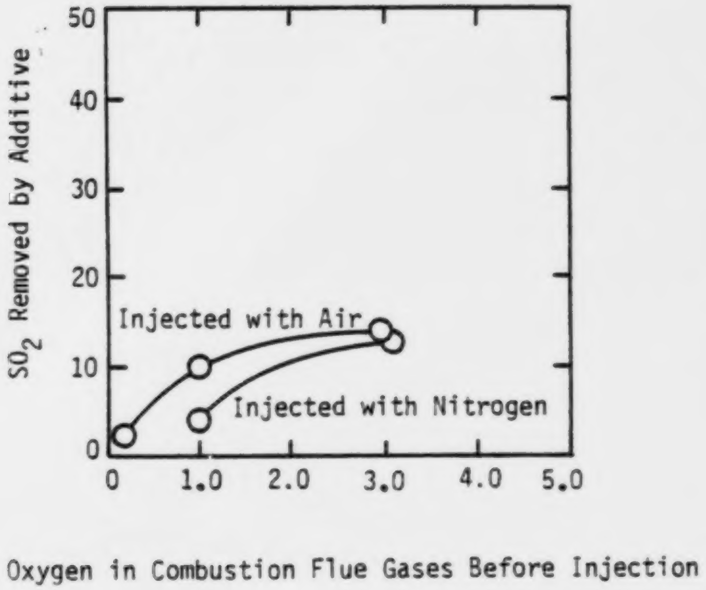

Figure 3-10. Effect of Excess Combustion Air on SO_2 Removal (Ref. 3).

caution until more definitive experiments can be accomplished.

3.2 Early Plant-Scale Studies

The pilot-scale results suggest that sulfur removal efficiency is primarily dependent upon sorbent distribution, residence time, and the T(t) history during the calcination/sulfation process once the sorbent has been chosen and the particle size specified. T(t) history and residence time are characteristics of the boiler and will be different for differing boiler designs (e.g., firing configuration and boiler size) and boiler operating conditions (e.g., load and excess air). Unfortunately, sufficient data are not available to determine a priori which boiler T(t) and residence time characteristics will result in high sulfur removal. A summary of SO_2 removal levels as a function of Ca/S stoichiometry for 12 different plant-scale test boilers is shown in Figure 3-11. Most of these data show sorbent utilization efficiencies of about 20 percent, although some data are as low as 5 percent or as high as 40 percent. In particular, the experimental conditions under which the widest spread in removal efficiencies are reported (Numbers 1, 2 and 12) were conducted in boilers having considerably different T(t) and residence time characteristics. Plant schematics for the TVA, Detroit Edison Company and Wisconsin Electric Power Company boilers are provided in Figure 3-12. The TVA boiler is wall-fired, the Detroit Edison boiler is tangentially-fired, and the Wisconsin Electric Power unit is vertical-fired (arch-fired); representative flow patterns for all three units are depicted in Figure 3-13.

For the wall-fired unit, temperatures in the burner zone are typically greater than 3000°F and, depending on load, combustion product temperatures drop to approximately 1400°F in 1 to 1.5 seconds. Typical T(t) characteristics for the TVA unit are shown in Figure 3-14. Because of the burner design, injecting the sorbent with the coal results in considerable overburning and low SO_2 removal efficiencies. To avoid this condition, the limestone was injected at various locations above the burner when the gas temperatures had dropped to about 2000°F. Inspection of Figure 3-14 shows that, at these injection conditions, the maximum residence time is on the order of, or less than, 0.5 seconds (i.e., before the gas temperatures drop below 1400°F). It is not surprising, LEGEND

Key	Investigator	Fuel	Sorbent	Flue Gas Temp. °F Average at Injection Point
1	Wisconsin Electric Co.	Coal	Limestone	3000
2	Detroit Edison Co.	Coal	Ground Dolomite	2800
3	Steag (W. Germany)	Coal	Ground Limestone	2400
4	Kansas Power & Light (C-E,Inc)	Coal	Limestone	2100
5	Union Electric Co (C-E,Inc)	Coal	Dolomite	2100
6	Energopomiar (Poland)	Coal & Gas	Dolomite	2100
7	Central Research Institute Of Electric Power (Japan)	Oil	Limestone	2100
8	Republic Coal & Coke	Coal	Dolomite	2300
9	Republic Coal & Coke	Coal	Dolomite	2800
10	General Motors	Coal	Dolomite	1900
11	General Motors	Coal	Limestone	1900
12	TVA	Coal	Limestone	2000

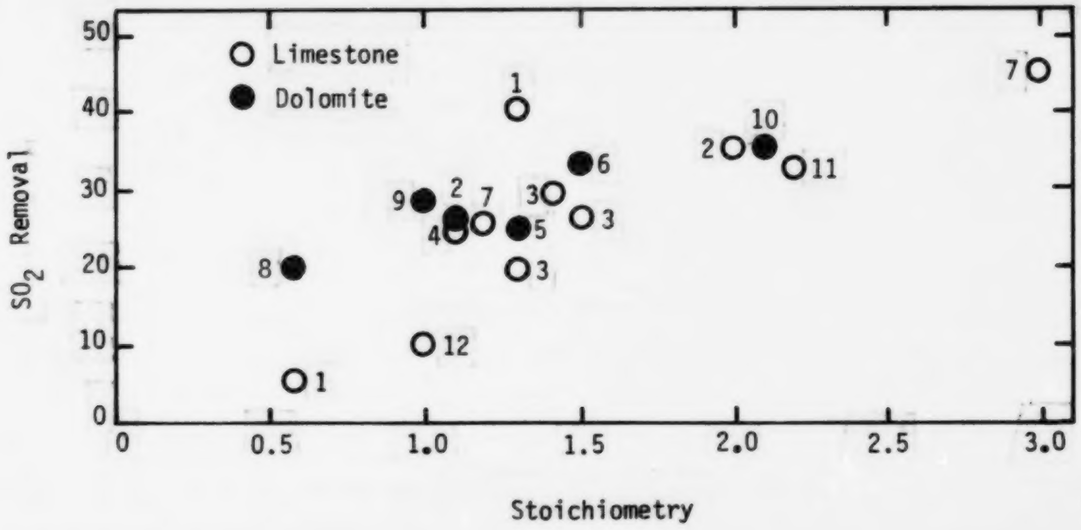

Figure 3-11. SO_2 Removal vs. Stoichiometry for Reported Plant-Scale Tests of Dry Limestone Injection Process (Ref. 4).

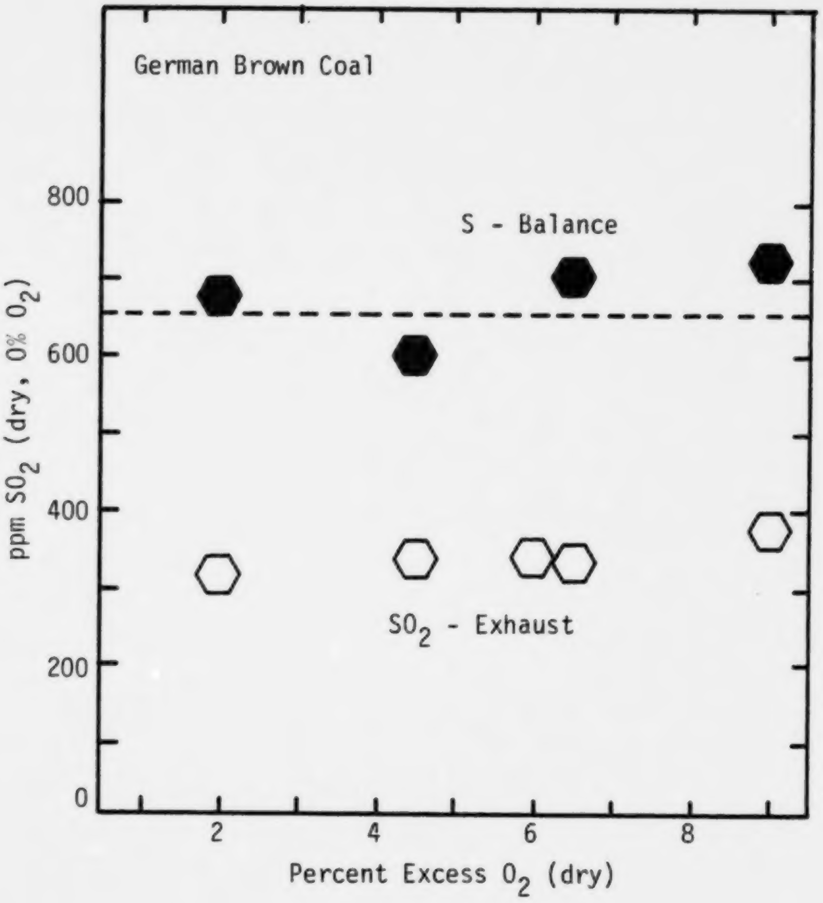

Figure 3-12. Sulfur Balance--Pulverized Coal.

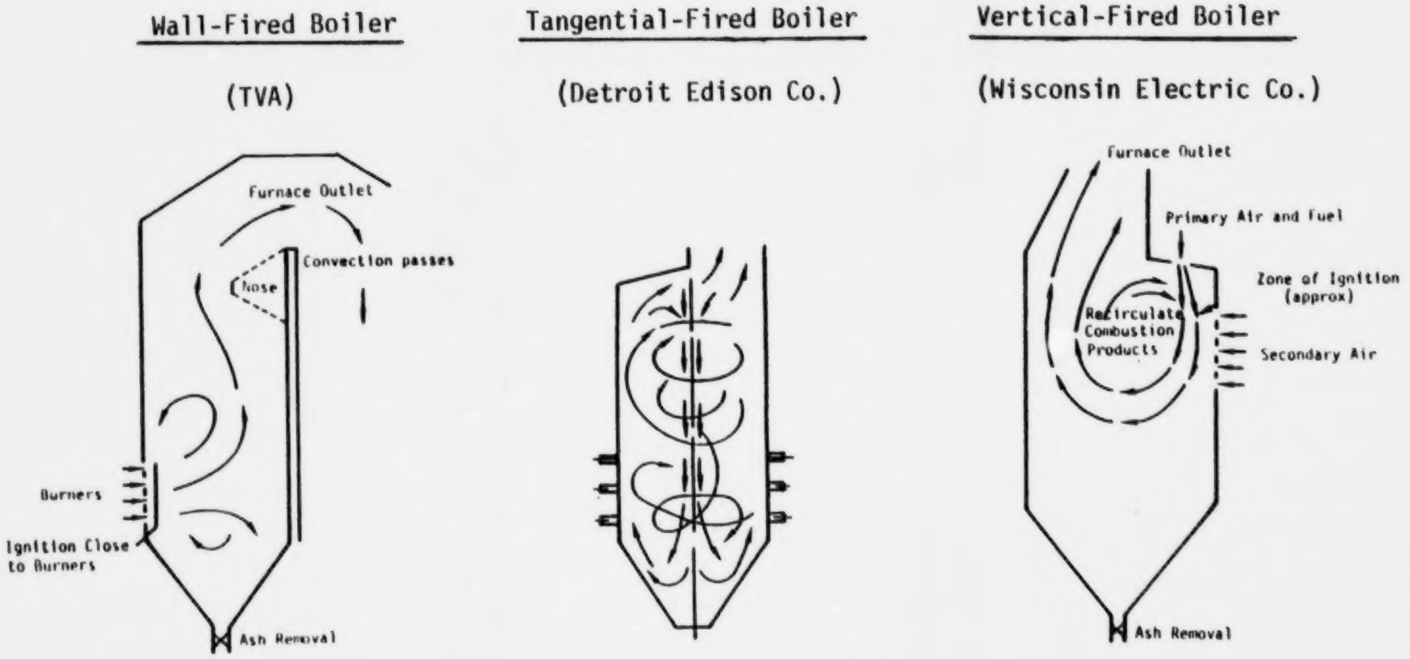

Wall-Fired Boiler

(TVA)

Tangential-Fired Boiler

(Detroit Edison Co.)

Vertical-Fired Boiler

(Wisconsin Electric Co.)

Furnace Outlet
Convection passes
Nose
Burners
Ignition Close to Burners
Ash Removal
Furnace Outlet
Primary Air and Fuel
Zone of Ignition (approx)
Recirculate Combustion Products
Secondary Air
Ash Removal

Figure 3-13. Field Scale Studies - General Combustion Chamber Flow Pattern.

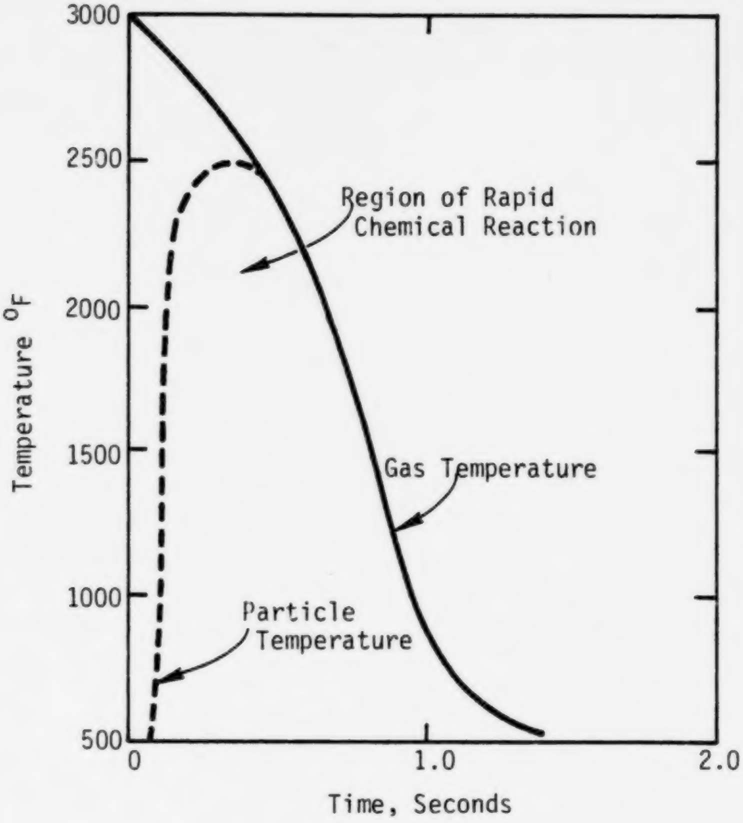

Figure 3-14. Time - Gas Temperature Profile and Limestone Residence Time for TVA unit.

therefore, that the sorbent removal efficiencies were only about 10 percent under these conditions. The boiler test conditions and specifications are shown in Table 3-2.

The tangentially-fired boiler provides a longer flame than the circular wall-fired high turbulence burner; therefore, the tangentially-fired burner tends to spread the combustion process by more gradually mixing the air with the coal. This should provide a more favorable initial temperature/time history for the sorbent. T(t) characteristics for this furnace are not available, so this is somewhat speculative. In these tests the sorbent was injected at one of two locations: 1) with the coal, or 2) in the upper row of burners only. When the dolomite was injected in the top row of burners at a 15 degree upward tilt and the gas temperature was about 2200°F, a 30 percent SO_2 removal efficiency was noted. Only slightly lower efficiencies occurred when the sorbent was injected with the coal. These results appear to be consistent with the more favorable T(t) characteristics and residence time provided by the tangentially-fired design over that of the front wall-fired turbulent burner/boiler configuration.

The most encouraging results were found with the vertical-fired unit wherein the burner fires overall lean and downward and additional combustion air is added from the side wall at discrete locations. In this way, the air is slowly mixed with the coal as it travels downward in the furnace. Eventually, the flame turns upward completing combustion as it rises into the top section of the furnace (Figure 3-13). This particular configuration should provide very favorable T(t), residence time, and T_{max} characteristics to maximize SO_2 removal. The results from these tests, also summarized in Table 3-2, show that very high SO_2 removal efficiencies, 40-50 percent, were obtained.

3.3 Recent Investigations

Three recent investigations at pilot and plant-scale are discussed in this section. Rheinish-Westfalische Electrizitatswerke (RWE), a German utility company, has conducted both small pilot-scale and plant-scale development studies of SO_2 capture by calcium compounds. Steinmüller has conducted tests at the IFRF in Holland using an exact-scaled version of their Staged Mixing Burner

Table 3-2. Field-Scale Results

Boiler Char, Test Conditions & Measurements	TVA Shawnee Unit No. 10	Detroit Edison Co. Pt. Clair	Wisconsin Elec. Power Co. Pt. Washington Units Nos. 1 & 2
Boiler			
• Manufacturer	B & W	C.E.	C.E.
• Firing Config.	Front Wall-Fired	Tangential-Fired	Vertical Fired
• Burners (No.)	16	16	20
• MW_C	150	170	85
• OFA Ports		No	No
Fuel			
• Heating Value Btu/hr	12,760	12,000	13,000
• Percent Sulfur	2.6	3.3	2.8
• Particle Size	70 percent 200	80 percent 200	65 percent 200
• Percent Ash	11	10	8
• Mine	Old Ben No. 24	Ohio Strip	West Virginia
Sorbent			
• Injection Method	Separate Nozzles	Through Burners	Through Burners
• Location	At Furnace Outlet	Top Burner Row	All
• Preparation	Separate from Coal	Separate from Coal	With Coal
• Injection Gas Temperature	2000°F	2200°F	As Coal
• Type	Limestone	Dolomite	Limestone
• Particle Size	Pulverizer Grade	Pulverizer Grade	Pulverizer Grade
Measurements			
• Percent SO_2 Removal	10	30	40 - 50
• Percent Stoichiometry	100	100	130

currently installed at the Weiher boiler. In the United States, recent studies have been conducted by EER under this contract (EPA Contract 68-02-2667) to demonstrate feasibility of SO_x control via sorbent injection in a pilot-scale (10×10^6 Btu/hr) version of the EPA Distributed Mixing Burner.

3.3.1 Rheinish-Westfalische Electrizitatswerke (RWE)

Dr. Hein of RWE has been studying SO_2 capture by calcium compounds for several years. The initial efforts concerned the inherent capture of SO_2 by the Ca contained within the coal structure. Using a small-scale, down-fired research facility (0.7 MW), data were obtained of exhaust SO_2 concentrations while burning a wide range of differing lignite coals. The exhaust SO_2 concentrations shown in Figure 3-15 were found to correlate quite well when plotted against Ca/S ratio obtained from analysis of the coals. While the conclusion is clear from this plot (i.e., higher Ca/S ratio fuels produce lower levels of SO_2 emissions), it is not possible to determine the independent effect of sulfur content on achieving SO_2 capture. The results are, nevertheless, encouraging in that they suggest the importance of calcium compounds in reducing SO_2.

These studies were then extended to a 60 MW_e corner-fired boiler at the Fortuna II Power Plant in West Germany. A number of differing lignite coals were burned in Niederaussem in an identical companion boiler to obtain baseline SO_2 emission levels. The results plotted in Figure 3-16 (no additive) show trends similar to those noted in the earlier pilot-plant studies. Four calcium compounds were then separately tested; 1) $Ca(OH)_2$, 2) $CaCO_3$, 3) Dolomite, and 4) CaO. These sorbents were pre-ground to 90 percent $<$90 micrometers and mixed with the brown coal before entering the pulverizer; the mixture was then fed directly to the burner fuel nozzles as shown in Figure 3-17. Note that for this brown coal, the furnace exit temperature is (as designed) 950-1000°C.

In the Fortuna II and Niederaussem boilers, the burners are positioned vertically with alternating air and coal slots (three levels of coal nozzles). These burners have no independent controls to change the fuel/air mixing characteristics. The results, shown in Figure 3-18, revealed that calcium hydroxide produced the highest sorbent utilization followed by dolomite, calicum carbonate

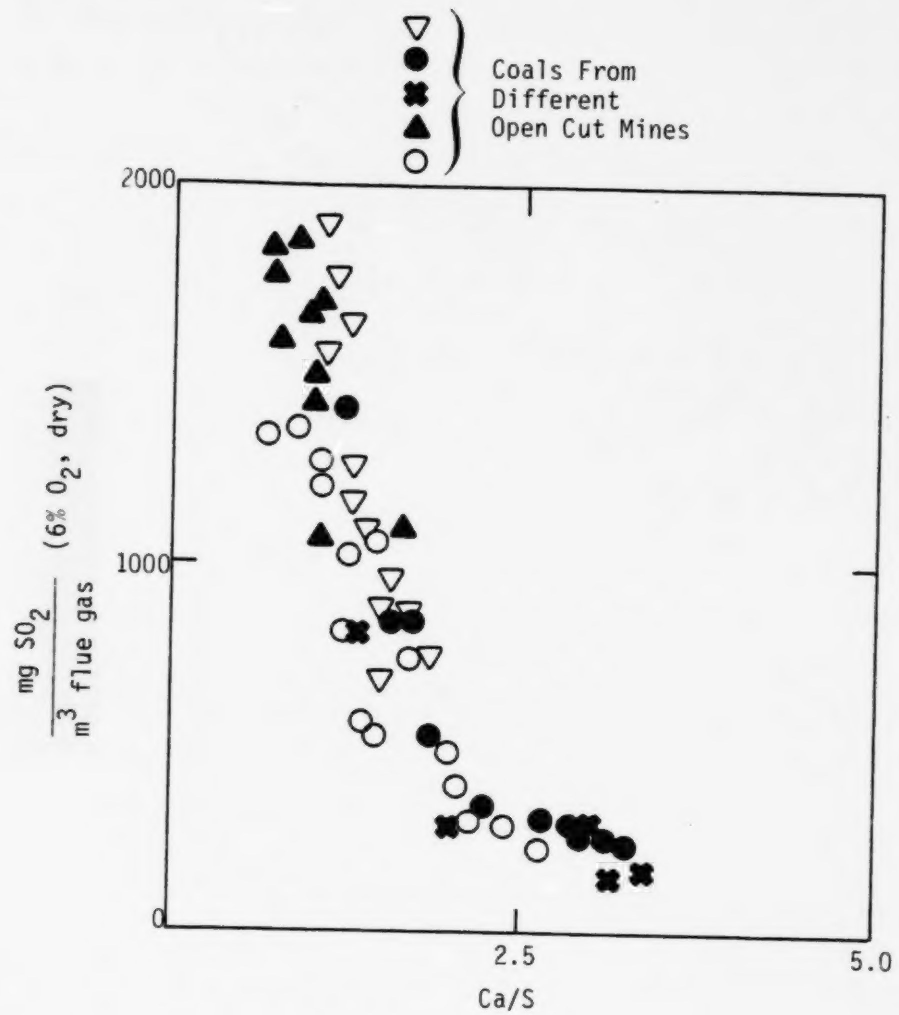

Figure 3-15. SO_2 Emission and Molar Ca/S Ratio (Ref. 5).

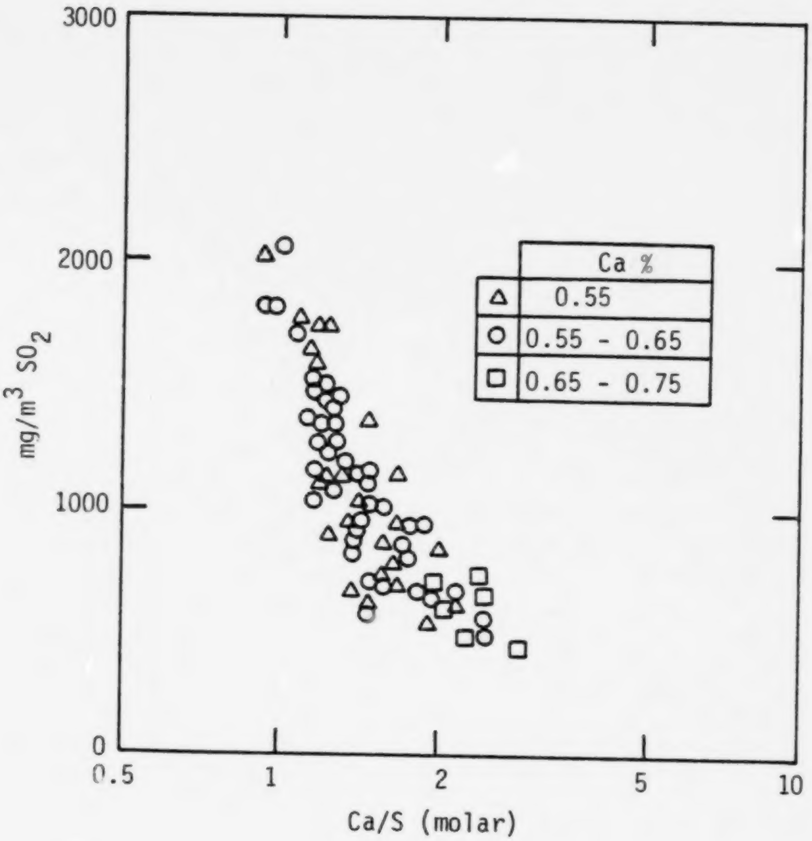

Figure 3-16. SO$_2$ Emission and Ca/S Ratio of the Fuel (Monthly Average Values for Boiler Fuels) (Ref. 5).

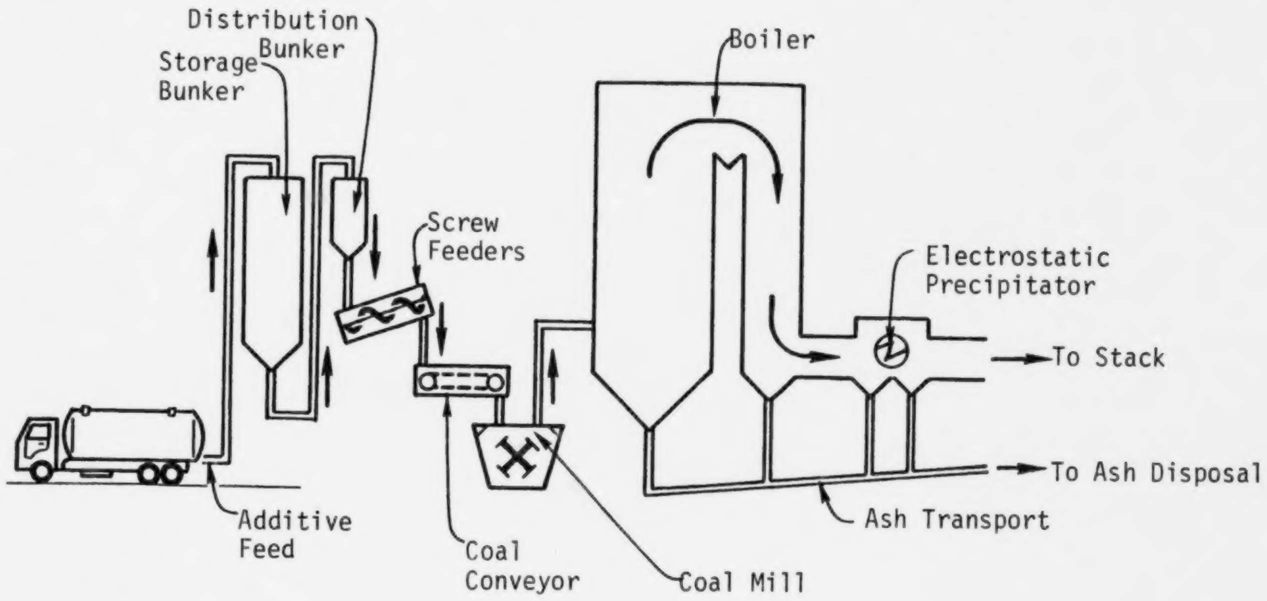
Distribution
Bunker
Storage
Bunker
Screw
Feeders
Boiler
Electrostatic
Precipitator
To Stack
To Ash Disposal
Ash Transport
Additive
Feed
Coal
Conveyor
Coal Mill

Figure 3-17. Installation of the Dry Additive System (Schematic) at the Fortuna II Power Plant - West Germany.

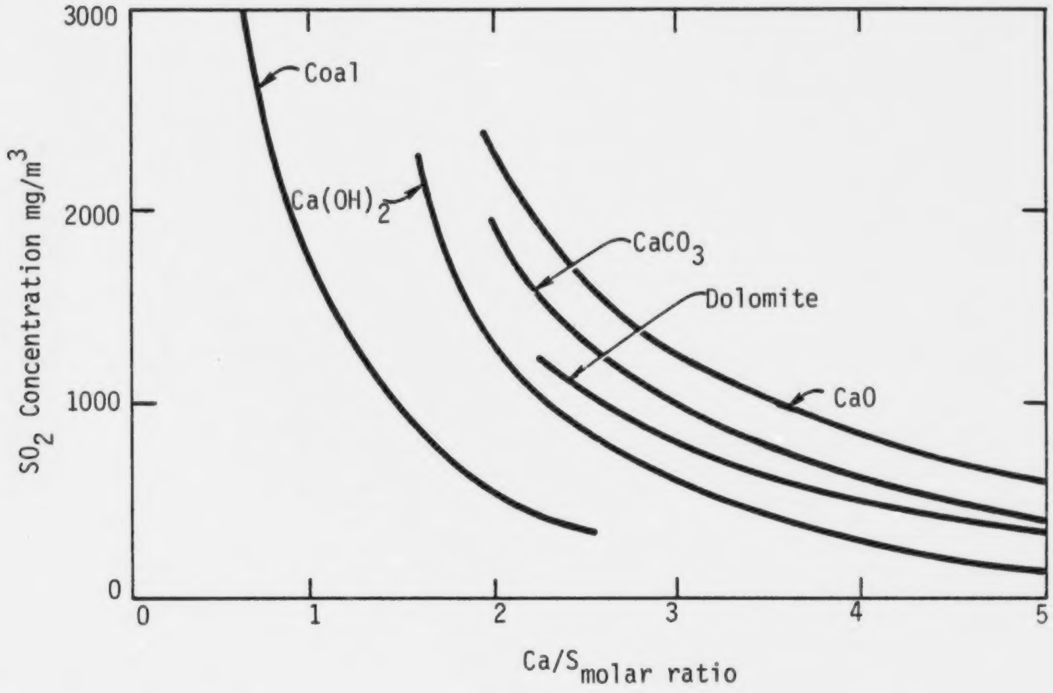

Figure 3-18. SO$_2$ Capture with Several Additives (Ref. 5).

and then by the calcium oxide. These results are explained by concluding that the CaO particle formed by having undergone decomposition in the combustion zone is more active than pure CaO. This is supported by results showing that after decomposition, the CaO particle formed from $Ca(OH)_2$ has the highest specific surface area followed by that from dolomite and then $CaCO_3$. The pure CaO has the lowest specific surface area. The results of Figure 3-19 clearly show that, for the RWE coal, the added Ca is less effective for SO_2 capture than the inherent Ca in the coal. At this time, it is not known what the controlling mechanism is. It may be controlled by 1) the intimacy of the inherent Ca to the evolving SO_2 within the particle, 2) the higher activity of the inherent calcium compounds as compared to the additive, or 3) a sulfur concentration effect not delineated in the data. Of further interest from Figure 3-19 are the levels of SO_2 in the flue gas, suggesting that the various coals have widely differing sulfur contents; however, not having specific information limits the ability to assess the impact of sulfur in the coal on the efficiency of the SO_2 capture process.

The Fortuna II Power Plant boiler has been under operation for about two and one-half years, burning a 0.3 percent S, 60 percent moisture brown coal with inherent Ca + Mg/S ratio of about 2.0. The latest information is that, using calcium hydroxide with particle size similar to typical PC firing as an additive, SO_2 reductions of 50 to 75 percent are being achieved at Ca/S of 2.5 to 5.0, respectively. It is possible that the high capture rates could be attributed to low furnace gas temperatures in the RWE furnace. Under these operating conditions, no slagging/fouling problems or changes in steam temperature have occurred.

Based on these successful results, a modern tower boiler will be retrofit with $Ca(OH)_2$ injection at the RWE Power Plant in Niederaussem. This will be completed in late 1982 or early 1983. The burner design for this unit is more sophisticated than that at Fortuna; in order to improve the early mixing characteristics of the coal/air, a series of air tubes in the form of a plus (+) has been placed in each coal nozzle and is designated as cooling for the coal duct. The trials are expected to take one to two years, and will concentrate on investigations of slagging and fouling, impacts on ESP operation, hopper ash

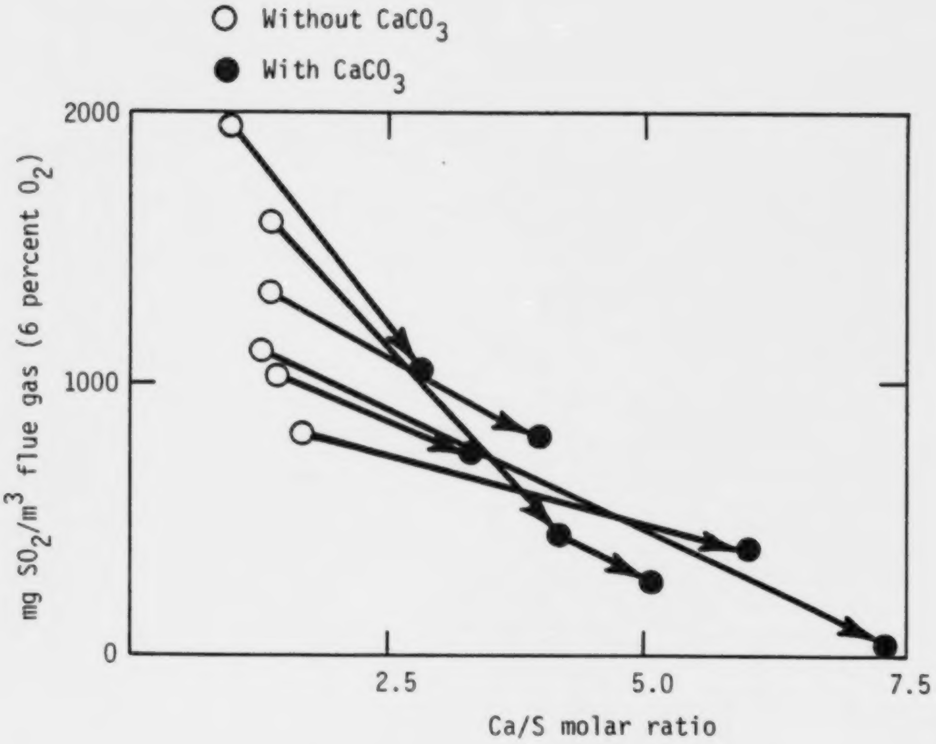

Figure 3-19. Emission Reduction with $CaCO_3$ (Ref. 5).

disposal, and other technical/operational problems, as well as $Ca(OH)_2$ pre-ground rather than pulverized at the plant.

3.3.2 Steinmüller

A schematic of the experimental set-up employed for the Steinmüller Staged Mixing Burner tests in the IFRF furnace is shown in Figure 3-20. Provision was made for the injection of various calcium based sorbents in three different positions, as indicated in the figure.

- Position 1: Sorbent mixed with coal in the coal transportation line;
- Position 2: Sorbent transported with a small quantity of compressed air and equally distributed in the four tertiary air ports;
- Position 3: The compressed air/limestone mixture could also be injected in four holes specially drilled in the ceramic quarl of the burner and localized somewhat further from the flame axis than the tertiary air ports existing in the original burner design. This system allowed the injection of additive directly in the external recirculation zone (labeled as E.R.Z.) of the flame.

Figure 3-21 is a schematic of the IFRF furnace which was used for this work. It is refractory-lined and partially cooled by the addition of water-cooled loops. A typical furnace temperature field is included in the figure as measured with the following nominal inputs:

- 240 kg/h Ruhr coal fired with 25 percent excess air and giving a total thermal input of 2.3 MW;
- 46 percent of the combustion air is injected through the tertiary air ports leading to a fuel-rich zone in the first part of the flame (equivalence ratio of 1.49).

This temperature field shows clearly that by injecting the sorbents in positions 2 and 3 it is possible to keep a large fraction of the lime particles away from the high temperature primary zone of the flame.

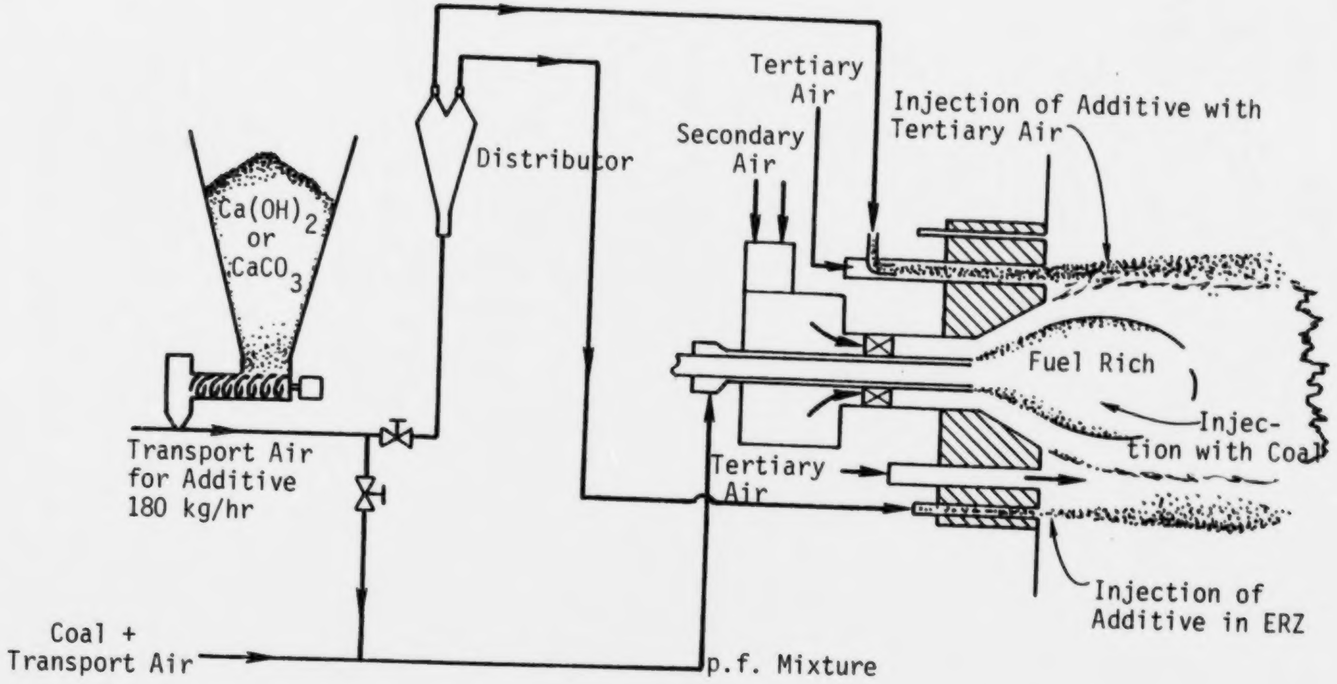
Ca(OH)$_2$
or
CaCO$_3$
Transport Air
for Additive
180 kg/hr
Distributor
Coal +
Transport Air
p.f. Mixture
Secondary
Air
Tertiary
Air
Tertiary
Air
Injection of Additive with
Tertiary Air
Fuel Rich
Injec-
tion with Coal
Injection of
Additive in ERZ

Figure 3-20. Schematic of Various Possibilities of Injection of the Additive for the Steinmuller Staged Mixing Burner.

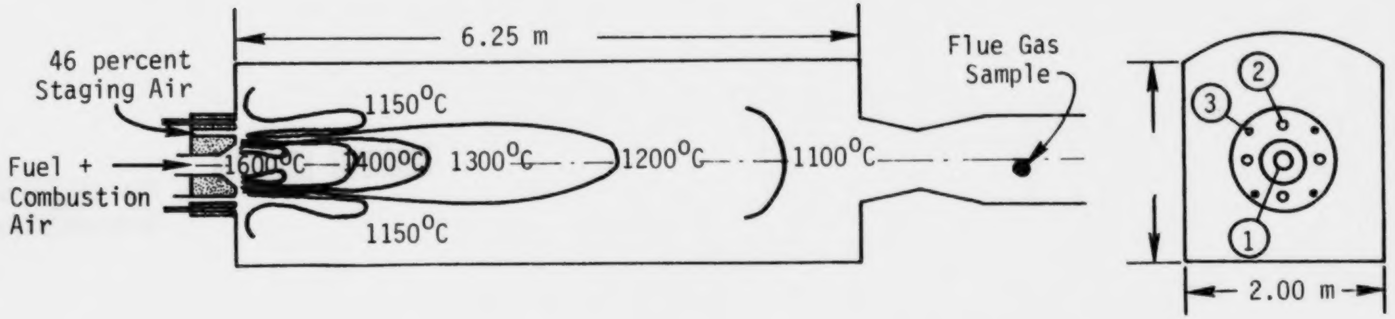

6.25 m
46 percent Staging Air
Fuel + Combustion Air
1150°C
1600°C
1400°C
1300°C
1200°C
1100°C
1150°C
Flue Gas Sample
2
3
1
2.00 m

1. Injection with fuel.
2. Injection with staging (tertiary) air.
3. Injection at periphery of flame.

Figure 3-21. Schematic of IFRF Furnace With Staged Mixing Burner and Typical Temperature Levels Measured With a 2.3 MW Coal Flame.

Figure 3-22 summarizes some typical results obtained with sorbent injection in position 3. The upper part of the figure depicts SO_2 removal rates as a function of the amount of $Ca(OH)_2$ injected in flames of various fuels; results from a fluidized bed limestone injection study are included for comparison. This graph shows that the desulfurization rates are very different from one fuel to another. In gas flames doped with SO_2 or H_2S very poor results are observed, while Saar and Ruhr coals, both having sulfur contents around 1.0 percent, the desulfurization is more effective (50 percent SO_2 removal, 25 percent sorbent utilization). This shows a very clear effect of the fuel type on the efficiency of sorbent utilization.

The lower half of Figure 3-22 shows sorbent utilization plotted against the SO_2 concentration for various fuels and additives. At low SO_2 concentration, the efficiency of utilization becomes a strong function of SO_2 concentration, showing that the process becomes diffusion limited. It can also be seen that changing the additive from $CaCO_3$ to $Ca(OH)_2$ and further to an activated $Ca(OH)_2$ increases the maximum sorbent utilization from 23 percent up to 50 percent.

Figure 3-23 shows how the principle of injection of the sorbent can affect the rate of desulfurization, especially in the case of combustion air staging. For the three different coals fired, it can be seen that the SO_2 removal rates are poor when the sorbent is mixed with the coal (Position 1), better when it is injected in the tertiary air ports (Position 2) and still better when it is injected in Position 3. With the Saar coal, it was also observed that the tertiary air velocity has an influence on the SO_2 capture. In this last case, at Ca/S = 2, the SO_2 removal rate can vary within the range from 1 to 2 by simply changing the location where the same sorbent is injected.

Figure 3-24 illustrates the variation of desulfurization rates as a function of the primary zone stoichiometric ratio. For three different fuels, Saar coal, Ruhr coal, and heavy fuel oil, it can be seen that the application of the staged mixing concept has a negative effect on SO_2 removal when the additive is mixed with the coal (Position 1), while it has a positive effect when the additive is injected at the periphery of the burner (Position 3). The poor results observed in the case of staged combustion when $Ca(OH)_2$ is mixed

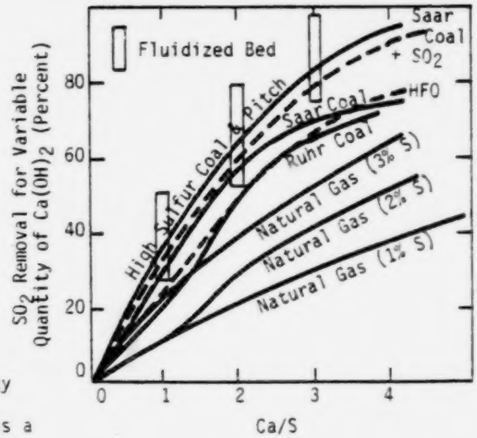

Maxiumum Efficiency of Utilization of Various Sorbents As a Function of SO_2 Concentration in Flue Gas

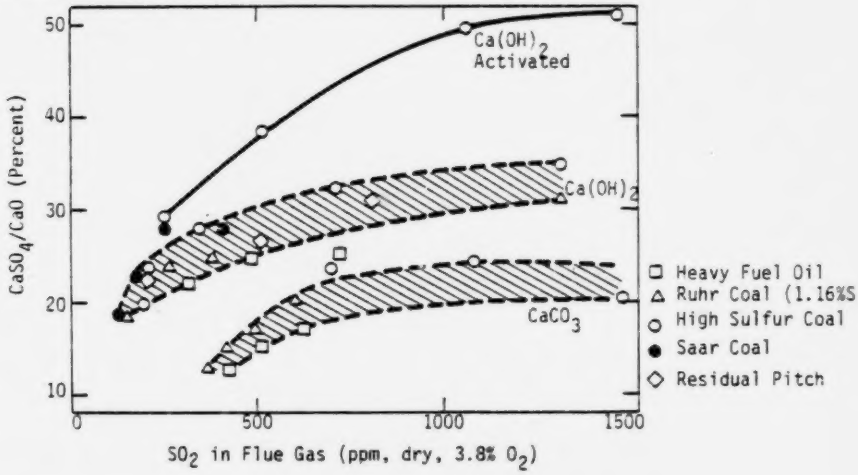

Figure 3-22. Typical Results of Desulfurization With Injection of Sorbent at the Periphery of the Flame (Position 3) (Ref. 6).

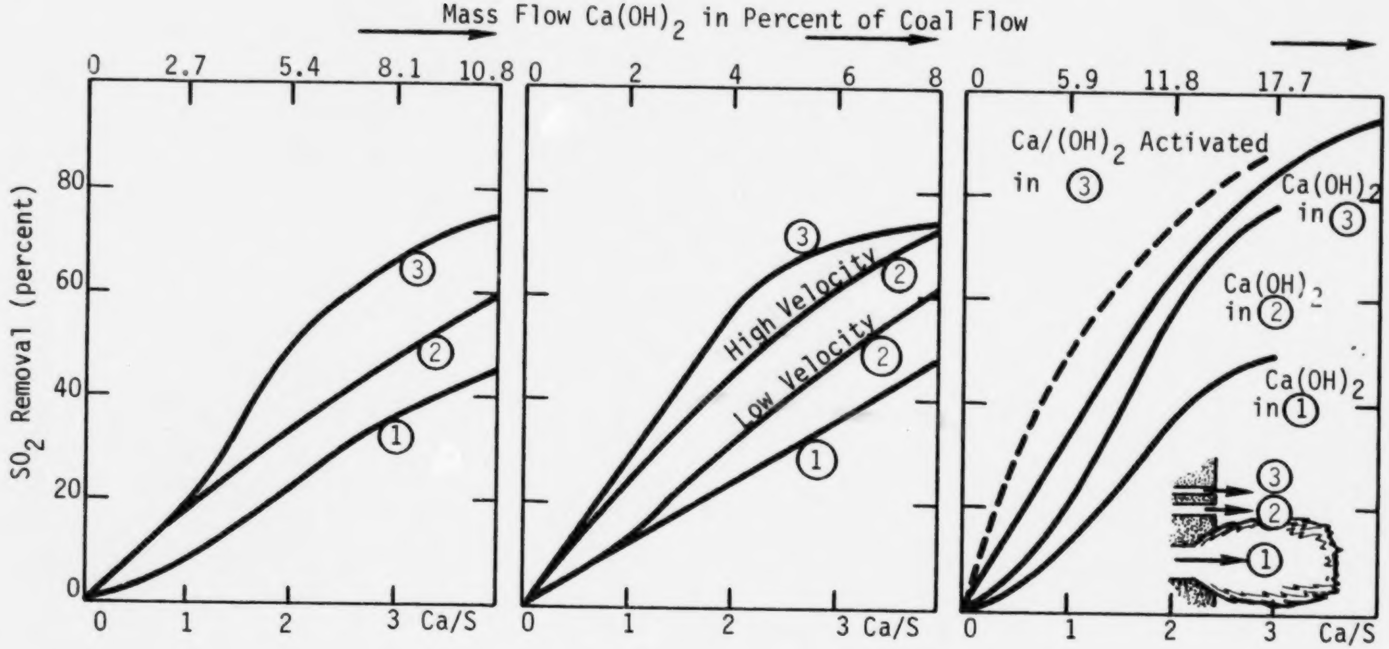

a) Ruhr Coal (1.16% S)

b) Saar Coal (0.85% S)

c) High sulfur Ruhr Coal (2.6% S)

Figure 3-23. Effect of Sorbent Injection Location on Desulfurization Rates for Three Different Coals (Ref. 6).

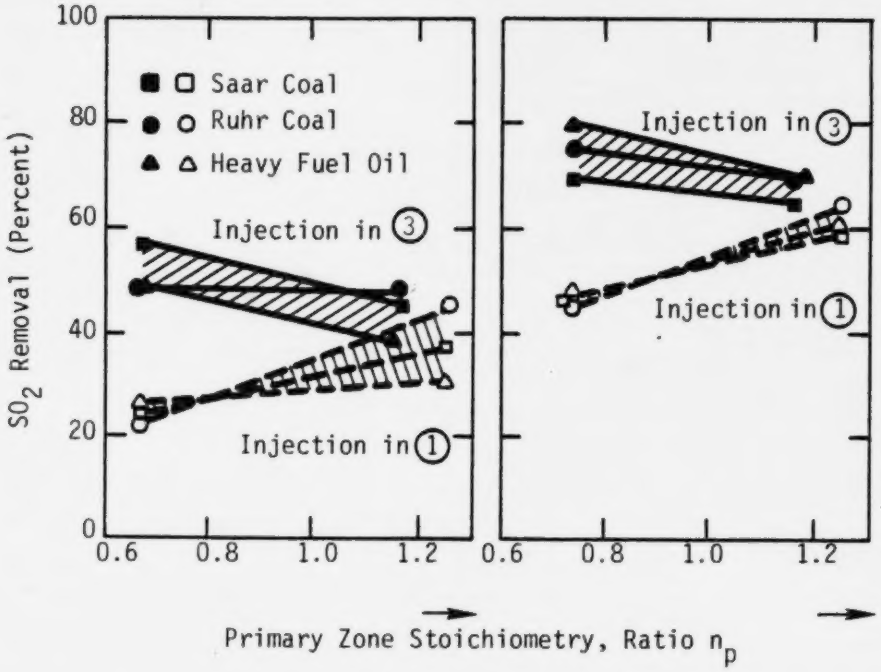

a) Ca/S = 2

b) Ca/S = 4

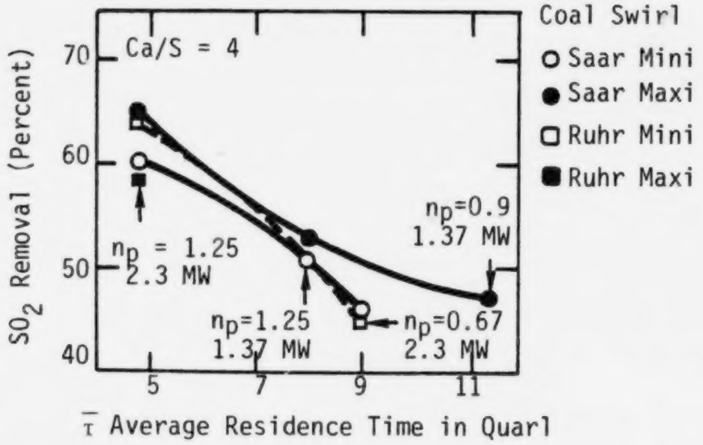

c) Injection of $Ca(OH)_2$ in Position 1

Figure 3-24. Effect of Staging on SO_2 Reduction Rates with Injection of $Ca(OH)_2$; Correlation With Average Residence Time in Burner Quarl When $Ca(OH)_2$ Is Mixed With Coal (Ref. 6).

with the coal are likely to be the result of a higher residence time of the sorbent particles in the hot zone of the flame, leading to dead-burning of CaO or to decomposition of $CaSO_4$. In fact, Figure 3-24c shows that when the additive is mixed with the coal, there is a good correlation between an estimated average residence time in the burner quarl ($\bar{\tau}$) and the SO_2 removal rate achieved. This correlation is applicable when $\bar{\tau}$ is varied by means of changing the overall thermal load or by means of changing the primary zone stoichiometric ratio. This indicates that the nature of the chemical field, fuel-lean or fuel-rich, does not play a major role in this case; it is simply the residence times of the sorbent in the quarl which influence the rate of desulfurization.

It is extremely interesting to note that the fuel/air mixing conditions which are the most favorable to a high efficiency in SO_2 capture by the direct sorbent injection method - namely the use of staged combustion - are also the conditions which produce a minimum quantity of NO_x. This is indicated in Figure 3-25 where the actual levels of reduced concentrations of NO_x and SO_x in the flue gases are given. By increasing the quantity of staging air, which leads to a reduction in the primary zone stoichiometric ratio from $n_p = 1.25$ (no staging, 25 percent excess air), down to $n_p = 0.67$ (46 percent staging, 25 percent excess air), it is possible to reduce the NO_x emission from about 650 ppm down to 350 ppm for both Ruhr and Saar coals. Under these conditions, the injection of a moderate amount of $Ca(OH)_2$ at the periphery of the burner (Ca/S = 2) brings the SO_2 emissions from 500 ppm down to 210 ppm with the Saar coal and from 830 ppm down to 430 ppm with the Ruhr coal. For the high sulfur coal, the SO_2 goes from 1900 ppm down to 800 ppm with Ca/S = 2.

3.3.3 EPA Pilot-Scale Studies

Sulfur capture tests with the EPA Distributed Mixing Burner were carried out in the thermal environment typical of water-wall boilers in the first generation small watertube simulator (SWS) which has since been dismantled. The unit is schematically illustrated in Figure 3-26 together with a layout of the support systems. The SWS could be fired at rates ranging from 4 to 16×10^6 Btu/hr. Other features of the SWS included:

- A ceramic front wall which could be moved to vary the furnace depth up to its maximum of 11 feet.

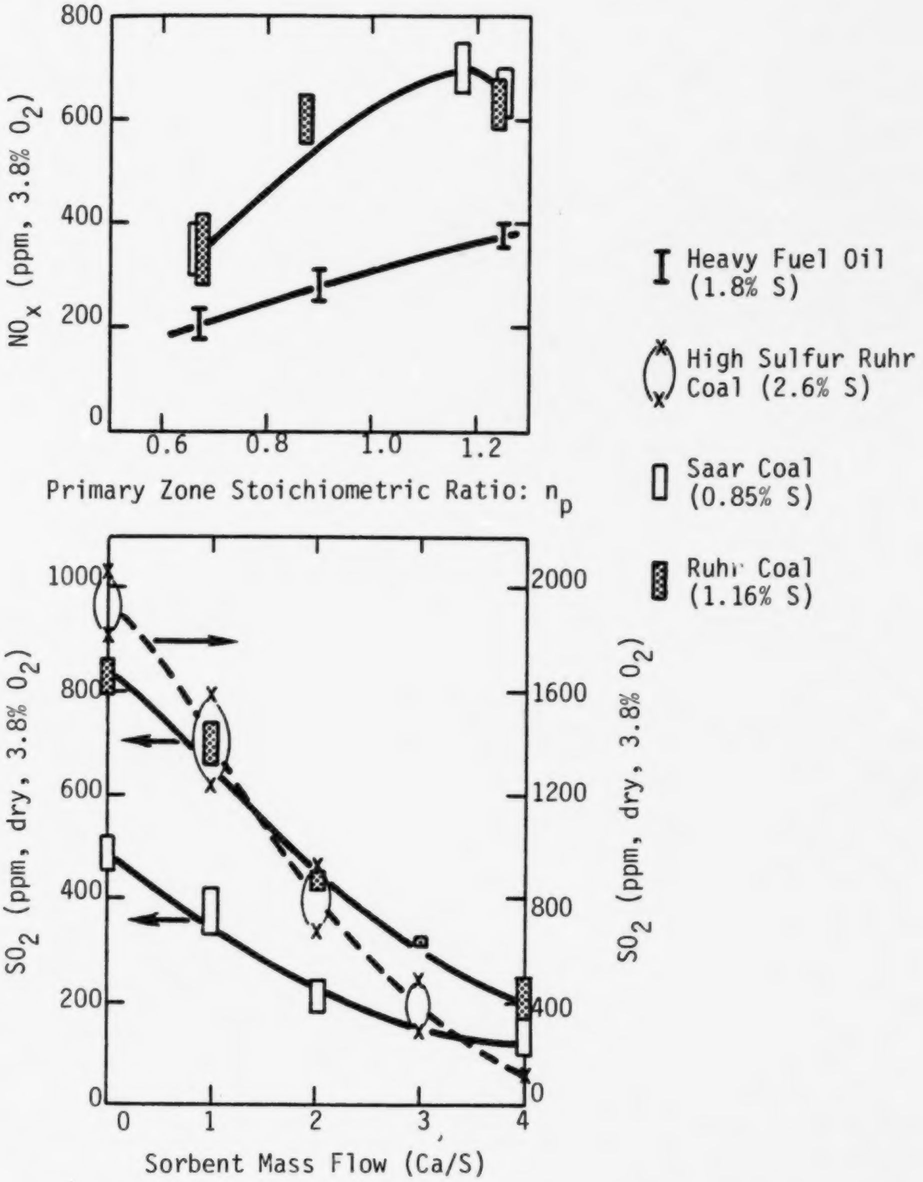

Figure 3-25. Actual Levels of SO_2 and NO_x Emission With Staged Combustion and With Injection of $Ca(OH)_2$ at the Periphery of the Burner (Position 3).

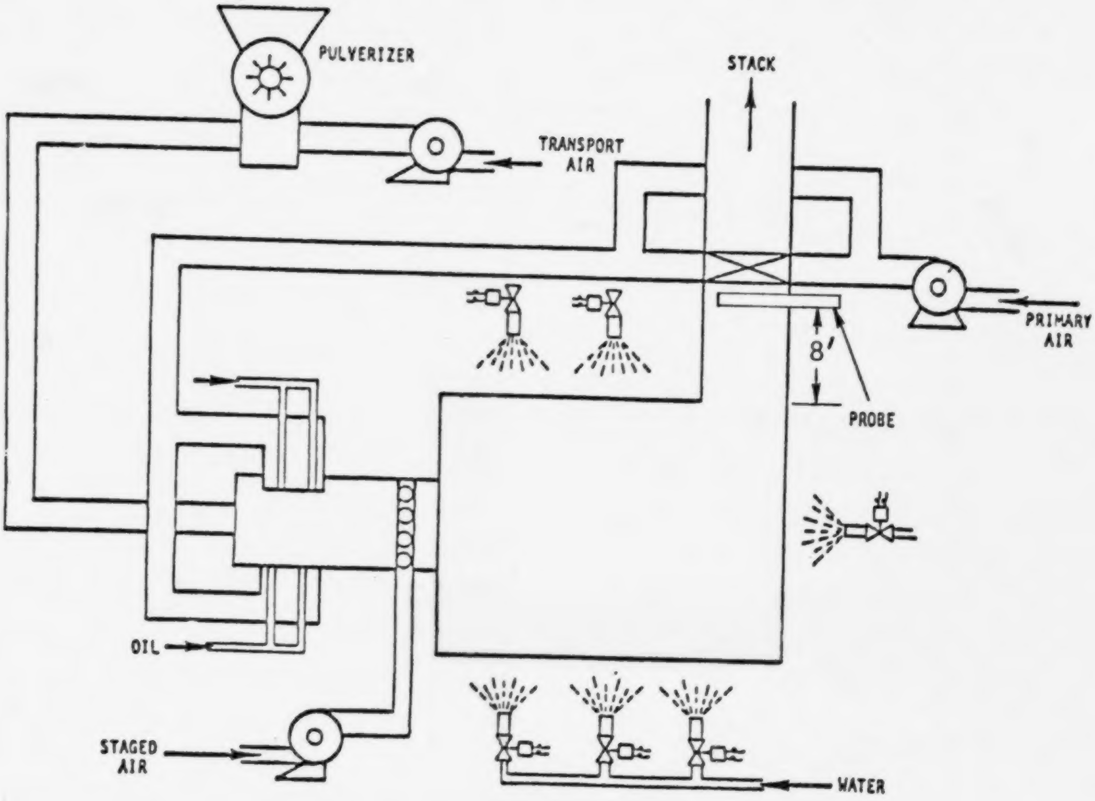
PULVERIZER
STACK
TRANSPORT AIR
PRIMARY AIR
8′
PROBE
OIL
STAGED AIR
WATER

Figure 3-26. Schematic of First Generation Small Watertube Simulator (SWS) and Support Facilities.

- sheet steel side and back walls which were cooled by a pulse water spray system and controlled to vary the wall temperature from 200 to 800°F;
- a stack heat exchanger that used the high temperature combustion products to preheat the incoming combustion air up to 600°F;
- multi-fuel capability.

The coal was pulverized by a high speed hammer mill and pneumatically transported to the burner with ambient air.

The DMB was operated under two very different conditions:

- Unstaged - No air flow in the staged air injectors;
- Staged - Secondary air flow zero.

These are extremes of operation which were used in an attempt to exaggerate any effect of mixing rate on SO_2 capture and NO_X/SO_X interaction. In all instances, the sorbent was batch-mixed with the coal before the pulverizer.

Figure 3-27 presents a sketch of the 12 x 10^6 Btu/hr Distributed Mixing Burner used in the sulfur capture tests. Coal and transport air are supplied via the annular coal injector and the remaining preheated combustion air is divided into two main streams:

- Secondary air is supplied at the burner throat in the duct surrounding the coal injector. The tangential momentum of this stream can be controlled by diverting some of the air through the swirl vanes.
- Staged air is supplied through injectors at the periphery of the burner exit on the firing wall.

Under low NO_X conditions, the burner is operated with less than the stoichiometric amount of air in the coal transport and secondary air streams.

All combustor input flows were monitored continuously. Combustion products were withdrawn from the flue exit duct prior to the heat exchanger, passed through a dry cyclone, and refrigerated to remove water vapor. The

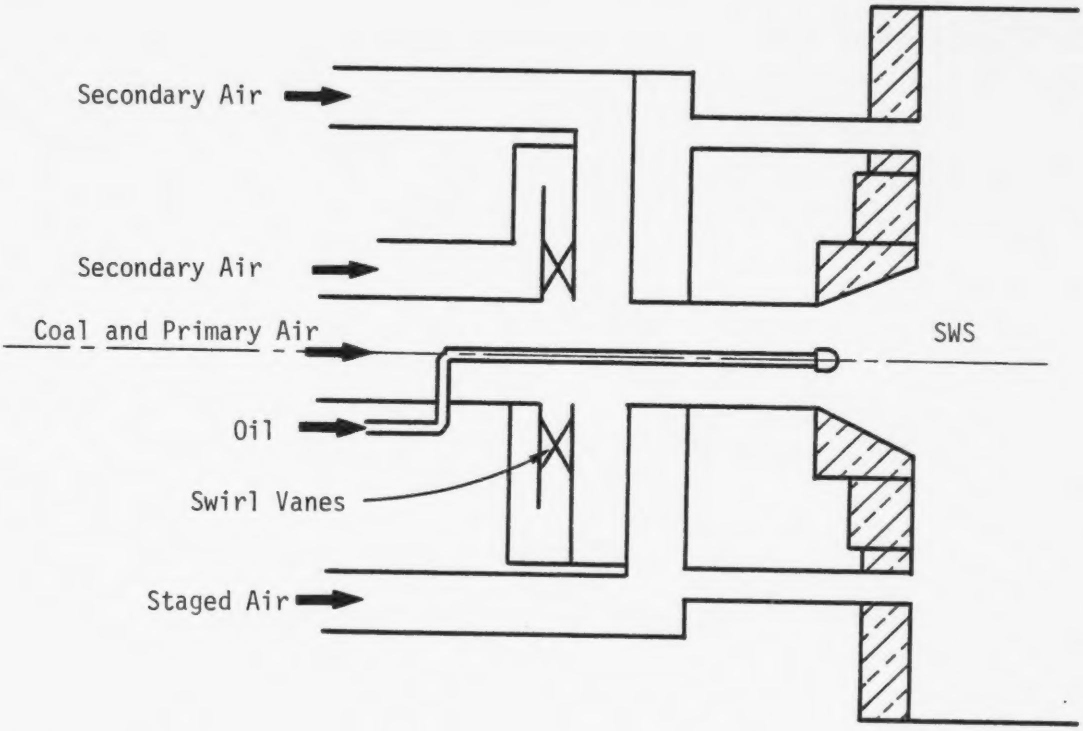
Secondary Air
Secondary Air
Coal and Primary Air
SWS
Oil
Swirl Vanes
Staged Air

Figure 3-27. Sketch of Distributed Mixing Burner.

combustion products were analyzed by the instruments listed in Table 3-3. Sample line material was Teflon and stainless steel and the extraction probe was cooled stainless steel.

A series of tests was conducted to ensure that appreciable amounts of sulfur were not being lost in the sample line. Calibration gas was passed through the entire sampling system after it had been used with sorbent addition; maximum sulfur loss was 5 percent.

A series of preliminary exploratory investigations was carried out to assess 1) the effect of sorbent type and sorbent ratio (calcium and sodium compounds were used) and 2) coal type upon sulfur capture, as well as to determine 3) whether there were significant advantages of operating under low NO_x conditions, and 4) whether or not sulfur capture influenced NO_x emissions. It is important to note that the DMB design is such that, under non-staging conditions, the coal/air mixing profile still minimizes the fuel/air mixing rate and is not equivalent to a pre-NSPS high-turbulence coal burner. Consequently, even though unstaged, the DMB flame characteristics are quite different from those produced with typical commercial turbulent burners.

Sorbent Type and Ratio

Two limestones and two sodium compounds were used in this study and their characteristics are shown in Table 3-4. The only significant difference between the two limestones was particle size; however, based on the work of several previous investigators, the largest size (74 μ) is below that where diffusion rate should control particle sulfation. The difference in the two sodium sorbents is that Trona is a hydrated form of sodium bicarbonate and, if the formation of water vapor during calcination is producing droplet communition, then the hydrate should increase the potential for this to occur.

Tests were first run without sorbent to determine the baseline operation and then with sorbent. For each case the sorbents were mixed with the coal prior to pulverization. The sorbent was preground and it cannot be expected that further size reduction takes place; however, the milling process tends to distribute the sorbent uniformly throughout the pulverized coal. The coal/sorbent/transport air mixture was then fed directly to the burner. Tests with and without sorbents were conducted over a range of excess air levels from about 1 to 9 percent excess O_2. The objective of the initial test series was to

Table 3-3. Analytical Instrumentation

Oxygen	Taylor Servomex (paramagnetic)
CO/CO_2	Anarad (NDIR)
SO_2	TECO (pulsed fluorescence)
NO/NO_x	Beckman (chemiluminescence)

Table 3-4. Sorbents Used in Sulfur Capture Tests

Sorbent	Major Constituent
Limestone (Vicron)	$CaCO_3$: 98.5 Size: 15 μm
Limestone (Mistrobrite)	$CaCO_3$: 98.2 Size: 74 μm
Trona	$Na_3H\ (CO_3)_2 \cdot 2H_2O$
Sodium Bicarbonate	$NaHCO_3$: 99.7%

obtain a rapid evaluation of the effectiveness of each sorbent and then to concentrate the subsequent efforts on the sorbent(s) showing the greatest potential. The results were repeatable and tests were typically conducted over an eight-hour time period so that any drifts in fuel composition or sorbent could be monitored. While some variations were observed, the differences were within experimental error, and in no case would the variations alter the conclusions from these experiments.

Typical results obtained with the limestone are shown in Figure 3-28. The upper line represents the baseline SO_2 emissions without sorbent and the overall level is approximately 580 ppm (at 0 percent O_2, dry) regardless of whether the burner is operated under full staging or unstaged conditions. Quantitative conversion of the fuel sulfur to gas phase SO_2 would result in 642 ppm, so under these operating conditions about 90 percent of the sulfur is in the form of SO_2 and 10 percent remains with the ash. When the sorbent was added, the SO_2 levels in the flue gases immediately dropped to between 250 and 170 ppm. This range depended on the split between the burner air (transport and secondary air) and the tertiary air, and therefore, on the T(t) and $\phi(t)$ characteristics. A summary of these results for the four sorbents is presented in Table 3-5.

Coal Type

The Utah coal (Table 3-6) is a relatively low sulfur coal which EER has been using as a baseline fuel for the burner development programs. Another coal available for testing at EER was a Western Kentucky coal having higher sulfur but nearly identical nitrogen levels. The moisture and ash content as well as the HHV of the W. Kentucky coal are similar to those of the Utah coal; thus, it was decided that for these feasibility studies, this selection would provide an adequate assessment of fuel sulfur effects.

The experimental procedures employed with the high sulfur coal were the same as those discussed for the Utah coal. The results are presented in Figure 3-29. Note that the SO_2 levels are considerably higher for this coal than for the Utah coal, which is reflective of the higher sulfur values in the Western Kentucky coal. The baseline values of SO_2 are about 3000 ppm which

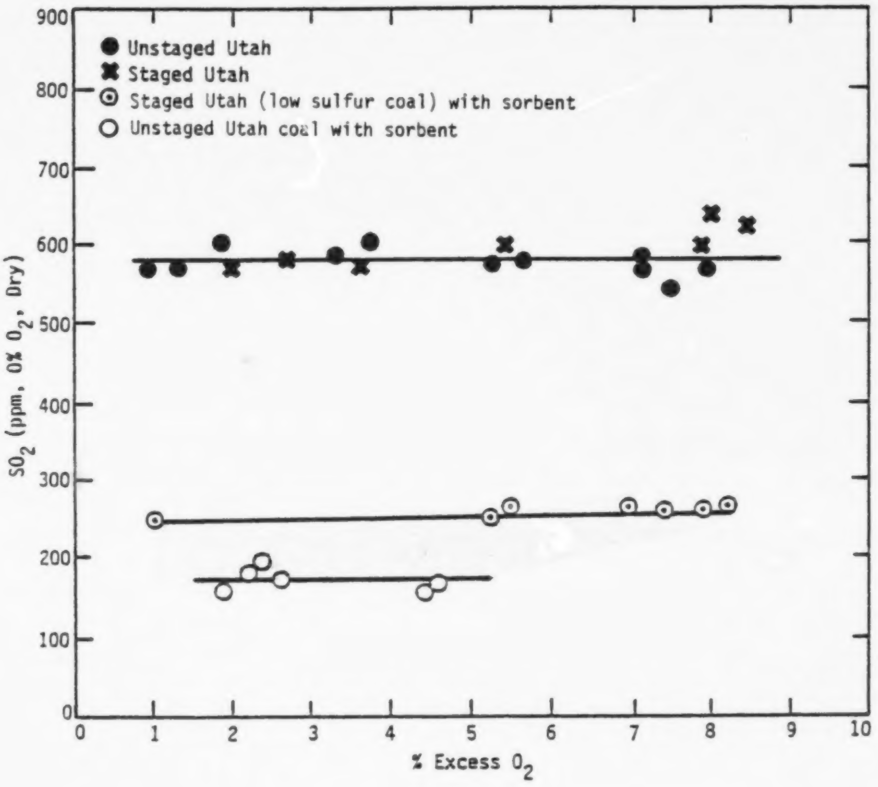

Figure 3-28. The Effect of the Addition of Limestone to the Utah Coal Prior to Pulverization on SO_2 Emissions (Ca/S = 1.0).

Table 3-5. Summary of Results

Coal	Sorbent	Percentage of Reduction of SO_2 Molar Ratio				
		$Ca/_{S=1}$	$Ca/_{S=2}$	$Ca/_{S=3}$	$Na/_{S=2}$	$Na/_{S=4}$
Utah (Low Sulfur)	Limestone	53	73	88		
	Trona				41	80
	Sodium Bicarbonate				52	

Table 3-6. Coal Composition

Characteristics	Origin	
	Utah	W. Kentucky
Proximate Analysis, % (as received)		
Moisture	6.39	3.68
Volatile	38.89	38.19
Ash	7.4	17.90
Fixed Carbon	47.32	40.23
Heating Value, Btu/lb	12,340	10,640
Ultimate Analysis, % (DAF)		
Carbon	79.45	77.57
Hydrogen	6.03	5.7
Nitrogen	1.44	1.63
Sulfur	0.74	3.8
Oxygen (by difference)	12.34	11.3

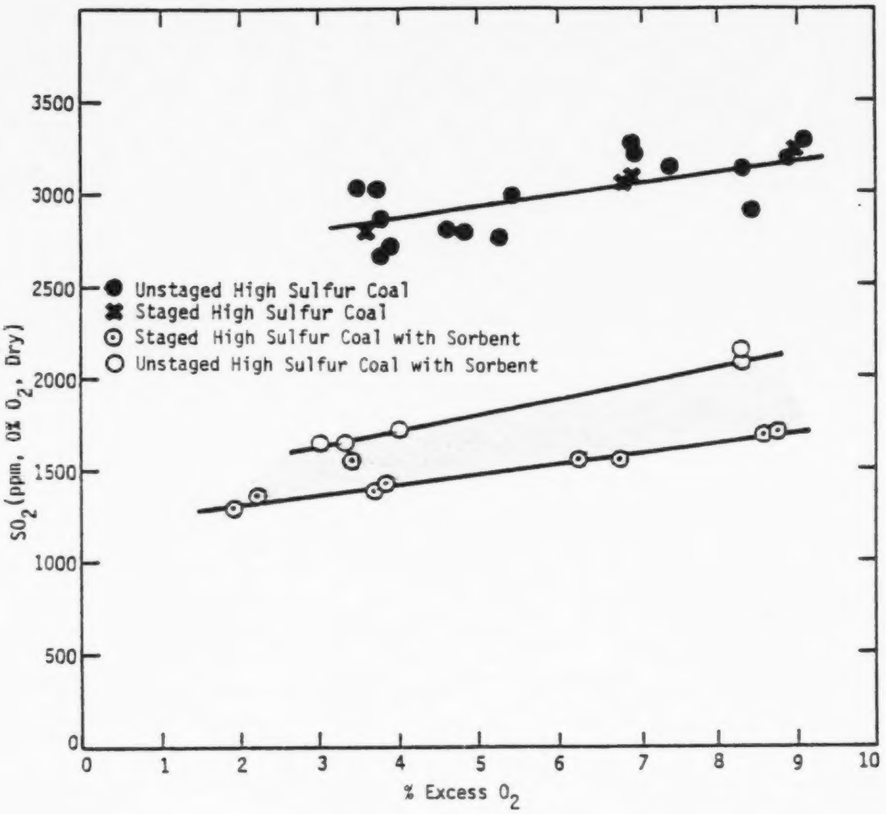

Figure 3-29. The Effect of the Addition of Limestone to the Western Kentucky Coal Prior to Pulverization on SO_2 Emissions (Ca/S = 1.0).

represents about 90 percent conversion of the sulfur into the gas phase. It is interesting that both coals had about the same conversion rate. Injection of limestone again reduced the SO_2 levels in the flue gas and the same band of SO_2 levels were observed depending on whether the burner was operating staged or unstaged. Of some interest, however, is that for the high sulfur coal the lower bound represents the staged (or low NO_x) operating mode, while for the low sulfur coal it is reversed. This suggests that there could be a tradeoff in T(t) characteristics with the SO_2 levels in the exhaust gas or that the Western Kentucky coal with a lower heating value and higher moisture requires a longer residence time at the lower temperatures (to avoid overburning before the sulfation process can be completed.

It should be noted that the percent reduction for both coals is approximately 50 percent, which is consistent with the results of previous investigators whose experiments indicate that sulfation rate is independent of sulfur dioxide concentration.

The limestone results are very encouraging in that the results suggest that the entire BET surface of the sorbent can be utilized when injected with the coal under controlled fuel/air mixing conditions. The sodium-based sorbents did not appear to offer any advantages over the calcium-based sorbent. It should also be noted that the two limestones with differing particle sizes gave identical results confirming that, for these small sizes, particle size no longer affects sorbent removal efficiencies. For the limestone, increasing the Ca/S ratio showed an increase in SO_2 reduction roughly in the same proportions as other investigators have found.

Staged versus Unstaged

The results presented above show that, for the coal alone, no difference in sulfur conversion occurs when operating under staged or unstaged conditions. Further, low NO_x operating conditions alone do not appear to increase or decrease the SO_2 emissions. When the sorbent was added, depending on the coal, different SO_2 removal characteristics did occur. For the high sulfur coal, low NO_x operating conditions enhanced SO_2 removal while the reverse is true for the Utah coal. It is unclear at this time, however, whether this difference is due to the properties of the coals or the combustion conditions produced by the low NO_x burner. NO_x emissions were determined during the tests on sulfur capture to ascertain whether NO_x/SO_x interactions could be observed. The results presented in Figure 3-30 show that no effect of sulfur capture was measured under any of the operating conditions even though from gas-phase kinetic considerations it might be expected that SO_x/NO_x would influence the overall NO_x emissions when the burner was operated staged.

3.4 Further Studies

Despite the many tests conducted to demonstrate the feasibility of SO_x control via dry sorbent injection (only a few of which were discussed in the previous sections), there are several reasons for additional investigations. For some of the system variables studied, the results of the various investigations are not in full agreement. Some of the effects noted have not been satisfactorily explained. Since most of the studies show that the burner design affects the SO_2 removal process, there is a definite need to assess the potential for sorbent injection in various burner configurations, both commercial and developmental. Finally, there is a need to clearly define the optimum operating envelope for application of this technology.

Under this contract, EER is engaged in a comprehensive development program at both bench and pilot-scales. During the period of performance covered by this report, pilot-scale studies were conducted in the LWS furnace using a 50×10^6 Btu/hr Steinmüller Staged Mixing Burner. The results of this study are discussed in Section 4. Additional pilot-scale tests are planned in the SWS, MT and LWS facilities. Tests of a 10×10^6 Btu/hr versatile DMB will be conducted in the SWS. These tests will allow identification of the effects of varying several burner design parameters. Based on the results, an optimum design will be specified. A 50×10^6 Btu/hr DMB will be built and tested in the MT and LWS, and a 120×10^6 Btu/hr burner of the same design will be constructed for LWS testing. The two larger burner tests will allow assessment of equipment scaling effects, the importance of thermal environment, and effects on boiler subsystems. These plans are detailed in Section 11.

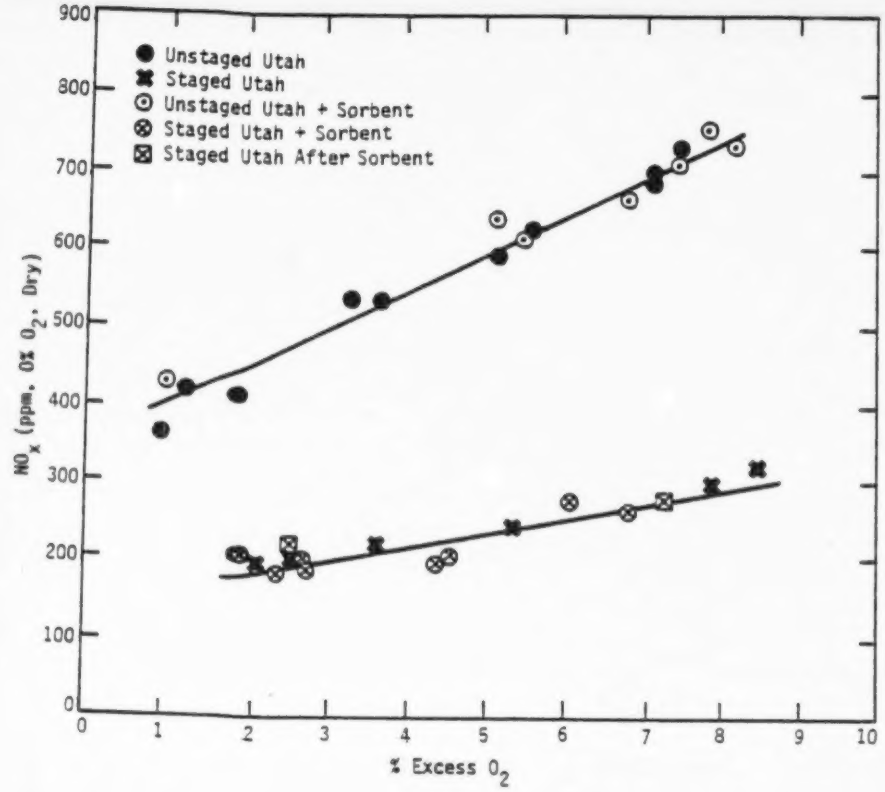

Figure 3-30. The Effect of Sorbent on NO$_x$ Emissions (Utah Coal Ca/S = 1).

4.0 STEINMÜLLER AND PROTOTYPE BURNER PILOT-SCALE STUDIES

This section discusses the results of tests conducted during this annual reporting period using Steinmüller and EPA prototype low NO_x burners in a large watertube simulator test facility. Tests were conducted without sorbent injection to characterize low NO_x operation of the burner, and with sorbent injection to assess the potential for in-situ SO_2 removal in controlled mixing pulverized coal burners.

4.1 Steinmüller Burner Tests

The results of a short experimental study carried out to determine the pollutant emission characteristics of a 50 x 10^6 Btu/hr (15 MW) coal fired staged mixing burner developed by the Steinmüller Company of Germany are discussed in this section. The studies were conducted in a large experimental test furnace at Energy and Environmental Research Corporation and complement a larger study which includes a comparison between research and commercial practice burner systems. The current studies focused primarily on emissions of NO_x and SO_x.

The burner used in these tests is depicted schematically in Figure 4-1, and some of the nominal input and operating parameters are listed in Table 4-1. The staged mixing burner is based on a standard circular burner design and consists of three concentric flow channels (core, primary, and secondary) with four outboard staging air ports located symmetrically on the perimeter of the main burner. This burner was scaled directly from Steinmuller staged mixing burners installed in a utility boiler in Weiher, Germany.

Pulverized coal suspended in 200^oF ($\sim 90^oC$) air entered through the annular primary channel and was discharge axially from the burner at 72 ft/sec (22 m/s). Core air was introduced in the center flow channel in an axial direction. The secondary was the only air flow stream that was introduced with a tangential momentum component. Swirl intensity variation was achieved by controlling the amount of air that bypassed the fixed-angle swirl vanes. This was accomplished by adjusting the axial position of the conical swirl vane assembly in the cone-shaped convergent channel. Staging air was introduced axially through the four outboard air ports around the burner. Both the secondary and staging air required 600^oF (315^oC) preheat and had bulk velocities of 115 ft/sec (35 m/s). In this reduced scale burner design, a

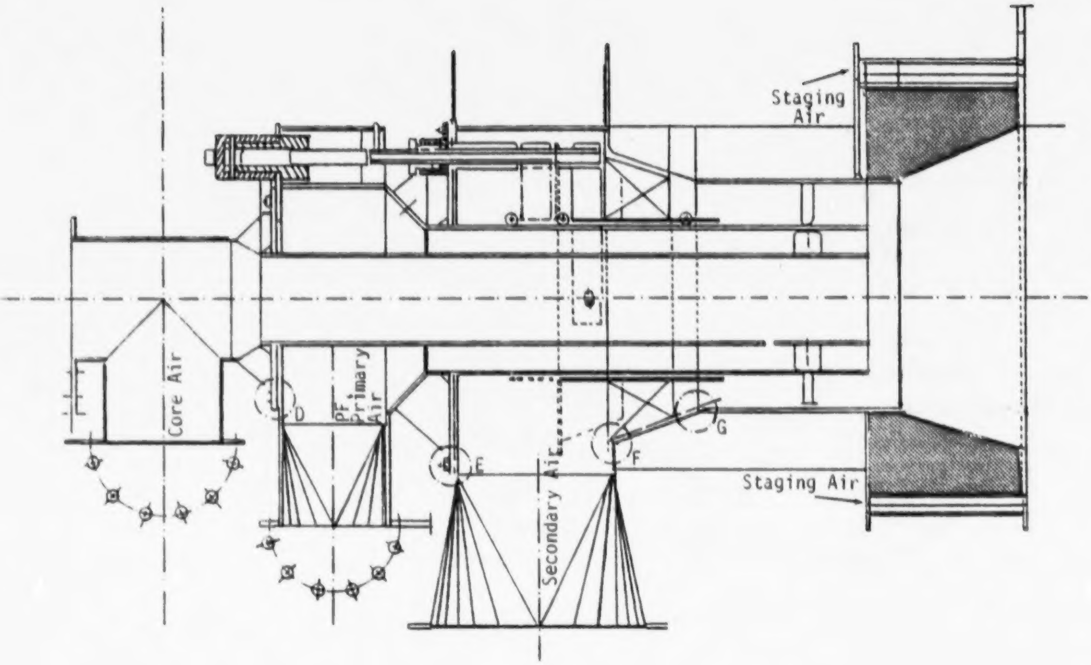
Staging Air
Core Air
PF Primary Air
D
E
F
G
Secondary Air
Staging Air

Figure 4-1. Schematic of the Steinmüller Staged Mixing Burner.

Table 4-1. Nominal Input and Operating Conditions for the Steinmuller Staged Mixing Burner Design.

Load Thermal	15	MW	51.2 MBtu/hr
Fuel HV	25.12	MJ/kg	10,800 Btu/lb
Moisture	10	%	10%
Stoich. air	8,53	kg/kg	8.53 lb/lb
Air Ratio n	1,25		1.25
Air Temperature	300	^oC	572^oF
Ratio p.a./p.f.	1,80	kg/kg	1.8 lb/lb
Velocity			
Primary Air	22	m/s	72 ft/sec
Secondary Air	35	m/s	115 ft/sec
Staging Air	35	m/s	115 ft/sec
Air Ratio Quarl	0,75		0.75
L/O of Quarl	0,55		0.55

quarl divergent half angle of 20^{0} and length to diameter ratio of 0.55 were employed.

The burner was designed such that about 20 percent of the theoretical air requirement was supplied by the primary air. Secondary air provided additional combustion air into the immediate region of the burner throat to give a burner zone stoichiometric ratio of 0.75. The remaining air was delivered through the staging air ports to provide an overall stoichiometric ratio of 1.25. The distribution of air to the various streams was controlled in the experimental system through the use of independently metered and regulated air supplies.

The only mechanically variable feature on this burner was the level of secondary air swirl applied; all other potential variables, such as coal nozzle position, were fixed in the basic burner design. The burner itself was constructed to normal commercial standards and tolerances according to detailed engineering designs supplied by Steinmüller.

The pilot-scale tests were conducted in the large watertube boiler simulator (LWS), which is a water spray cooled test furnace partially refractory-lined to provide a thermal environment typical of coal-fired boilers. Figure 4-2 shows an artist's sketch of the test furnace and presents a list of its characteristics. The system is direct-fired. Coal is fed from a crusher to a weigh-belt feeder prior to being pulverized in a Raymond bowl mill. The pulverized coal is then transported to the burner with premetered primary air. Combustion air is preheated in a direct-fired heat exchanger, meterd, and supplied to the burner.

In Table 4-2, several LWS furnace thermal parameters are presented and compared to those for the Weiher boiler in which the Steinmuller burner is presently installed. It should be noted, however, that the Weiher boiler data are only approximate and are estimated from information available in the open literature. It should be noted also that this boiler is of the "tower" type, is opposed wall fired, and that the furnace contains an internal division wall. At high firing rate, it can be seen that the LWS furnace would result in thermal conditions similar to those for the field boiler. The test burner was, however, designed only for a firing rate of 50 x 10^{6} Btu/hr (15 MW) such that the furnace is underfired, making it difficult to compare results directly.

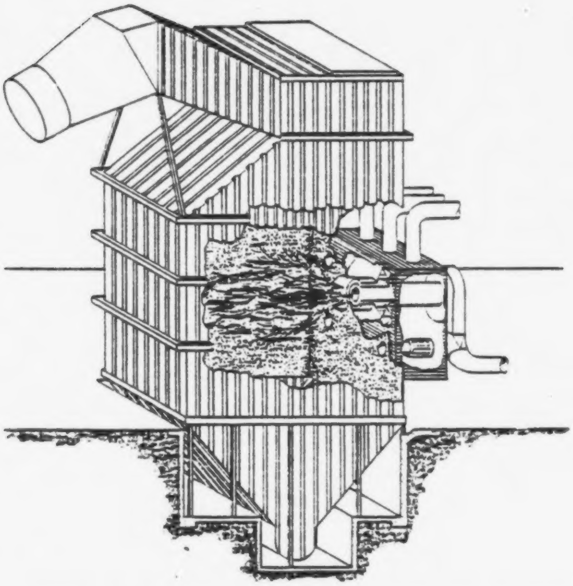

Parameter		Value	
Firing			
Configuration	Primary Optional	Single Wall Opposed or Corner	
Firing Rate	Minimum Maximum	50 x 10^6 Btu/hr 150 x 10^6 Btu/hr	
Dimensions			
Firing Depth		22 ft.	
Width		16 ft.	
Rear Wall Height		20 ft.	
Knuckle-to-Nose Height		27.5 ft.	
Nose Angle		37° (from horizontal)	
Hopper Angle		52° (from horizontal)	
Height Above Ground Level		35.7 ft.	
Total Vertical Height		50.5 ft. (pit to top)	
Cooled Surface Area			
Burner Zone		704 ft.^{2}	
Total Furnace		1951 ft.^{2}	
Volume			
Burner Zone		3520 ft.^{3}	
Total Furnace		11,544 ft.^{3} (to nose)	
Insulation		All Sidewalls knuckle-up 16 ft.	
Cooling		Spray-cooled on all surfaces	
Thermal Environment			
Heat Release/Cooled Surface		213,068 Btu/hr ft^2	In burner zone at maximum firing rate
Heat Release/Volume		42,614 Btu/hr ft^3	

Figure 4-2. Characteristics of the LWS Test Furnace.

Table 4-2. LWS Operating Parameters

Parameter	Burner Firing Rate (10^6 Btu/hr)			Weiher Boiler*	Units
	50	70	100		
Heat Release Per Unit Area (Total Furnace)	28.5	39.5	56.4	-	10^3 Btu/hr/ft^2
Burner Zone Liberation Rate - BZLR	78.1	109.4	156.2	176	10^3 Btu/hr/ft^2
Heat Release Per Unit Volume (Total Furnace)	4.3	6.0	8.6	10.6	10^3 Btu/hr/ft^3
Residence Time (Total Furnace)	12.8	9.1	6.4	5.1	Sec
Residence Time (Burner Zone)	6.18	4.41	3.09	2.5	Sec
Furnace Exit Temperature	1420	1600	1900	1920	^oF

* Approximate data only.

Three different coals were fired in the Steinmuller burner, all of which were high volatile bituminous coals with low ash content. Detailed analyses of these coals and the size distributions of the pulverized fuels as fired are presented in Tables 4-3 and 4-4. The Saar coal is a West German coal specially imported for these tests, and is included to link these data to those generated elsewhere with the Steinmuller burner. Saar coal is the principal fuel used in the Weiher boiler and was used in the pilot scale development testing of the burner. The Utah and Indiana are both U.S. coals. The Utah coal has been fired extensively at EER in many of the bench scale and burner development programs, and as such represents the baseline coal providing a link to comparable DMB data. It will be noted also that the nitrogen and sulfur contents of the Utah and Saar coals are similar, although the Utah coal has a considerably higher volatile content. The Indiana coal is included primarily becuase of its high (2.56 percent) sulfur content.

During the initial burner commissioning and system shakedown tests, some problems were encountered in obtaining stables flames for all input conditions and burner settings. The reasons for this instability were not immediately apparent, and some time was spent adjusting parameters to improve performance and define suitable operating ranges. It was considered that the relatively cold furnace enclosure might be limiting the flame stability range, although successful operating experience with other burners suggested that this was not the case. In order to broaden the stability range, coal grindings were selected which were somwhat finer than might normally be used for such high volatile fuels. Also it was found necessary to operate the burner with a secondary air swirl level which was close to the maximum adjustment. Swirl level was, however, found to have no effect on the emissions of NO_x, except when flame stability was impared, and was thus discounted as a significant variable parameter. A small amount of core air (bled from the secondary windbox) was also found to improve stability. Unfortunately, the flame stability performance of the burner when firing Saar coal was worse than for the two U.S. coals. This created some difficulties in meeting all the proposed test conditions, and the limited coal supplies and test period precluded a lengthly trouble shooting effort.

Where stable operation was achieved, the resulting flames were luminous and intense, with ignition generally occurring within the burner quarl

Table 4-3a. Analysis - Utah Coal

PROXIMATE ANALYSIS (%)	As Received	Dry Basis
Moisture	2.84	-
Ash	7.22	7.43
Volatile Matter	41.95	43.18
Fixed Carbon	47.99	49.39
	100.00	100.00
Calorific Value (Btu/lb)	12,731	13,103
Sulfur (%)	0.85	0.85
Mineral Matter Free (Btu/lb)	-	14,273
ULTIMATE ANALYSIS (%)		
Moisture	2.84	-
Carbon	71.70	73.80
Hydrogen	5.63	5.80
Nitrogen	1.46	1.50
Sulfur	0.85	0.87
Ash	7.22	7.43
Oxygen (difference)	10.30	10.60
	100.00	100.00
ELEMENTAL ANALYSIS OF ASH	Analysis, %	
SiO_2	63.01	
Al_2O_3	15.91	
TiO_2	1.87	
Fe_2O_3	4.85	
CaO	4.94	
MgO	1.22	
Na_2O	0.99	
K_2O	1.24	
P_2O_5	0.38	
SO_3	4.11	

Table 4-3b. Analysis - Indiana Coal

PROXIMATE ANALYSIS (%)	As Received	Dry Basis
Moisture	5.75	-
Ash	11.15	11.82
Volatile Matter	36.47	38.69
Fixed Carbon	46.63	49.49
	100.00	100.00
Calorific Value (Btu/lb)	11,527	12,230
Sulfur (%)	2.41	2.56
Mineral Matter Free (Btu/lb)	-	14,102
ULTIMATE ANALYSIS (%)		
Moisture	5.75	-
Carbon	64.91	68.87
Hydrogen	4.84	5.14
Nitrogen	1.37	1.45
Sulfur	2.41	2.56
Ash	11.15	11.82
Oxygen (difference)	9.57	10.16
	100.00	100.00

ELEMENTAL ANALYSIS OF ASH	Analysis, %	
SiO_2	51.25	
Al_2O_3	21.07	
TiO_2	1.96	
Fe_2O_3	16.99	
CaO	2.12	
MgO	0.92	
Na_2O	0.29	
K_2O	2.24	
P_2O_5	0.16	
SO_3	1.71	

Table 4-3c. Analysis - Saar Coal

PROXIMATE ANALYSIS (%)	As Received	Dry Basis
Moisture	1.54	-
Ash	7.16	7.27
Volatile Matter	34.35	34.89
Fixed Carbon	56.95	57.84
	100.00	100.00
Calorific Value (Btu/lb)	13,164	13,369
Sulfur (%)	0.84	0.85
Mineral Matter Free (Btu/lb)	-	14,536
ULTIMATE ANALYSIS (%)		
Moisture	1.54	-
Carbon	74.60	75.76
Hydrogen	4.88	4.95
Nitrogen	1.32	1.34
Sulfur	0.84	0.85
Ash	7.16	7.27
Oxygen (difference)	9.66	9.83
	100.00	100.00

ELEMENTAL ANALYSIS OF ASH	Analysis, %	
SiO_2	43.27	
Al_2O_3	26.06	
TiO_2	1.31	
Fe_2O_3	10.80	
CaO	6.20	
MgO	3.52	
Na_2O	0.28	
K_2O	2.66	
P_2O_5	0.16	
SO_3	5.83	

Table 4-4. Pulverized Coal Size Analyses

U.S. Seive Size	Microns	Weight % Residue on Sieve		
		Indiana	Utah	Saar
50	300	0.1	0.35	0.9
100	150	7.7	3.5	3.2
140	100	20.5	10.0	10.1
200	75	22.9	24.1	28.2

or within 2 inches (5 cm) of the burner exit. The visible flame envelope was typically 8 to 12 feet (2.5 to 3.5 meters) in length and 6 to 8 feet (2 meters) in diameter. Stable flames were obtained for a range of burner zone stoichiometry levels (SR_B) of 0.6 to 1.0 and for a burner load range of 39 x 10^6 to 74 x 10^6 Btu/hr (11.5 to 22 MW).

Discussions were held with Steinmüller throughout the course of the test period with regard to the stable operating range of the burner. As a result of these discussions, it transpired that the detailed burner drawings were in error with regard to the set-back of the inner core-air pipe. Unfortunately, this error was not discovered until close the the end of the limited test period and appropriate modifications could not be made.

4.1.1 Emissions of NO_x

The emissions characteristics of the burner were determined as a function of three basic variable parameters. These were: burner zone stoichiometry (SR_B), based on the total air flow (primary plus secondary) into the burner zone; overall excess air level (SR_T); and burner load. Other parameters such as primary air/coal stoichiometric ratio (SR_p) and swirl level were held constant. Swirl level was found to have no influence on NO_x emission levels, except when changes in swirl level changed flame stability. The nominal input conditions for the burner were:

Load	50 x 10^6 Btu/hr (15 MW)
SR_p	0.21
SR_B	0.75
SR_T	1.25

Results obtained for NO_x and corresponding CO emissions are presented in the following discussion on a coal by coal basis.

Utah Coal

Experimental NO_x and CO emission characteristics for the Steinmüller burner firing Utah coal are shown in Figures 4-3, 4-4, and 4-5, where emission values are normalized to 0 percent oxygen in the stack. Figure 4-3 illustrates the effect of varying burner zone stoichiometry, where NO_x values range from 120 ppm to 290 ppm for an SR_B of 0.6 to 0.9 respectively. Due to stability limitations, it was not possible to operate the burner in an overall fuel lean

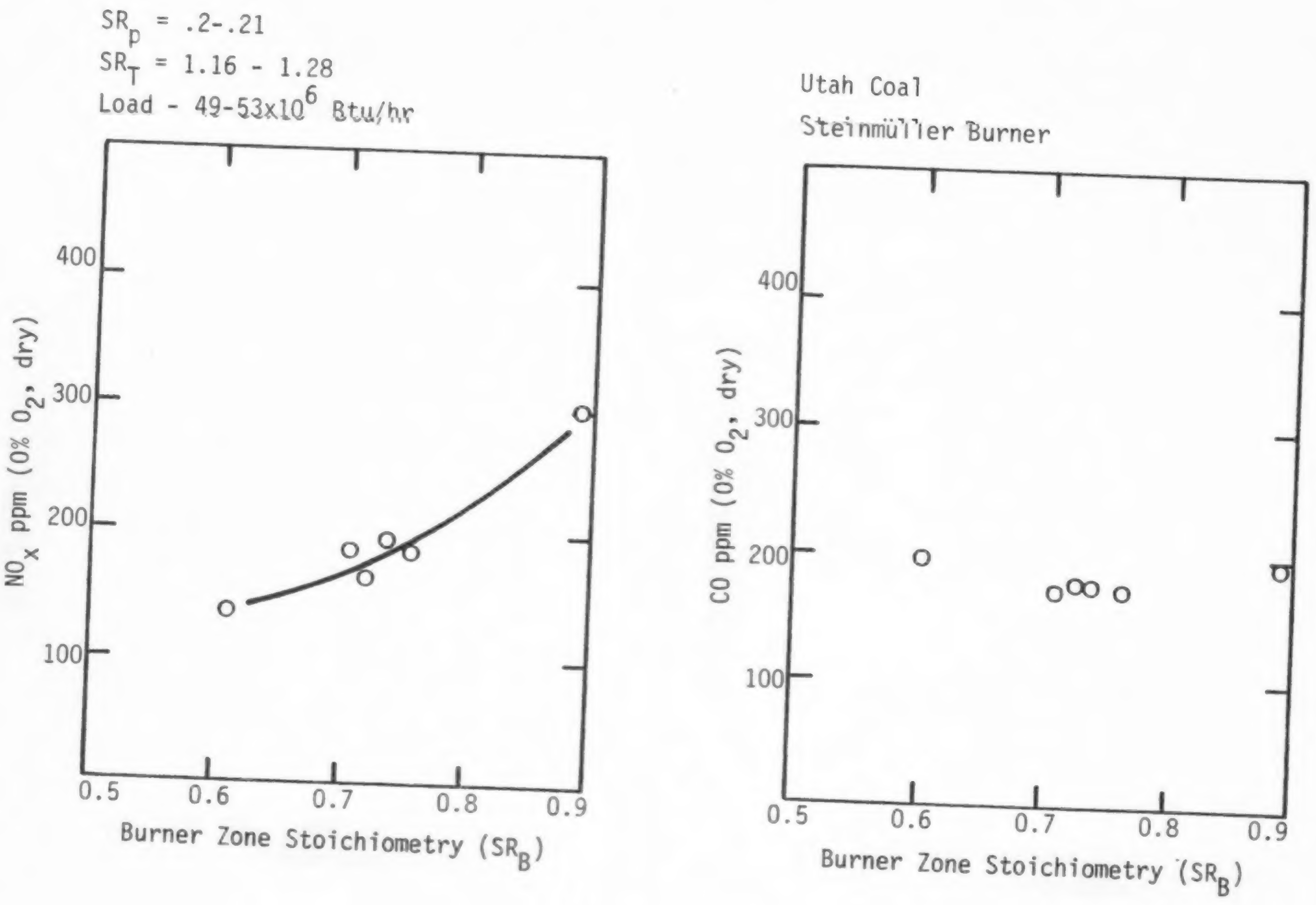

Figure 4-3. Effect of Staging on Emissions, Utah Coal.

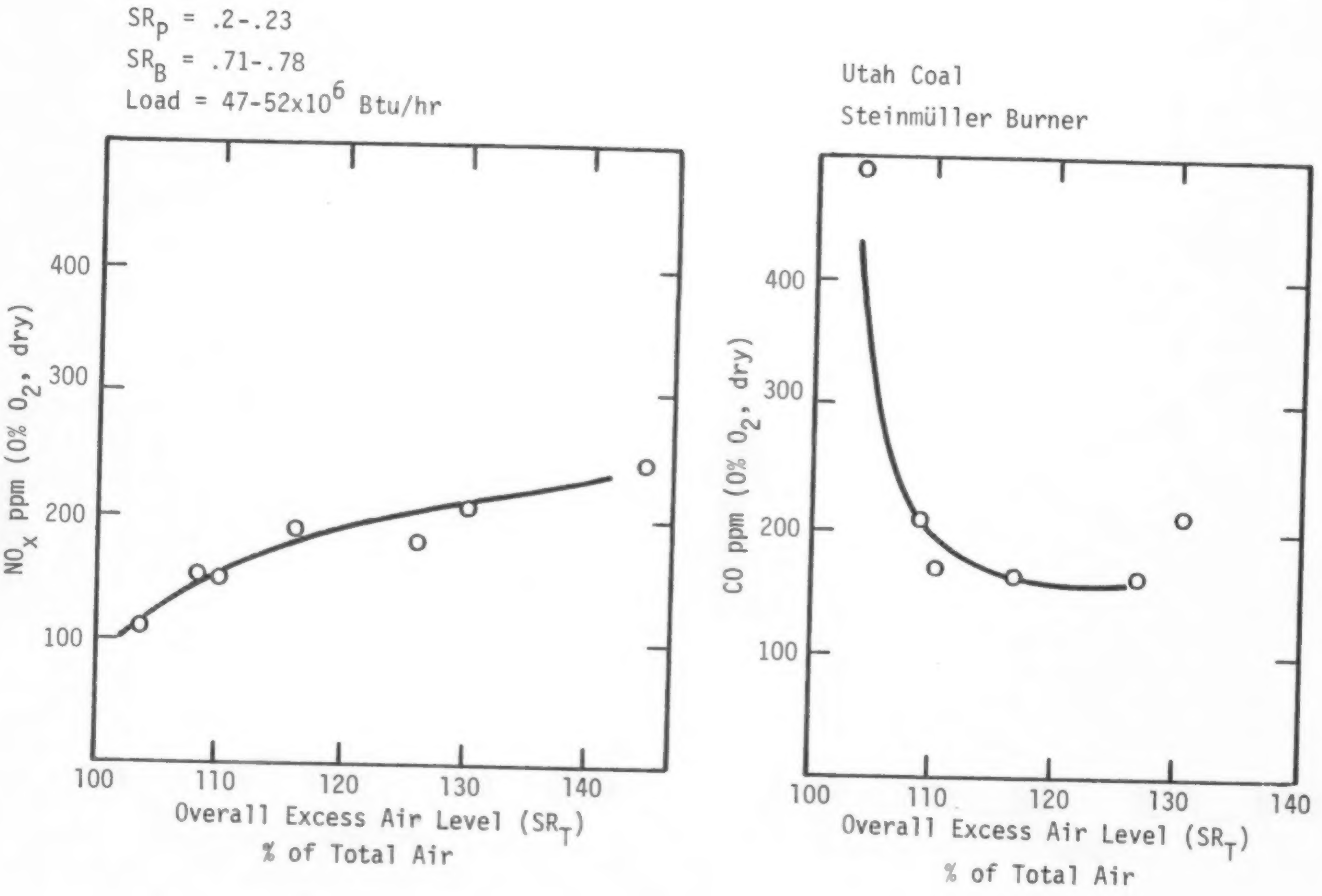

Figure 4-4. Effect of Excess Air on Emissions, Utah Coal.

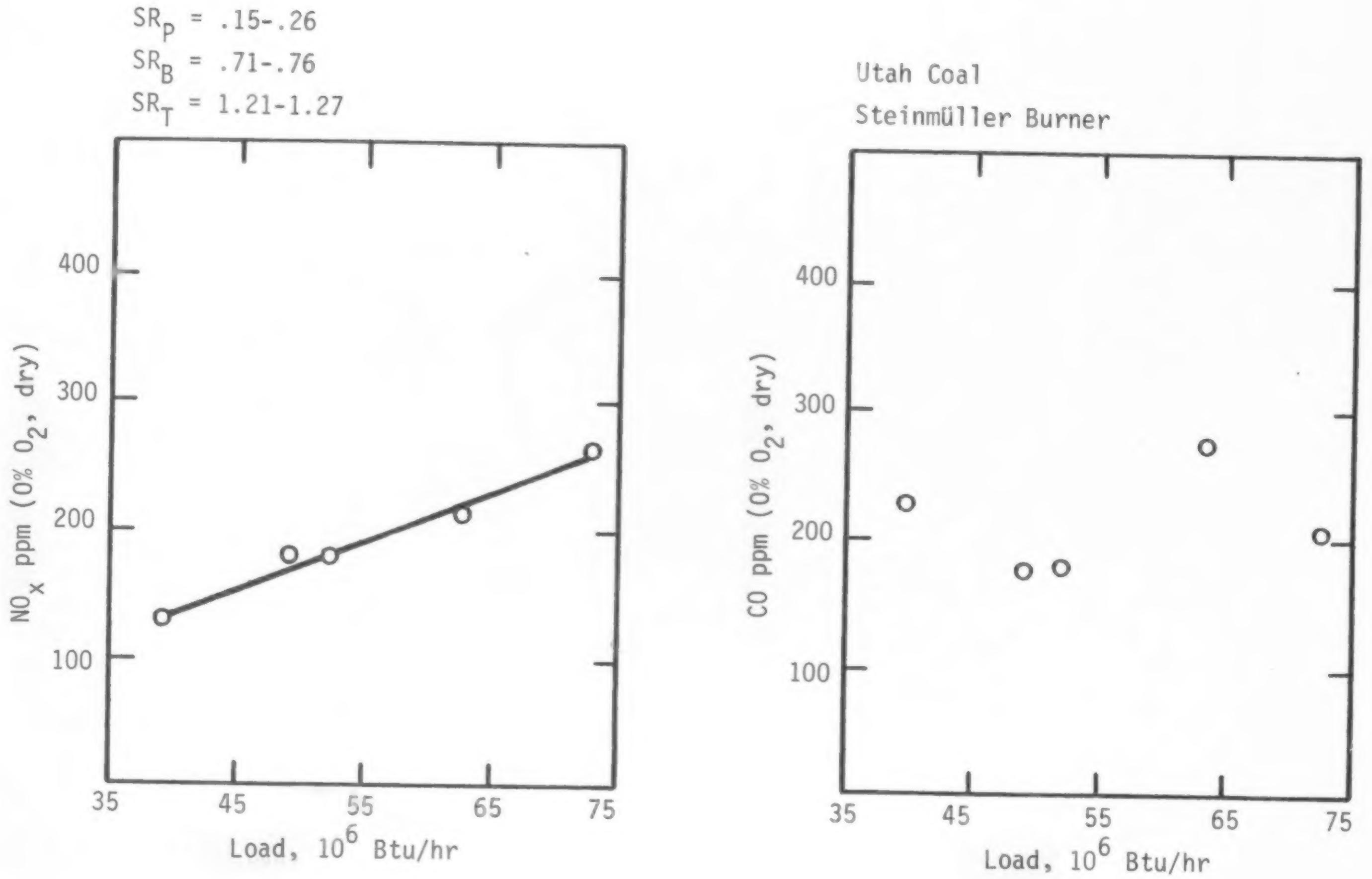

Figure 4-5. Effect of Burner Load on Emissions, Utah Coal

mode. At the burner nominal operating point ($SR_B = 0.75$), the NO_x emission is 190 ppm and CO typically 175 ppm. This CO level is higher than might be expected, but is nevertheless characteristic of the low furnace firing density employed. The CO level was found to remain relatively constant for the range of SR_B investigated while the trend in NO_x emissions is characteristic of burners of the distributed mixing type. Overall excess air level (Figure 4-4) varied in the range $SR_T = 1.3 - 1.45$ was found to have only a moderate effect on NO_x emissions while excess air levels below $SR_T = 1.1$ resulted in a significant increase in CO production. The influence of burner load on NO_x was also found to be moderate, resulting in an emission of 250 ppm (Figure 4-5) at the maximum load investigated of 72×10^6 Btu/hr (21 MW).

Indiana Coal

Experimental results for NO_x and CO emissions for the Indiana coal are presented in Figures 4-6, 4-7 and 4-8. It will be noted here that NO_x emissions are considerably higher (350 ppm at nominal conditions) than those observed for the Utah coal, despite a comparable fuel nitrogen content, and would tend to indicate a relatively strong coal effect. This difference has been observed also for other burners firing the Indiana coal. However, for burners of the distributed mixing type operating under optimum staged conditions, the limited data that are available (Figure 4-9) show no significant coal effect. This would seem to indicate that the present Steinmüller burner configuration is not necessarily the optimum for low emissions performance.

The effects of excess air and burner load are presented in Figures 4-7 and 4-8; in both cases, the magnitude of the effect is much stronger than that observed with the Utah coal.

Saar Coal

It was with the German Saar coal that the previously mentioned stability problems were most apparent; consequently, it was not possible to operate the burner at all desired operating points. At nominal staging conditions, it was necessary to overfire the burner in order to avoid high CO emissions. Thus, many of the basic data were obtained at a nominal input of 60×10^6 Btu/hr (17.6 MW). The data presented in Figures 4-10 through 4-12 are not entirely consistent with those for the other two coals tested. Nevertheless, some comparable trends are apparent in the data. Figure 4-12 shows the effect of

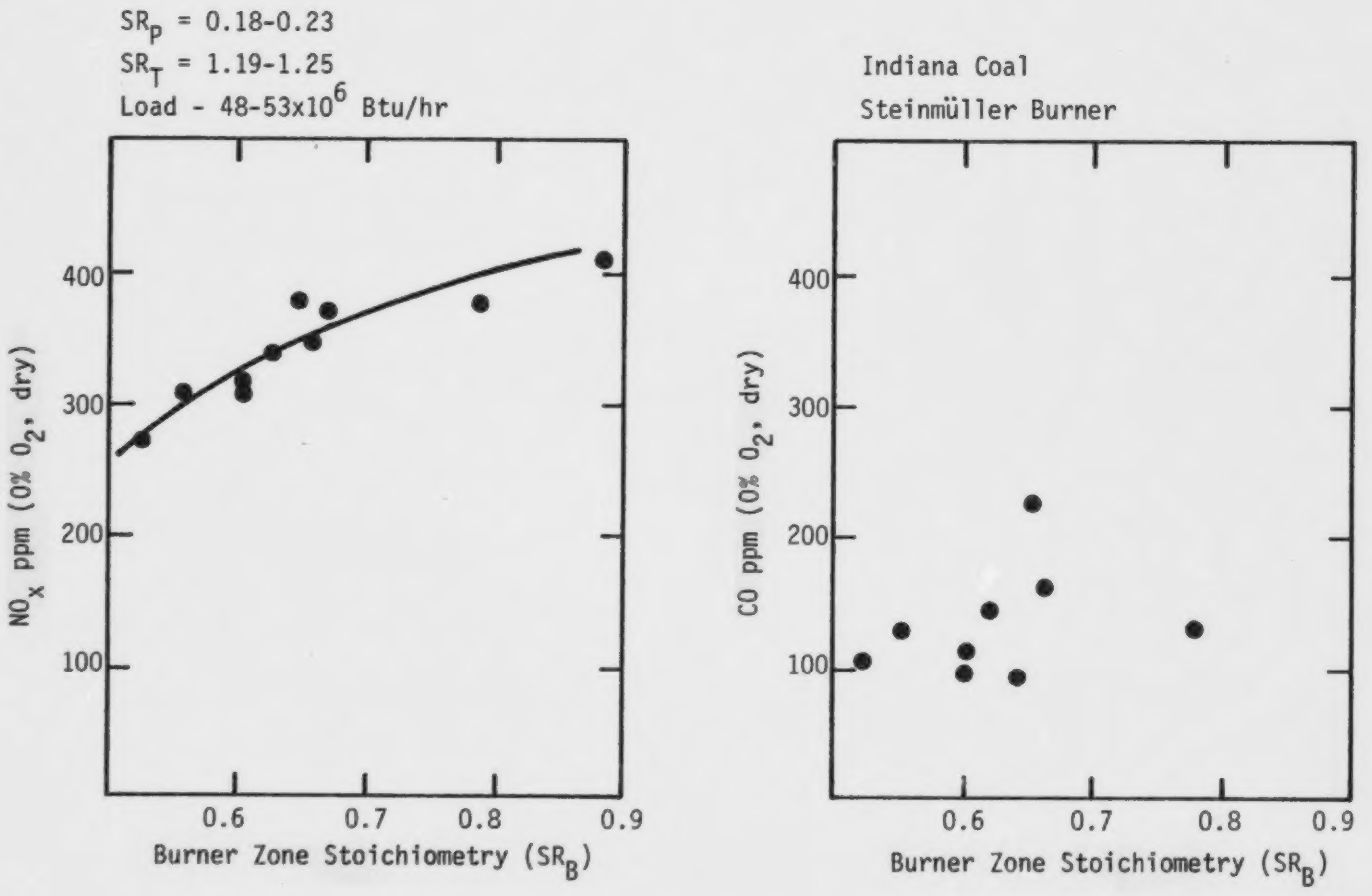

Figure 4-6. Effect of Burner Zone Stoichiometry - Indiana Coal.

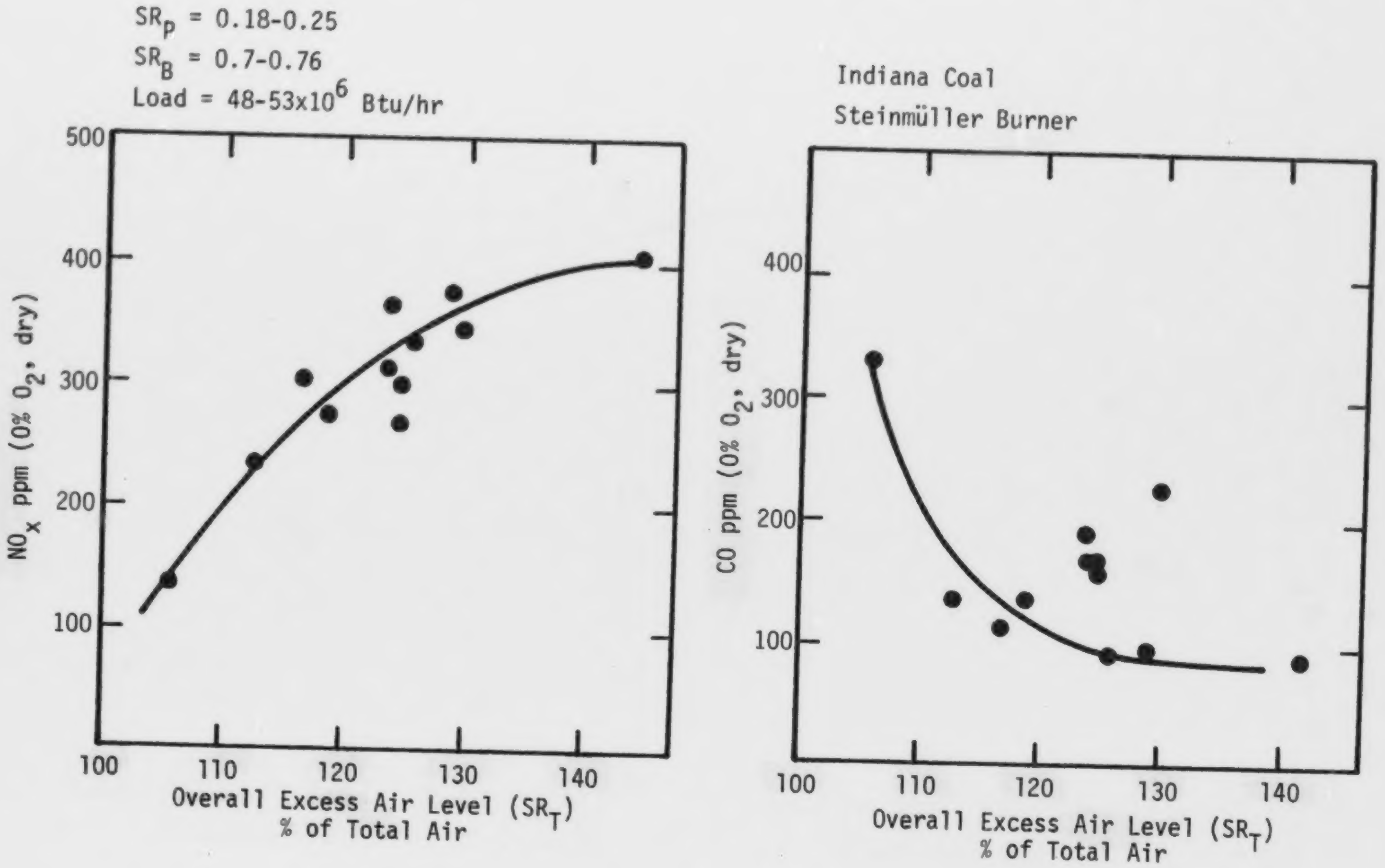

Figure 4-7. Effect of Excess Air, Indiana Coal.

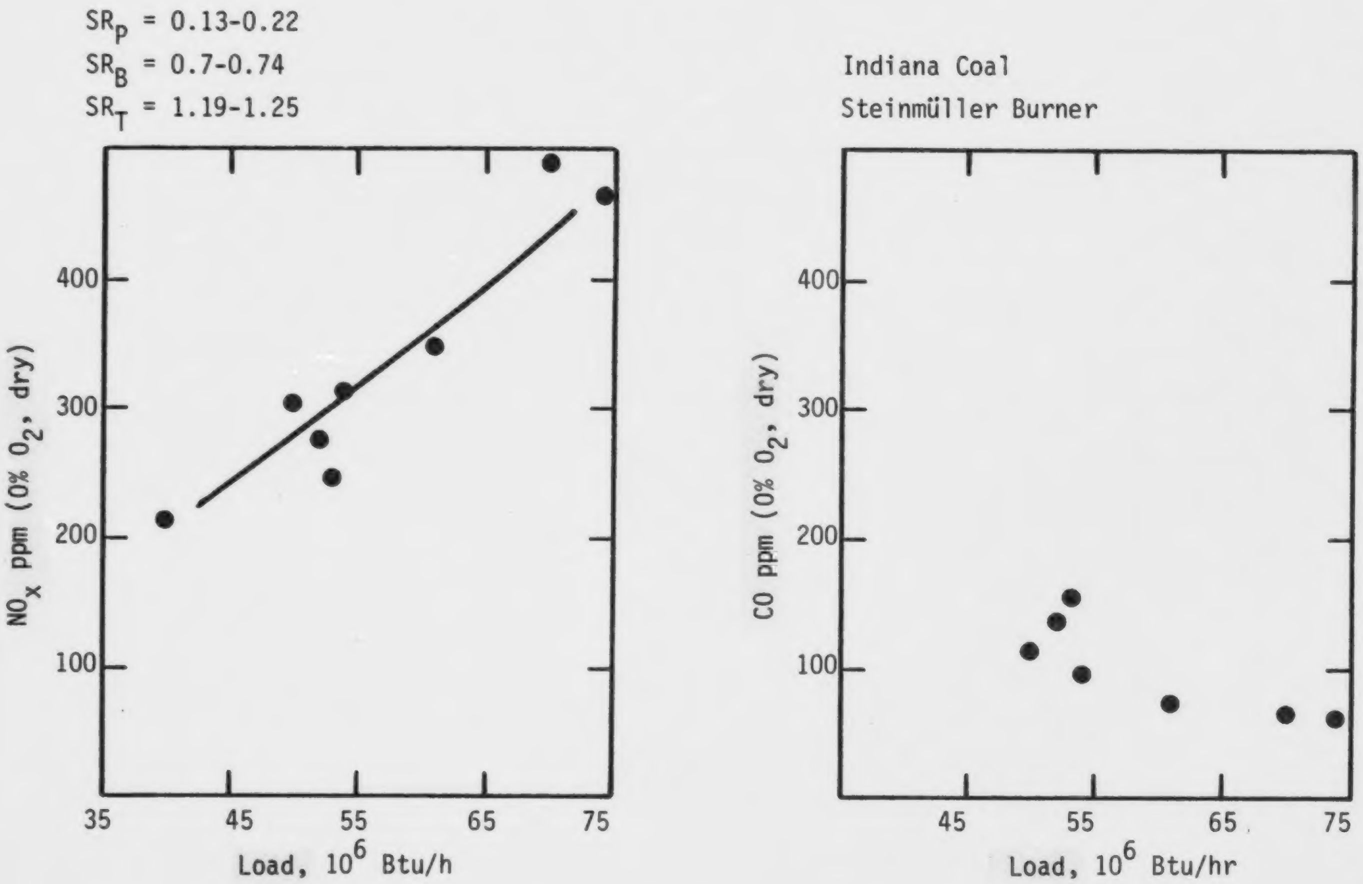

Figure 4-8. Effect of Burner Load, Indiana Coal.

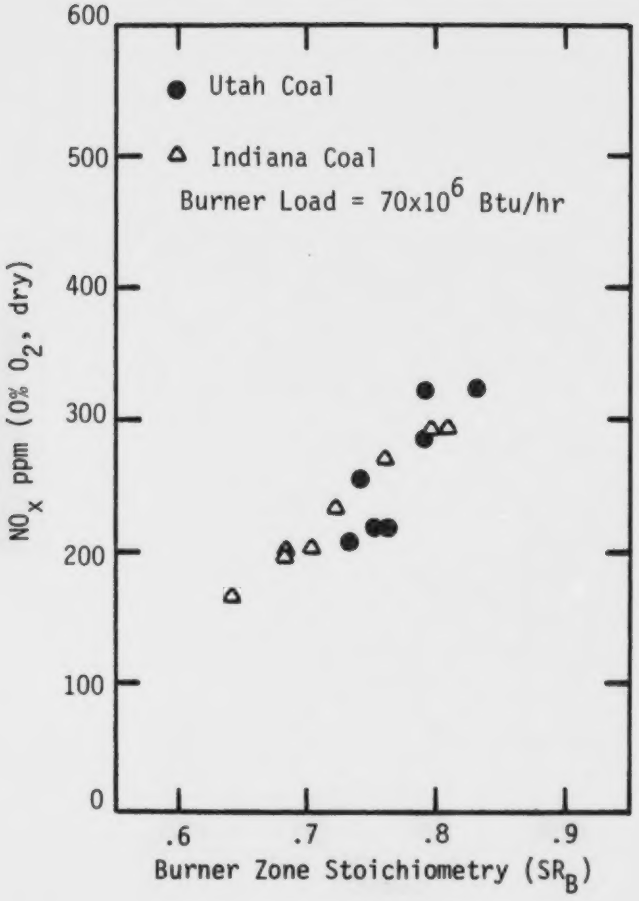

Figure 4-9. Effect of Coal Type - EPA Prototype 3 Burner.

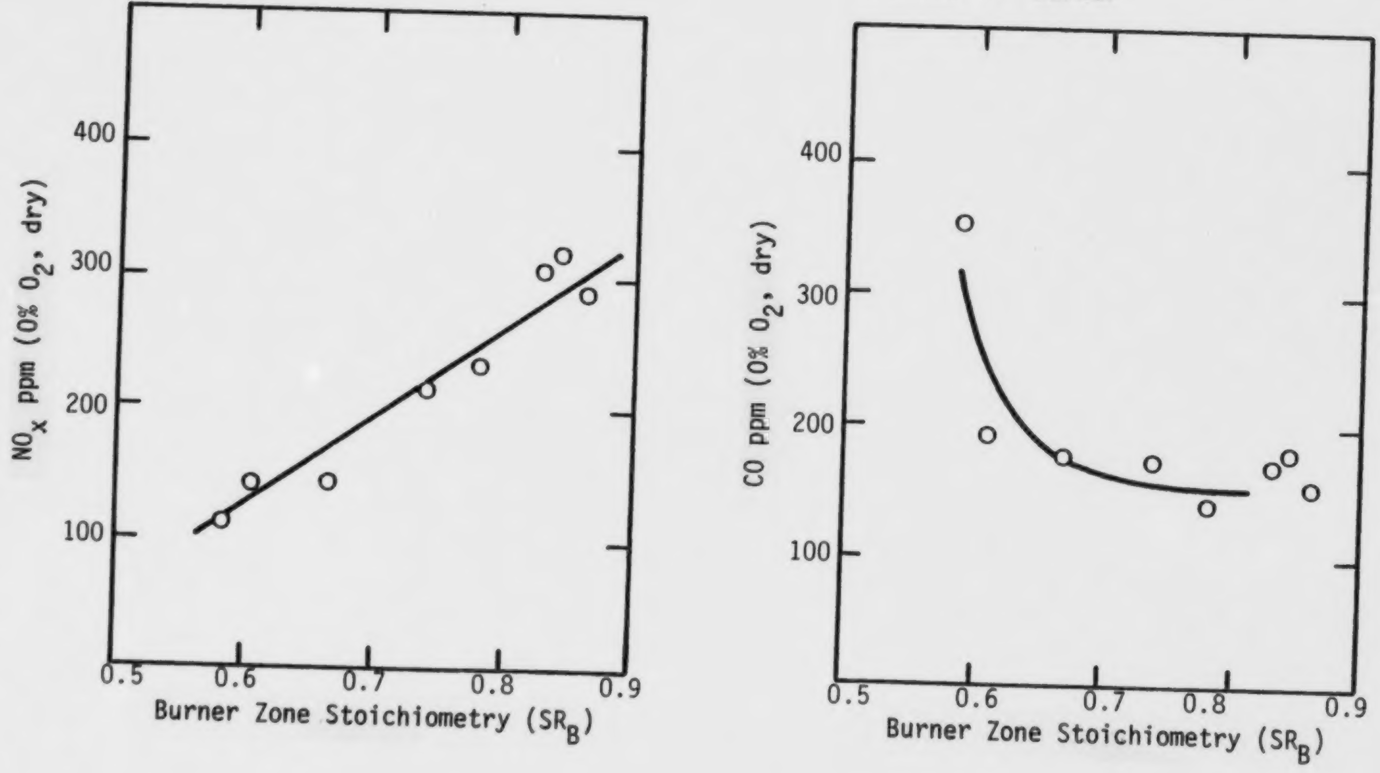

SR_T = 1.1-1.14
SR_p = .16-.2
Load = 58-62x10^6 Btu/hr

Saar Coal
Steinmüller Burner

Figure 4-10. Effect of Burner Zone Stoichiometry - Saar Coal.

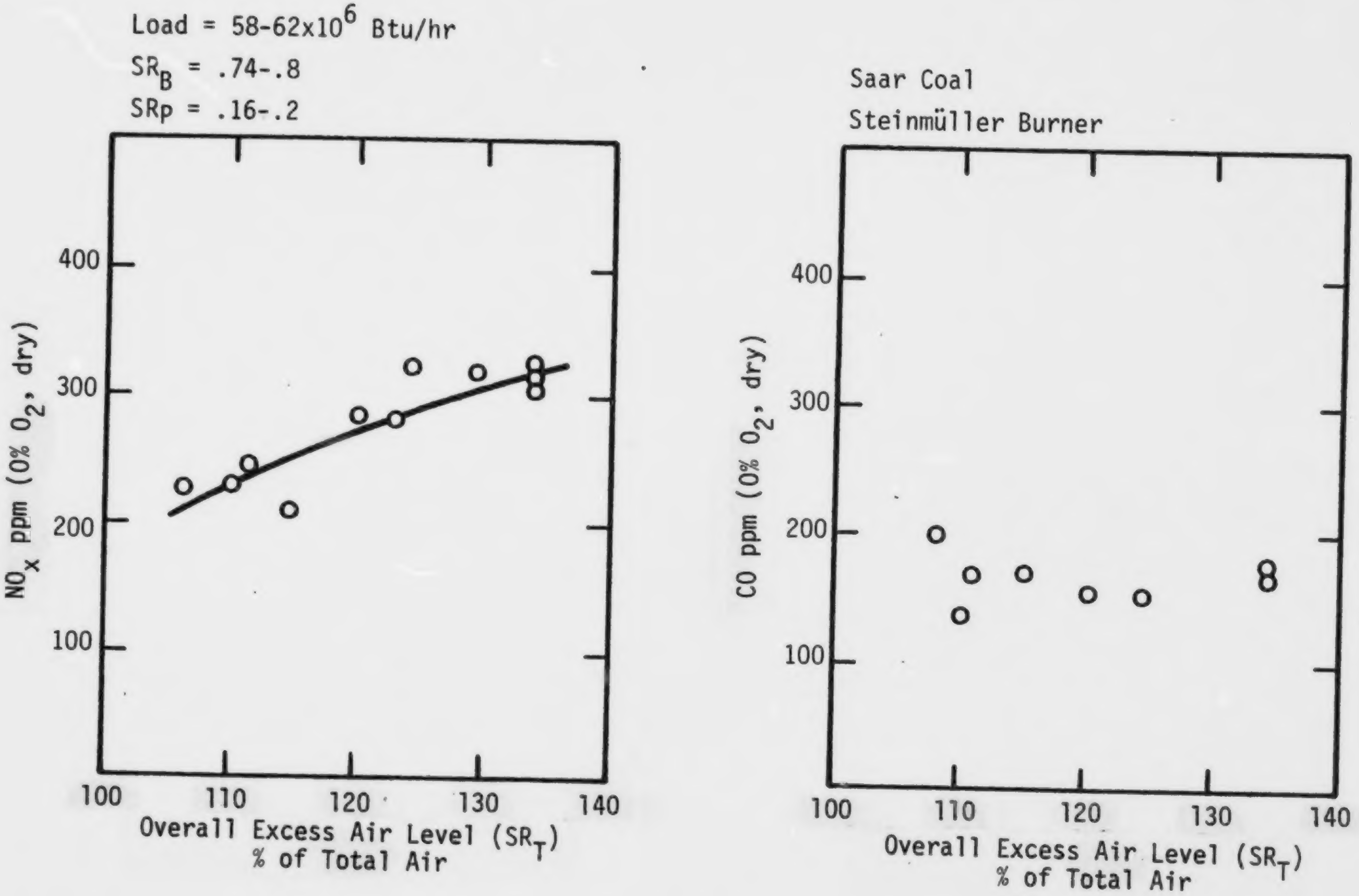

Figure 4-11. Effect of Excess Air, Saar Coal

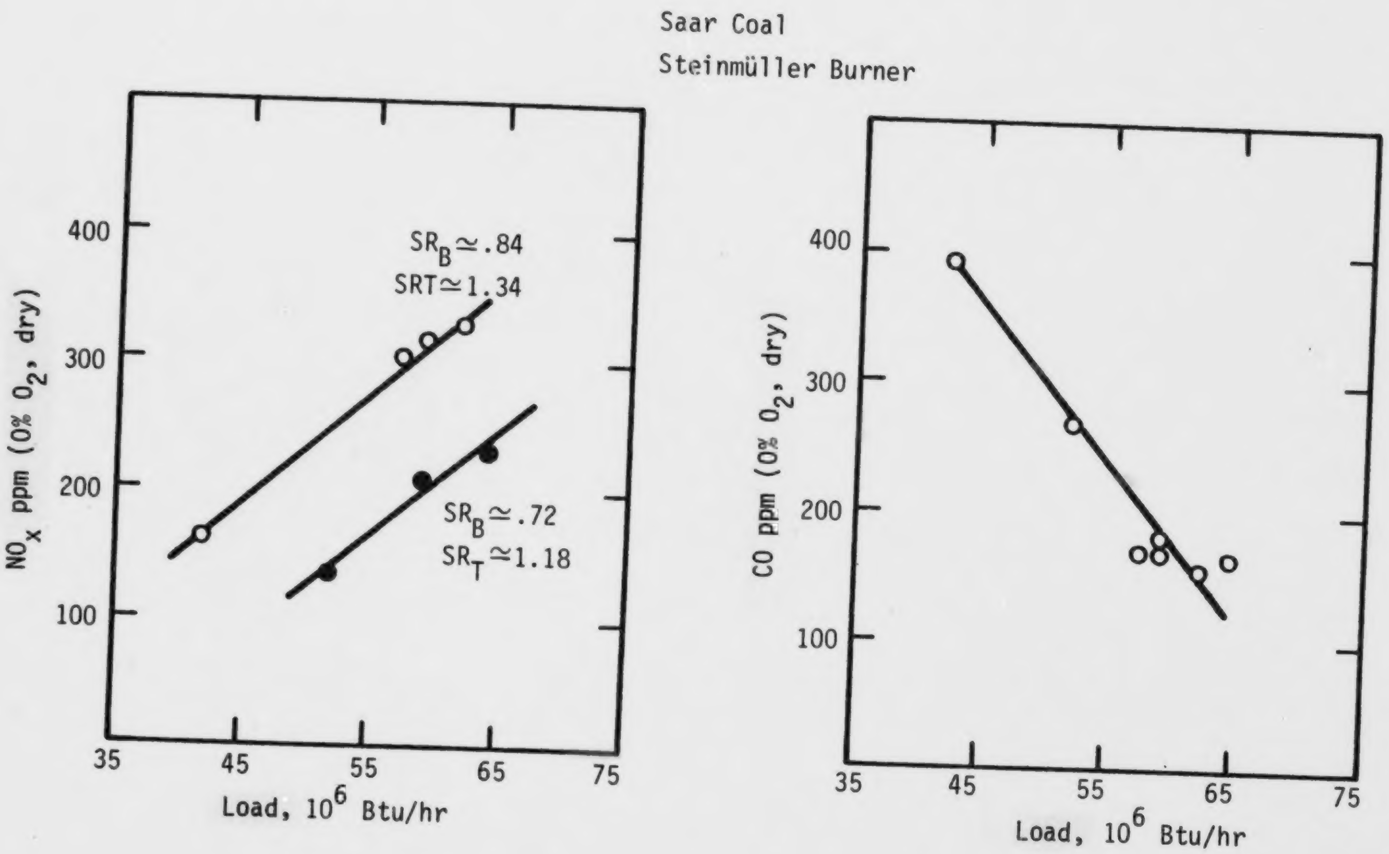

Figure 4-12. Effect of Burner Load, Saar Coal.

burner load on CO emissions. When the results are extrapolated back to nominal burner operating conditions at 50 x 10^6 Btu/hr (15 MW), an NO_x level of 180 ppm is suggested. This level is comparable with the data obtained for the Utah coal. It should be noted that the relative effects of both burner zone stoichiometry and excess air are also similar. The effect of increasing load is, however, much stronger than that observed for Utah coal, and is in fact more comparable to the trends seen with Indiana coal. It is not clear whether this trend is real or perhaps associated with flame stability.

4.1.2 Reduction of SO_2 by the Injection of Sorbents

In addition to the characterization of NO_x emissions, which represent the main objective of this study, a brief series of experiments was carried out in order to determine the potential for SO_2 removal by the direct injection of calcium-based sorbents. These studies were carried out without modification to the burner, and without optimization of conditions for sulfur capture.

In the SO_2 emission reduction studies the sorbent, either limestone or calcium hydroxide, was added to the coal prior to pulverization or was injected through the outboard staged air ports in suspension. In this second configuration, the sorbent was not mixed with the tertiary air stream, but added through separate injectors placed on the axis of the staged air ports.

Previous work on this subject has shown the need for careful design and control of sampling conditions in order to avoid the erroneous results obtained when hot flue gases are passed over solid particulate matter containing active sorbents in sampling probes. In this case, a specially designed sampling system, developed in small scale experimental work, was adapted for use in the LWS furnace system. This sampling system is shown in Figure 4-13. The essential component is a "phase discrimination probe" which aerodynamically separates gaseous and solid phases to avoid the problems normally associated with more conventional filter probes. From the sampling probe, the hot gases pass through a short heated sample line, without further treatment, directly into a Dupont NDUV continuous SO_2 analyzer. This sample system has been adopted by EER as the standard system for SO_2 monitoring in the presence of sorbents, and has shown good consistent performance when compared to wet chemical and other analytical techniques.

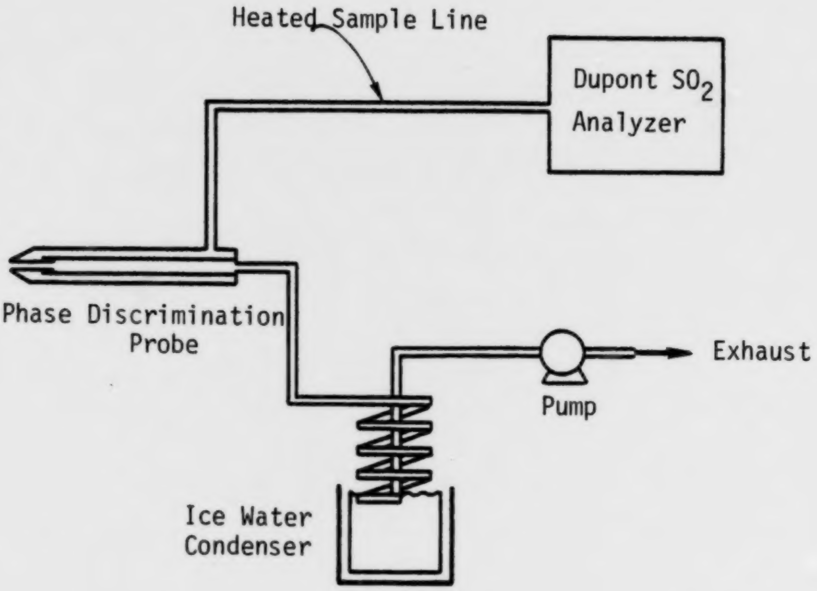
Heated Sample Line
Dupont SO_2 Analyzer
Phase Discrimination Probe
Exhaust
Pump
Ice Water Condenser

Figure 4-13. Schematic of the SO_2 Sampling System.

Sulfur capture values for this study are based on SO_2 emissions measured without additive and not upon expected sulfur dioxide concentrations based upon input sulfur content. This definition thus relates to SO_2 removal by the added sorbent and is desirable for two reasons. First, the distribution of sulfur in coal is not uniform and can vary with time during the course of an experiment, thus yielding a potentially wide range of "baseline" SO_2 emission levels. Second, still active sorbent can accumulate on cooled furnace surfaces and can lead to furnace inherent SO_2 removal in addition to that due to the directly injected sorbent. The amount of SO_2 removed in this way depends upon the nature and amount of the deposit and upon the local furnace conditions, and will thus vary with both experimental system and firing conditions.

Shown in Figure 4-14 are data which illustrate the effect of coal sulfur content on SO_2 removal when using $Ca(OH)_2$ sorbent. Sulfur capture with the two low-sulfur coals (Utah and Saar) is much less than for the higher sulfur Indiana coal. For the low-sulfur coals, sulfur capture appears to increase almost linearly with added calcium, and there is not a significant difference in capture when the sorbent is added either with the coal or in the tertiary air. For the high-sulfur Indiana coal, there is considerably more scatter in the experimental data and it would appear that tertiary air addition can, in some cases, results in a marginal improvement in sulfur capture. Figure 4-15 allows a comparison to be made between the effectiveness of $Ca(OH)_2$ and $CaCO_3$ as the sorbent. It is difficult to draw definitive conclusions from such limited data, although it appears that the hydroxide is more effective than the carbonate under these conditions.

4.2 Prototype Burner Tests

Tests were also conducted in the LWS using a 70 x 10^6 Btu/hr, EPA Distributed Mixing Burner (DMB) which incorporated Foster Wheeler commercial burner components. This burner, shown in Figure 4-16 without outboard staging air ports, is the prototype design for the WIPCO utility boiler under the EPA low NO_x demonstration program (68-02-3127). This design has an annular coal injector and dual annular secondary air passages with independent flow rate and swirl controls.

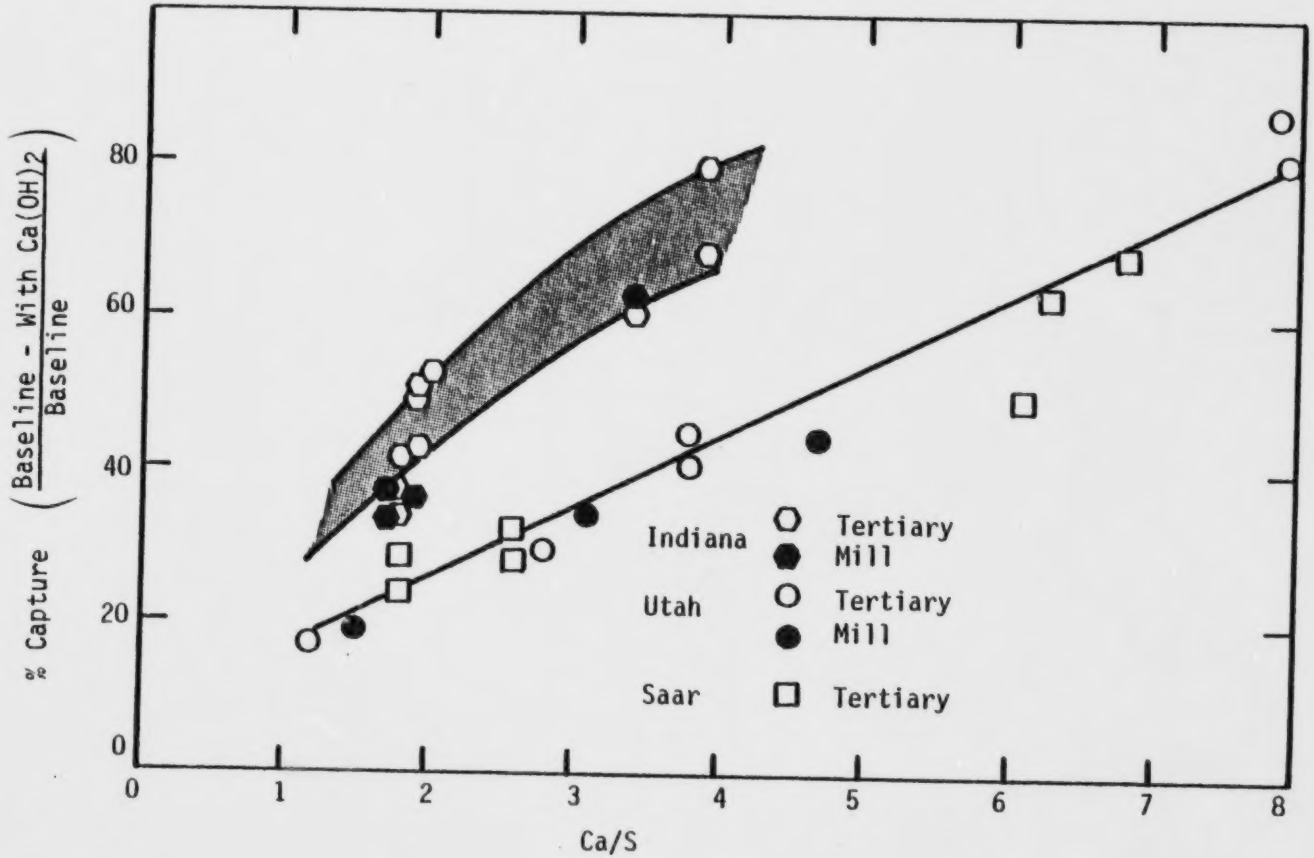

Figure 4-14. Comparison of Sulfur Capture for Two Coals Using Calcium Hydroxide as the Sorbent and the Steinmuller Low NO_x Burner.

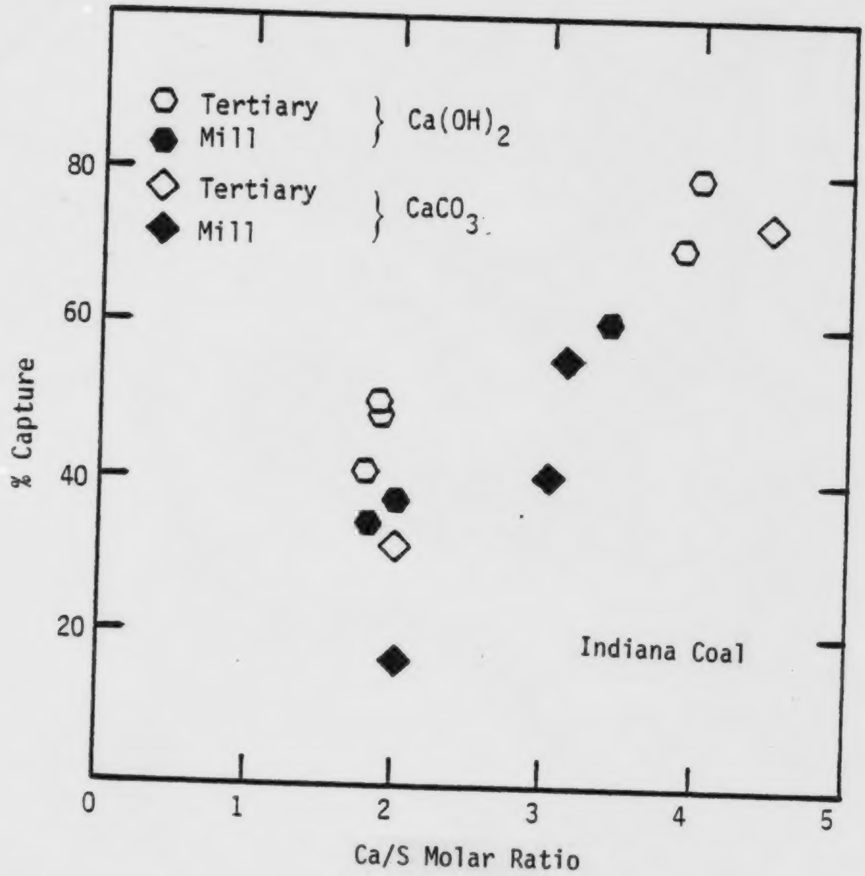

Figure 4-15. Comparison of Sulfur Capture with Calcium Hydroxide and Calcium Carbonate with the Steinmüller Burner.

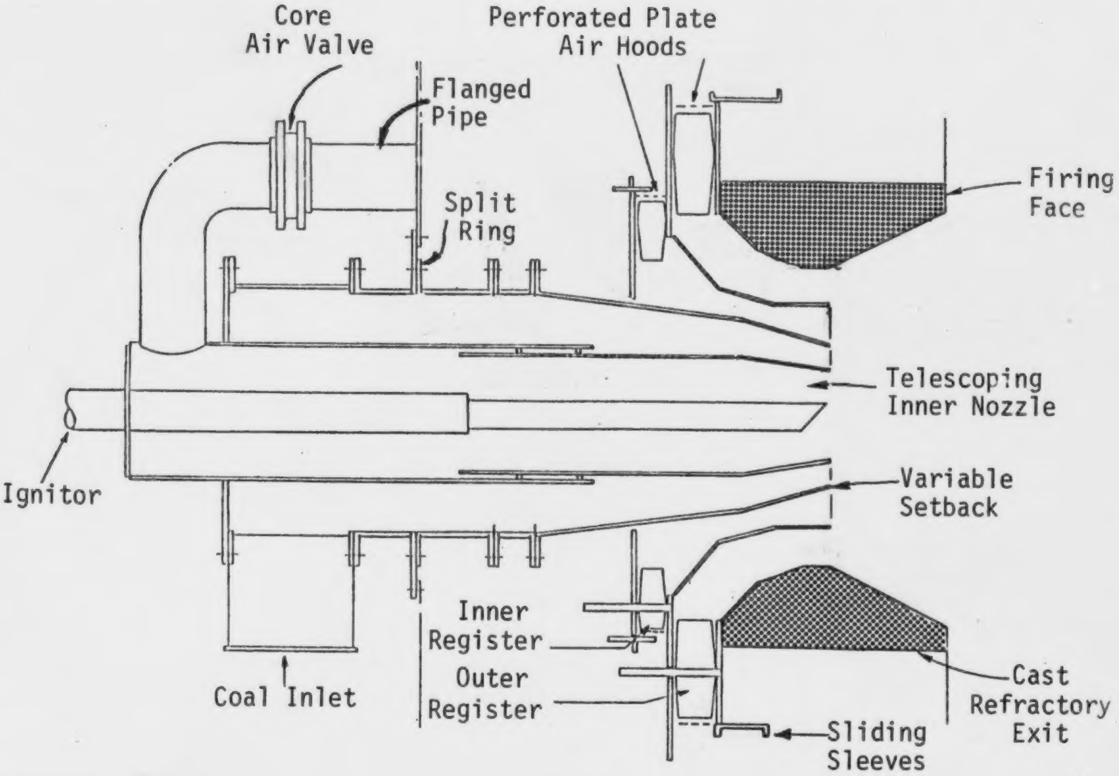
Core Air Valve
Perforated Plate Air Hoods
Flanged Pipe
Split Ring
Firing Face
Telescoping Inner Nozzle
Ignitor
Variable Setback
Inner Register
Outer Register
Coal Inlet
Cast Refractory Exit
Sliding Sleeves

Figure 4-16. EPA Prototype DMB with Foster Wheeler Burner Components (Tertiary Ports Not Shown).

The prototype burner was tested in the optimized low NO_x configuration developed for installation in the WIPCO boiler. The tests were conducted under Contract 68-02-3127. Figure 4-17 summarizes the NO_x emissions for this test series. Note that there is essentially no fuel effect on NO_x emissions for these two fuels.

While the prototype DMB was installed in the LWS for NO_x emission optimization under 68-02-3127, a brief series of tests was conducted under this contract to characterize the potential for SO_2 removal via dry sorbent injection. Two basic injection configurations were utilized: sorbent mixing with the coal prior to pulverization, and sorbent injection through the tertiary air ports. As in the Steinmüller burner tests, the sorbent was not distributed in the tertiary air; rather, the sorbent injection nozzle was located on the tertiary air port axis. Limestone was the only sorbent used for this limited test series.

Figures 4-18 and 4-19 show that the sulfur capture results achieved with the two injection configurations were comparable. The figures also show that a variation of one of the sorbent introduction methods (i.e., sorbent injection through only the two lower tertiary air ports) resulted in higher sulfur capture. This configuration was tested for practical reasons; the WIPCO boiler arrangement is such that it will be impossible to inject sorbent through all four tertiaries, but it may be possible to introduce the sorbent through the lower two ports. Initially, the higher capture values attendant with this configuration were attributed to a T(t) effect resulting directly from the fact that the sorbent had to pass through the entire flame zone. To further study this effect, a test was conducted in which sorbent was injected through only the top two tertiary ports. Surprisingly, sulfur capture for this test was comparable to that for lower tertiary injection. The explanation currently offered for this phenomenon is that the effect is directly dependent on the injection velocity. During the two port injection studies, the same sorbent/transport air ratio was employed, but the injector area was halved, resulting in higher injection velocities. These higher speed jets are characterized by significantly increased entrainment of hot combustion gases from the flame zone. Thus, the effect is attributed to the T(t) history, but not in the direct sense originally thought.

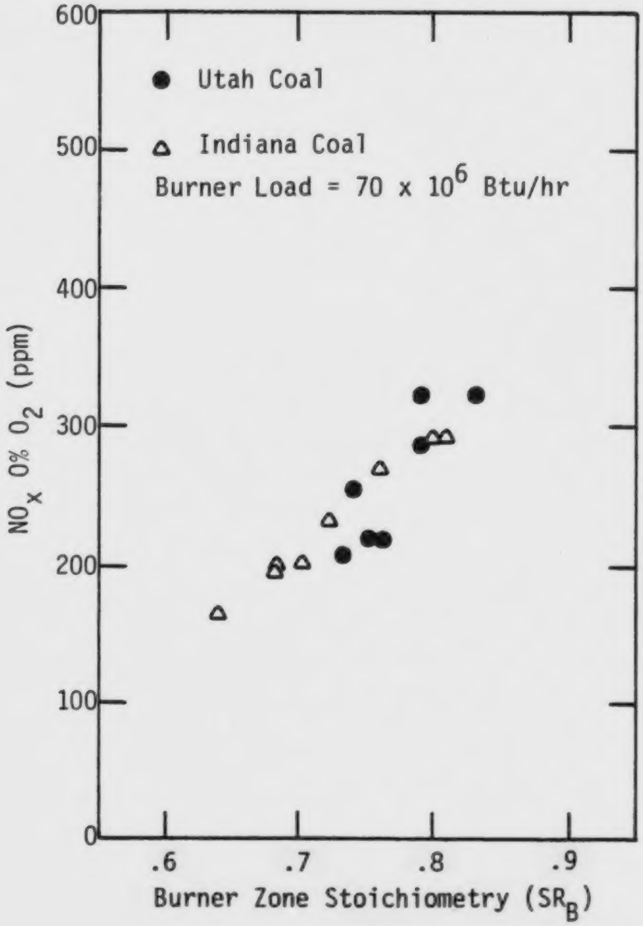

Figure 4-17. Prototype DMB NO_x Emissions.

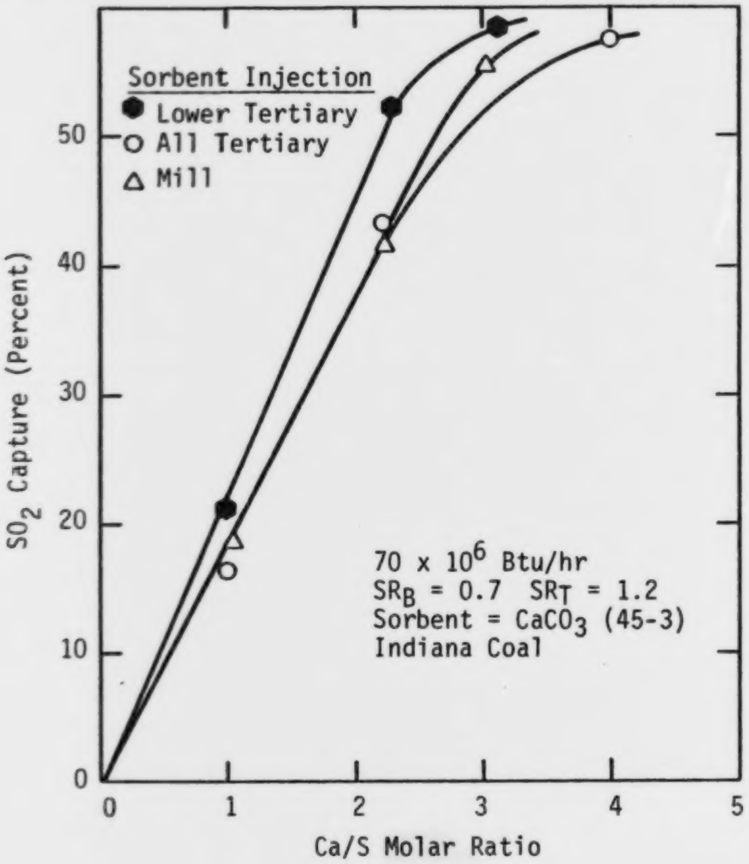

Figure 4-18. Effect of Sorbent Injection Location - EPA Prototype DMB, Indiana Coal.

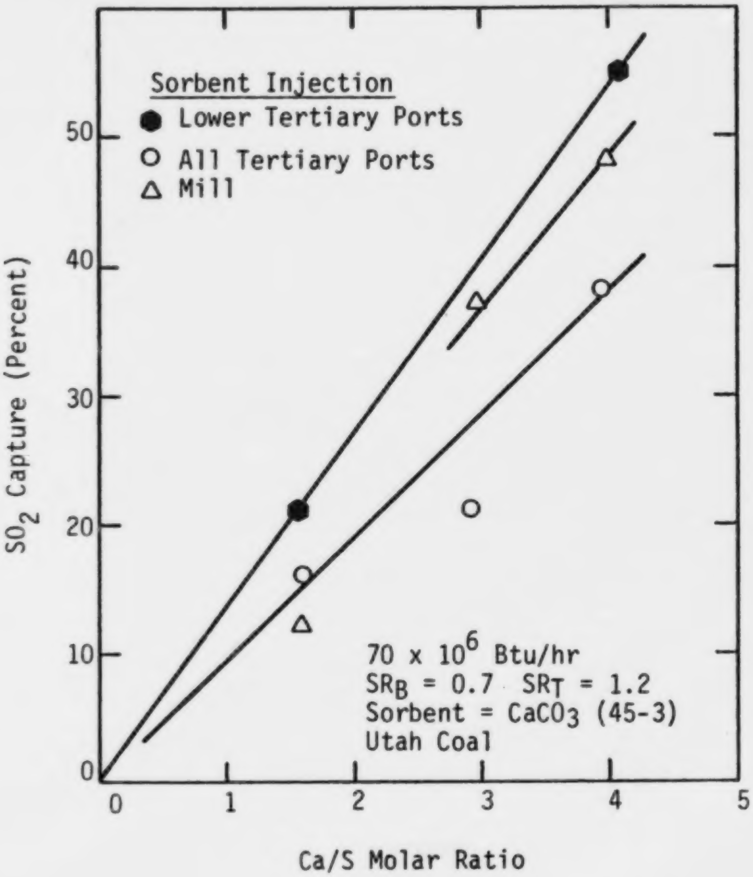

Figure 4-19. Effect of Sorbent Injection Location - EPA Prototype DMB, Utah Coal.

For the prototype burner tests, the sulfur capture results were verified by performing sulfur balances. Figure 4-20 shows that sulfur balances conducted from flue gas analysis and fly ash analysis agreed very well; therefore, a high level of confidence is attached to these results. Figure 4-20 also points out that the sulfur capture rates achieved with the Indiana coal were higher than those noted with Utah coal. This is consistent with observations of previous studies in which higher sulfur capture values are noted with higher sulfur content coals.

4.3 Comparison of Results

Data are available from a number of sources against which the present results can be compared to provide some insight into the relative performance of different burners at different scales, and how small and pilot scales results relate to full scale. For the Steinmüller burner, data are available both from the pilot scale development tests carried out at the IFRF in a 2.3 MW (7.8 x 10^6 Btu/hr) furnace, and from the field boiler (Weiher boiler) which was retrofitted for staged combustion. In both cases, the fuel fired was the German Saar coal. Also, the results of the Steinmuller and EPA prototype DMB tests can be compared.

Results from the different facilities showing the effect of burner zone stoichiometry for the Steinmüller burner are compared in Figure 4-21. Here it can be seen for the three facilities, Weiher boiler, IFRF furnace, and LWS, that although the absolute levels of NO_x emissions are different, the relative trends are comparable. Shown also are some results obtained with the Saar coal on a small 70 x 10^3 Btu/hr (20 kW) bench scale furnace with a premixed burner. There also, despite the significantly different system configuration, the relative effect of staging is comparable for $SR_B > 0.7$. For $SR_B < 0.7$, NO_x emissions show a characteristic upturn. Shown in Figures 4-22 and 4-23 are the effects of overall excess air and burner load on NO_x emissions, where again trends are comparable for the three different facilities.

As a general conclusion, the fact that relative behavior can be reproduced for similar equipment fired in different facilities is well known, and burner manufacturers have found that when two burners are tested in a research facility (such as the LWS), the ratio of NO_x emissions measured in the test facility, under comparable conditions will be comparable to the ratio of emis-

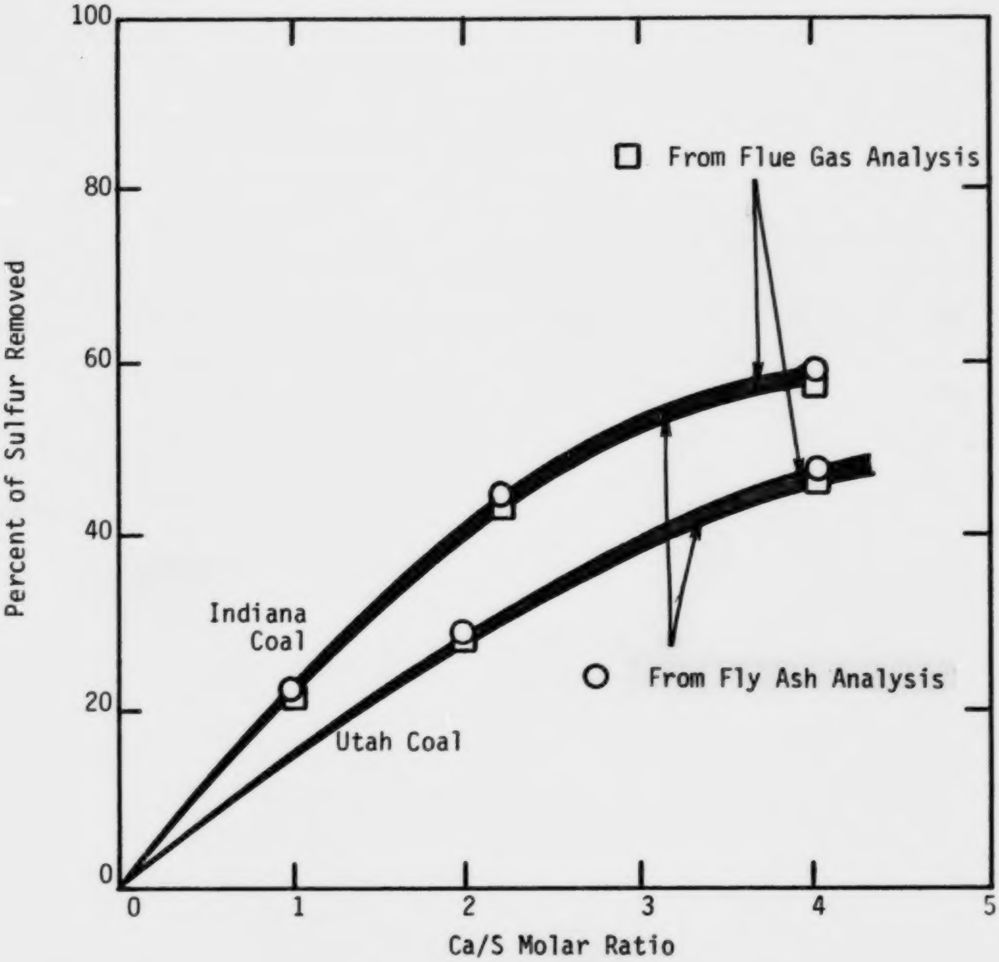

Figure 4-20. Sulfur Balance - EPA Prototype DMB, Limestone Injected Through All Four Tertiary Ports.

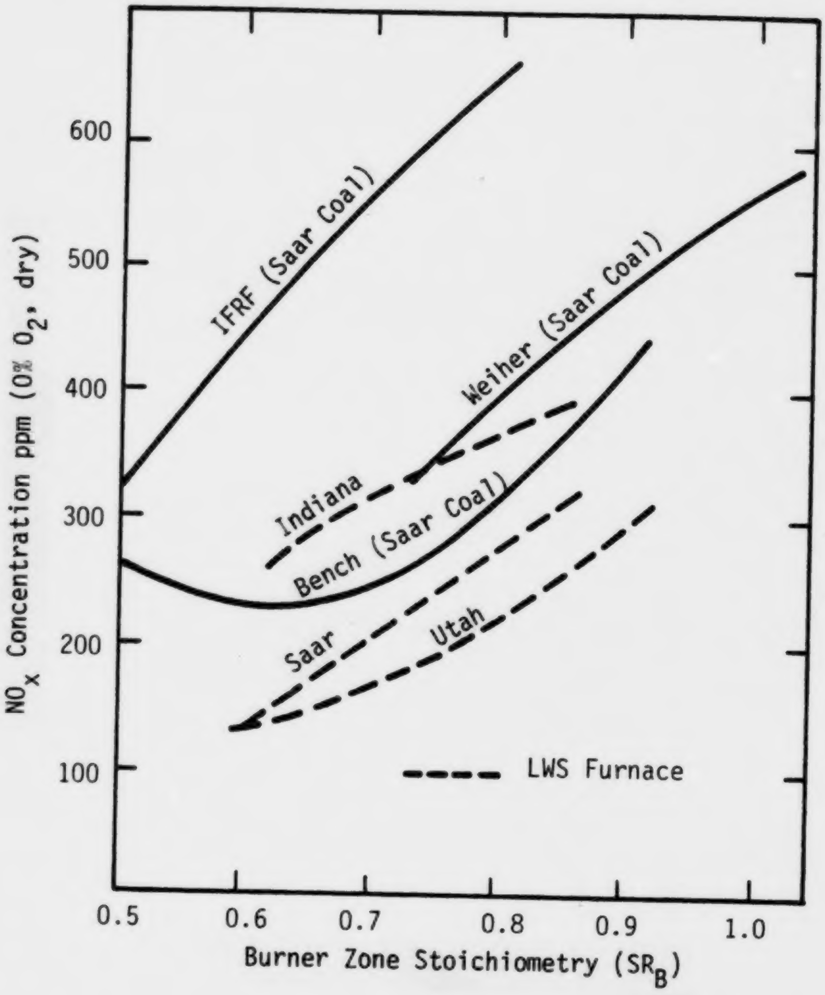

Figure 4-21. Effect of Burner Zone Stoichiometry on NO$_x$ Emissions ~ Comparison of Data, Steinmüller Burner.

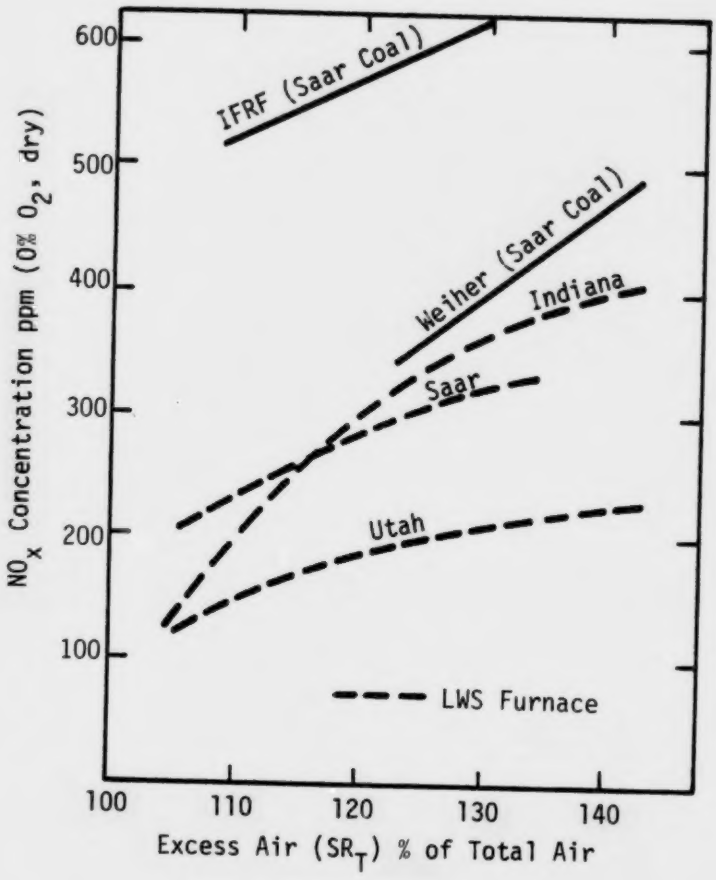

Figure 4-22. Effect of Excess Air on NO_x Emissions - Comparison of Data, Steimuller Burner.

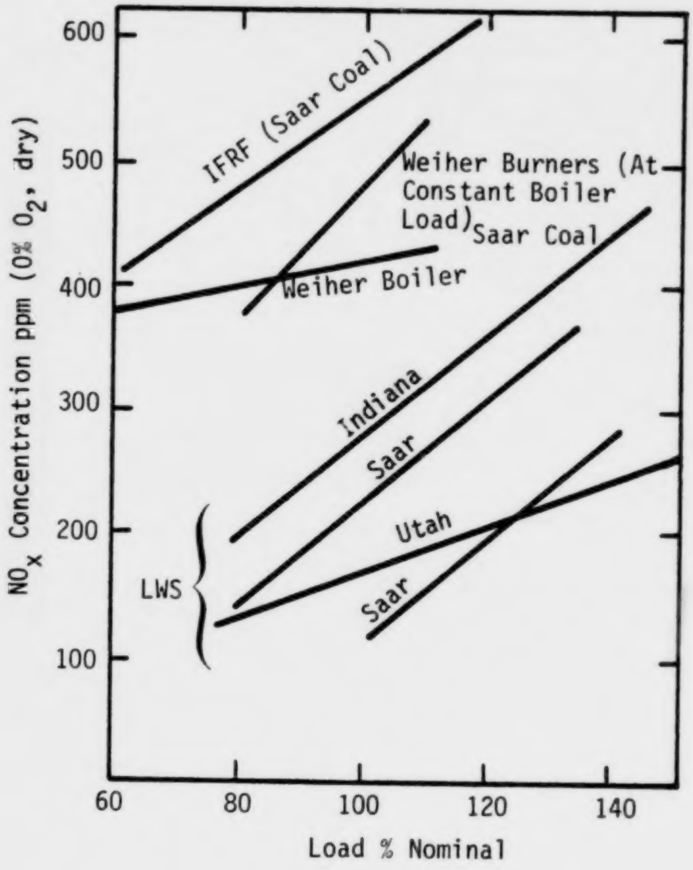

Figure 4-23. Effect of Load on NO$_x$ Emissions ~Comparison of Data, Steinmüller Burner.

sions when operated in field conditions. This knowledge can thus be used to translate experimental data to field conditions, providing some baseline comparison is available.

The results of Figures 4-21 through 4-23 show that the absolute emission levels are clearly different for the different facilities. Under approximately similar burner conditions, NO_x levels are 600 ppm in the IFRF furnace, 350 ppm in the Weiher boiler, and 230 ppm in the LWS. It is not clear whether these differences relate to burner scaling or to differences in the thermal environment, or to a combination of both.

In scaling the Steinmüller burner for the various tests, a hybrid approach has been taken which is a compromise between constant velocity, geometry and residence time scaling. In this approach, burner throat velocities are maintained constant since this maintains burner pressure drop and minimum p.f. transport velcoity, and quarl length is varied (longer at the smaller scale) to compensate for different residence times in the near burner region. There is, however, insufficient scale related information on this type of approach to permit a determination of how this might affect NO_x emissions. Some data have been generated which indicate that an increase in quarl length, for a given burner and input conditions, results in an increase in NO_x emissions, and this may go some way towards explaining differences observed in the different scales.

In terms of the effect of thermal environment, there are again some differences between the different systems, which might influence both burner performance and NO_x emissions. Because of surface to volume ratio considerations, small scale furnace systems must operate with a considerably increased wall temperature in order to preserve comparability of overall heat extraction. In the IFRF furnace, for example, wall temperatures are typically 900 - 1000°C compared to the approximately 600°C of operating boilers. In the tests carried out in the LWS furnace, the flue gas (furnace exit) temperature was typically 1420°F (770°C) which is somewhat cooler than the 1000 - 1100°C of the IFRF furnace and the field boiler, and is indicative of a much colder furnace environment. This might be expected to result in lower emissions of NO_x, particularly of the thermal component. However, results for the EPA prototype DMB burner system fired in the old (heavily cooled) LWS furnace and in the new (partially refractory-lined) LWS furnace are presented in Figure 4-24 and show that firing in the higher temperature furnace results in comparable NO_x emission levels. Additional data included in Figure 4-23 illustrate the two types of load effect observed in the Weiher boiler. In one case, the load variation is achieved by allowing total boiler load to change, and in the other case, boiler load is held constant and burner load varied by using more or fewer burners for the same total output. It is clear from these results that the effect of burner variables (in this case, principally burner velocity) is much stronger than the thermal effect achieved by varying total boiler conditions.

The Steinmüller sulfur capture results may be compared to recent studies carried out with a pilot-scale (2.5 MW) version of the Steinmüller burner in the IFRF experimental furnace. A summary of the results of this study is given in Figure 4-25, and shows that substantially higher SO_2 removal levels were achieved under comparable burner input conditions. Experimental data which have been obtained to date concerning the effect of parameters on SO_2 removal suggest that thermal considerations are of primary importance and that higher temperatures (typically >1200°C) lead to lower SO_2 capture efficiencies due to "dead-burning" of the sorbent. In light of these results, one would, therefore, expect lower capture values from the IFRF furnace (exit temperature 1000-1100°C) than from the LWS furnace (exit temperature 770°C). That the IFRF data show the reverse trend would seem to indicate that in larger scale systems operating with practical combustion equipment, there are parameters other than those of a purely thermal nature which can influence sulfur capture independently. The understanding of the physical and chemical mechanisms involved in the sulfur capture process is the subject of much current on-going research, both at bench-scale and in large pilot-scale systems such as the LWS furnace.

Figure 4-26 summarizes results from the Steinmüller and EPA prototype DMB burners in several furnaces; results from Steinmüller tests in the LWS and in the IFRF furnace are included along with LWS and BSF test data from the prototype burner. Several observations can be made regarding these data. First, the BSF data (BSF operation was at conditions selected to match the flue gas

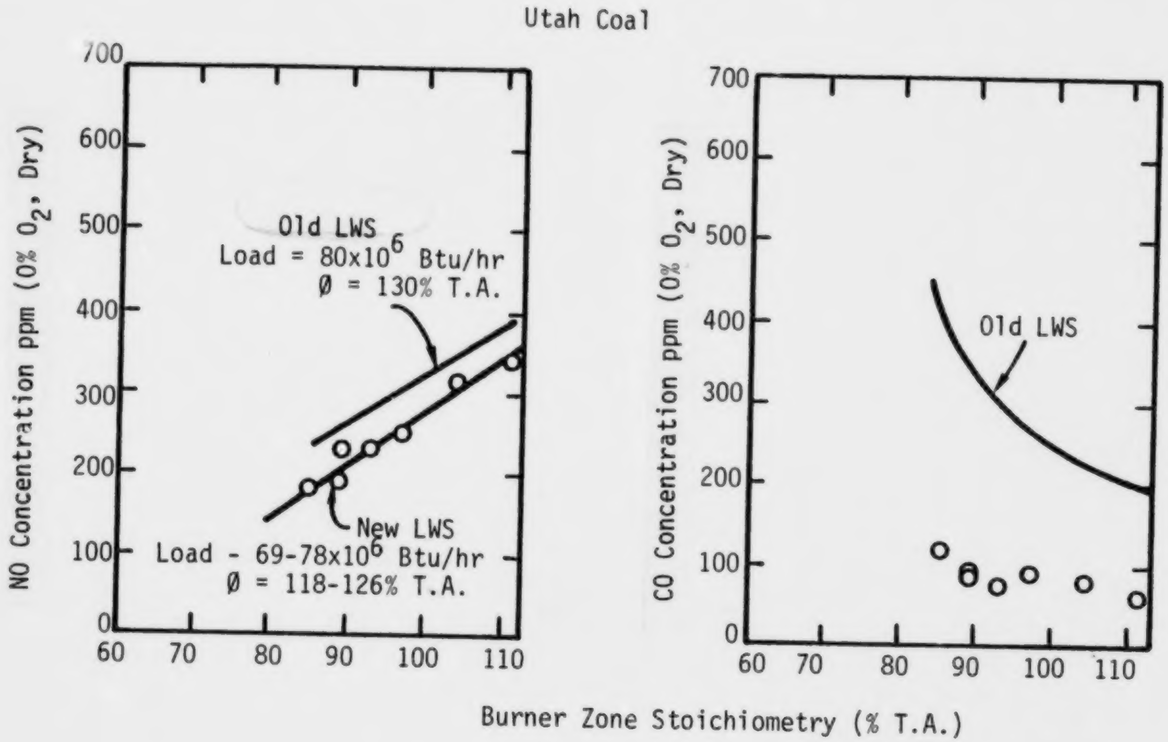

Figure 4-24. NO_x and CO Emissions for the EPA Prototype DMB Fired in the LWS Furnace.

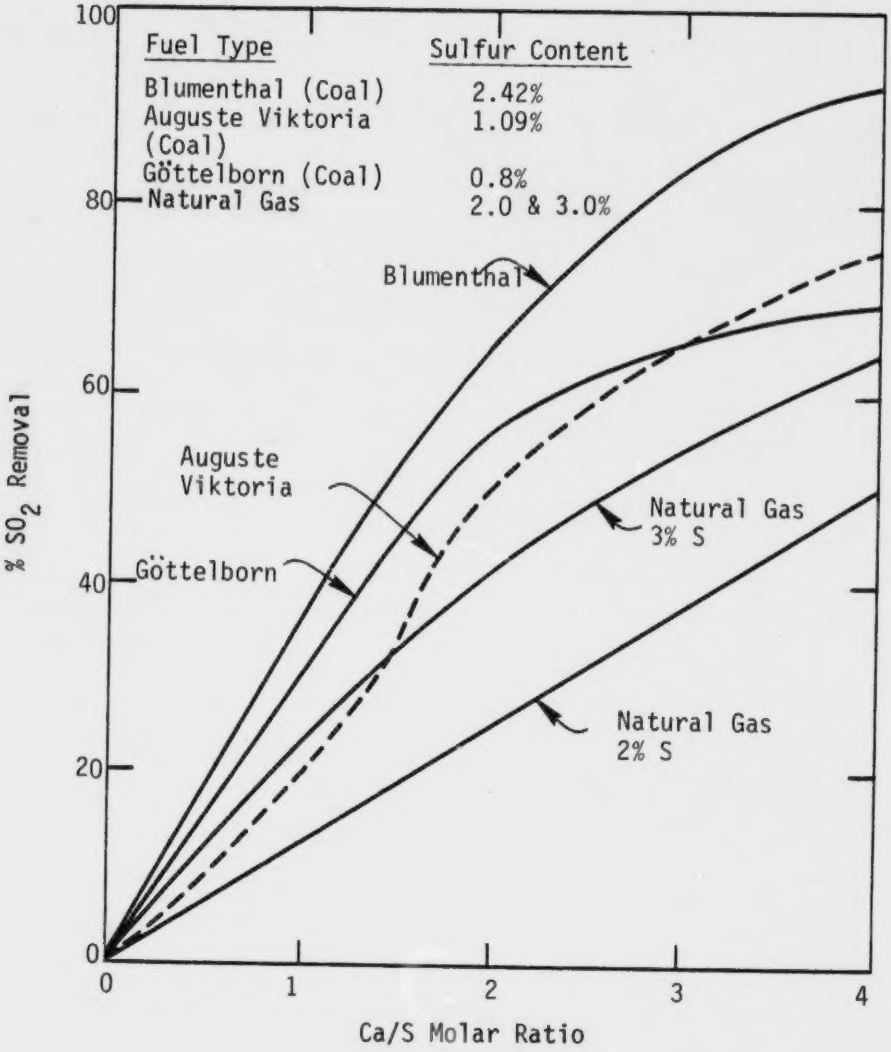

Figure 4-25. Summary of Results Obtained with the Steinmüller Burner in the IFRF Furnace.

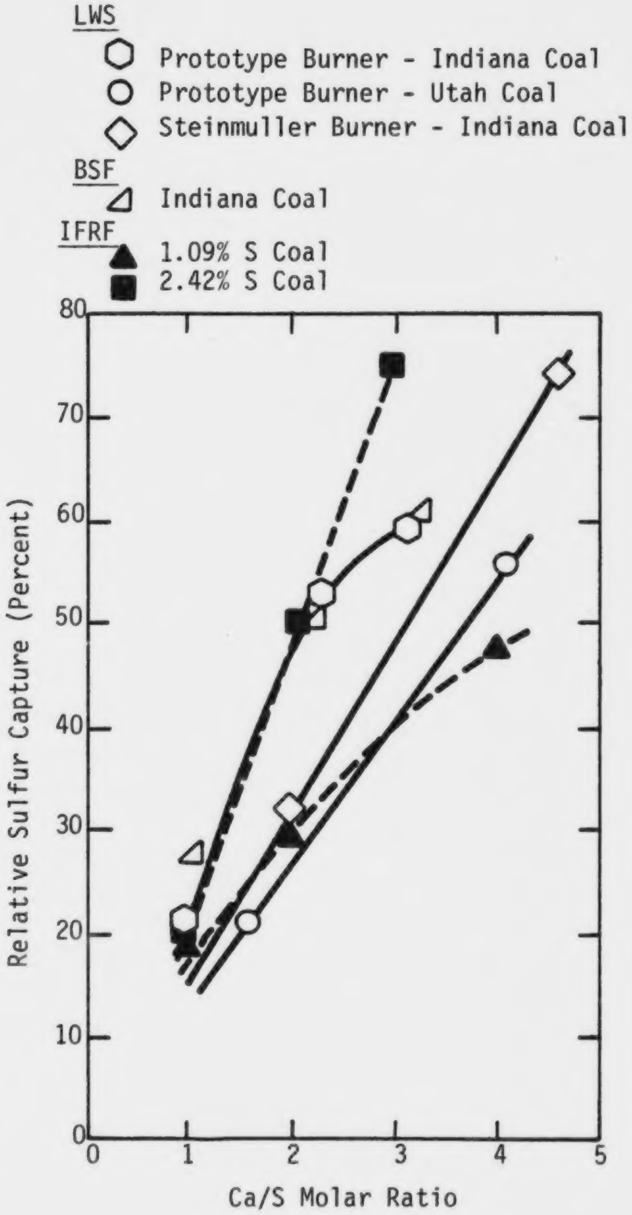

Figure 4-26. Comparison of Steinmuller and DMB Data - Limestone Injected in Tertiary Ports.

temperature and mean residence time of the LWS tests) show good agreement with the LWS data for Indiana coal. Both of these tests showed results in agreement with the high-sulfur coal IFRF data. This is surprising in light of the high furnace temperature employed at IFRF. At the present time, no explanation has been offered for this phenomenon.

Comparing the prototype and Steinmüller LWS results with Indiana coal, it is seen that the prototype burner resulted in higher sulfur capture even though the burners were operated at comparable conditions. This is perhaps indicative of the influence of burner design conditions, although it should be noted that neither burner was optimized for SO_2 capture for these tests. Finally, the prototype burner LWS results with Utah coal and the low-sulfur coal IFRF test results show good general agreement. This indicates that burner effects may be unimportant for low-sulfur coals; again, these results are from burners which were not optimized for SO_2 capture and, therefore, should be treated with caution.

In general, the pilot-scale tests indicate the need for more definitive assessments of the parameters controlling SO_2 capture via dry sorbents. Specifically, studies should focus on the potential for application of this technology in field boilers, and the optimum burner design and operating parameters required to maximize sulfur capture without affecting NO_x emissions or boiler efficiency.

5.0 THE COAL/SULFUR/SORBENT SYSTEM IN PULVERIZED FUEL COMBUSTION: EVOLUTION, OXIDATION AND RETENTION OF SULFUR

The mechanisms of sulfur pollutant formation in a pulverized coal furnace are inextricably intertwined with the mechanisms of coal combustion. A global view of coal sulfur shows that the sulfur introduced into the furnace will ultimately end up as a gaseous emission--either SO_2 or SO_3 or as part of a solid compound retained in the boiler or associated with the flyash. The sulfur introduced to the furnace is essentially all in reduced sulfur compounds while the sulfur leaving the furnace, whether gas or solid, is oxidized. The direct injection of alkali metal sorbents into the pulverized fuel (pf) furnace is intended to increase the proportion of sulfur in the solid phase at the furnace exit.

The reactions involved in the oxidation of coal sulfur and the reactions which govern the ultimate phase of the sulfur are exceedingly complex and are by no means well understood. The following section is an overview of the current understanding of the factors affecting sulfur oxidation and retention in pulverized coal fired furnaces. The basic mechanisms of sulfur evolution and oxidation are discussed; then the complication of dry sorbent/sulfur interaction is addressed. The information presented is extracted from a number of excellent reviews of coal combustion mechanisms, coal sulfur interactions and sulfur sorbent interactions. This section is not intended to be an exhaustive review of the subject and the interested reader is directed to the review articles referenced.

As mentioned earlier, the mechanisms of sulfur oxidation and retention in a pulverized fuel furnace with or without the complication of added dry sorbents cannot be separated from the basic mechanisms of coal combustion. Figure 5-1 is a schematic illustration of the basic processes occurring during pulverized coal combustion. The illustration is extremely simplistic and is offered as a conceptual guide only. The addition of solid sorbents into the combustor complicates the sulfur chemistry throughout the system. The basic interactions of these solid sorbents with the sulfur is included in the cartoon. Calcium carbonate is used only as an example of an alkali metal sorbent--the basic interactions illustrated are applicable to other dry sorbents (such as magnesium or sodium based carbonates).

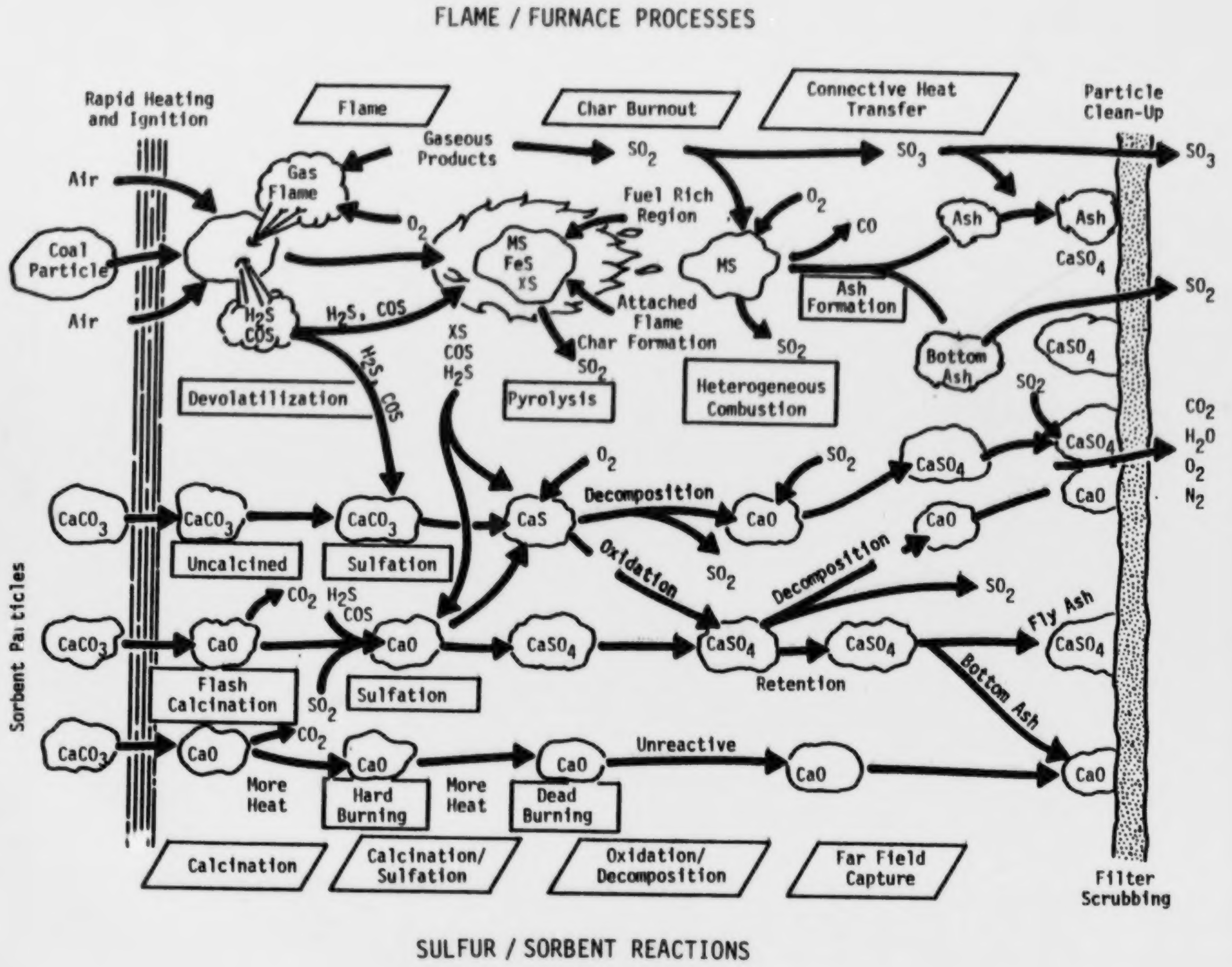
FLAME / FURNACE PROCESSES
Rapid Heating and Ignition
Flame
Char Burnout
Connective Heat Transfer
Particle Clean-Up
Air
Coal Particle
Air
Gas Flame
H_2S COS
Gaseous Products
O_2
H_2S, COS
MS FeS XS
Fuel Rich Region
Attached Flame
Char Formation
SO_2
MS
O_2
CO
SO_2
SO_3
Ash
Ash
$CaSO_4$
Ash Formation
Bottom Ash
SO_3
SO_2
$CaSO_4$
CO_2
H_2O
O_2
N_2
Devolatilization
Pyrolysis
Heterogeneous Combustion
XS
COS
H_2S
Sorbent Particles
$CaCO_3$
$CaCO_3$
Uncalcined
$CaCO_3$
Sulfation
CaS
O_2
Decomposition
Oxidation
CaO
SO_2
SO_2
$CaSO_4$
$CaSO_4$
CaO
CaO
Decomposition
SO_2
$CaCO_3$
CaO
Flash Calcination
CO_2
H_2S
COS
CaO
SO_2
Sulfation
$CaSO_4$
$CaSO_4$
Retention
$CaSO_4$
Fly Ash
$CaSO_4$
Bottom Ash
$CaCO_3$
CaO
CO_2
More Heat
CaO
Hard Burning
More Heat
CaO
Dead Burning
Unreactive
CaO
CaO
Calcination
Calcination/Sulfation
Oxidation/Decomposition
Far Field Capture
Filter Scrubbing
SULFUR / SORBENT REACTIONS

Figure 5-1. Conceptual View of Sulfur and Sorbent Transformations During Coal Combustion.

This review section will first discuss coal sulfur chemistry including: the amount and type of sulfur found in American coals, studies on sulfur devolitization and pyrolisis, the gas phase chemistry of typical sulfur specie in a coal flame, and finally, char burnout and retention of sulfur in the solid. After the background information on coal sulfur chemistry is presented the effect of the coal flame on alkali metal sorbents will be discussed. Factors affecting sorbent utilization and sulfation capacity will be reviewed. And finally flame/sorbent/sulfur interactions will be discussed with an emphasis on reaction rates and kinetics.

5.1 Coal Sulfur Chemistry

The amount and type of sulfur containing emissions from a coal fired plant depends upon the coal type and sulfur content, the sulfur distribution in the coal and, to some extent, the conditions under which the coal is burned. This section first considers the amount and type of sulfur found in American coals; it then reviews coal sulfur combustion from devolatilization through pyrolisis and oxidation. The gas phase kinetics of likely sulfur intermidates is discussed. There is little information available on the role of sulfur in heterogeneous combustion or char burnout phase of coal combustion. A substantial amount of the sulfur remains in the char and must be oxidized. Some sulfur, depending on coal type and composition, remains in the flyash and in the boiler; this inherent capture is also discussed.

5.1.1 Coal Sulfur, Its Forms

The total amount of sulfur in coal is extremely variable; it can range from less than 0.5 percent in some high grade Western coals to as high as 9 percent in certain Eastern bituminous coals. Coal sulfur is generally divided into two classes: inorganic and organic sulfur. The ratio of organic-to-inorganic sulfur in coal varies with coal type and seam, as does the total amount of sulfur in coal. Two classes of inorganic sulfur have been traditionally distinguished, the disulfides and the sulfates. The organic sulfur is all of the sulfur which is bound in the hydrocarbon matrix.

The working definition of the classes of sulfur are as follows (Attar, 1978):

- the sulfate sulfur is the equivalent of the amount of sulfate ion which dissolves in 2:3 HCL in 30 minutes;

- the pyritic sulfur is the sulfur equivalent of the iron which dissolves in boiling 2N HCN_3 in 30 minutes;
- the organic sulfur is the difference between the total sulfur and the sum of the sulfate and pyritic sulfur.

The total sulfur is usually determined from the amount of SO_2 that is evolved when the sample is burned.

For many coals the major portion of the sulfur exists in the inorganic component as FeS_2. The sulfate sulfur rarely exceeds 0.1 weight percent and is often negligible. However, it does increase if the coal is exposed to air.

The iron sulfide, FeS_2, appears in two crystalline forms: the pyrite (cubic) and the marcasite (rhombic). Since most of the FeS_2 is pyritic, the name pyrites is often used to designate all of the FeS_2. The chemical reactivity of these two forms is believed to be similar; therefore they are rarely considered separately. It is generally considered that the majority of the FeS_2 exists as loose crystals which form vein-like structure in the organic coal seam. The density of the pyrites is approximately 5.0. Since the density of the organic material is generally less than 1.5 g/cm^3, a large fraction of the pyrites can be separated from the organic material by flotation type techniques.

The sulfate sulfur is thought to be primarily in the form of calcium and iron sulfates or their hydrated forms ($CaSO_4 \cdot 2\ H_2O$ or $FeSO_4 \cdot 7\ H_2O$) and again believed to be loose crystals.

There is considerable uncertainty regarding the molecular structure of the organic sulfur. Most of the information available has been derived from the examination of smaller molecular products which were obtained by breaking the organic coal matrix. The organic sulfur is generally believed to bivalent and the dominant form is thought to be aromatic. Solomon (1977) estimates that approximately 60 percent of the sulfur resides in heterocyclic rings. Attar (1978) estimates 40 to 70 percent of the total organic sulfur in bituminous coals is thiophenic (aromatic). Table 5-1 shows the classes of organic sulfur that are generally considered to be significant in coal. These classes are

Table 5-1. Coal Sulfur Forms.

A)	INORGANIC		
		Pyritic	FeS_2
		Sulfate	$CaSO_4 \cdot 2H_2O$, $FeSO_4 \cdot 7H_2)$
B)	ORGANIC		
		Mercaptan or Thiol	RSH
		Sulphide or Thio-ether	RSR'
		Disulphide	RSSR'
		Thiophenic (aromatic)	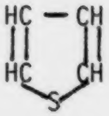
		Thiopyronic	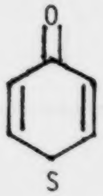

general and somewhat speculative as the categories are based on solubility, depolymerization, and pyrolysis studies, and in most instances are not the result of direct analysis.

Table 5-2 shows data on the total sulfur content of coals from the major coal-producing states throughout the United States. These data illustrate the wide range of sulfur contents, even in common coal fields. Table 5-3 shows similar data for the major coal-producing areas throughout the world. Again, there is a wide variation although some countries including Columbia, Indonesia, Turkey, India, Australia, New Zealand, Holland, Spain, and Czechoslovakia have a prevalence of low sulfur coals. Several industrialized countries are considering importing certain Australian, Russian and East European coals because of their low sulfur content. The regional distribution of coals having similar sulfur contents in the United States is also very typical of that found in the Soviet Union. Thus, it has been suggested (Yurovskii, 1960) that the processes involved in the formation of coal sulfur are very similar throughout the world.

Figure 5-2 presents data on the organic and pyritic sulfur content of a wide variety of coals, including those currently on hand at EERC. As this figure indicates, there is a substantial variation in the relative amount of each type of sulfur and, therefore, it is reasonable to expect that the efficiency of dry SO_2 control may be a function of both the total sulfur content and the sulfur distribution. Thus, some understanding of the fate of the fuel sulfur during the combustion process is needed.

5.1.2 Coal Combustion: An Overview of Sulfur Transformations in Coal Burning

The burning of coal in a large, pulverized coal furnace involves the complex interaction of physical and chemical processes. Unfortunately, the reactions and transformations of coal-sulfur compounds are among the most complex and possibly the least understood of all the chemical processes occurring in a coal-fired furnace. Until recently, the mechanisms controlling the oxidation of fuel sulfur in an actual coal flame have received little attention.

It is conceptually helpful to follow the combustion behavior of a single coal particle as illustrated in Figure 5-3 which is a detail from Figure 5-1. When a particle is injected into the furnace, rapid heating of the particle

Table 5-2. Total Sulfur of U.S. Coals.

State, District	Minimum Sulfur Content		Maximum Sulfur Content		State-wise Average Sulfur Content	
	Coal Bed (Section)	S_{total}, %	Coal Bed (Section)	S_{total}, %	Number of Analyses Used	S_{total}, %
Alabama	Helena	0.5	Jefferson	3.1	37	1.24
Arkansas	Fillpot	0.7	Charleston	3.1	11	1.76
California	Not indexed (Eimedor)	2.0	Not indexed (Monterey)	4.5	4	2.60
Colorado	Nai-renkkol	1.0	(Rio Blanco)	9.0	22	5.39
Georgia	Etna	1.0	Durham	8.0	3	3.33
Illinois	Jefferson	1.3	(Franklin)	8.0	21	3.82
Indiana	V (Pike)	0.6	Minshell	4.6	28	2.84
Iowa	Nodaway	3.0	Not indexed	7.3	14	5.08
Kansas	Beaver (Borbu)	2.0	Beaver (Sivenors)	4.1	6	3.23
Kentucky	Elkhorn	0.5	Kentuck-14 (Ohio)	4.5	58	1.89
Maryland	Minedeer	0.6	Upper Kittanning	3.8	15	1.96
Michigan	Not indexed (Saginaw)	1.2	Not indexed (Huron)	7.7	8	3.49
Missouri	Jordan	1.6	Beaver	5.7	18	3.88
Montana	Not indexed (Rosebud Field)	0.3	(Broadwater)	8.0	10	1.73
New Mexico	(Sandwall)	0.4	White Ash	1.1	13	0.72
North Dakota	(Wind)	0.3	Morton	1.4	9	0.66
Ohio	Pittsburg	0.4	Lower Kittanning	5.7	36	2.84
Oklahoma	Stigler	0.5	(Craig)	6.0	19	1.88
Pennsylvania (anthracite)	Pie	0.4	Egg	0	86	0.68
Pennsylvania (bituminous)	Lewis Pitening	0.5	Upper Kittanning	5.5	92	2.02
Tennessee	Sewanee	0.6	Coll-creek	3.9	30	1.49
Texas	(Milam)	1.0	Palo Pinto	4.1	6	2.12
Utah	(Morgan)	0.5	(Iron)	6.1	14	1.63
Virginia	Jewell	0.5	Hernen	2.8	32	0.97
Washington	Whatcom	0.3	Stevens	2.0	16	0.91
West Virginia	Welch	0.5	(Marshall)	4.4	94	1.31
Wyoming	(Fremont)	0.5	(Big Horn)	2.1	7	0.81

Table 5-3. Sulfur Content of World Coals.
(Yurovskii, 1960).

Country	S_{total}, %
Japan	0.3 - 3.34
India	0.29 - 0.82
Africa	0.98 - 4.18
Australia	<1.0%
Canada	0.3 - 0.6
England	0.3 - 2.04
Chile	0.73 - 5.8
Brazil	0.85 - 3.42
Poland	0.6 - 1.7
Czechoslovakia	0.44 - 0.78
Hungary	0.35 - 5.14
Rumania	0.19 - 3.08
Yugoslavia	0.60 - 6.2
USSR	0.20 - 9.4

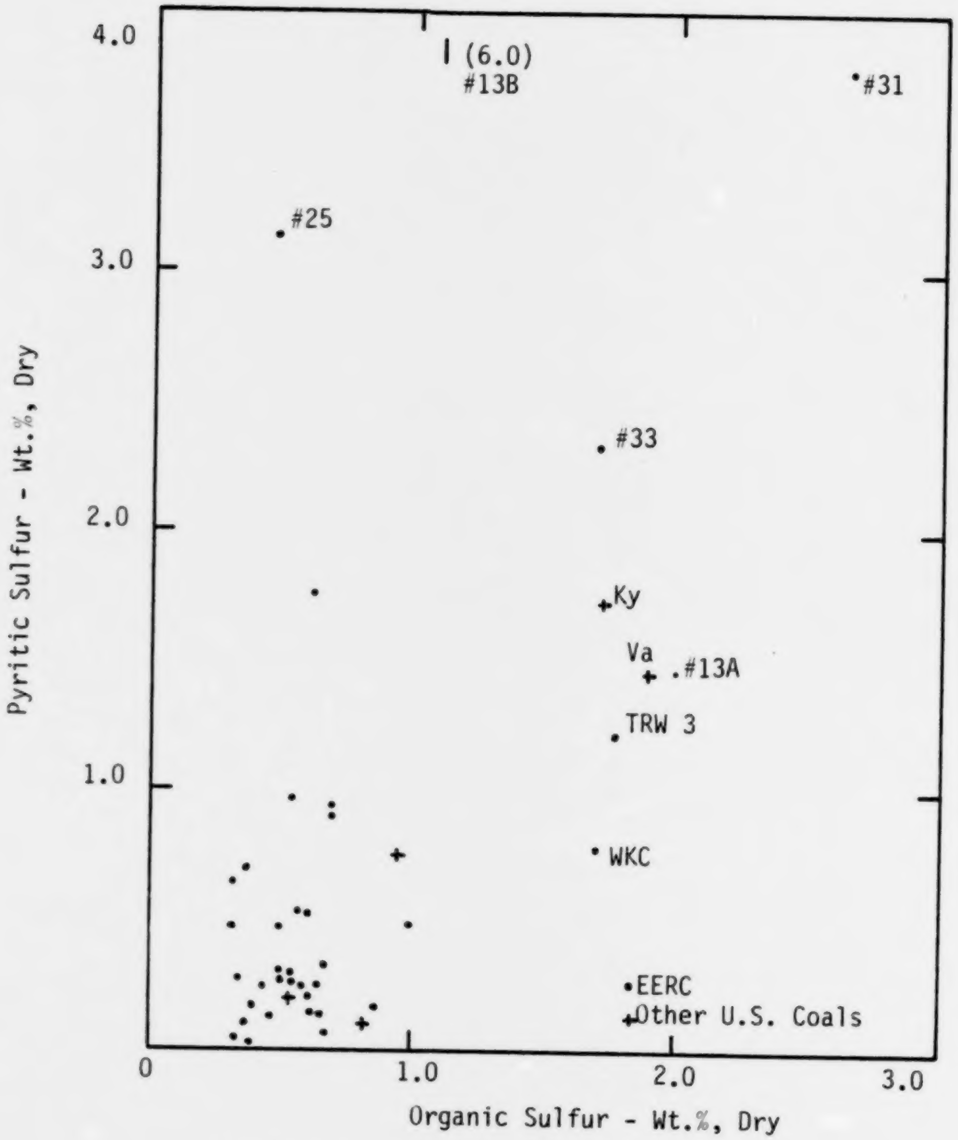

Figure 5-2. Sulfur Distribution in Some Typical U.S. Coals

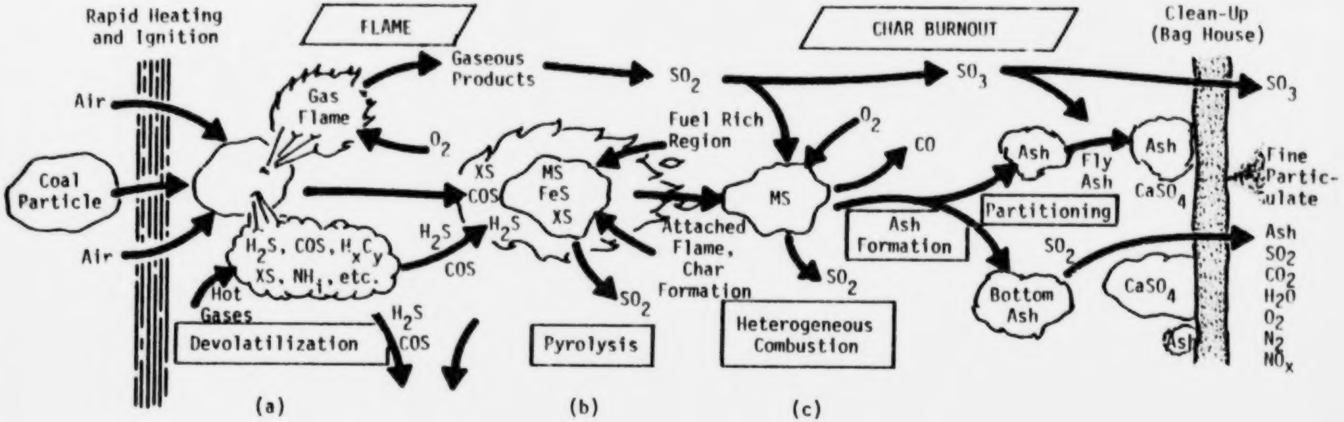
Rapid Heating and Ignition
FLAME
CHAR BURNOUT
Clean-Up (Bag House)
Air
Coal Particle
Air
Gas Flame
Gaseous Products
O_2
SO_2
SO_3
SO_3
Fuel Rich Region
O_2
CO
XS
COS
H_2S
MS
FeS
XS
MS
Ash
Fly Ash
Ash
$CaSO_4$
Fine Partic-ulate
H_2S, COS, H_xC_y
XS, NH_i, etc.
H_2S
COS
Attached Flame, Char Formation
Ash Formation
Partitioning
SO_2
Ash
SO_2
CO_2
H_2O
O_2
N_2
NO_x
Hot Gases
H_2S
COS
SO_2
SO_2
Bottom Ash
$CaSO_4$
Ash
Devolatilization
Pyrolysis
Heterogeneous Combustion
(a)
(b)
(c)

Figure 5-3. Combustion Behavior of a Single Coal Particle.

drives off light volatile gases in jets from the particle. These volatile gases play a role in flame stability and are probably oxidized far from the particle surface (see Figure 5-3a). As the particle heats up, devolatilization proceeds, sometimes accompanied by softening and swelling of the coal particle (depending on the coal type), at a decreasing rate as the volatile content of the coal is depleted. Eventually, Wendt (1980) assumes, there must be a point at which the volatilization rate is slow enough to allow the stabilization of a diffusion flame attached to the coal particle (see Figure 5-3b). Pyrolysis of sulfur and nitrogen containing hydrocarbons then occurs in the fuel rich regions of this diffusion flame.

Heterogeneous burnout of the coal carbon commences when volatiles are no longer evolved from the particle surface (see Figure 5-3c). It should be remembered that coal particles are irregular in shape and pores, cracks, and bubbles may form in the particle; it is possible for part of a particle to undergo heterogeneous combustion while volatiles are being evolved and burning at and near another part of the particle surface.

One should bear in mind that, while there is a cloud of burning gas and each coal particle will evolve volatiles and undergo heterogeneous char burnout, all three processes are interdependent and are occurring simultaneously in a pulverized coal flame. The separation of these processes is a conceptual aid only.

The fate of the various sulfur compounds in coal during these three parts of the combustion process depends on both the coal type and burning conditiions, most notably the heating rate and burning temperature.

5.1.3 Coal Sulfur Devolatilization

During pulverized-coal devolatilization the sulfur side chains (-SH) and the linking sulfur chains (-S-) in aliphatic compounds are believed to rupture early in the heating sequence leading to the rapid evolution of volatile sulfur. The thiophenic structure, however, is more stable and does not decompose until temperatures of about 1200^{0}K are attained (Malte, 1979). Solomon (1977) has studied the devolatilization of pulverized coal heated under vacuum in a mesh to temperatures around 1000^{0}C at a rate of 600^{0}C/second. He found that the gases evolved from the coal particles consistently exhibited enhanced sulfur content and, in fact, relative to the sulfur content of the original coal, the sulfur content of the volatile gas was often greater by a factor of two (mass basis) with the dominant specie being H_2S. In particular, his preliminary results indicate that:

- approximately 40 precent of the organic sulfur is volatilized under the conditions investigated;
- the organic volatiles are primarily mercaptans and small sulfides; the aromatic rings remain in the char;
- organic sulfur is more volatile than coal carbon or nitrogen, but less volatile than oxygen or hydrogen;
- there is no clear simple relationship between organic sulfur devolatilization and temperature;
- the inorganic sulfur interacts with the organic matrix during devolatilization.

Figure 5-4 shows typical data from the work of Solomon as replotted by Malte (1979).

Figure 5-5 summarizes the data obtained by Sarofim et al. (1978) in their laminar flow, drop-tube furnace experiments with a Pittsburgh seam No. 8, HVA bituminous coal, and a Montana lignite coal. They too found that sulfur was not as difficult to remove from the coal as carbon and nitrogen, but more difficult than hydrogen and oxygen. Their data indicate that both the rate of sulfur devolatilzation and the total amount of sulfur devolatilized are temperature dependent. At 1900°K sulfur evolution was initially very rapid but up to 50 percent of the sulfur could be retained in the char. At 1260°K sulfur evolution was slower and the asymptotic retention of sulfur was as high as 70 percent. In the case of the Montana lignite similar trends were observed. Again, asymptotic retention of sulfur at temperatures below 1510°K is approximately 50 percent, and there are indications that sulfur can be essentially completely devolatilized at extremely high temperatures.

It is known that pyrites decompose upon heating by the reaction: $FeS_2 \rightarrow FeS + S$ (400°C); $FeS \rightarrow Fe + S$ (900°C), where the sulfur released is volatile.

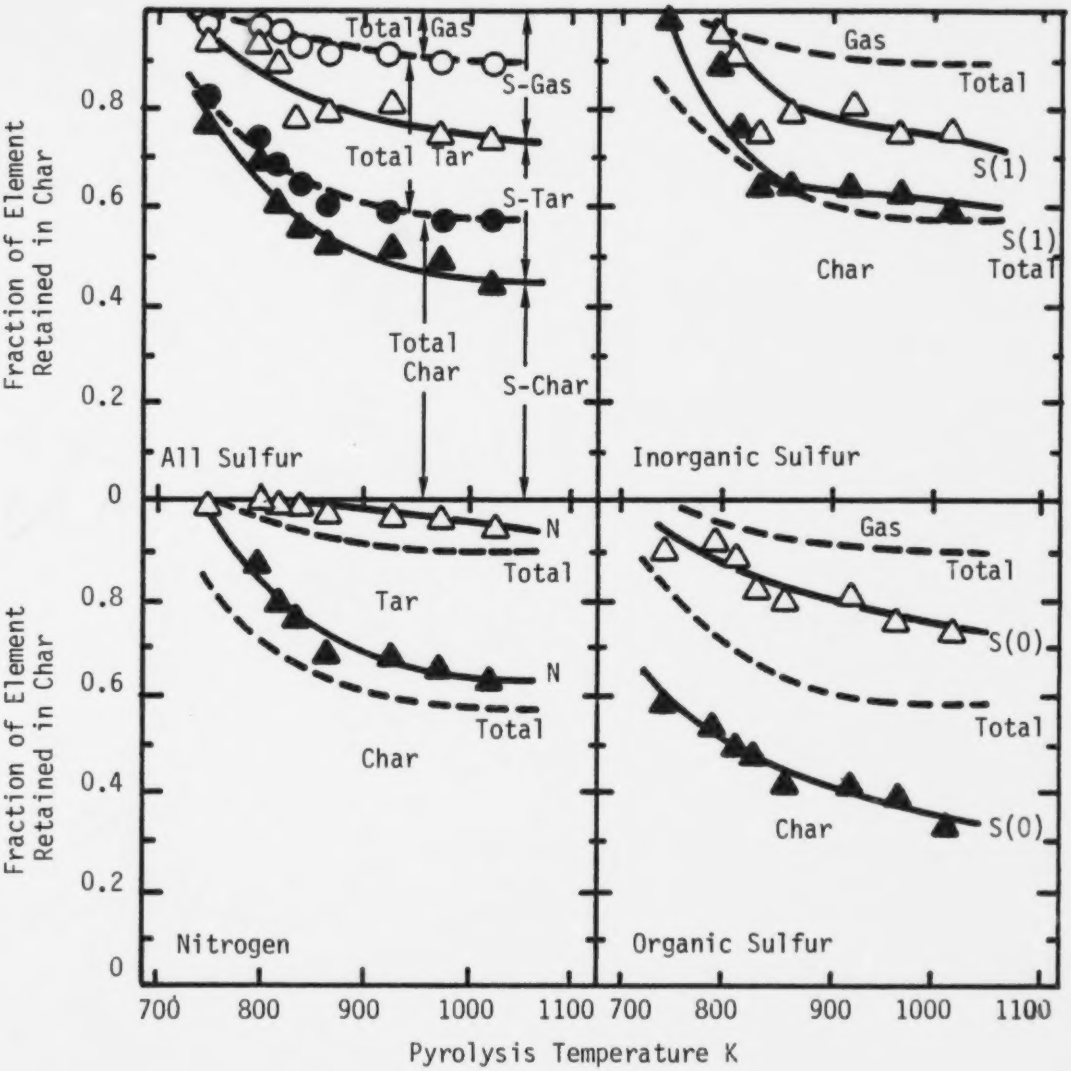

Figure 5-4. Sulfur Evolution Data (Solomon).

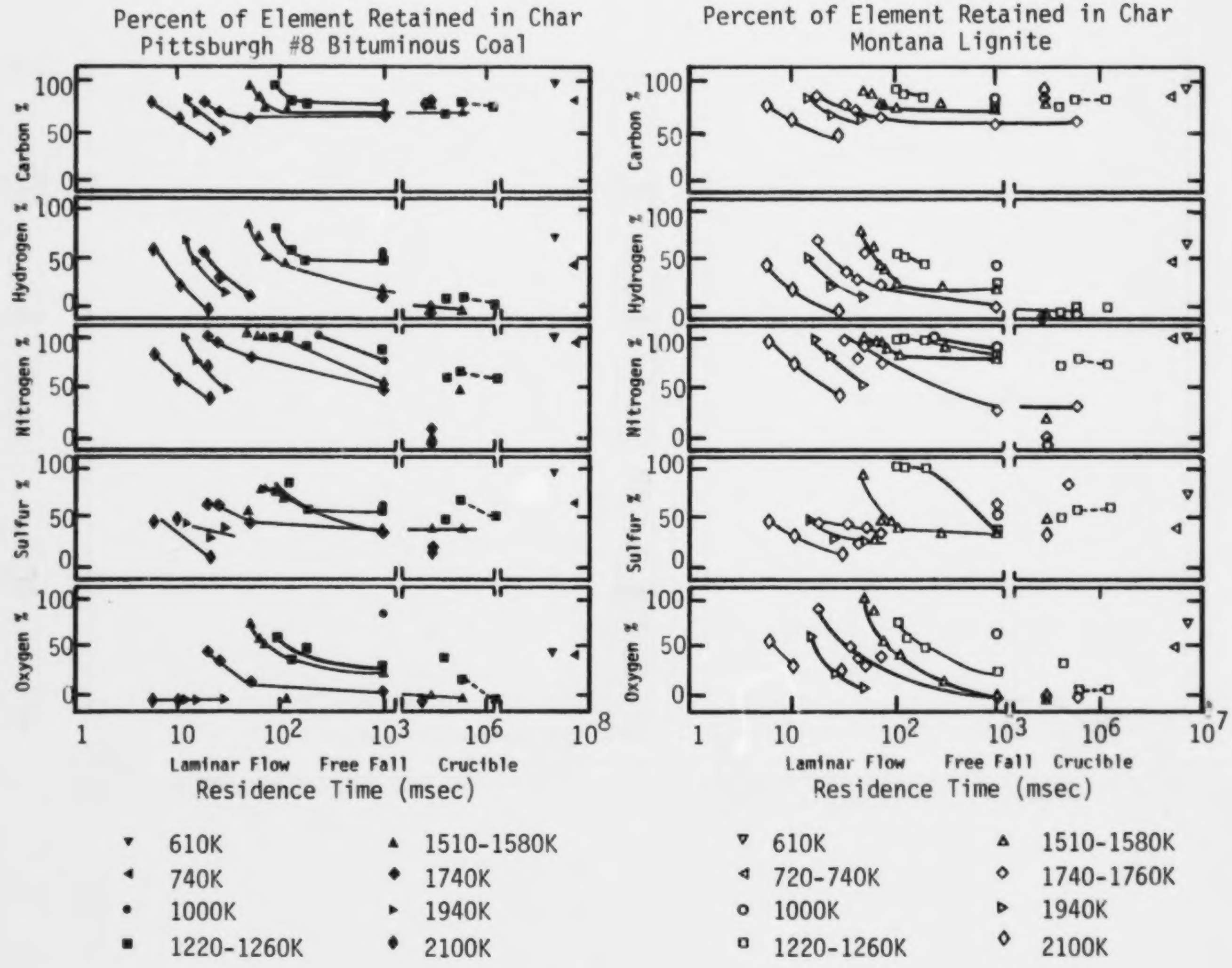

Figure 5-5. Elemental Loss During Devolatilization.

Solomon was able to determine a rate constant for this pyrite volatilization in coal with a series of screen-heating experiments. His proposed rate constant is time and temperature dependent and is given by:

$$X = (1 + e^{-tA_0 \exp(-E/RT)})$$

where

t = devolatilization time at T, in sec

$A_o = 4.8 \cdot 10^2$

E = 16.7 Kcal

T = temperature in ^oK

This activation energy (16.7 Kcal) is lower than that measured for pyrite decomposition (42 and 68 Kcal). This is not unreasonable since the decomposition of pyrite in coal is undoubtedly more complex than that of simple pyrites.

There are also indicatons that pyritic sulfur may react with the coal matrix. Pyrolysis studies of coal have indicated that sulfur originating in the pyrites may be found bound to the organic matrix. Analysis of the tars produced during Solomon's devolatilization studies showed an increase in sulfur content of the tar component which could be related to coal parent type and devolatilization temperature. The sulfur content of these tars increased over the original organic sulfur content with increasing temperature and with increasing pyrite content of the parent coal. Bass (1981) also observed an enhancement in the organic sulfur content of char samples from a burning fixed bed of coal. Attar (1978) has proposed a H_2S intermediate in the sulfur exchange process and Bass postulates a reaction of the form $SO_2 + Cx+1 \rightarrow C_xS + CO_2$. The mechanisms for this organic sulfur enhancement are unclear and require further investigation.

Thus, in summary, the pyrolysis data avilable to date indicate that while a substantial portion of the organic sulfur will be evolved during the devolatilization process a significant amount of sulfur, particularly sulfur originally part of the inorganic component, may remain in the char phase and be oxidized heterogeneously. Hence, both types of subsequent combustion (gas phase and heterogeneous) are certain to be important in the production of sulfur oxides and in any in situ capture process.

5.1.4 Gas Phase Chemistry of Coal-Sulfur Compounds

Regardless of their source (fuel oil, coal, or smelter ores), the gas phase combustion of sulfur compounds probably involves pyrolysis of large molecules to more simple compounds such as hydrogen sulfide, carbonyl sulfide, small mercaptans and the like, followed by oxidation and subsequent interaction of the sulfur oxides (SO, SO_2, SO_3) with other gas phase species. The most likely gaseous sulfur components of a coal combustion system are: hydrogen sulfide, carbonyl sulfide, carbon disulfide, sulfur dioxide and trioxide, and small molecular weight mercaptans. The following summary of gas phase sulfur chemistry is mostly extracted from excellent review articles by Cullis and Malcahy (1972) and Bauer et al (1973). Unless otherwide noted, all mechanisms and rate data presented are from high temperature flame or shock tube studies.

5.1.4.1 Hydrogen Sulfide (H_2S)

Hydrogen sulfide is probably the primary reduced gas phase sulfur compound in coal combustion. Unfortunately, its oxidation in hydrocarbon systems has not been completely investigated. Most kinetic studies of H_2S oxidation have been carried out at low temperatures. Bowman and Dodge (1977) have studied the thermal decomposition of H_2S in a shock tube and propose a mechanism and rates for its decomposition (see Table 5-4). The oxidation of H_2S is fast and proceeds through the path:

$$H_2S \rightarrow HS \rightarrow SO \rightarrow SO_2$$

Merryman and Levy (1967) have studied the formation of SO_2 in low pressure hydrogen sulfide flames, determining rates for the reactions:

$$H_2S + O \rightarrow OH + SH \qquad (1)$$

$$SO + O_2 \rightarrow SO_2 + O \qquad (2)$$

Cullis and Mulcahy (1972) have reviewed available rate data (including Merryman and Levy's work) and give likely elementary reactions (and their rates) involved in the H_2S oxidation mechanism. A tentative overall mechanism for hydrogen sulfide oxidation based on this data is given in Table 5-5.

Table 5-4. Thermal Decomposition of Hydrogen Sulfide.

Reaction*	A	B	$E/_R$ (K)
(1)* $H_2S + M \rightleftarrows HS + H + M$	11.3	0	37,300
(2) $H + H_2S \rightleftarrows HS + H_2$	9.9	0	860
(3) $HS + HS \rightleftarrows H_2S + S$	10.0	0	0
(4) $H + HS \rightleftarrows H_2 + S$	10.3	0	0
(5) $S + HS \rightleftarrows S_2 + H$	8.8	0.5	0
(6)* $S + H + M \rightleftarrows HS + M$	9.0	0	0

*where reaction rate is given by $k_x = 10^A\ T^B \exp(-E/RT)\ m^3/\text{kg mole sec}$

Table 5-5. Hydrogen Sulfide Oxidation.

Reaction*	A	B	$E/_R$ (K)
(1) $H_2S + H \rightleftarrows HS + H_2$	9.9	0	860
(2) $H_2S + OH \rightleftarrows H_2O + HS$	9.3	at 300K	
(3) $H_2S + O \rightleftarrows OH + HS$	8.2	0	750
(4) $HS + O \rightleftarrows SO + H$	11.2	at 300K	
(5) $HS + H \rightleftarrows H_2 + S$	10.3	0	0
(6) $HS + O_2 \rightleftarrows SO + OH$	<7.8	300K	
(7) $SO + O_2 \rightleftarrows SO_2 + O$	7.4	assumed at 1200K	
(8) $SO + OH \rightleftarrows SO_2 + H$	10.8	at 300K	
(9) $SO + O + M \rightleftarrows SO_2 + M$	11.5	at 300K	
(10) $S_2 + O \rightleftarrows SO + S$	9.6	at 1050K	
(11) $S + O_2 \rightleftarrows SO + O$	9.1	at 300K	
(12) $SO + H \rightleftarrows S + OH$			

*where reaction rate is given by $k_x = 10^A\ T^B \exp(-E/RT)\ m^3/kg$ mole sec

5.1.4.2 Carbon Disulfide (CS_2)

Carbon disulfide is found as a sulfur containing product of coal pyrolysis although it is not a major form of sulfur in the parent coal. It may be a product of the reaction of carbonyl sulfide and hydrogen sulfide or of carbon and sulfur:

$$C + S_2 \rightarrow CS_2 \qquad (3)$$

Carbon disulfide is probably a component in coal combustion, but its importance is not known; therefore, results from pyrolysis studies should be applied to combustion at high temperatures with discretion.

Hofmann et al (1969) studied the oxidation of carbon disulfide in isothermal flames at temperatures above 900°C and correlated their experimental results with known rate data to produce the mechanism tabulated in Table 5-6. These correlations were done with a computer-kinetics program eliminating the usual steady-state assumptions. It must be noted again that the proposed rates are tentative with all reaction rates except 2-33 and 2-25 known within a factor of three. The rate of reaction 2-35 was adjusted in the computer runs to give the closest correlation between observed and calculated results.

5.1.4.3 Carbonyl Sulfide (COS)

Carbonyl sulfide is probably an intermediate in the oxidation of organic sulfur compounds found in coal. The reaction:

$$CO_2 + H_2S \rightleftarrows COS + H_2O \qquad (4)$$

has been proposed as part of the hydrogen sulfide oxidation system in hydrocarbon flames. Hofmann et al (1970) studied the oxidation of carbonyl sulfide in the 1000°C region in an isothermal flame. The results of these studies coupled with a review of available rate data were used to propose a possible mechanism for the oxidation of carbonyl sulfide (Table 5-7).

5.1.4.4 Sulfur Dioxide and Trioxide (SO_2 and SO_3)

Sulfur dioxide is the major gaseous sulfur product of coal-burning systems. Although the mechanisms of SO_2 production in coal-burning systems are not well-understood, the interactions of SO_2 with other components of combustion exhausts have been more intensely studied than any other sulfur system. The SO_2/SO_3 system has received much attention because SO_3 reacts readily with water to form

Table 5-6. Carbon Disulfide Oxidation at 927°C, 30 torr Pressure

Reaction	Rate Constant (cm^3/mole sec)	Number
$O + CS_2 \rightleftarrows CS + SO$	2.2×10^{13}	2-36
$O + CS_2 \rightleftarrows COS + S$	3.0×10^{12}	2-38
$O + CS \rightleftarrows CO + S$	1.0×10^{14}	2-37
$O + COS \rightleftarrows CO + SO$	6.6×10^{12}	2-22
$SO + O_2 \rightleftarrows SO_2 + O$	2.4×10^{10}	2-90
$S + O_2 \rightleftarrows SO + O$	1.0×10^{12}	2-21
$CS + O_2 \rightleftarrows CO + SO$	2.5×10^{10}	2-33
$S + CS_2 \rightleftarrows CS + S_2$	1.5×10^{13}	2-29
$O + S_2 \rightleftarrows SO + S$	4.0×10^{12}	2-39

Table 5-7. Carbonyl Sulfide Oxidation at 997°C, 74 torr Pressure

Reaction	Rate Constant (cm^3/mole sec)	Number
$O + COS \rightleftarrows CO + SO$	7.5×10^{12}	2-22
$O + COS \rightleftarrows CO_2 + S$	1.6×10^{12}	2-23
$S + O_2 \rightleftarrows SO + O$	1.0×10^{12}	2-21
$SO + O_2 \rightleftarrows SO_2 + O$	2.8×10^{10}	2-90

sulfuric acid which corrodes boilers, duct work, precipitators, and other machinery. Sulfur trioxide also raises the dew point of a gas considerably, limiting the heat that can be extracted from combustion gases before condesation and subsequent corrosion occur.

The SO_2/SO_3 system is probably the best understood of the sulfur dioxide interactions in coal flames. Merryman and Levy (1971) have studied sulfur trioxide flame chemistry in premixed hydrogen sulfide and carbonyl sulfide flames. The authors observed that the SO_3 concentration increased with increasing total pressure in the early part of the flame in accordance with the three-body reaction:

$$SO_2 + O + M \rightleftarrows SO_3 + M \tag{5}$$

Mechanisms for the production and depletion of SO_3 were proposed (Table 5-8) and rates for reaction 5 and the reaction:

$$SO_3 + O \rightleftarrows SO_2 + O_2 \tag{6}$$

were determined. The rate constant for reaction 5 is $k_5 = 2.4 \times 10^{17} \exp(-2500/RT)$ cm^6/mole sec, and that for reaction 6 is $k_6 = 6.5 \times 10^{14} \exp(-10800/RT)$ cm^3/mole sec (which takes into account the reaction:

$$SO_3 + H \rightleftarrows SO_2 + OH \tag{7}$$

which may occur in the hydrogen sulfide flame). The rates obtained for reaction 6 in the two flames were slightly different before allowance for reaction 7 in the hydrogen sulfide flame was made. Fenimore and Jones (1965) determined a rate of 6.4×10^{12} cm^3/moles sec for reacton 6 at 1600^oK. This rate is in reasonable agreement with the later results of Merryman and Levy (1969). Levy also suggested that staged combustion results in an increase in SO_3 production in the flame zone.

The gas phase sulfur chemistry discussed above is certainly not exhaustive but it can be used to give a general understanding of the reactions involving gaseous sulfur compounds which may take place in a coal flame.

The interactions of these gaseous species with solids in the flame system, dry alkali additives and ash will be discussed in Section 5.3.

Table 5-8. Reactions Involved in SO_3 Production and Depletion in COS and H_2S Flames.

Reaction	Rate Constant	Number	Comments
$SO_2 + O + M \rightleftarrows SO_3 + M$	2.4×10^{17} $\exp(-2500/RT)$	2-5	c
$SO_2 + 1/2\ O_2 \rightleftarrows SO_3$		2-17	
$SO_2 + O \rightleftarrows SO_3 + h\nu$		2-18	
$SO_3 + O \rightleftarrows SO_2 + O_2$	a) 2.8×10^{14} $\exp(-12000/RT)$	2-6	a
	b) 6.5×10^{14} $\exp(-10800/RT)$		b
$SO_3 + H \rightleftarrows SO_2 + OH$		2-7	

a - in COS flame

b - in H_2S flame

c - in $cm^6/moles^2$, sec

5.1.5 Char Sulfur Oxidation and Inherent Capture

The mechanisms of char-sulfur oxidation are far less understood than those of gas-phase sulfur oxidation. The controlling reactions may take place in the crevices and pores of the particle and rupture may occur depending on the physical characteristics of the coal. As previously noted, a substantial portion of the inorganic sulfur may remain in the char phase. It is known that the decomposition of mineral sulfur depends upon the temperature and surrounding atmosphere. Calcium-sulfate decomposition increases with increasing temperature in an oxidizing atmosphere while the decomposition of pyrites in an inert atmosphere is accompanied by sulfur sublimation.

Fundamental data on the oxidation of actual fuel-bound sulfur molecules are very limited. Slaughter and Pershing (University of Utah) have recently conducted oxidative pyrolysis studies on Indiana coal particles (total S=2.2%, organic S=0.6%) and their results indicate that sulfur is oxidized preferentially to carbon, even when O_2 availability is limited. With free-stream conditions of 0.8 percent O_2 and 2100°F, 90 percent of the fuel sulfur was evolved and oxidized to SO_2, but only 60 percent of the initial carbon appeared in the gas phase as CO or CO_2. These data suggest that even in the center of a large fuel jet, large amounts of SO_2 will be formed quickly.

5.1.5.1 Role of Inherent Alkali, Sulfur Retention

Some portion of the sulfur in a given coal may be "captured" by the mineral matter inherent in the coal. This "inherent" sulfur capture has received little direct attention, but it is likely that reactions between the coal sulfur and the alkaline mineral matter in the coal account for the majority of the retention effect.

The data available on inherent sulfur capture in pilot- and full-scale systems are very limited and must be considered carefully because of the difficulties associated with making accurate SO_2 and SO_3 measurements, and because of the variability of fuel sulfur with time in a given coal-fired unit.

Some of the best data on inherent sulfur capture are the result of research programs at the Canadian Combustion Research Laboratory (Brown et al., 1978) and at Shell Development (Schwartz, 1979). Brown and co-workers studied the neutralization of sulfur by lignite ash in a 1600 lb/hr steam, pilot-scale research boiler. The lignite coals used in their work, one from N. Dakota and two from Saskatchewan, were characterized by sulfur levels below 0.7 percent on an "as-received" basis and moderate-to-high levels of alkaline ash constiuents. The purpose of their research was to determine the influence of the alkaline ash on the SO_2 emissions and the effect of combustion parameters on this sulfur capture. Scwartz and his associates conducted similar studies using a Texas lignite, two subbituminous coals from the Powder River Basin and a Beulah, N. Dakota lignite obtained from the Grand Forks Energy Research Center (GFERC). This work was conducted in a laboratory-scale (micro) combustor which was fired at a nominal rate of 0.25 lbs of coal/hr. Preliminary experiments indicated that the SO_2 emissions obtained in this small unit were typical of field data with these same coals. In both studies, considerable care was taken to obtain accurate measurements of SO_2 and SO_3 in the exhaust gases and of the sulfur and alkaline-ash composition of the coal feed.

Figure 5-6 is a composite plot made from the tabulated data of both investigators. This figure shows the percent capture (based on the measurement of SO_2 plus SO_3) as a function of the sulfur level in the coal (DAF). These data indicate the following:

- Inherent sulfur capture levels in excess of 30 percent are possible with certain coals.
- Both subbituminous and lignite coals exhibit this characteristic.
- Bench-scale studies appear to produce results similar to large-scale combustion equipment.

All of the coals tested in both studies have calcium-to-sulfur ratios greater than 1.0.

The data shown in Figure 5-6 were all obtained by dividing the measured SO_x emissions by the theoretical SO_x emissions based on the inlet fuel sulfur content. To demonstrate that this sulfur was indeed being captured in the solid phase, Brown and co-workers measured the sulfur content of the particulate phase and of the residual boiler ash. Table 5-9 summarizes the results of these tests. The data indicate that in three of the four tests, Brown was able to close the sulfur balance to within less than 5 percent. They also suggest that a substantial portion of the sulfur is actually being retained in the boiler ash. Thus, it appears that the phenomena of inherent sulfur capture is

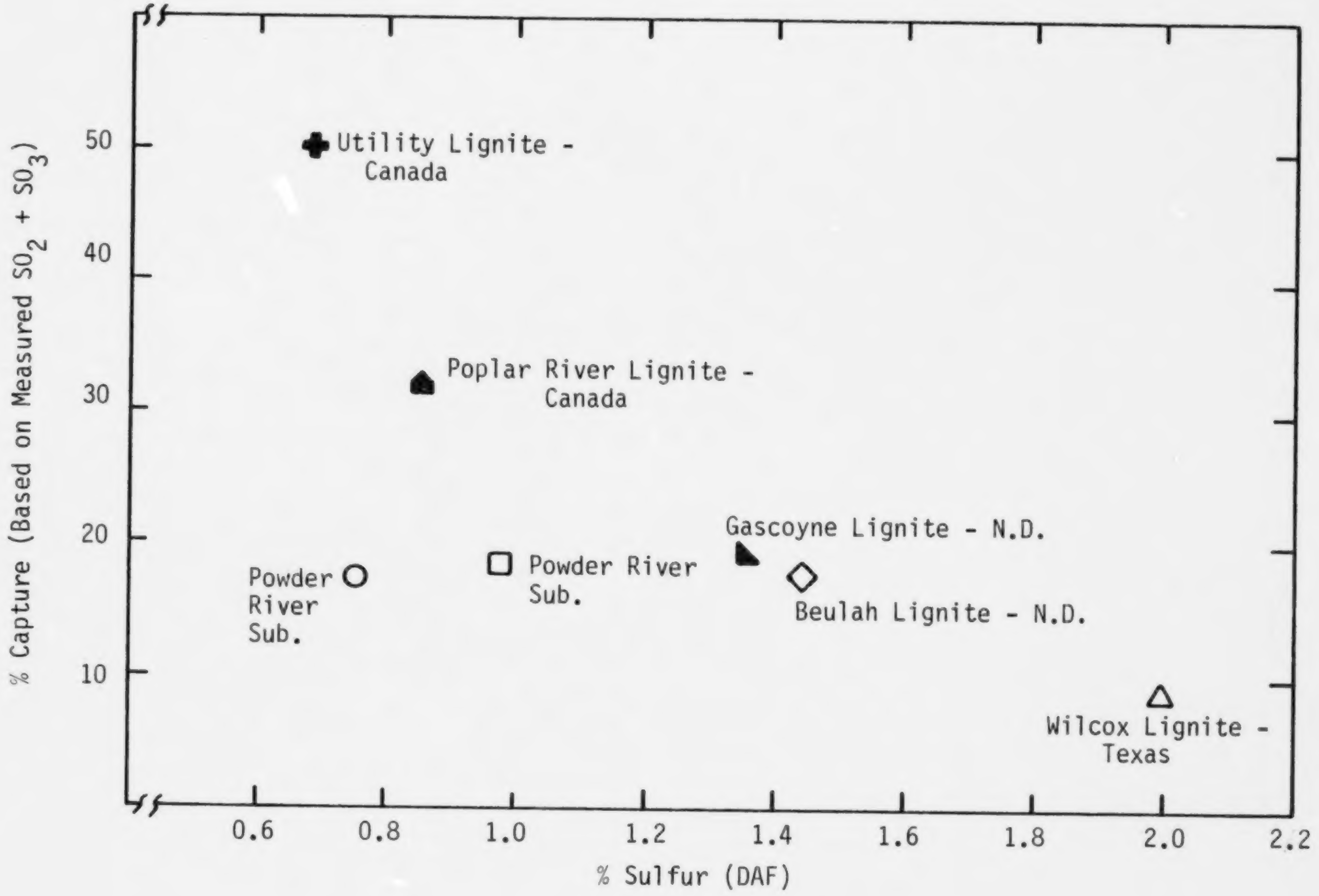

Figure 5-6. Inherent Sulfur Capture Results.

Table 5-9. Sulfur Balances for Gascoyne Lignite (Brown, et al, 1978).

Test No.		1	2	3	4
Excess Oxygen	%	4.9	4.9	3.0	3.0
Sulfur Input	kg/hr	0.912	0.999	0.956	0.956
Sulfur Outputs					
as SO_2	%	58.1	74.1	81.6	81.2
as SO_3	%	--	1.8	1.7	1.9
Particulates	%	8.0	8.9	8.5	8.9
Sulfur retained in Boiler	%	16.4	14.3	12.1	12.1
Total Accountable Sulfur	%	82.5	99.1	103.9	104.1

real and depending on the composition of the coal, can have a significant impact on the SO_x emissions.

The particulate data shown was based on measurements made before the electrostatic precipitator. To determine the actual solid sulfur emissions to the atmosphere, measurements were also made after the ESP. This fine particulate matter was analyzed for moisture and sulfur content. The results indicated that the solid phase sulfur emissions (in the particulate) constituted less than 0.03 percent of the total input sulfur, and less than 0.05 percent of the total sulfur emission. Sulfate emissions may, however, be significant.

Although neither Brown nor Schwartz was particularly interested in the efficiency of the alkali utilization in the studies, their data can be used to consider this important parameter. Figure 5-7 shows the results of calculations based on their experimental data and indicates that the alkali content of the lignites and subbituminous coals in these experiments is far from completely utilized. The percent utilization was calculated based on the ratio of the measured SO_x emissions to the theoretical (computed from fuel sulfur content) and the calcium-to-sulfur molar ratio. The data indicate that utilizations on the order of 15 percent are typical of the work in the micro-combustor at Shell and in the pilot unit at CCRL.

In summary then, we have followed the sulfur in coal through the combustion process (as illustrated in Figure 5-2) from an overview of the sulfur found in coal, its evolution into the gas phase during rapid devolatilization, its pyrolysis in the gas phase and at the coal surface, its gas phase kinetics; its heterogeneous oxidation in the coal char, and its retention in the solid phase as bottom or fly ash. This review makes it apparent that many key factors governing coal sulfur combustion and retention are very poorly understood. That such processes as pyrolysis, burning in rich zones at the coal face, and heterogeneous oxidation in the coal char take place is a good assumption based on current knowledge but mechanistic details of such phenomena are lacking. The next sections add to the overall scheme the complication of alkali metal salts and their interacton with the flame and sulfur components.

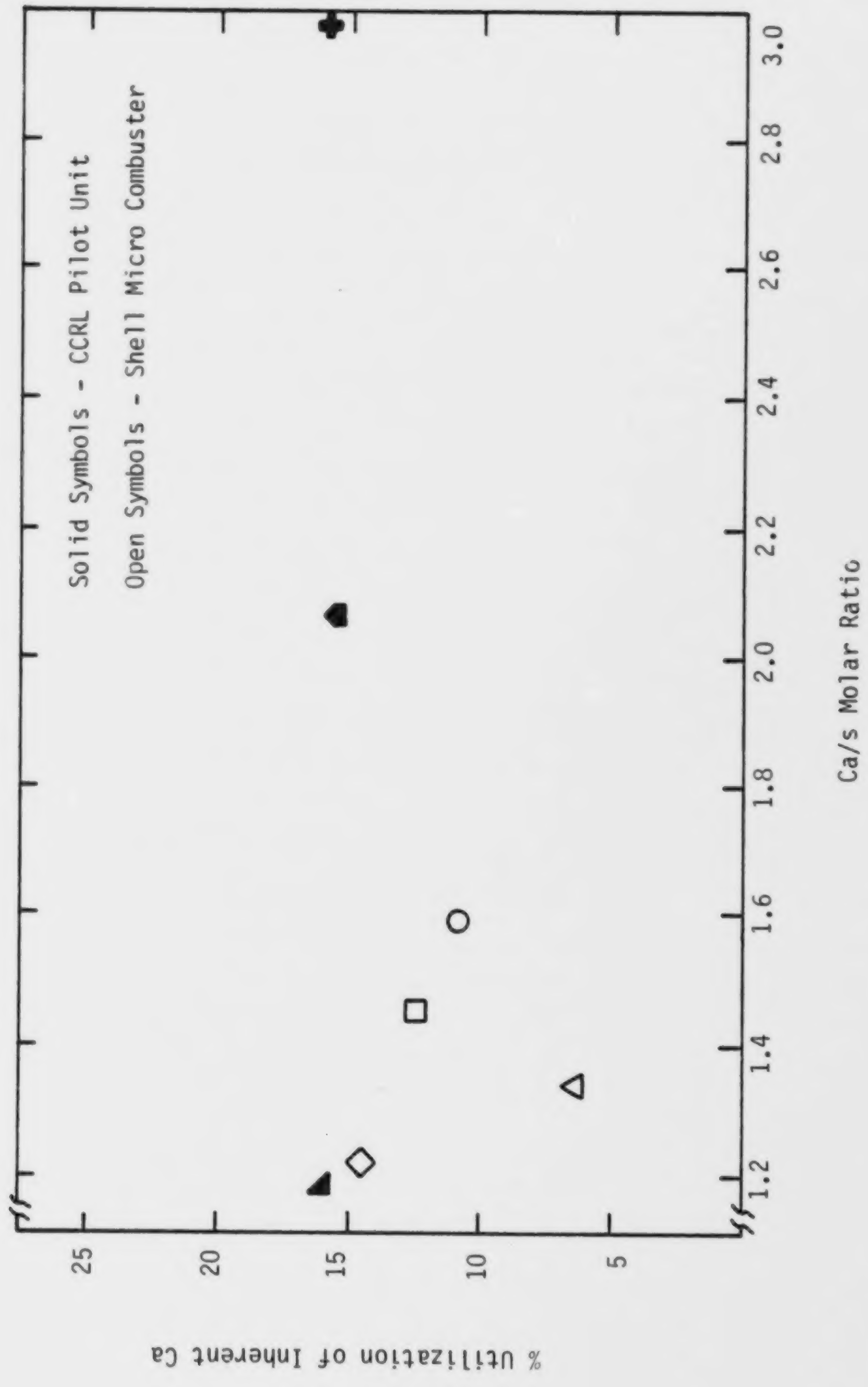

Figure 5-7. Calcium Utilization.

5.2 Alkali Sorbents Addition: Interactions of the Coal/Sulfur/Sorbent System

Having established the background for coal combustion and the basic coal-sulfur evolution, oxidation, and retention processes, we must superimpose the physical and chemical interactions of alkakli sorbent additives with the coal sulfur chemistry. A portion of Figure 5-1 is repeated here as Figure 5-8; the reader's attention is now drawn to follow the progress of the sorbent particles through the furnace. Calcium carbonate is used as a representative alkali metal sorbent for illustrative purposes.

One should note that Figure 5-8 implies that the sorbent is injected with the coal particles. Although this is mechanically the easiest way to introduce the sorbent into the furnace, and is conceptually the simplest to follow, it may not be the most effective way to capture sulfur in the furnace. The low NO_x distributed mixing burners have two stage air injection systems as has been discussed earlier. Alkali sorbents may be introduced with the coal into the central reducing atmosphere of the flame or may be injected around this rich core with the tertiary or staging air. On a macroscopic level and in terms of overall thermal and chemical history of the sorbent these two injection modes may be very different, but on a microscopic, single particle level there are only a few possible processes. These processes are illustrated in Figure 5-8 as follows: a) A sorbent particle is injected and immediately reacts as the carbonate with some sulfur species then continues through the furnace where it may oxidize, decompose or remain the same; b) A sorbent particle is injected and calcines, giving off carbon dioxide and forming a porous reactive oxide which continues through the furnace. The oxide may overheat and dead burn, encounter some sulfur species and react, or pass through the furnace unreacted; c) further downstream the sorbent may still react with a sulfur compound, the reacted sorbent may oxidize or decompose or the oxide may be retained on a surface (such as a bag house filter) and react with SO_2 passing over it.

Sections 5.2.1 and 5.2.2 deal with these furnace/sulfur/sorbent interactions. Section 5.2.1 reviews sorbent characteristics that affect sulfation capacity and reactivity and the effect of boiler conditions (especially thermal history) on these characteristics. Section 5.2.2 deals with the kinetics of the sorbent sulfur system; especially the $H_2S/CaO/CaCO_3$ and SO_2/CaO reactions.

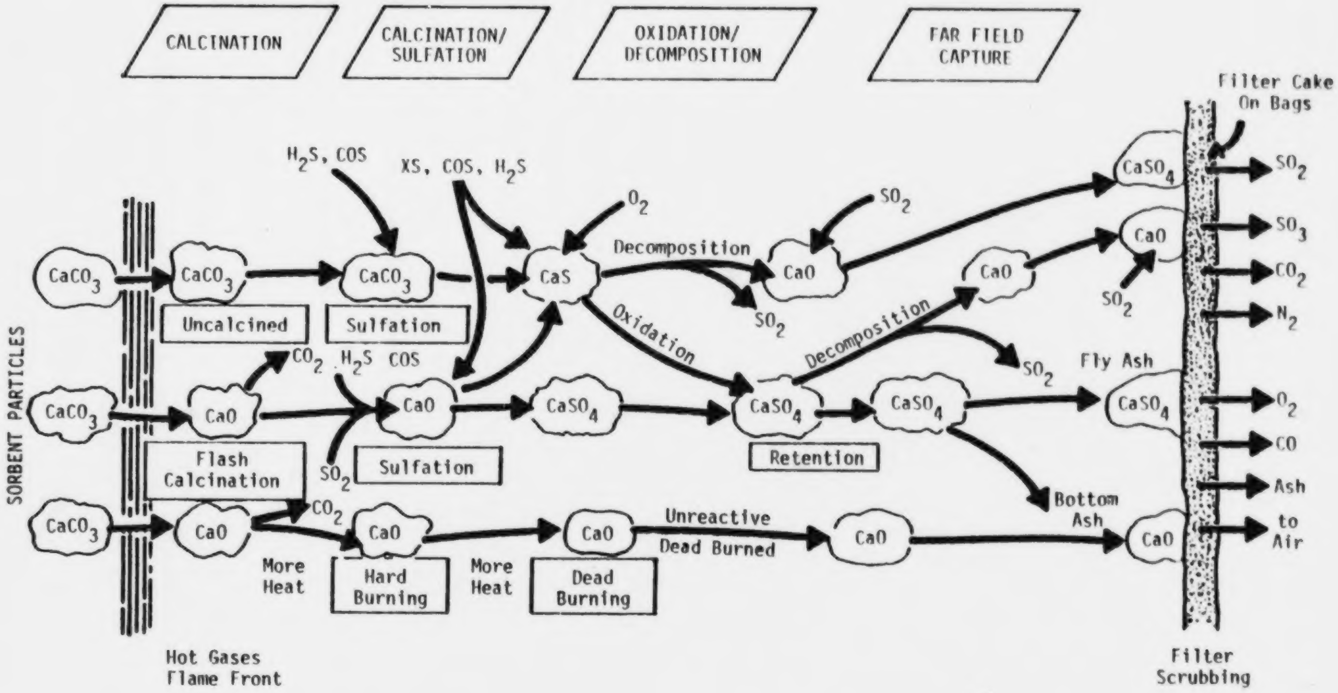
CALCINATION
CALCINATION/ SULFATION
OXIDATION/ DECOMPOSITION
FAR FIELD CAPTURE
SORBENT PARTICLES
$CaCO_3$
$CaCO_3$
Uncalcined
H_2S, COS
$CaCO_3$
Sulfation
XS, COS, H_2S
O_2
CaS
Decomposition
CaO
SO_2
SO_2
Oxidation
$CaCO_3$
CaO
Flash Calcination
CO_2
H_2S COS
CaO
SO_2
Sulfation
$CaSO_4$
$CaSO_4$
Retention
Decomposition
SO_2
CaO
$CaSO_4$
Fly Ash
Bottom Ash
$CaCO_3$
CaO
CO_2
More Heat
CaO
Hard Burning
More Heat
CaO
Dead Burning
Unreactive
Dead Burned
CaO
$CaSO_4$
CaO
SO_2
$CaSO_4$
CaO
Hot Gases
Flame Front
Filter Cake On Bags
SO_2
SO_3
CO_2
N_2
O_2
CO
Ash
to Air
Filter Scrubbing

Figure 5-8. Possible Transformations and Interactions of Sorbent Particles in a Coal-Fired Furnace.

5.2.1 Sorbent Characteristics: Furnace Effects and Effects on Calcination, Reactivity and Capacity

Clearly sorbent characteristics, including reactivity and sulfation capacity, are not independent of the furnace/flame system. The effects of varous parameters, including gaseous environment and thermal history, on sorbent characteristics will be discussed. Fundamental studies discussed by Borgwardt (1971), Coutant (1971) and Ishihara (1970) as well as review reports by Sliger et al (1972) and Battelle Memorial Institute (1966) are the sources for the information discussed. This is not intended to be an exhaustive review and the interested reader is referred to the sources cited for more detailed information. In particular, the articles by Borgwardt and Coutant are excellent sources. Three studies are singled out below as being both representative and sufficiently significant to warrant detailed discussions. Borgwardt (1971) presents results of a study directed toward the identification of fundamental mechanisms controlling the ulimate utilization of various sorbent calcines in isothermal, nondispersed reactors. The results of this study define the potential impact of these parameters under idealized reaction conditions. In another study conducted by Ishihara (1970) Borgwardt's studies were extended to include some of the more practical system processes to be encountered in boilers, such as, (1) a temperature/time history (non-isothermal), and (2) the sorbent calcine dispersed in a SO_2 laden flue gas. Different boiler designs have differing temperature/time histories, and the third significant study, that by Battelle (1966) extended the above efforts to include a broad range of temperature/time histories sufficient to cover the full range encountered in practical commercial boilers. Further, since boilers will utilize uncalcined sorbents, the raw sorbent material was used by Battelle.

All of these studies were designed to investigate the reactions of SO_2 with calcined sorbents which would occur in fuel lean regions; the possibility of the direct reaction of uncalcined sorbent with reduced sulfur species was not considered. These reactions become real possibilities only in a staged combustion system such as the DMB and have received little attention until recently.

The results from these studies which characterized fuel lean combustion systems have shown that three distinct processes must be optimized in order that in situ sulfur capture by sorbents be both technically and economically feasible. Firstly, the sorbent must be calcined under temperature/time histories that not only provide rapid evolution of the CO_2 but also insure a resulting particle morphology which is ideal for the overall sulfation step and which maximizes the sulfation capacity of the sorbent. Secondly, the sulfation reaction rate must be maximized to insure that the sulfation process is accomplished rapidly. While this is somewhat dependent on the particle physical characteristics it is also dependent upon the specific chemical makeup of the calcine as well as both the SO_2 and O_2 concentrations, and temperature/time history. Thirdly, the overall utilization of the sorbent must be maximized in order to minimize the amount of sorbent required. Since intra-particle diffusion is extremely slow, the pore diffusion resistance is considered to be the limiting step in achieving full utilization (i.e., 100 percent) of the sorbent particle. Unfortunately, unless the intra-particle structure can be utilized within the residence times typical of commercial boiler systems then overall sorbent utilization efficiencies will be limited to that attainable from total reaction of SO_2 with the calcine contained on the particle surface (which is the BET surface area of the sorbent).

The following discussion is divided into the three process steps described above: (1) factors affecting sorbent calcination; (2) factors affecting sorbent reactivity, and (3) factors affecting sorbent utilization. Although for convenience of presentation these processes have been divided it is not meant to imply that when injected into the boiler all processes occur sequentially.

5.2.1.1 Factors Affecting Sorbent Calcination

The term calcination refers to the dissociation of the CO_2 from the carbonate anion of an alkali metal carbonate when heated. The large number of sorbents studied for boiler application can generally be grouped into those containing calcium, magnesium and/or sodium (K_2CO_3 has been studied for MHD application as well as other carbonate compounds). For these three compound classes the general calcination reactions are:

Calcium Carbonate: $CaCO_3 \xrightarrow{\text{Heat}} CaO + CO_2$

Magnesium Carbonate: $MgCO_3 \xrightarrow{\text{Heat}} MgO + CO_2$

Sodium Bicarbonate: $2NaHCO_3 \xrightarrow{\text{Heat}} Na_2CO_3 + H_2O + CO_2$

It is believed that during calcination the sorbent particles do not change their physical size but do undergo significant increases in pore diameter (and therefore BET surface). This fact is clearly seen from inspection of the data shown in Table 5-10. Eleven different raw sorbents are compared for pore characteristics before and after calcination at 1100°C. Note first that there is a wide variation in pore size between the various sorbents ranging from 0.01 to 4μ diameter after calcination. This fact alone suggests that even though a sorbent is classed in a general category such as "calcite" there can be wide variations in surface and pore characteristics which may be attributed to the details of the calcination process or the physical structure of the sorbent. As shown in Table 5-10 the overall pore volume of all of the stones increased more than an order of magnitude (~40 times) when calcined at 1100°C.

Borgwardt indicated that this was accomplished without any significant change in particle diameter. Another characteristic reported by Borgwardt (although not shown in Table 5-10) is that the BET surface after calcination was almost independent of initial particle size. This observation is supported by Ishihara's work where several limestones were "instantaneously" calcined in a dispersed reactor at 2190°F, and almost identical specific surface areas resulted regardless of initial particle size (see Table 5-11). (The initial specific surface area was inversely proportional to particle diameter). It is also interesting to note that flash calcination resulted in about the same final surface area for all of the limestones, suggesting that when calcined quickly rather than slowly, as in Borgwardt's case, the final particle BET surface will be independent (or a weak function) of differences in particle composition. Figure 5-9 shows the change in specific surface area of several sizes of Mie limestone due to flash calcination. The surface area change ranged from an order of magnitude for the 3 μm stone to forty times for the 20 μm stone. If these results are extrapolated to particle sizes in the range of Borgwardt's it suggests that rapid calcination in a dispersed reactor will produce surface areas about one order of magnitude greater than those produced in the lower temperature fixed bed. It is not known whether this characteristic will continue to hold for even larger particle sizes. If it does not it appears that small initial particles sizes will result in greater final total surface areas than will large initial particle sizes.

Table 5-10. Physical Characteristics of Several Raw Stones and Their Calcines.

Stone or Mineral	Raw Stone	Stone Calcinated at ∿1100C	
	Mean Pore Volume cc/g	Pore Volume cc/g	Mean Pore Diameter (μ)
Calcite	0.004	0.30	2.1
Limestone	0.020	0.29	0.60
Limestone	0.007	0.32	0.44
Dolomite	0.010	0.42	0.27
Dolomite	0.026	0.40	0.30
Magnesite	0.042	0.34	0.01
Aragonite	0.020	0.36	4.0
Dolomite	0.018	0.36	0.42
Marble	0.89	1.21	1.6

Table 5-11. Specific Surface Area of Calcined Limestone and Hydrated Limes Heated Rapidly.

Sorbents	Mass Mean Particle Size μ	Specific BET Surface Area m^2/g
Mie limestone	57	9.4*
	20.5	23.8
	20.5	22.1
	3.4	22.8
Hikawa limestone	49	18.9
	12	22.2
Joban limestone	17	28.2
	14	24.4
Ishige limestone	12	6.5
Tokunosima limestone B	14	15.5
Hydrated lime	5.8	16.0

*Incomplete decomposition

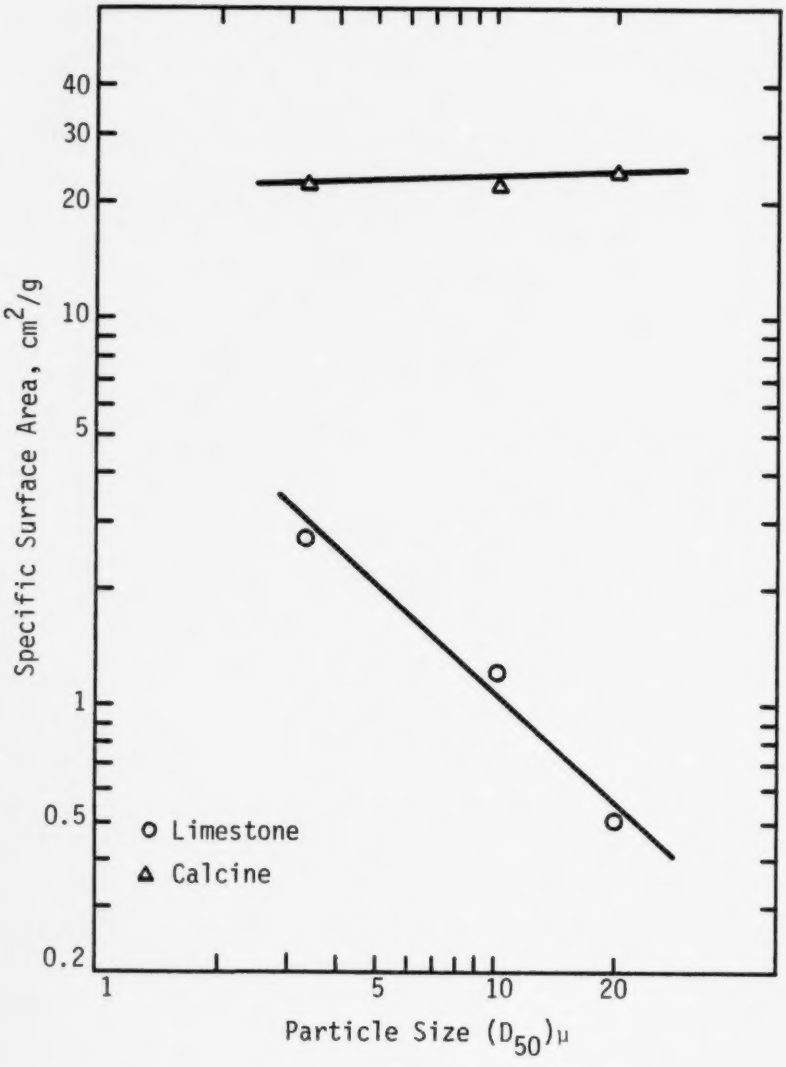

Figure 5-9. Change of Specific Surface Area of Limestone by Calcination and Reaction in Combustion Gases.

Pore characteristics and physical dimensions of the calcine are dependent upon the calcination temperature, as shown in Figure 5-10 (adapted from Borgwardt, 1972). Note that when the particles are subjected to gas temperatures of 1800°F or greater in a fixed bed reactor the overall surface area (BET) decreases although the mean pore diameter continues to increase. This decrease in BET surface, called overburning, has a slight but not severe effect on the reaction rate of the calcine. Higher temperature calcination results in deadburning which is accompanied by complete loss of calcine reactivity. Borgwardt speculates that the loss in surface area of the hard burned calcines was due to some shrinkage of and crystallite growth in the particles. Ishihara found similar results in the dispersed bed reactor studies where calcination was almost instantaneous. In those experiments the decrease in specific surface area was found to occur at gas temperatures of 2190°F rather than at 1800°F as reported by Borgwardt. This difference is probably because the particle temperature significantly lags gas temperature under the rapid heating rates used by Ishihara.

The physical properties of calcined sorbents are dependent on the time/temperature history experienced by the particles during calcinaton. Also, different sorbents of the same class undergo the transitions from softburning to hardburning and finally deadburning at conditions which are specific to a given sorbent. A schematic is presented in Figure 5-11 showing the general effect of increasing the particle temperature during calcinaton on its physical and chemical characteristics. While the temperatures listed are dependent on the specific sorbent, they are representative for most of those of interest. These results suggest that if particle temperatures (not necessarily gas temperatures) can be kept below about 2000°F during calcination then maximum particle specific surface areas and therefore, high chemical reactivity will result.

5.2.1.2 Factors Affecting Sorbent Reactivity

There have been several fundamental studies of the factors affecting sulfation of alkali metal oxides. Studies have shown the major variables which affect calcined sorbent reactivity are: particle size, pore diameter and size distribution, specific surface area, and chemical composition. These variables are not necessarily independent and are affected by the reacting environment but an attempt has been made to separate their effects in the following discussion.

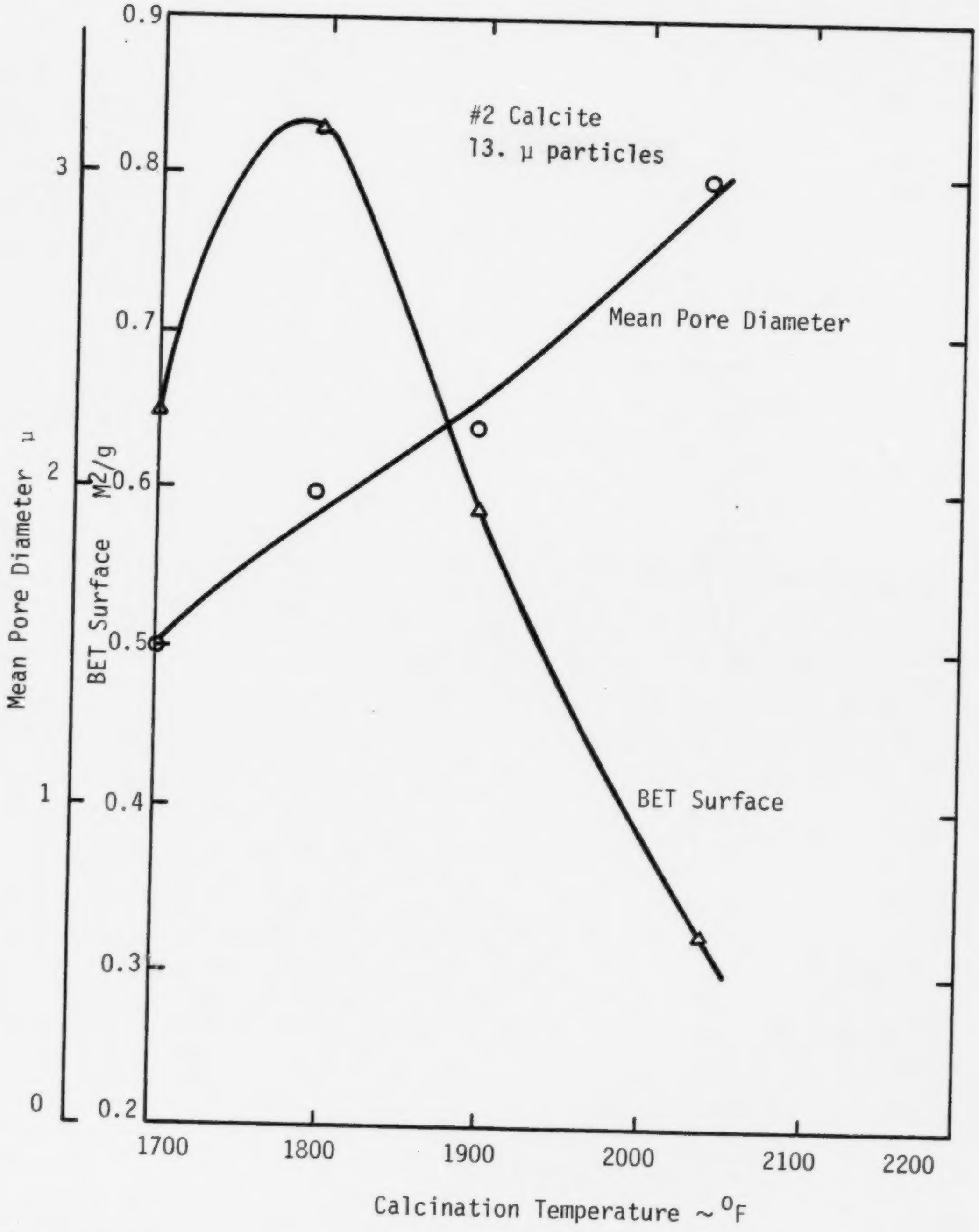

Figure 5-10. Effect of Calcination Temperature on Particle Physical Characteristics (120 minutes).

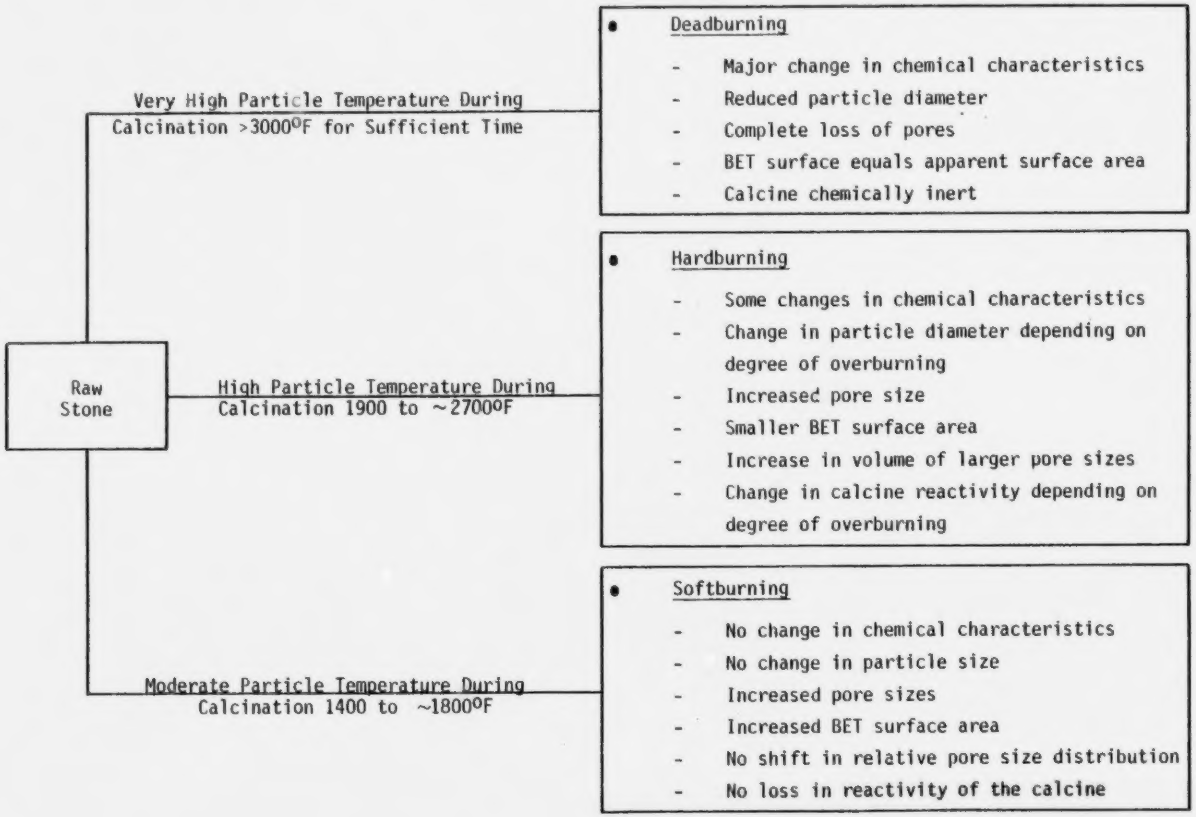
Raw Stone
Very High Particle Temperature During Calcination >3000°F for Sufficient Time
High Particle Temperature During Calcination 1900 to ~2700°F
Moderate Particle Temperature During Calcination 1400 to ~1800°F
• Deadburning
- Major change in chemical characteristics
- Reduced particle diameter
- Complete loss of pores
- BET surface equals apparent surface area
- Calcine chemically inert
• Hardburning
- Some changes in chemical characteristics
- Change in particle diameter depending on degree of overburning
- Increased pore size
- Smaller BET surface area
- Increase in volume of larger pore sizes
- Change in calcine reactivity depending on degree of overburning
• Softburning
- No change in chemical characteristics
- No change in particle size
- Increased pore sizes
- Increased BET surface area
- No shift in relative pore size distribution
- No loss in reactivity of the calcine

Figure 5-11. General Summary of Effect of Calcination Temperature on Particle Physical and Chemical Characteristics.

Particle specific surface area and pore diameter are interrelated and therefore will be discussed together. The results from the previous section suggested that increasing the temperature during calcination will result in a decrease in BET surface and a corresponding increase in pore diameter.

Using Borgwardt's data for particle sizes in the 100μ range the effect of pore diameter on reaction rate of CaO with SO_2 can be assessed as shown in Figure 5-12. The data plotted in this manner shows that as the pore diameter decreases the reaction rate initially increases suggesting that the number of small pores is increasing with a corresponding increase in the active surface-to-volume ratio. A maximum reaction rate is then achieved when the mean pore diameter has decreased to approximately 0.2 to 0.4μ, followed by a rapid decrease in the reaction rate. The maximum in the CaO reaction rate curve is probably due to the interaction of two competing reaction controls: (1) CaO reaction rate, and (2) SO_2 diffusion rate. These results suggest that very large or small pore sizes are undesirable and there is an optimum range of pore size where the reaction rate is maximized. Borgwardt's data further suggests that the critical minimum pore diameter causing a decrease in reaction rate may be dependent on the particle size. As shown in Figure 5-13 as the particle size decreases the reaction rate for the smallest pores tend to increase almost exponentially. If the results can be extrapolated to sizes less than 96μ then the reaction rate for small pores would tend to approach that of the intermediate sizes and it is possible that reaction rate for very small particles may be independent of both pore size and particle size.

The above results indicate that the effects of surface area and pore size on sorbent reactivity are complex but an ideal scenario can be imagined: select a sorbent with pores sufficiently large enough to give a good reaction rate and which expands or fragments when the sorbent is heated above the temperature where optimum sized pores are formed. As such a sorbent is heated the reaction rate would increase and if it swelled or fragmented at the correct temperature the downturn in reaction rate due to diffusion limitations would be eliminated.

In summary, the results imply that to maximize the sulfation reaction rate it is important to match the sorbent pore growth characteristics with an optimum temperature/time profile.

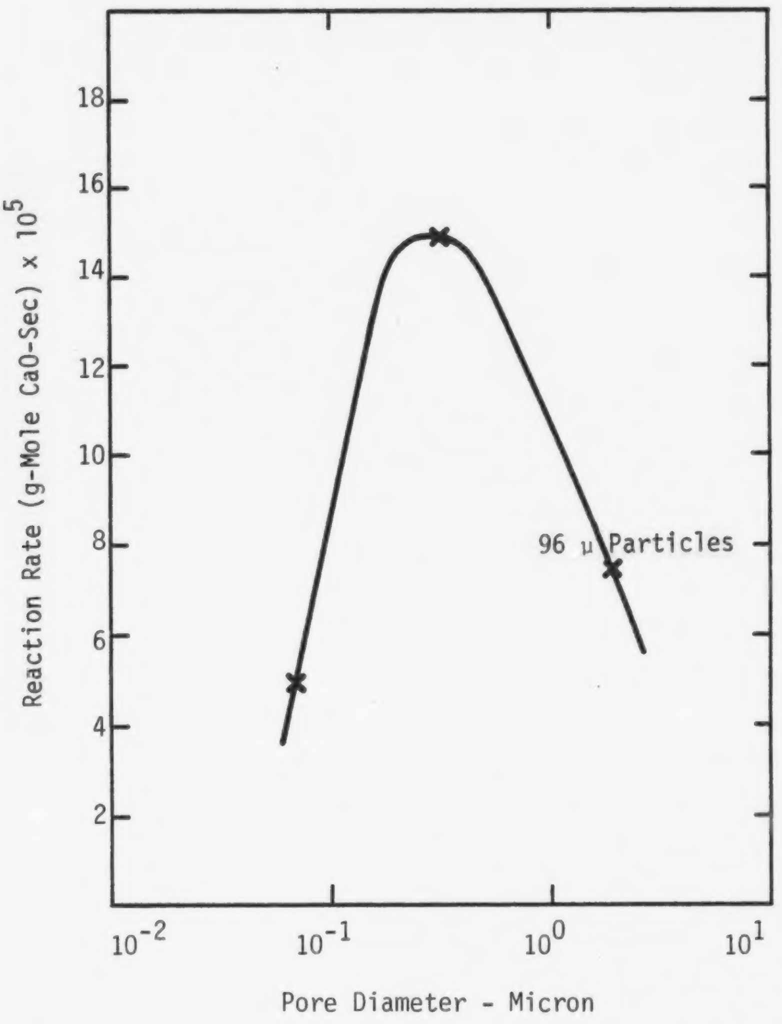

Figure 5-12. Effect of Pore Diameter on Reaction Rate 96 μ Particles.

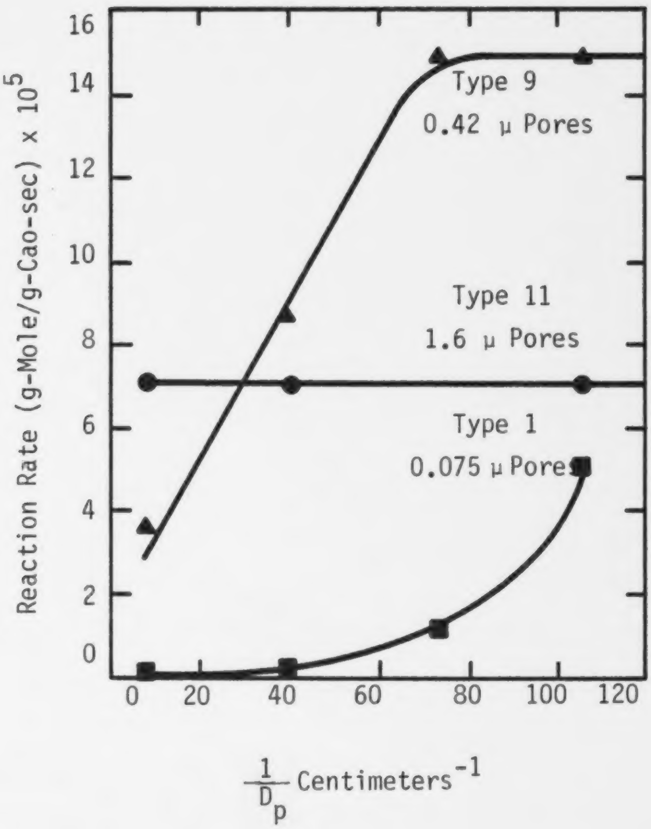

Figure 5-13. Reaction Rate at Constant Sulfation as Affected by the Pore Size of the Calcine, Illustrating Zero, Linear, and Expotential Responses to $1/\overline{D}_p$.

The effect of particle diameter on reaction rate is somewhat complicated by the fact that, depending on the pore diameter, the reaction rate can be extremely sensitive to particle size or insensitive as was shown in Figure 5-13. The effect of particle diameter on reaction rate for four different limestones is shown in Figure 5-14. For the intermediate range of pore sizes note that as the particles become very large the reaction rate appears to be approaching zero and limestone utilization can be considered to be limited by reaction on the particle surface. This is not unexpected since diffusion into the inner particle will become more difficult as the particle becomes larger. As the particle size decreases the reaction rate tends to increase first rapidly then more slowly as particle size becomes very small.

If the results of Ishihara (presented earlier) which indicated that after rapid calcination at a given temperature the BET surface area is independent of the initial particle size are applicable to these studies then the results shown in Figure 5-14 are an independent comparison of particle size and reaction rate. Therefore, for the range of particle sizes of interest to boiler applications, where rapid calcination is expected to occur, variation in particle size independent of any other change would not be expected to have a large impact on sorbent reactivity.

5.2.1.3 Factors Affecting Sorbent Capacity

When a sorbent particle is injected the hot gas or combustion environment it heats up, calcines, and may react with sulfur species in the surrounding gases. The onset of calcination is very rapid for small particles injected into hot environments. Figure 5-15 (Sliger et al) shows the calculated time required to heat particles injected into hot gas. As shown in Figure 5-16 (Coutant), calcination and sulfation may occur while the particle temperature continues to increase toward the gas temperature. The time required for calcination is dependent on the gas temperature and as shown in Figure 5-17, about 90 percent calcination can be achieved in about 1.0 second for gas temperatures of 2028°F. Note that at the conditions specified for this calculation the sulfation process is not completed until after the particle temperature had reached a maximum temperature. If both the calcinaton process and the reaction rate for sulfation are maximized and both processes are complete before the particle temperature reaches levels at which overburning occurs, then maximum sorbent utilization

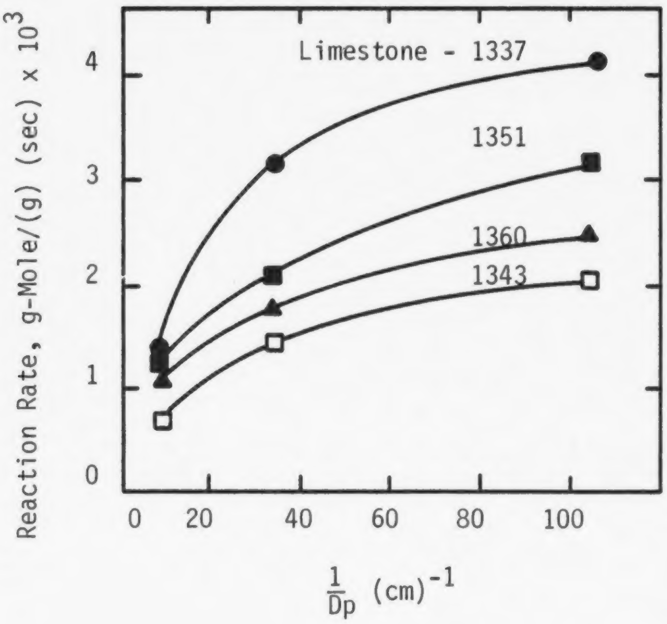

Figure 5-14. Reaction Rate vs. $1/\overline{D}_p$
Sulfate Loading = 2×10^{-3} g. moles/g

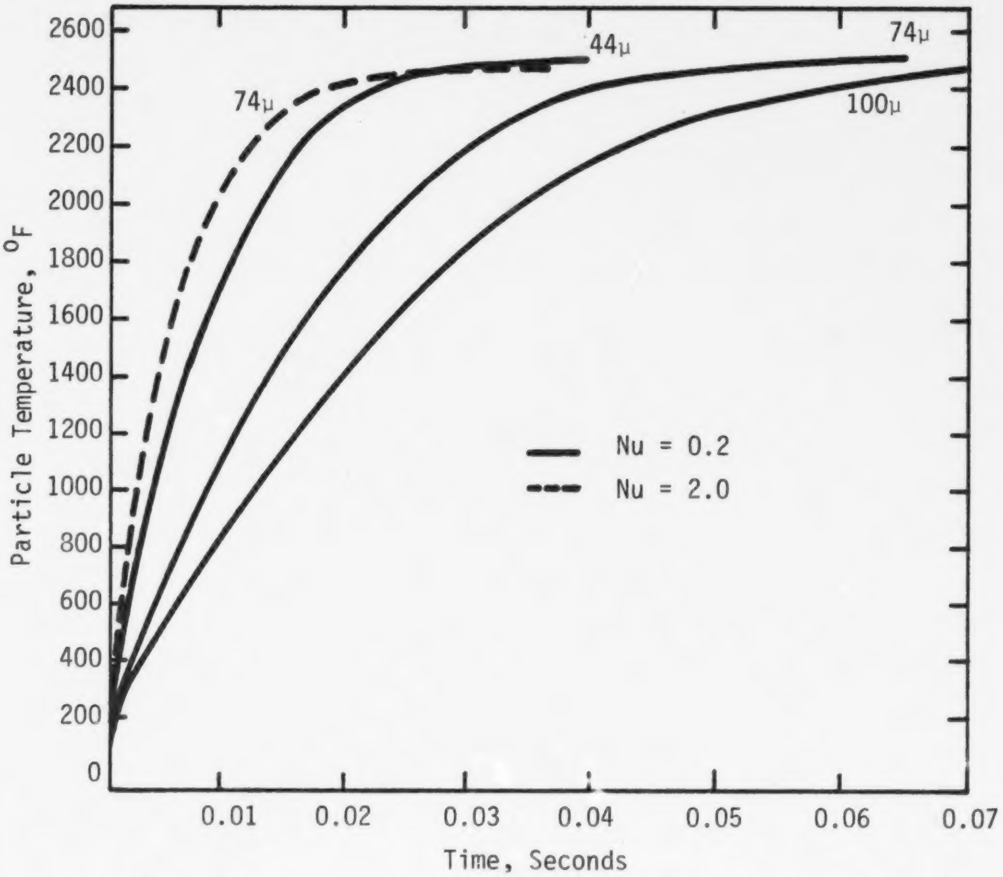

Figure 5-15. Particle Heat-Up Time for Limestone.

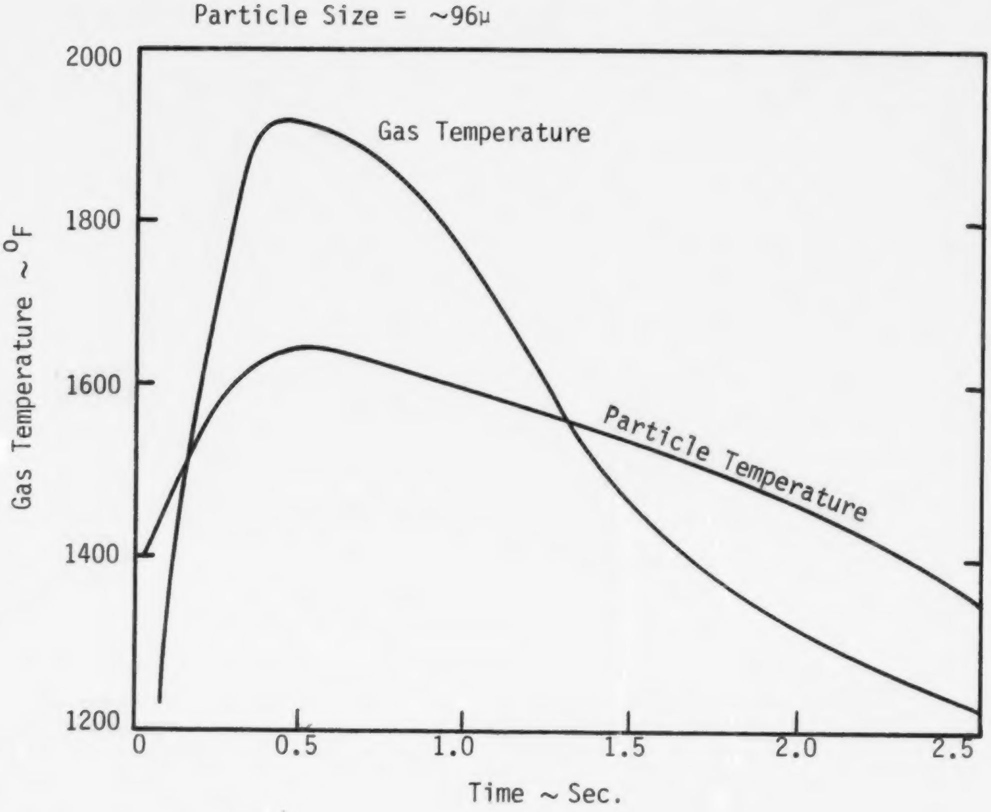

Figure 5-16. Typical Particle Heat-Up Characteristics.

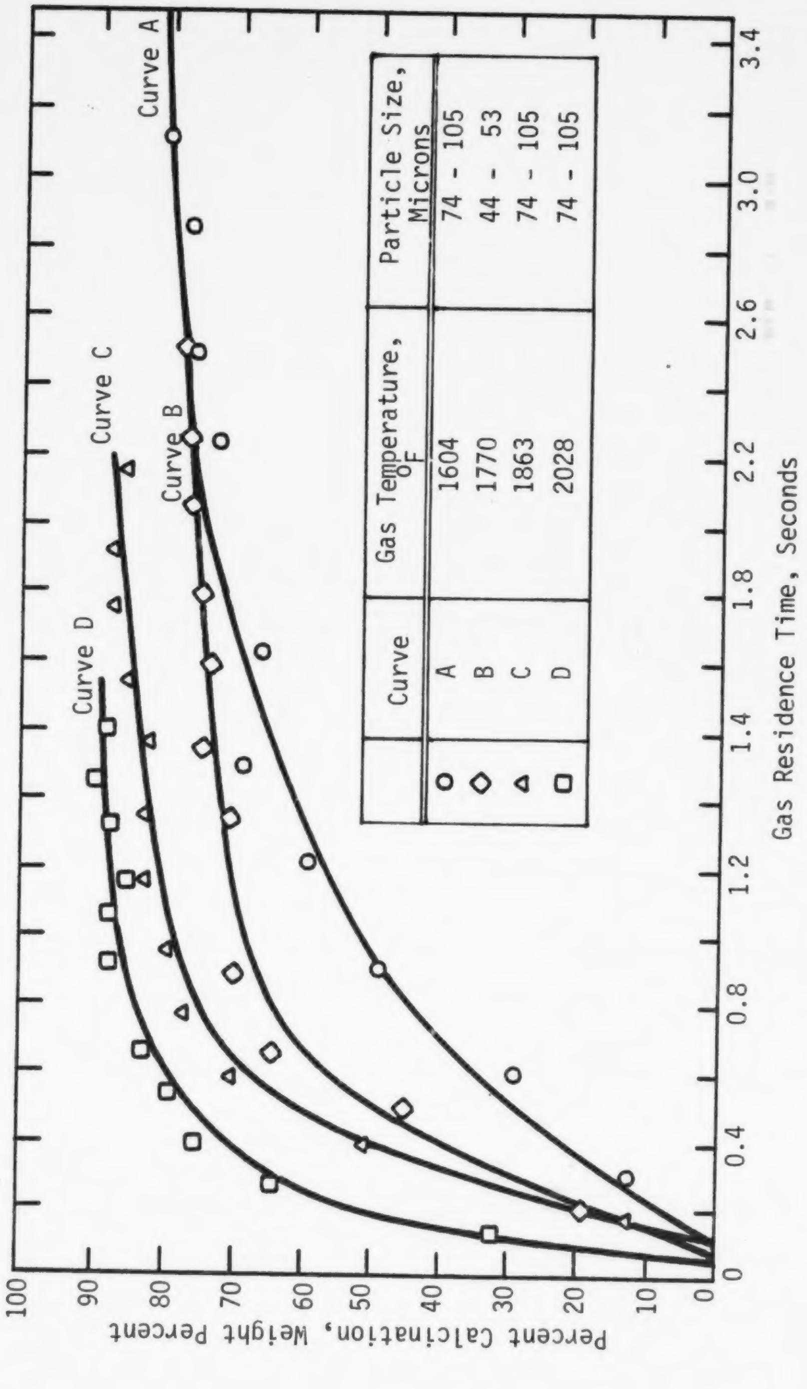

Figure 5-17. Effect of Gas Temperature on Calcination.

will occur. Further, good distribution of the sorbent in the gas stream is also necessary in order to maximize utilization of all of the avilable sorbent particles. Theoretically the major requirement is that the sorbent be distributed in an identical manner as that of the coal so that quantitative reaction between the calcine and sulfur can results.

If both the calcination and sulfation process steps are optimized then the major limits to 100 percent utilization of the sorbent are sufficient residence time for diffusion of sulfur into all pores of the particle and into the solid portions of the material and elimination of any subsequent decomposition or disproportionation of the reacted sorbent. If sufficient residence time can be provided for pore diffusion then the maximum utilization of the available sorbent would be about 50 percent (equivalent to conversion of all sorbent on the BET surface of most stones). Since the proposed application is for boilers and the residence times are on the order of 2-3 seconds then intraparticle diffusion will not be a significant factor for practical particle sizes. Based on this type of limiting process and considering only "lean" reactions (in an oxidizing atmosphere) Borgwardt proposed a parameter, the "Effectiveness Factor," which relates the amount of CaO which reacts with SO_2 to form $CaSO_4$ to the amount of CaO initially available for reaction. The initially available CaO is only that on the particle surface and thus is related to the specific surface area. Based on this definition an effectiveness factor of one suggests that the entire BET surface has undergone reaction while for values much less than one, the reaction is confined to the outer particle surface. It is not surprising, therefore, to find that when all other factors such as temperature or SO_2 concentration are held constant the sorbent utilization is a function of particle size, pore size, residence time and sorbent type.

For large particles, greater than 100 microns, Borgwardt has shown that the major variable affecting utilization efficiency is the mean pore diameter. Typical results for 250 micron particles are shown in Figure 5-18. For these particle sizes, pore diameters greater than approximately 0.7 microns are reaction rate controlled while diffusion tends to become limiting for smaller pore sizes. Pore sizes even as large as 0.7 microns can result in significant diffusion resistance since the reaction of CaO to form $CaSO_4$ results in a large increase in volume (~173 percent). As shown schematically below, for very large pores the space is more than adequate to accommodate the larger $CaSO_4$

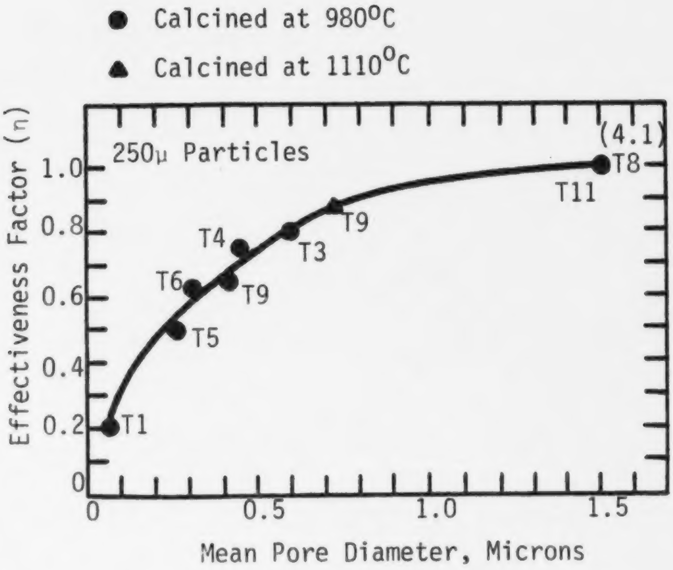

Figure 5-18. Relationship Between Effectiveness Factor and Pore Size.

molecules so that the change in diffusional resistance would be minimal. For

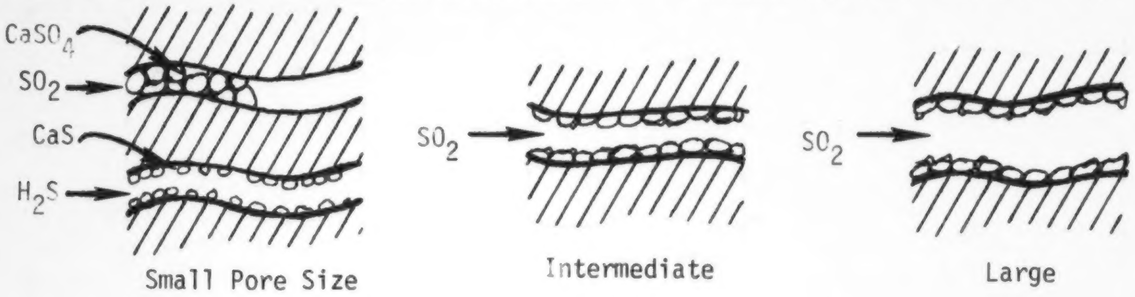

the intermediate sized pores the diffusional resistance would increase, however, if sufficient residence times were available then complete utilization would still be attainable. As the pore sizes become smaller the increase in $CaSO_4$ will eventually completely fill the void space, and in fact, since the reaction proceeds inward, would result in blocking the opening and thereby confining the reaction to the outer surface. Using this model it is apparent that the smaller the particle size then the smaller the pore diameter can be for a given utilization efficiency. According to Borgwardt, and suggested previously, the sulfation process is reaction rate controlled for small particles having pore sizes after calcination of 0.1μ or greater while it is diffusion rate controlled for large particles. It would appear then that it should be much easier to achieve high utilization of the CaO using small particles than large particles.

The maximum utilization of 50 percent of the CaO is further suggested as a limit by Borgwardt in Figure 5-19. These results show a continual decrease in pore volume as the sulfation process proceeds while the particle volume remained constant until the solid conversion reached 50 percent CaO conversion. When the conversion reached that of complete conversion of all CaO on the specific particle, surface expansion of the particle, accompanied by a significant decrease in reaction rate, occurred. It should be noted that some sorbents such as dolomite, aragoniate, and marl have exhibited the capability of achieving greater than 50 percent utilization of the calcine. In these cases the high utilization is attributed to the fact that these sorbents have greater specific surface/volume ratios; however, it should be noted that the impurity of the sorbent dictates that greater quantities are required than that for the more pure substances. In other cases (e.g., nacholite) there is some evidence to suggest that high utilization can result from particle communition (rupture resulting in many fine particles) during calcination.

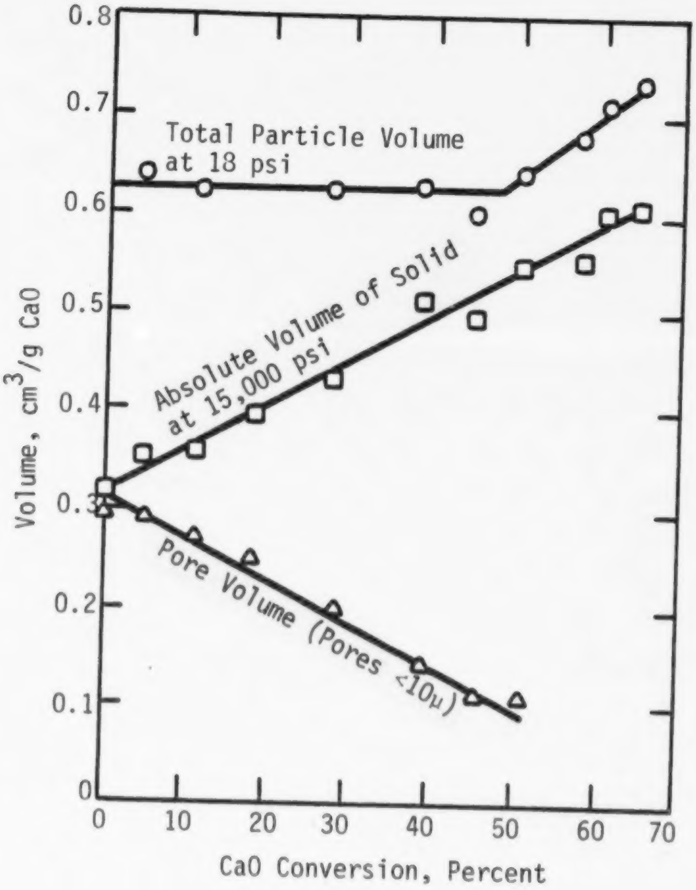

Figure 5-19. Pore Volume and Particle Volume as a Function of Conversion in 0.025 cm Particles.

The effect of pore size on sorbent capacity may be limited to regions in the furnace where the reactions are between the calcined sorbent and SO_2, or, in locally fuel lean regions. The reaction of H_2S or COS with a calcine, CaO for example, results in CaS formation. The formation of CaS on the particle surface and in the pores will not result in increased diffusional resistance as the CaS molecules are not significantly larger than the CaO molecules. The sorbent capacity is still probably limited to the available BET surface area even in fuel rich regions as intraparticle diffusion rates wil still be significant, but the minimum pore size constraint is relaxed.

Utilization efficiencies approaching 100 percent can only be achieved if the inner recesses of the particles are allowed to enter into the reaction. If a sorbent could be found which undergoes melting and/or evaporation at the temperature conditions occurring in boilers then the reaction as the particle cools in passing through the furnace would be on a single molecule basis rather than on a particle basis and a much higher utilization efficiencies would be attainable. This approach is of course that being used in the high temperature systems for MHD applications using KCO_3 where very high utilization efficiencies are achieved. Some work has also been carried out with cupric oxide at low temperatures (1360^{o}F) and found to result in significant absorption of SO_2 (40 percent weight change). For the higher temperatures in boilers (approaching 3000^{o}F) the CuO should melt (M.P. 1865^{o}F) and although the porosity would be destroyed it is possible that the total absorption of SO_2 into the liquid phase would be much greater than for the solid. These represent only two possibilities for obtaining greater sorbent utilization.

5.2.2 Kinetics of Sorbent Sulfur Reactions

The kinetics of the sulfation reactions between SO_2 and many alkali metal sorbents has received considerable attention; several excellent reviews of the subject have been published. The report prepared by Sliger et al of the M.W. Kellogg Co. for the EPA (1972) and articles by Borgwardt (1970-2) and Ishihara were the major sources for the material discussed in this section.

The use of staged combustion systems for NO_x reduction in pf boilers and the increasing interest in coal gasifiers has added impetus to the study of H_2S and COS reactions with solid additives. Freund (1980) and Yang (1979) have recently published articles dealing with the reactions of H_2S with limestone/ dolomite and COS with CaO respectively.

It is clear that sorbent characteristics play a key role in sorbent/sulfur kinetics and that these characteristics are in turn affected by the furnace environment as well as reactions with the sulfur compounds. The preceeding sections dealt with the effect of the furnace on the sorbents (calcination and deadburning) and the effect of sorbent characteristics on the sulfur sorbent reactions. This section will separate, as much as possible, the kinetics of the sulfur sorbent reactions. The focus of the following discussion will be the effect of external (controllable or furnace induced) parameters on the sulfur sorbent reactions. These parameters include sulfur species concentration, temperature, gaseous environment (i.e. O_2, H_2O, CO_2 concentrations) and residence time. The reactions of SO_2 with calcined limestone will be discussed then the kinetics of the H_2S calcium carbonate and calcium oxide systems and finally the reaction of calcium oxide with COS. This is not an extensive review but rather an overview designed to help direct the current research.

The effect of SO_2 concentration on reaction rate has been studied in both fixed bed (Borgwardt, 1972) and dispersed phase reactors (Ishihara, 1970) and found to be an important parameter. The experimental approach taken by Ishihara more closely models the particle size, temperature and temperature/time characteristics of commercial boilers. In Ishihara's experiments the sorbent was injected into a flue gas of known SO_2 concentration and allowed to react until exiting the stack. Ninety-six samples were taken at discrete locations along the reactor length and SO_2 concentrations determined. The ratio of calcium oxide reacted to the total calcium oxide input was then determined. Typical results are shown in Figure 15-20 for three different initial sulfate loadings. The initial reaction rate was then determined as the tangent to the curves passing through the origin. It is important to realize that in these experiments the temperature of the reacting gas varied with time so that any $\Delta n/\Delta t$ is not a total derivative but a partial derivative ($\partial n/\partial t$). This information was used to develop the Arrhenius plot shown in Figure 5-21 for the reaction rate constant ($K_1 = Ae^{-E/RT}$) as a function of 1/T. These results are particularly revealing in that they show that the reaction rate has a first order dependence on the sulfur dioxide concentration. In addition note that the initial reaction

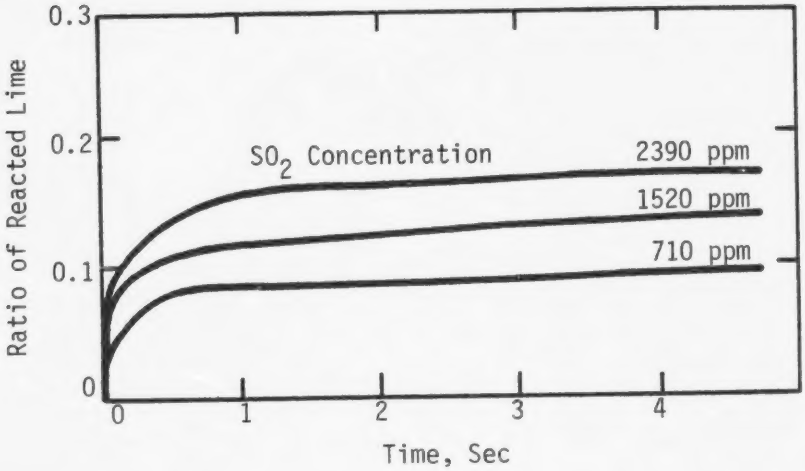

Figure 5-20. Relation Between Ratio of Reacted Lime and Sulfur Dioxide Concentration (Joban Limestone).

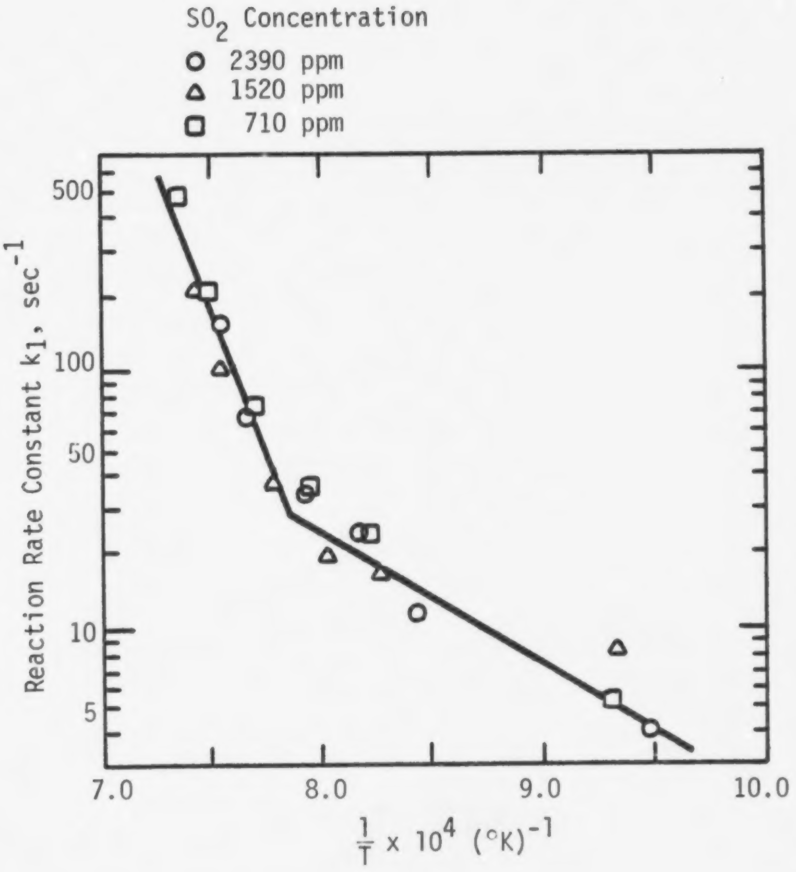

Figure 5-21. Arrhenius Plot for the Reaction of CaO with SO_2 Showing the Effect of SO_2 Concentration (Joban Limestone).

rate constant at high temperature drops rapidly until a temperature of about 1800°F and then the reaction rate constant decreases more gently. These results suggest that as the reaction proceeds the activity of the calcine decreases. From the nature of these experiments it is unlikely that this decrease is due to overburning; the authors suggest that initially the sulfation process is reaction rate limited and that plugging of the pores as sulfation proceeds leads to the diffusion rate controlling the reaction.

As mentioned earlier the sorbent reactivity (and therefore the reaction rate) is affected by the sorbent type. Data presented in Figure 5-22 (Borgwardt, 1971) show that the reaction rate also depends on the calcine type. These experiments conducted with fixed beds under isothermal conditions clearly show that (depending on the particular sorbent selected) an order of magnitude difference in reaction rate can occur.

The influence of SO_2 concentration on reaction rate characteristics are particularly interesting when viewed as the relationship of the ratio of reacted lime with SO_2 concentration as shown in Figure 5-23. These results (and also Coutant, 1971) show that the ratio is almost independent of the concentration of sulfur dioxide. For example, a fivefold increase in SO_2 concentration only increases the percentage of SO_2 captured by about 4 percent. Consequently, it would be expected that for almost any flue gas sulfur concentration level the percentage reduction in SO_2 concentration with addition of sorbents will be nearly constant. These results are almost identical with those of Battelle (1966) which suggests that the amount of SO_2 that can be removed from a gas stream is proportional to the gas SO_2 concentration to the 3/2 power.

The gas temperature at the sorbent injection point also affects the reaction rate, as demonstrated by the data plotted in Figure 5-24 (Ishihara, 1970). If the sorbent pore size is large enough (and constant) the reaction rate is directly related to the BET surface area. The data corresponding to mean pore diameters greater than about 0.2μ are plotted in Figure 5-25 (Borgwardt,1971) and clearly illustrate the linear relationship. These results show that for sorbents having pore sizes large enough so that diffusion is not controlling, the larger the specific surface area the greater the reaction rate. Dispersed phase reactor experiments (Figure 5-26) have also given similar results as

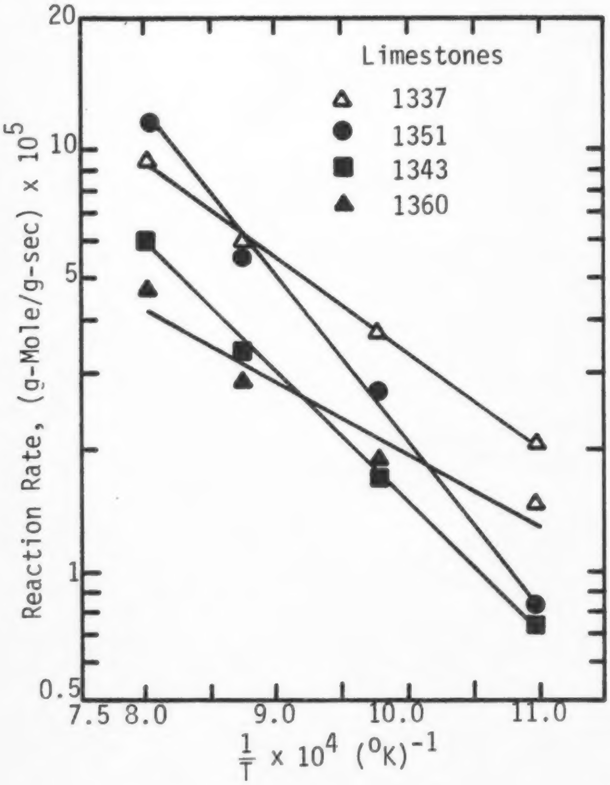

Figure 5-22. Arrhenium Plots for the Reaction of Sulfur Dioxide with Four Limestones.

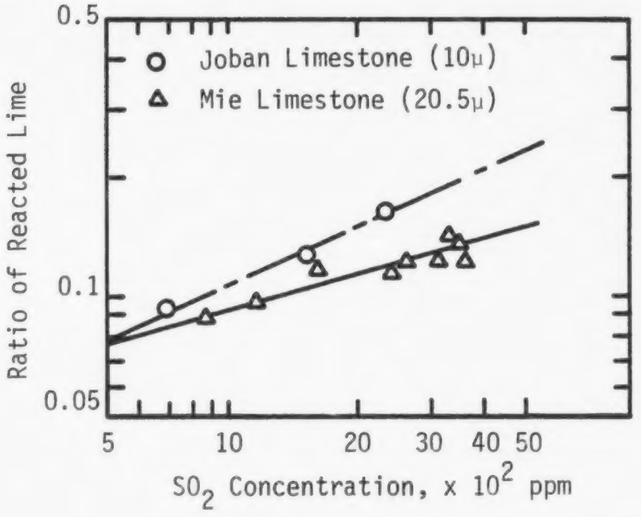

Figure 5-23. Relation Between SO_2 Concentration at Injection Point and the Reactivity of Lime.

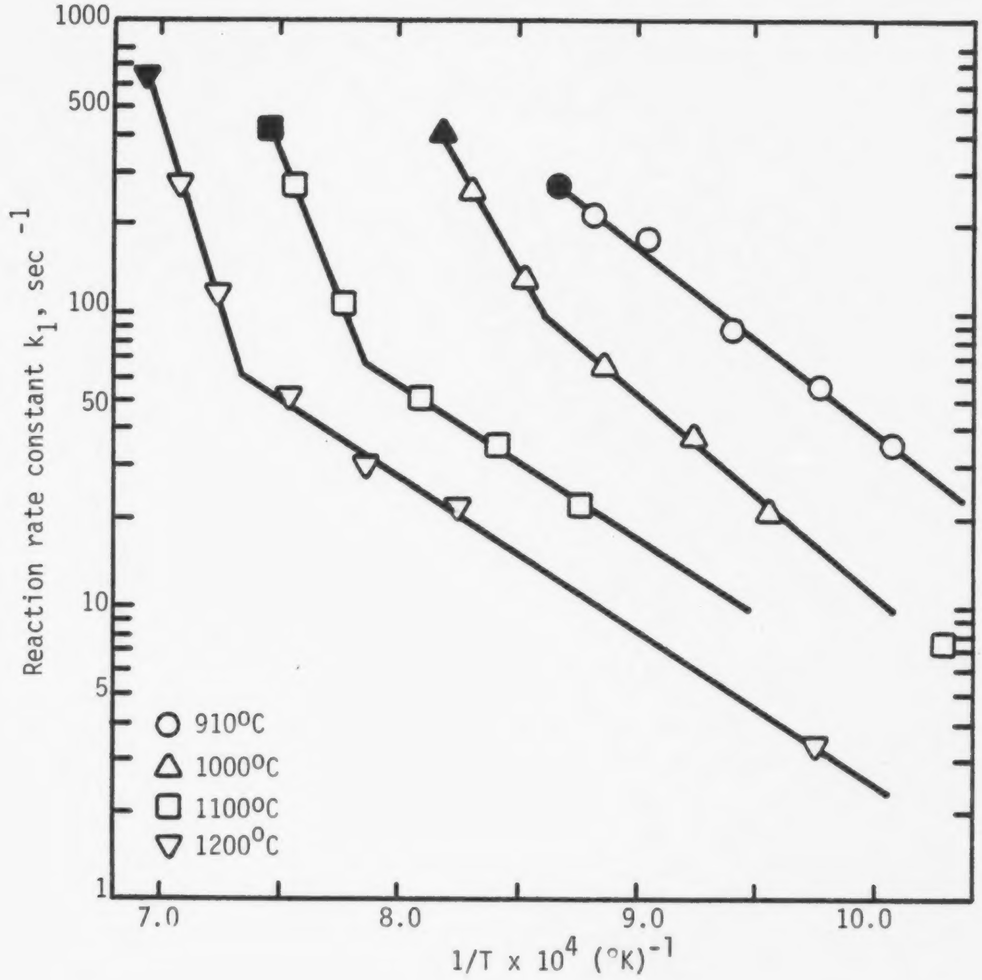

Figure 5-24. Arrhenius Plot for the Reaction of CaO with SO_2 Showing the Effect of Gas Temperature at Injection Point.

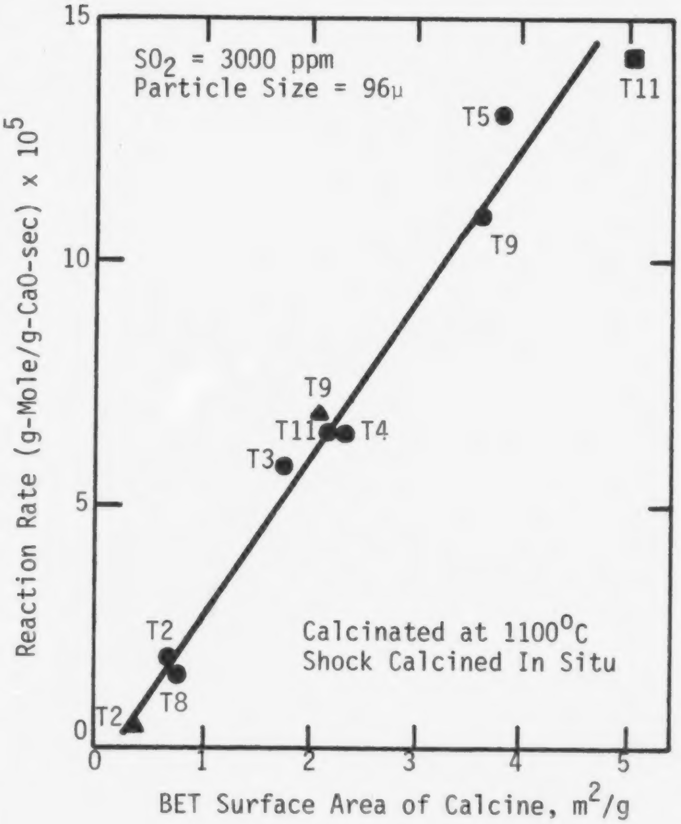

Figure 5-25. Reaction Rate vs. Surface Area.

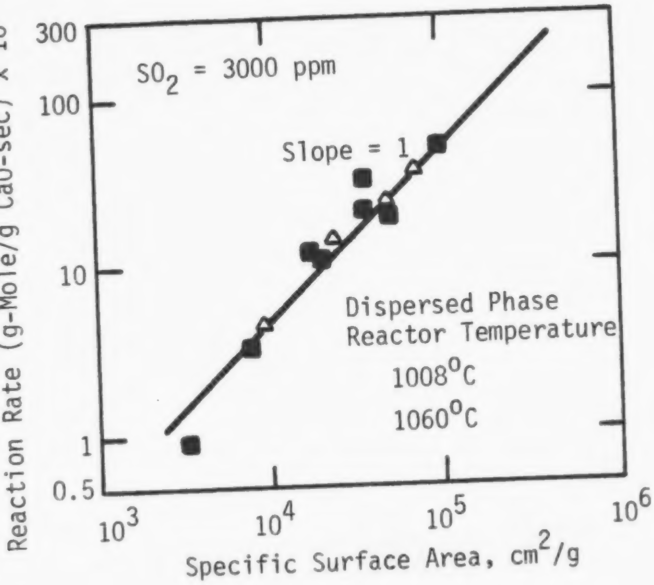

Figure 5-26. Comparison of Initial SO_2 Reaction Rates in a Dispersed-Phase Reactor.

those of Borgwardt so that these results should not be considered limited to fixed bed reactors.

The new, low NO_x, distributed mixing burners have combustion regions which are overall fuel rich. The sulfur capture by dry alkali additives may occur in these fuel rich regions. The possibility of such capture and the kinetics of H_2S/COS reactions with calcined and uncalcined sorbents is discussed in the following paragraphs.

The kinetics of the reaction between carbonyl sulfide and calcium oxide has been studied by Yang and Chen (1979). They measured the rate of sorbtion of COS by CaO at one atmosphere and temperatures from 500° to 900°C. They assessed the effects of CO concentration, flow rate of COS over the CaO bed, temperature and COS concentration on the reaction rate (see Figure 5-27a, b, c, d). The interplay between the chemical reaction rate and the COS diffusion into the CaO rate was interpreted using a grain model. The reaction

$$CaO + COS \rightarrow CaS + CO_2 \tag{8}$$

is first order with respect to COS as can be seen from the initial rate data (from Figure 5-27d) plotted in Figure 5-28.

The reaction of H_2S with CaO has been studied by Westmoreland et al (1977) and Pell et al (1971). At 700°C and 1 percent H_2S the initial reaction rates for the reaction

$$CaO + H_2S \rightarrow CaS + H_2O \tag{9}$$

are given by the two investigators as

$$\left(\frac{dX}{dt}\right)_{t=0} = 1 \times 10^{-4}\ S^{-1} \quad \text{(using reagent powder, Westmoreland)}$$

and

$$\left(\frac{dX}{dt}\right)_{t=0} = .6 \times 10^{-4} S^{-1} \quad \text{(using dolomite powder, Pell)}$$

these rates are similar to that measured by Yang for the COS reaction

$$\left(\frac{dX}{dt}\right)_{t=0} = 1.3 \times 10^{-4} S^{-1} \quad \text{(using reagent powder, Yang).}$$

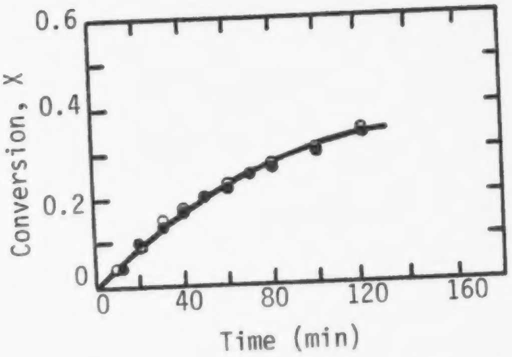

Fig. 5-27a. Reaction Rate of CaO with COS (0.1%) at 500°C; in N_2(●) and in N_2 with 10% CO(○).

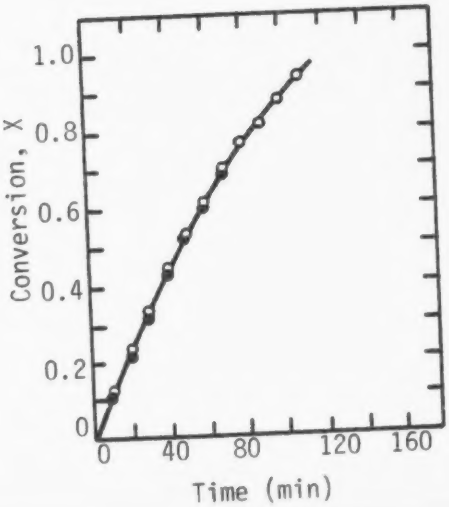

Fig. 5-27b. Effect of Flow Rate on Reaction Rate at 900°C with 0.1% COS and 10% CO in N_2; with Flow Rates of 1000 SCCM (○) and 2000 SCCM (●).

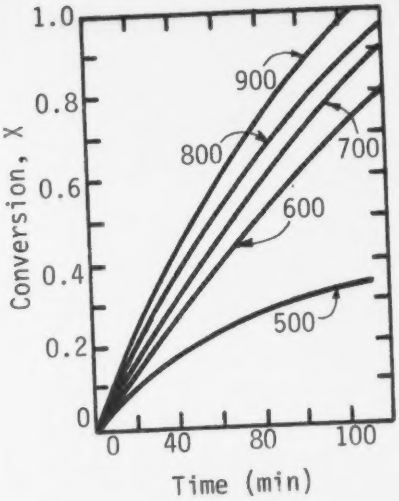

Fig. 5-27c. Effect of temperature on Reaction Rate with 0.1% COS and 10% CO in N_2.

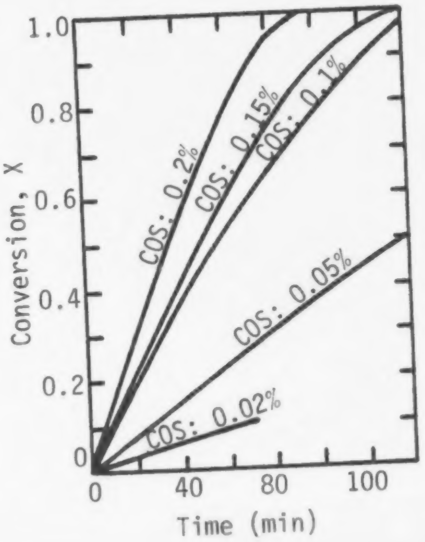

Fig. 5-27d. Effect of COS Concentration on Reaction Rate at 800°C with 10% CO and the Marked COS Compositions in N_2.

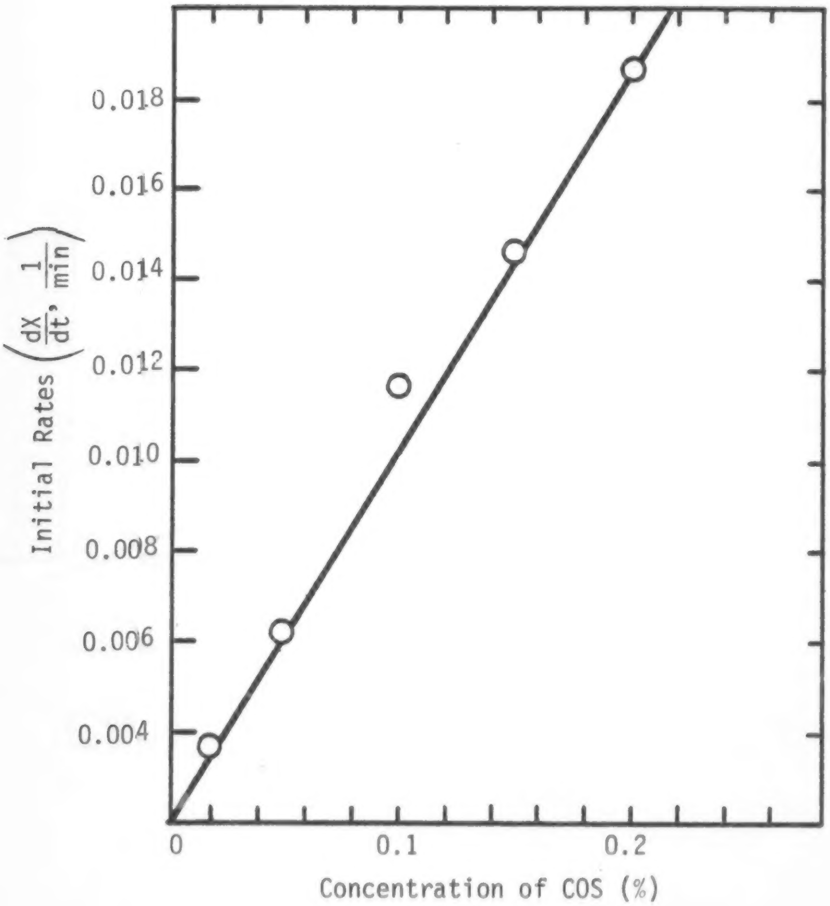

Figure 5-28. Analysis of the Reaction Order with Respect to COS at 800°C.

The reaction rates of either reduced sulfur species with CaO are similar under similar conditions; the reaction of H_2S with $CaCO_3$ is, however, much faster than the reaction of H_2S with CaO. Figure 5-29 compares the reaction rates of CaO and $CaCO_3$ with H_2S (from the data of Pell and Ruth respectively).

In summary, sulfur evolved from the coal may react with dry sorbents either as reduced species (H_2S or COS) or oxidized species (SO_2 or SO_3) and the reactions may take place before during or after calcinaton of the carbonate. There is evidence that reacton of the reduced species with uncalcined stones may be the most favorable for the formation of CaS at high temperatures.

Equilibrium calculations show that the product of reaction in rich regions, CaS, is stable at higher temperatures than the lean reaction product ($CaSO_4$- see Figure 5-30). However, it is unlikely that significant amounts of CaS could be retained in the solid when the coal is sufficiently burned out for efficient boiler operation. The direct oxidation of CaS to $CaSO_4$, retaining the sulfur in the solid phase, is an appealing possibility, but little information on the time/temperature/gaseous environment required for this direct oxidation exists. The equilibrium calculations show a sharp drop in stable solid sulfur species at SR = 1.0; this drop implies that the route from CaS to $CaSO_4$ with the sulfur remaining in the solid is unlikely at boiler temperatures. These are equilibrium distributions, however, and if the shift from rich to lean is fast the sulfur may remain in the solid phase.

We have now established a background of information about coal sulfur, its evolution from the coal during pf combustion, its oxidation and gas phase kinetics in a flame. We have also followed a sorbent particle through the boiler and have reviewed the effects of the boiler on sorbent characteristics and the effect of sorbent characteristics on sulfur capture. We have lightly reviewed the kinetics of sulfur/sorbent reactions and have looked at predicted equilibrium species distribution. In summary many factors affect the final fate of sulfur (either emitted as a gaseous specie or retained in the solid phase) in a pf boiler when dry sorbents are added. These factors include:

1) sorbent properties, type, particle size, surface area, pore size and size distribution;

2) the effect of the flame and furnace on the sorbent including;

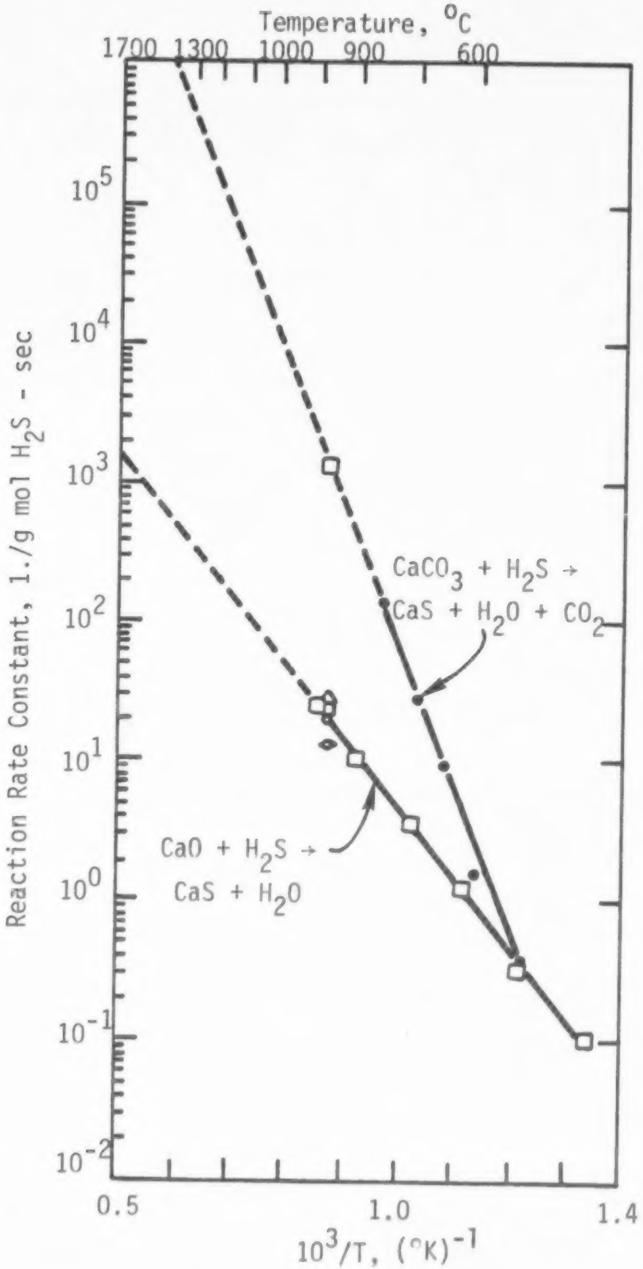

Figure 5-29. Extrapolation of Reaction Data to High Temperatures.

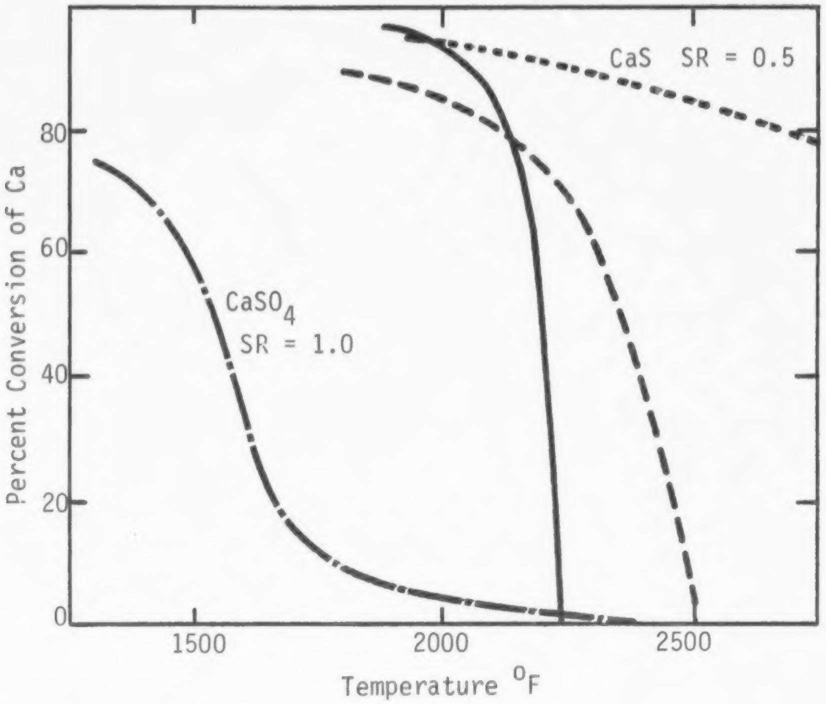

Figure 5-30. Relative Stability of CaS and $CaSO_4$, Equilibrium Calculations.

3) calcination, deadburning, and decomposition of reacted sorbent;

4) the sulfur evolution from the coal, including rate of evolution and species evolved;

5) gas/solid chemistry of the sulfur compounds including oxidation and the kinetics of sulfur/solid reactions; and

6) the furnace time/temperature profile which is inextricably bound to the coal combustion process and which has an overriding effect on all of the above processes.

6.0 EXPERIMENTAL PLAN--BENCH-SCALE STUDIES

Two sets of bench-scale studies (at two firing levels) were planned. Studies were planned for two existing small-scale tunnel furnaces (propane- and coal-fired at 70,000 to 100,000 Btu/hr) and an existing small-scale, coal-fired furnace (70,000 to 100,000 Btu/hr) with a convective heat-transfer section. The small-scale studies were planned for and conducted during the design and construction of the Boiler Simulator Furnace (BSF). Information generated by the small-scale studies was used to specify design and operating criteria for the BSF and to plan the initial experiments in the BSF. Section 6.1 describes the experiments planned for the small-scale facilities, and Section 6.2 describes the BSF test plan.

6.1 Small-Scale Studies

A set of experiments designed to identify those parameters which have a significant effect on the capture of SO_2 by a solid sorbent in a gas flame was planned. The experiments were expected to establish the effect of combustion conditions and sorbent characteristics on sulfur/solid-sorbent interactions. The data obtained during these experiments was used to plan studies of sulfur capture by solid sorbents in pulverized-coal flames. The parameters and conditions which warranted further study were defined. The parameters of interest included:

- Excess air level
- Temperature history
- Additive sulfur form
- Water vapor
- Residence time
- Sorbent type
- Ca/S ratio

The screening studies were designed only to direct more complete investigations of those parameters which prove to have significant effects on sulfur capture. More detailed investigations were planned for the BSF studies.

The effect of excess air on sorbent utilization at the baseline thermal load (50,000 Btu/hr) was determined by charging the total combustion air flow rate.

The effect of sulfur species oxidation state was determined by changing the sulfur additive from SO_2 to H_2S for the same thermal and stoichiometric conditions.

The temperature history of the solid sorbent, and the temperature regime experienced by the reacting solid-sorbent/SO_2 pair was modified by adding a cooling coil designed to remove 20,000 Btu/hr from the furnace below the burner.

The effect of staged combustion on sulfur capture was studied by adding the combustion air to the furnace in two stages. The first-stage ran fuel rich (at SR's from .5 to .9) and the second-stage air was added at a point about 28 inches below the propane burner. Powdered $CaSO_4$ and CaS (respectively, the probable reaction products of fuel-lean and fuel-rich firing of sulfur/solid-sorbent doped flames) were added to the furnace in order to define the role of sorbent decomposition in the overall sulfur capture scheme.

6.2 Test Plan, Boiler Simulator Furnace

The initial experimental studies in the Boiler Simulator Furnace are directed at establishing which sorbent and fuel characteristics and which combustion conditions have effects on sorbent utilization. Subsequent testing will involve a more detailed examination of the controlling mechanisms through the use of extensive internal measurement techniques. The current work is exploratory in nature and relies primarily on exhaust and postflame measurements with continuous analyzers. The planned work was divided into three basic test sequences:

Series A	Combustion Parameter Screening
Series B	Thermal Environment Studies
Series C	Fuel and Sorbent Effects

Each test series has been further divided and the purpose of each will be discussed in detail in the following sections. It should be remembered that each series was planned and then somewhat revised to investigate questions raised by the results of the earlier experiments.

6.2.1 Combustion Parameters: Series A, Purpose and Scope

The purpose of the series A tests was to define the role of combustion parameters in the effectiveness of limestone injection. The first part of the tests used a subscale distributed-mixing burner with outboard tertiary air ports. (The burner was velocity-scaled from the EPA prototype low-NO_x burner). The combustion parameters of interest in the DMB studies were:

- Firing rate
- Heat extraction rate
- Sorbent location
- Overall excess air
- Burner-zone stoichiometry
- Tertiary air velocity

The same sorbent and fuel was used for all of the tests. Firing rate was changed by changing both coal and air flow rates. Heat extraction was varied by inserting cooling lances in the radiant section. Sorbent was injected into the tertiary air, the primary air, or with the coal. Overall excess air was increased by increasing the tertiary air only (maintaining the burner-zone stoichiometry at 0.6). Burner-zone stoichiometry was varied by changing the secondary/tertiary air split; and, finally, the tertiary air velocity was changed by changing the diameter of the tertiary air ports. Table 6-1 shows the overall test matrix for the fuel lean screening studies. The results of these experiments were used to plan the external staging studies and will be discussed in Section 10.

The external staging studies were performed in the BSF using the same fuel injector and primary and secondary air supply methods, but the staging air was added downstream at the base of the postflame section rather than through the tertiary air ports at the burner face. Sorbent was added, either with the primary air, at the base of the postflame section (before staging air addition), or with the staging air.

Table 6-1. Test Matrix--Series A-2--Staged Combustion Screening

● - Baseline "Pivot" Points   2 - Secondary Importance

				SORBENT LOCATION											
				TERTIARY PORTS WITH N_2			PRIMARY AIR WITH COAL			BASE OF PFC *			NO ADDITIVE		
				SR_1			SR_1			SR_1			SR_1		
				0.6	0.75	0.9	0.6	0.75	0.9	0.6	0.75	0.9	0.6	0.75	0.9
NORMAL LOAD (800,000 BTU/HR)	ADDITIONAL COOLING 100,000	STAGING AIR	MID					○		2	○	2			
			BOT		○		○	●	○		○		○	●	○
	ADDITIONAL COOLING NONE	STAGING AIR	MID							2	2	2			
			BOT				2	○	2				2	○	2
LOW LOAD (500,000 BTU/HR)	ADDITIONAL COOLING 100,000	STAGING AIR	MID							2	2	2			
			BOT				2	○	2				2	○	2
	ADDITIONAL COOLING NONE	STAGING AIR	MID												
			BOT				2	2	2						

* MEASURE REDUCED SULFUR SPECIES AT MID LEVEL WITH AND WITHOUT SORBENT

The purpose of the external staging studies was to determine the effect of first-stage stoichiometry on sulfur evolution from the coal and sorbent utilization. These were also screening studies, detailed, in-flame measurements were not planned. Table 6-2 shows the overall test matrix for external staging studies. The test matrix was modified from the originally planned matrix because the results of the DMB studies pointed out new questions; including the effect of first-stage stoichiometry, the sulfur speciation at the sorbent injection point, and second-stage temperature. The external staging portion of Series A testing was also completed during this reporting period. The results are discussed in Section 10.

6.2.2 Thermal Environment: Series B, Purpose and Scope

The purpose of the second series of tests is to further investigate the role of thermal environment in sulfur capture. The results obtained in the combustion parameter screening studies (Series A) indicated that temperature has a strong effect on sorbent utilization. The external staging studies also indicated that primary-zone stoichiometry and second-stage flame may have an effect on sulfur capture. The interpretation of the data is clouded by the effect of temperature and stoichiometry on gasification of the coal. Series B is therefore divided into two parts: Propane/H_2S studies and coal-fired studies.

The first set of experiments planned will clarify the effect of primary-zone stoichiometry on the sulfur species distribution and the effect of sulfur species distribution on sorbent utilization. Propane doped with H_2S will be used as the fuel because in a coal flame the sulfur species concentrations and distribution are a function of the coal burnout, and thus of the primary-zone stoichiometry. The use of propane/H_2S instead of coal will eliminate the complication caused by sulfur devolatilization and coal burnout. The test series will also quantify the retention of sulfur in the solid phase across the second-stage flame. This data should clarify the role of CaS and should determine the conditions required to shift the solid sulfur compound from CaS to $CaSO_4$ without decomposing all of the solid sulfur species to SO_2. Table 6-3 shows the test matrix planned for the propane/H_2S thermal environment studies and Figure 6-1 shows the H_2S and sorbent injection locations and the sampling points in the furnace.

Table 6-2. External Staging Studies Test Matrix

● Baseline "Pivot" Point

			No Additive			Sorbent Location															
						Primary Air With Coal				Base of PFC With N_2				Base of PFC With 15% TA				With Staging Air			
			SR_1			SR_1				SR_1				SR_1				SR_1			
			.6	.75	.9	.6	.75	.90	1.1	.6	.75	.90	1.1	.6	.75	.9	1.1	.6	.75	.90	1.1
Normal Load 800,000 Btu/hr	Cooling	Yes	○	○	○	○	○	○		○	○	○						○	○	○	
		No	○	○	○	●	○	○	○	○	○	○			○	○	○				
Low Load 500,000 Btu/hr	Cooling	Yes																			
		No	○	○	○	○	○	○	○												
Propane H_2S	Cooling	Yes	○	○	○									○	○	○	○				
		No																			

Table 6-3. Thermal Environment Studies--Propane-Fired

● - Baseline "Pivot" Point

2 - Secondary Importance

				No Preheat No Cooling			No Preheat						No Preheat H_2S Ins. Postflame Rad.Cooling	
							Radiant Zone Cooling--Top			Postflame Cooling				
				Sorbent Location			Sorbent Location			Sorbent Location			Sorbent Location	
				Burner	Post-flame	Second Stage	B	PF	2^{nd} S	B	PF	2^{nd} S	B	PF
Fuel Sulfur Content		SR_1	0.5				2				2			
			0.7				2				2			
			0.9				2				2			
			1.1				2				2			
	Match Ind. (∿2%)	SR_1	0.5		✓		✓	✓	2	2	✓		✓	✓
			0.7		✓		●	✓	2	2	✓		✓	✓
			0.9		✓		✓	✓	2	2	✓		✓	✓
			1.1		✓		✓	✓	2	2	✓		✓	✓
	3%	SR_1	0.5				2				2			
			0.7				2				2			
			0.9				2				2			
			1.1				2				2			

2--Secondary Importance

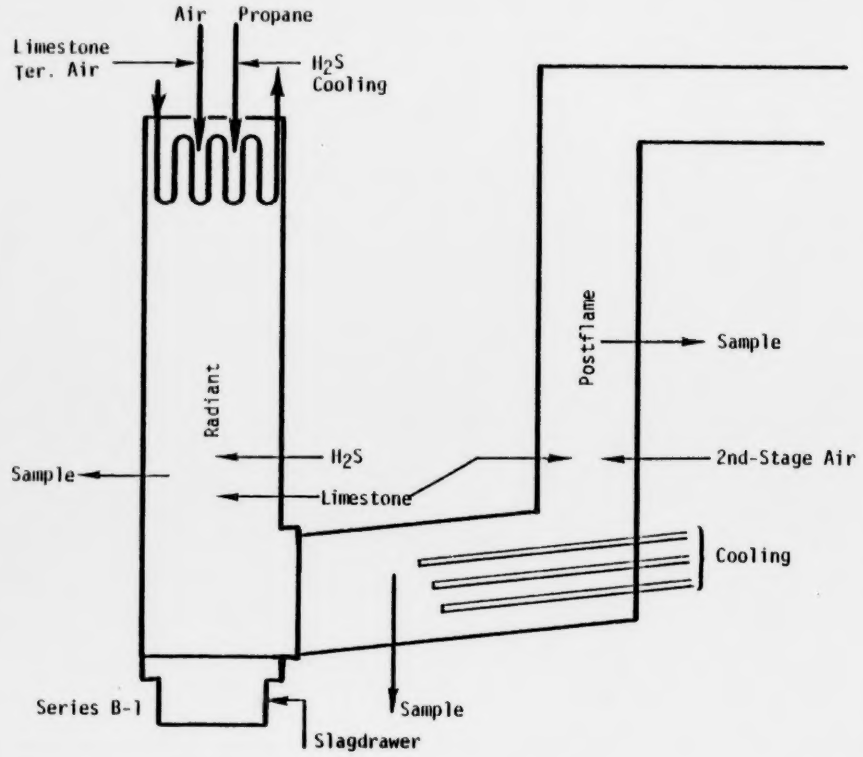
Air
Propane
Limestone
Ter. Air
H_2S
Cooling
Radiant
Postflame
Sample
H_2S
Limestone
2nd-Stage Air
Sample
Cooling
Series B-1
Sample
Slagdrawer

Figure 6-1. Sample, Sorbent Injection, and H_2S Injection Locations for Propane-Fired Experiments (Series B-1).

The purpose of the coal-fired thermal environment studies is to clarify the effect of the furnace time/temperature profile on sorbent utilization. Table 6-4 shows the test matrix palnned for the coal-fired thermal environment screening studies. Both internally staged (staging air added through tertiary air ports at the burner face) and externally staged (staging air added at the base of the postflame section) conditions will be investigated. The time/temperature profile will be modified by cooling either or both the radiant furnace at the burner and the postflame section (at the transition). The radiant zone will be cooled with water-cooled coils on the furnace wall. Cooling rods inserted in the horizontal transition section will be used for second-stage cooling. Sorbent will be added with the coal or with the staging air. Peak flame temperatures (first and/or second stage) will be reduced by dilution of the combustion air with nitrogen. The effect of primary-zone stoichiometry on sulfur species evolution and on sorbent utilization will also be investigated.

The results of these screening studies will be used in conjunction with the combustion parameter studies to define the combustion conditions which will be used for the fuel/sorbent effects experiments (discussed in the next section).

6.2.3 Fuel and Sorbent Effects: Series C, Purpose and Scope

The purpose of this test series is to screen various fuel and sorbent characteristics for their effect, if any, on sorbent utilization. This test series is severely limited in scope. It is likely that several parameters will require more detailed investigaton to define their effects.

The sorbent parameters of interest include: particle size, surface area, composition, pore volume, and pore size distribution. The fuel parameters of interest include: coal type, sulfur content, sulfur distribution (organic/inorganic), ash content and composition, and moisture. All of these parameters cannot be investigated extensively or even independently; for example, sorbent particle size cannot be changed without changing the sorbent surface area.

Several basic experiments have been planned to screen the parameters listed and to define which parameters, under which conditions require further investigation. The test matrix for Series C is shown in Table 6-5.

Table 6-4. Thermal Environment Studies--Coal-Fired

● - Pivot Points

2 - Secondary Importance

		No Additional Cooling		Heat Extraction With H_2O Cooling Tubes			Thermal Diluent-N_c				Combinations		
							Everywhere		TA or SA		Post-flame Cooling	Max. Pre-heat	Cooling Top
		Max. Preheat	No Preheat	Top Rad.	Bottom Rad.	Post-flame	15%	30%	15%	20%	30% N_2 With SA	30% N_2 With SH	30% N_2 Every-where
Excess Air SR_B = 1.1, SR_T = 1.2	Sorbent Location TA												
	PA	✓	2	●	2		2	✓					✓
	None	✓	2	✓	2		2	✓					✓
DMB SR_B = 0.6, SR_T = 1.2	Sorbent Location TA	✓	2	●	2		2	✓					✓
	PA	✓	2	✓	2		2	✓		2			✓
	None	✓	2	✓	2		2	✓					✓
External Stage SR_1 = 0.75 SR_T = 1.2	Sorbent Location SA	✓	✓				✓	2	2	✓	2	✓	
	PA	✓	✓	2			✓	✓	2	✓	2	✓	
	None	✓	✓	2			✓	✓	2	✓	2	✓	
External Stage SR_1 = 0.6 SR_T = 1.2	Sorbent Location SA	✓	✓				✓	2	2	✓	2	✓	
	PA	✓	●	2			✓	✓	2	✓	2	✓	
	None	✓	✓	2			✓	✓	2	✓	2	✓	

Table 6-5. Test Matrix for Fuel/Sorbent Studies (Series C)

Sorbent Composition	Sorbent Size	Excess Air* $SR_B=1.1$ $SR_T=1.2$				DMB*, $SR_B=0.6$, $SR_T=1.2$ Sorbent w/T.A.				Sorbent w/Coal				Staged* $SR_T=0.6$ $SR_T=1.2$			
		Coal				Coal				Coal				Coal			
		IN	UT	AL	ND	IN	UT	AL	ND	IN	UT	AL	ND	IN	UT	AL	ND
Vicron Calcite	45-3	○	2	2	2	●	○	○	○	○	2	2	2	●	○	○	○
	15-15	2				○				2				○			
$Ca(OH)_2$						○	2	2	2	2				○			
Michigan Marl						○	2	2	2	2				○			
$CaMg(CO_3)_2$						○ 2	2	2	2	2				○			

* assume 800,000 Btu/hr, wall cooling

● - Baseline "Pivot" Point

2 - Secondary Importance

The sorbents which will be used for these studies have been selected; they are: Vicron 45-3, the baseline calcium carbonate used for all the other test series; Vicron 15-15, the same calcium carbonate but with a small particle size; a dolomite used in the TVA studies; a calcium hydroxide (of roughly the same particle size as the baseline carbonate); and a Michigan marl (a carbonate which gave exceptionally high utilization in the TVA studies). This set of sorbents will not define the effect of all of the sorbent variables of interest, but it will define which variables need further investigation and may provide a basis for comparing the results in the BSF with earlier pilot- and full-scale studies.

The list of fuel characteristics which may influence sulfur capture is even longer than the list of sorbent characteristics; furthermore, it is even more difficult to vary only one characteristic of a coal than it is to vary one characteristic of a sorbent. The particular coals which will be used for this portion of the test series have not been selected; however, the desideratum for coal selection has been defined.

The coals which will be used will all have roughly the same sulfur content as the Indiana coal (2.4 percent). The Indiana coal is low in inorganic sulfur (only 25 percent of the sulfur is pyritic). A coal similar to the Indiana, but with most of the sulfur as pyrite, will be used to investigate the role of coal sulfur type. A coal with a high calcium content (Ca/S = 1 - 2) will be selected, and a coal with a high moisture content will be used. The baseline sorbent, Vicron 45-3, will be used with all the coals.

The five coals used for the fuel screening studies will give an indication of which of these fuel characteristics have significant effects on sulfur capture. Measurements of sulfur species in the rich zone will indicate the effect of these fuel characteristics on sulfur evolution from the coal.

7.0 EXPERIMENTAL FACILITIES

The experiments described in this report were performed in a number of facilities at different scales. The facilities at EER used in these investigations included: a pilot-scale furnace, the SWS, designed to fire at a rate of 120 MBtu/hr, three bench-scale furnaces designed to fire at 70,000 to 100,000 Btu/hr, and a new facility, the BSF, constructed for the bench-scale parameter screening studies. The following sections briefly describe the pilot and small-scale facilities. The design, construction and shakedown testing of the new Boiler Simulator Furnace is discussed in detail.

7.1 Pilot-Scale Facilities

The pilot-scale facility used for the experiments described in Section 4 has been described in detail in earlier reports including the second and third annual reports for EPA Contract 68-02-2667 and by Folsom, et al., 1980 (ref.7). Briefly, the furnace used is a watertube similator (LWS) designed for a maximum firing rate of 150 MBtu/hr, and configured like a conventional boiler. The furnace is spray-cooled with water and the inner walls are partially lined with refractory. The furnace is wall-fired. The fire box at burner level is 22-feet deep and 16-feet wide.

7.2 Small-Scale Facilities

Three small furnaces, designed for throughput rates from 70,000 to 100,000 Btu/hr were used for preliminary testing. All three of the furnaces have been described in detail in other reports. The coal-fired Argon furnace was used extensively for the nitrogen oxides emissions studies which were reported in the third annual report for EPA Contract 68-02-2667. The second small coal fired furnace, with convective sections, was described in detail in ref. 8, (Reese, et al.). Both furnaces used premixed coal burners and were fired with coal/air for the preliminary experiments reported in Section 10. Figures 7-1 and 7-2 are schematics of the two furnaces.

The preliminary gas-phase studies were carried out in a down-fired tunnel furnace (Figure 7-3) similar in dimensions and capacity to the coal-fired Argon furnace. The furnace was equipped with a diffusion burner which allowed both

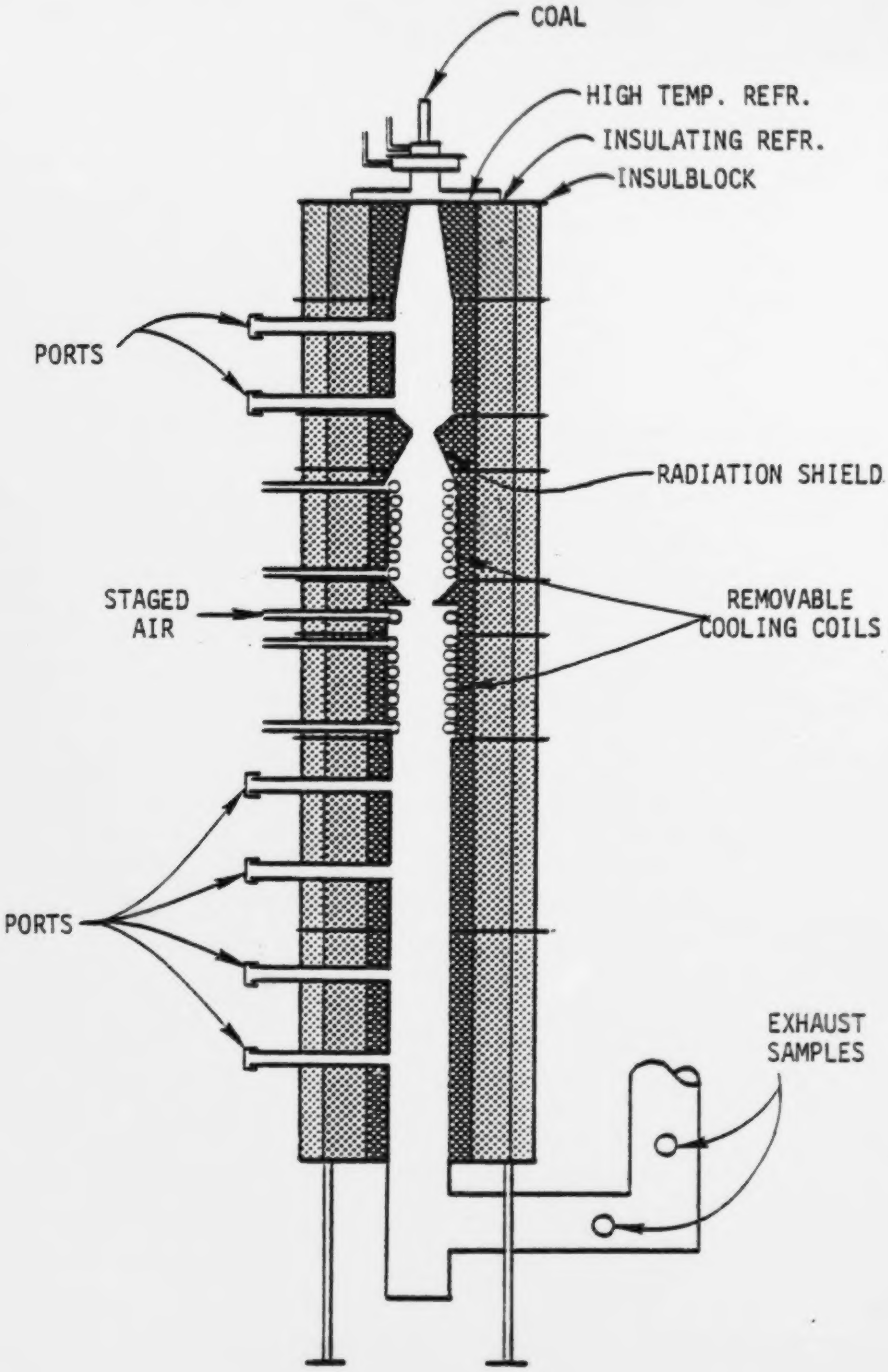
COAL
HIGH TEMP. REFR.
INSULATING REFR.
INSULBLOCK
PORTS
RADIATION SHIELD
STAGED AIR
REMOVABLE COOLING COILS
PORTS
EXHAUST SAMPLES

Figure 7-1. Bench-Scale Reactor, Coal/Argon Fired.

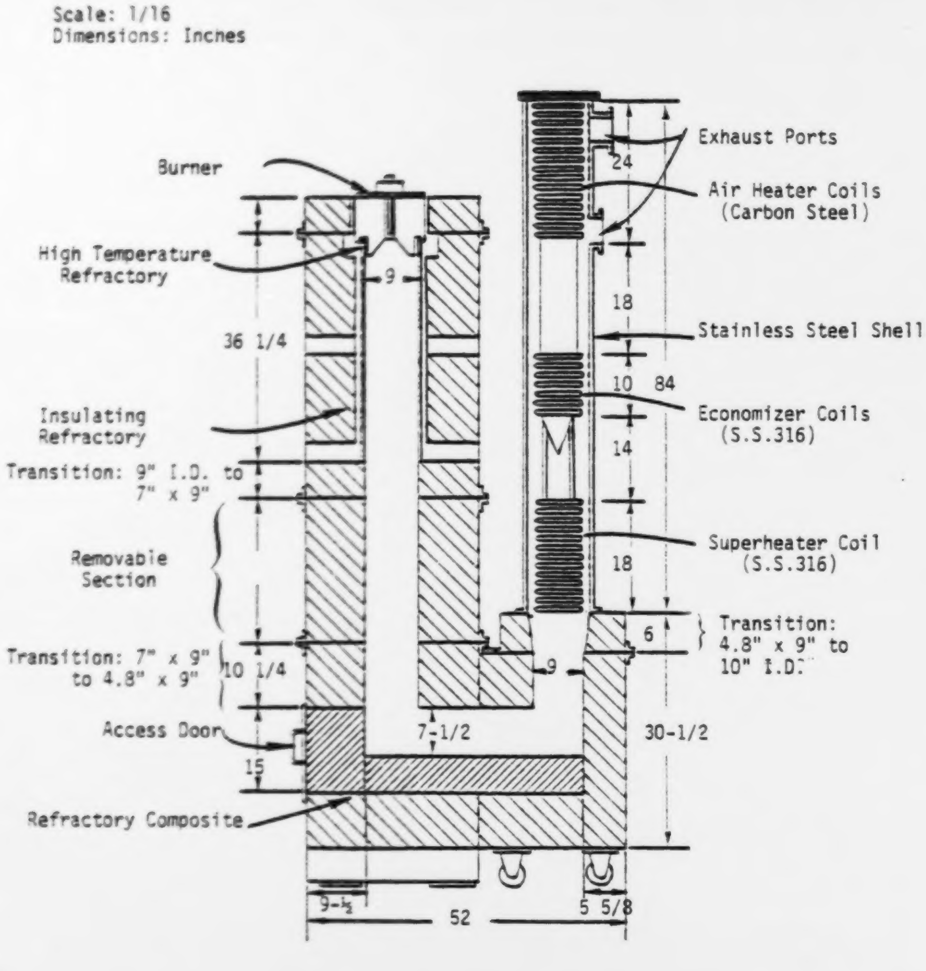
Scale: 1/16
Dimensions: Inches
Burner
High Temperature Refractory
9
36 1/4
Insulating Refractory
Transition: 9" I.D. to 7" x 9"
Removable Section
Transition: 7" x 9" to 4.8" x 9"
10 1/4
Access Door
15
Refractory Composite
7-1/2
9
9-½
52
5 5/8
Exhaust Ports
Air Heater Coils (Carbon Steel)
24
18
Stainless Steel Shell
10
84
Economizer Coils (S.S.316)
14
Superheater Coil (S.S.316)
18
6
Transition: 4.8" x 9" to 10" I.D.
30-1/2

Figure 7-2. Cross-Section Schematic of the Combustor, Convective Furnace.

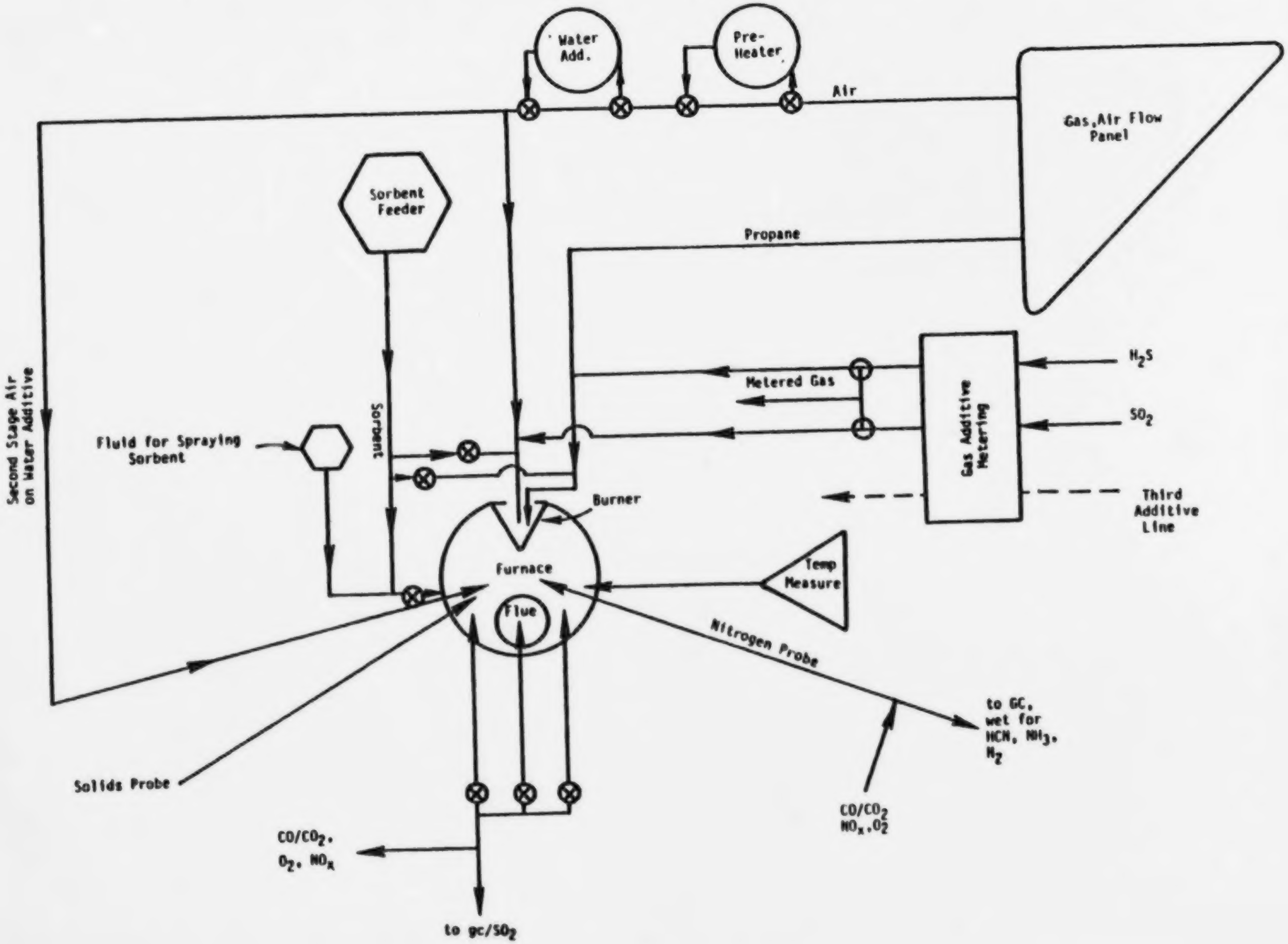
Water Add.
Pre-Heater
Air
Gas,Air Flow Panel
Sorbent Feeder
Propane
Second Stage Air on Water Additive
Metered Gas
H_2S
SO_2
Gas Additive Metering
Third Additive Line
Sorbent
Fluid for Spraying Sorbent
Burner
Furnace
Flue
Temp Measure
Nitrogen Probe
to GC, wet for HCN, NH_3, H_2
Solids Probe
CO/CO_2, O_2, NO_x
CO/CO_2 NO_x, O_2
to gc/SO_2

Figure 7-3. Schematic of Experimental System for Gas Phase Sulfur Experiments, Argon/Propane Furnace.

radial and axial gas injection (Figure 7-4). The furnace was fired with propane and air. Sulfur species were added either to the combustion air or to the fuel. The sulfur additives, either H_2S or SO_2, were metered from bottles of pure gas through a stainless steel critical-orifice flow metering system (Figure 7-5). Solid sorbents were metered into the combustion air with a volumetric screw feeder (Figure 7-6). The solids feeder had an agitated, air-stirred feed bin which emptied into an air transport line which, in turn, flowed into the main combustion air line. All of the air and fuel flow rates were measured with high-accuracy Brooks rotameters. The gas furnace was used to perform preliminary screening studies, the experiments required auxiliary equipment including: air preheaters for the combustion air, cooling lances, steam injection and secondary air injectors. The sampling and analytical systems development are described in Section 8. Much of the sample system development and testing work was performed with the propane fired tunnel furnace.

7.3 Boiler Simulator Furnace

The Boiler Simulator Furnace (BSF) was developed for studying sulfur pollutants from boilers as part of Task 2 of EPA Contract No. 68-02-2667. The furnace, as originally proposed, had a firing rate of 120×10^3 Btu/hr. After reviewing the system requirements, particularly the problem of heat loss from a system of this size, it was decided to increase the firing rate to 1×10^6 Btu/hr. The eightfold increase in heat input rate necessitated a redesign of the BSF. The BSF design and construction and shakedown are discussed in the following sections.

7.3.1 Design Criteria and Program Requirements

The BSF experimental furnace system is designed to produce combustion conditions typical of a wide variety of coal combustor firing schemes including:

- Wall firing
- Tangential Firing
- Turbo
- Arch
- Tower
- Steamer
- Cyclone

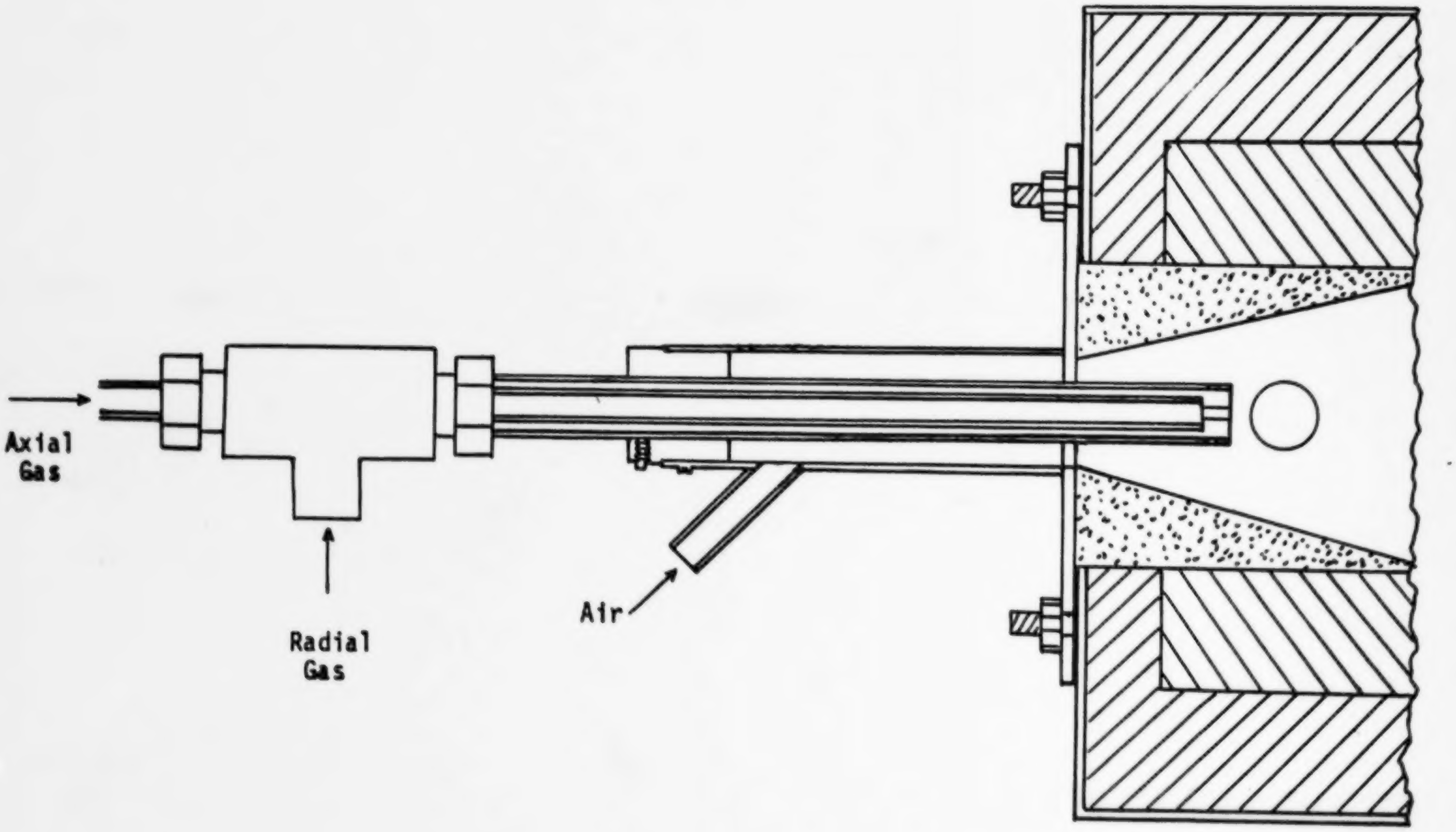
Axial Gas
Radial Gas
Air

Figure 7-4. Burner Schematic, Propane/Argon Furnace.

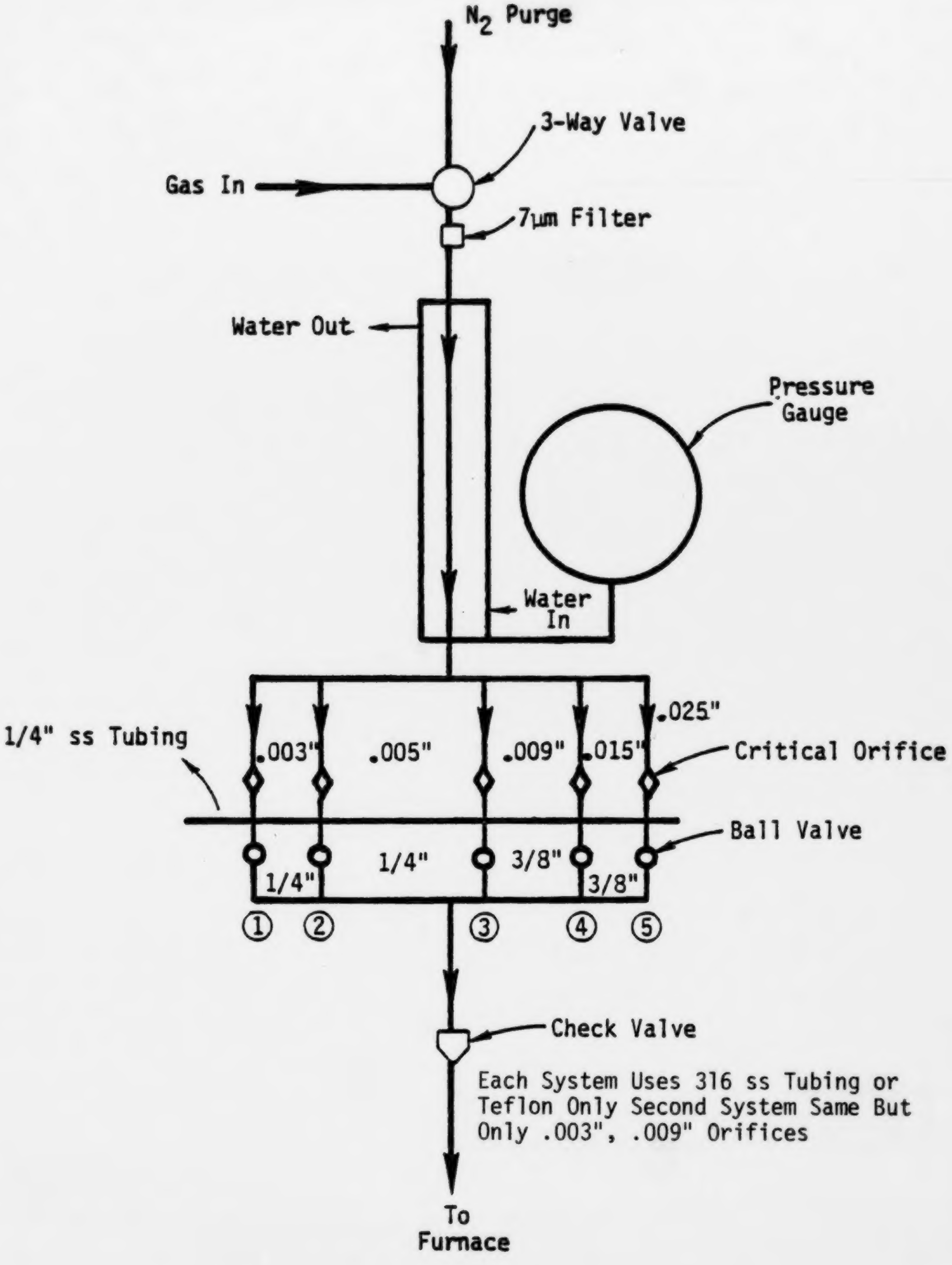
N_2 Purge
3-Way Valve
Gas In
7μm Filter
Water Out
Pressure Gauge
Water In
1/4" ss Tubing
.003"
.005"
.009"
.015"
.025"
Critical Orifice
Ball Valve
1/4"
1/4"
3/8"
3/8"
①
②
③
④
⑤
Check Valve
Each System Uses 316 ss Tubing or Teflon Only Second System Same But Only .003", .009" Orifices
To Furnace

Figure 7-5. Gas Additive System.

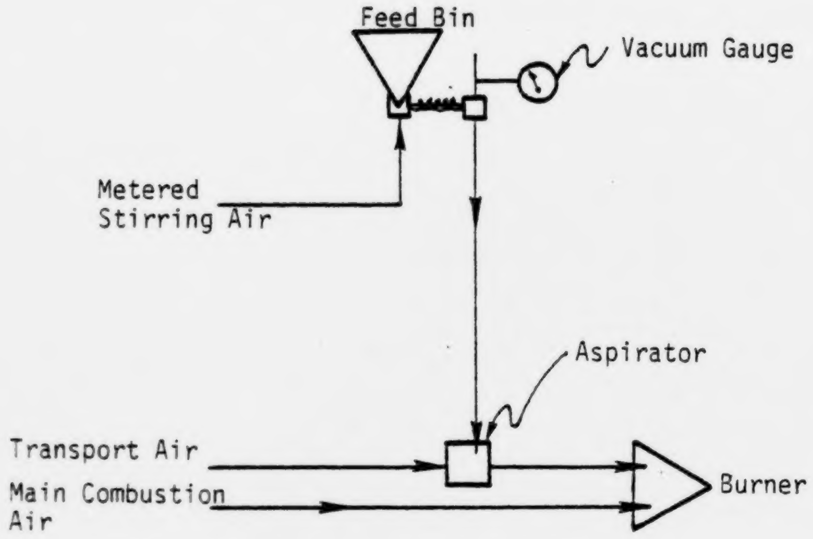
Feed Bin
Vacuum Gauge
Metered Stirring Air
Aspirator
Transport Air
Main Combustion Air
Burner

Figure 7-6. Solids Transport System, Propane/Argon Furnace.

This is no attempt to simulate directly the hardware of each of these types of firing systems; the BSF design tries to include conditions typical of the various systems. In particular, the unit is designed to simulate the time/temperature stoichiometry history of an actual full scale, utility boiler. It includes detailed consideration of the flame zone, radiant zone, convective passages and the particle collection equipment. Additionally, it is designed to operate over a wider range of combustion conditions than are typical of current commercial practice.

The design criteria include the following:

- Independent control of wall temperature throughout the furnace and convective sections;
- Fuel consumption rate nominally 80 lbs/hr;
- Variable burner design;
- Variable preheat of all combustion air streams;
- Simulation of large particle-loss to furnace bottom;
- Ability to quickly and easily clean interior sections;
- Potential for near adiabatic operation by minimizing heat losses;
- Ease of access for sampling probes.

The experimental facility is suitable for the nitrogen and sulfur oxides studies currently in progress and is also suitable for investigations on particulate formation, slagging and fouling.

7.3.1.2 Design Approach

The BSF design was based on the program requirements using information obtained from a review of experimental furnaces in the combustion pollution research community. A summary of the characteristics of these furnaces is shown in Table 7-1.

The experimental goals required that the experimental conditions be controlled and measured accurately to discriminate between the individual effects of the many operating variables. The BSF design includes adequate control and metering capabilities to facilitate efficient experimentation and minimize data scatter.

Table 7-1. Summary of Data Obtained on Other Research Furnaces

Unit ID	Furnace Configuration	Firing Arrangement	Furnace Dimensions	Furnace Pressure	Primary Fuel	Nominal Capacity (Btu/hr)
BYU	V,R,T,C	Down	8"φ x 60" H	ATM	P.C.	350×10^3
Aerotherm	R,S	Wall,Corner	Main 39" Cube	ATM	P.C.; #2, #6 Refuse	1.5×10^6
	H,R,T,S		Extn 33"φ x 10^1L			
CE-CMHF	V,R,C,T	Down	NK	ATM	P.C.	NK
RWE, Germany	V,R,B	Down	NK	ATM	P. Brown Coal	6×10^6
Grand Forks	V,R,C,T	Up	30"φx 8'H	ATM	P.C.	0.5×10^6
B&W Stirling	V,R,B	Wall	10'W x 12½' D	ATM	P.C.	47×10^6
B&W PCF Main	H,T,S	Wall	40"x40"x80"L	ATM	P.C.	4×10^6
	H,C	Staging	4½'φ x 8'L	ATM	P.C.	DO
Shell-MCU	V,T	Down	2"φ x 3'H	ATM	P.C.	4×10^3
Shell-LCF	V,B	Wall	NK	ATM	P.C.	1.5×10^6
U. of Ariz.	V,R,T,C	Down	6"φ x 84"H	ATM	P.C.	60×10^3
IFRF No. 1	H,R,T,S	Wall	79"Wx81"x248"L	ATM	Oil, Gas	6×10^6
IFRF No.2	H,R,T,X	Wall	47"Wx47"Hx185"L	ATM	Gas	3.5×10^6
EERC Coal	V,R,T,C	Down	6"φ x 108"H	ATM	P.C.	70×10^3
EERC EPRI	V,R,T,C,S	Down	7"φ x 32.5"H 7"x4-7/8"x16¼"H	ATM	P.C.	70×10^3

V - Vertical; R - Refractory lined; T - Tunnel; C - Cylindrical; S - Retangular;

H - Horizontal; B - Boiler; P.C. - Pulverized Coal; NK - Not known.

Table 7-1. Summary of Data Obtained on Other Research Furnaces, Cont.

Unit ID	Nominal T. Sec.	Heat Release Rate		Heat Extraction	
		Btu/hr-ft^3	Btu/hr-ft^2	Radiant	Conv.
BYU	0.32	2.0×10^5	3.34×10^4	None	None
Aerotherm	1.99	Main=3.19×10^4	Main=2.8×10^4	None	Dow Therm
	2.50	Extn=1.74×10^4	Extn=1.74×10^4		
CE-CMHF	NK	NK	NK	NK	NK
RWE, Germany	NK	NK	NK	Water	Water
Grand Forks	5.0	1.35×10^4	8.44×10^3	None	Air
B&W Stirling	4.06	1.57×10^4	4.35×10^4	None	Water
B&W PCF Main	1.18	5.4×10^4	4.49×10^4	None	Water
	2.02	3.15×10^4	3.15×10^4	Water	Water
Shell-MCU	1.0	6.12×10^4	2.55×10^3	Heated	None
Shell-LCF	NK	NK	NK	Steam	None
U. of Ariz.	1.45	4.38×10^4	5.45×10^3	None	None
IFRF No. 1	9.66	6.74×10^3	1.12×10^4	Water	None
IFRF No.2	4.29	1.48×10^4	1.45×10^4	NK	NK
EERC Coal	1.61	4.95×10^3	4.95×10^3	Water	None
EERC EPRI	0.95	6.70×10^4	9.159×10^3	None	Air

V - Vertical; R - Refractory lined; T - Tunnel; C - Cylindrical; S - Retangular;

H - Horizontal; B - Boiler; P.C. - Pulverized Coal; NK - Not known.

The system was designed to minimize down time in order to support the long duration experimentation required for slagging and fouling studies. The need for continuous 24-hour operation dictates that automatic functions be incorporated to minimize labor expenses.

7.3.1.3 System Overview

The Boiler Simulator experimental facility can be divided into these major systems:

- Fuel
- Additive
- Air
- Burner
- Furnace
- Clean-up
- Data acquisition.

The key design considerations are illustrated in Figure 7-7. In the following section the design concepts for each subsystem are described.

7.3.1.4 Fuel System

The fuel system consists of two subsystems:

- Pulverized Coal - Test Fuel
- Gas - Overnight Firing

The coal system design requirements were:

- Pulverization of coal to the desired particle size distribution;
- Safe storage;
- Metering and feeding to the burner.

After reviewing the two alternatives to produce the pulverized coal, batch pulverization was preferred over on-line pulverization. The advantages of batch pulverization included:

- Better control of primary air/coal ratio;

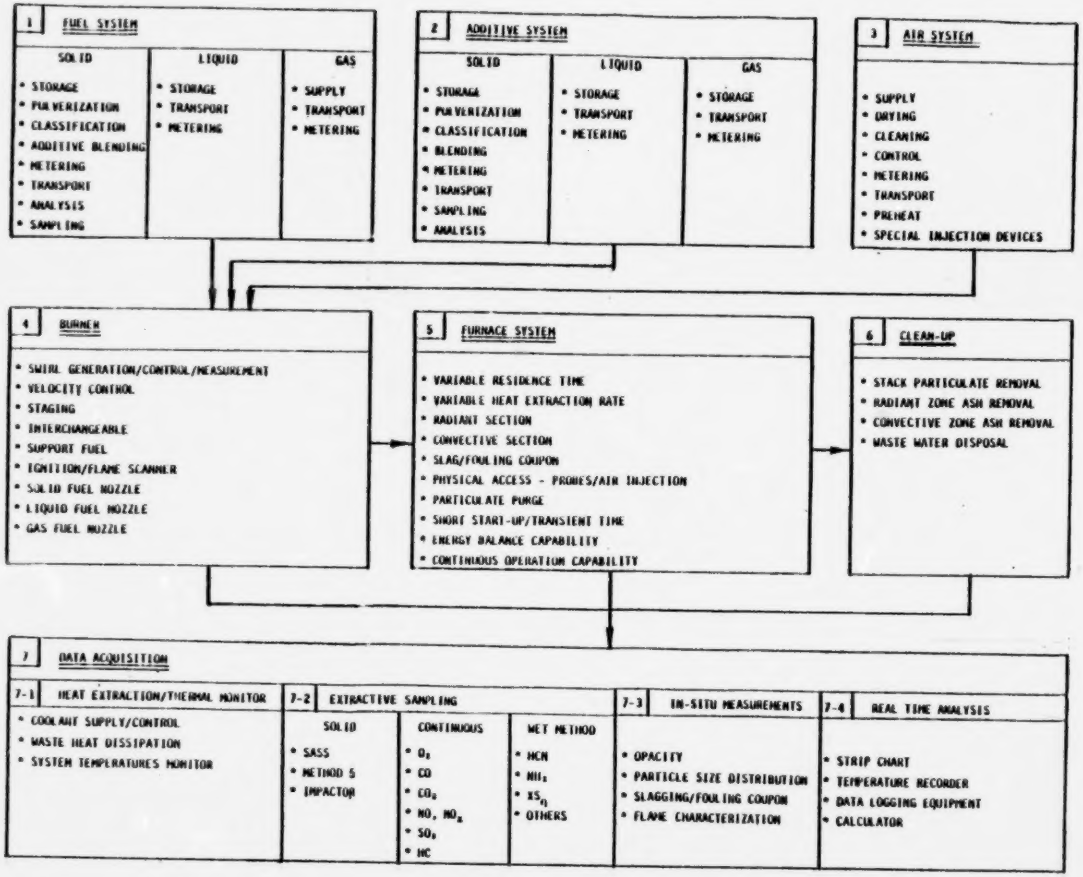
1 FUEL SYSTEM
SOLID
• STORAGE
• PULVERIZATION
• CLASSIFICATION
• ADDITIVE BLENDING
• METERING
• TRANSPORT
• ANALYSIS
• SAMPLING
LIQUID
• STORAGE
• TRANSPORT
• METERING
GAS
• SUPPLY
• TRANSPORT
• METERING
2 ADDITIVE SYSTEM
SOLID
• STORAGE
• PULVERIZATION
• CLASSIFICATION
• BLENDING
• METERING
• TRANSPORT
• SAMPLING
• ANALYSIS
LIQUID
• STORAGE
• TRANSPORT
• METERING
GAS
• STORAGE
• TRANSPORT
• METERING
3 AIR SYSTEM
• SUPPLY
• DRYING
• CLEANING
• CONTROL
• METERING
• TRANSPORT
• PREHEAT
• SPECIAL INJECTION DEVICES
4 BURNER
• SWIRL GENERATION/CONTROL/MEASUREMENT
• VELOCITY CONTROL
• STAGING
• INTERCHANGEABLE
• SUPPORT FUEL
• IGNITION/FLAME SCANNER
• SOLID FUEL NOZZLE
• LIQUID FUEL NOZZLE
• GAS FUEL NOZZLE
5 FURNACE SYSTEM
• VARIABLE RESIDENCE TIME
• VARIABLE HEAT EXTRACTION RATE
• RADIANT SECTION
• CONVECTIVE SECTION
• SLAG/FOULING COUPON
• PHYSICAL ACCESS - PROBES/AIR INJECTION
• PARTICULATE PURGE
• SHORT START-UP/TRANSIENT TIME
• ENERGY BALANCE CAPABILITY
• CONTINUOUS OPERATION CAPABILITY
6 CLEAN-UP
• STACK PARTICULATE REMOVAL
• RADIANT ZONE ASH REMOVAL
• CONVECTIVE ZONE ASH REMOVAL
• WASTE WATER DISPOSAL
7 DATA ACQUISITION
7-1 HEAT EXTRACTION/THERMAL MONITOR
• COOLANT SUPPLY/CONTROL
• WASTE HEAT DISSIPATION
• SYSTEM TEMPERATURES MONITOR
7-2 EXTRACTIVE SAMPLING
SOLID
• SASS
• METHOD 5
• IMPACTOR
CONTINUOUS
• O_2
• CO
• CO_2
• NO, NO_x
• SO_2
• HC
WET METHOD
• HCN
• NH_3
• ΣS_n
• OTHERS
7-3 IN-SITU MEASUREMENTS
• OPACITY
• PARTICLE SIZE DISTRIBUTION
• SLAGGING/FOULING COUPON
• FLAME CHARACTERIZATION
7-4 REAL TIME ANALYSIS
• STRIP CHART
• TEMPERATURE RECORDER
• DATA LOGGING EQUIPMENT
• CALCULATOR

Figure 7-7. Summary of Design Criteria for Boiler Simulator Furnace.

- Improved particle size consistency;
- Elimination of operation problems associated with on-line milling.

Coals were pulverized in a maximum 5 ton batch using a Raymond bowl mill in conjunction with a bag house as shown in Figure 7-8. This 5 ton batch supplied 10 days of 8-hour testing. The coal powder was stored in five air-tight bins in a CO_2 atmosphere to reduce fire hazard.

Experience at EER indicates that an accurate and stable fuel feed system is crucial to the quality of the data. A loss-in-weight type twin-screw metering feeder was selected because it provides stability as well as operation ease. The feeder also provided an analog signal which can be used in the data acquisition system. Figure 7-9 shows a schematic of the coal system. Experience with the coal feed system is discussed in Section 7.3.2.

A propane system was used to fire the furnace overnight. The system functioned automatically and maintained furnace temperatures unattended during periods when coal fired testing was not being performed. Figure 7-10 shows the propane system.

7.3.1.5 Additive System

Sorbent was added to the furnace in several ways: pulverized with the coal, added with the coal in the primary air, added with the staging air (either at the burner face or downstream) or added directly into the furnace with a small amount of transport gas (either air or nitrogen). The sorbent was fed with a small twin screw volumetric feeder supplied by Ktron. Experience with the sorbent feed system is discussed in Secton 7.3.2. The sorbent was transported from the feeder to the injection location with metered gas (either air or N_2). Pressures at the feeder exit were regulated to prevent plugging of the delivery tube or asperation of sorbent from the feeder. The sorbent transport system is depicted schematically in Figure 7-9.

7.3.1.6 Combustion Air System

A maxiumum of 260 SCFM of air was needed to support a 1×10^6 Btu/hr furnace. The combustion air system (see Figure 7-11) consists of:

- Supply
- Metering

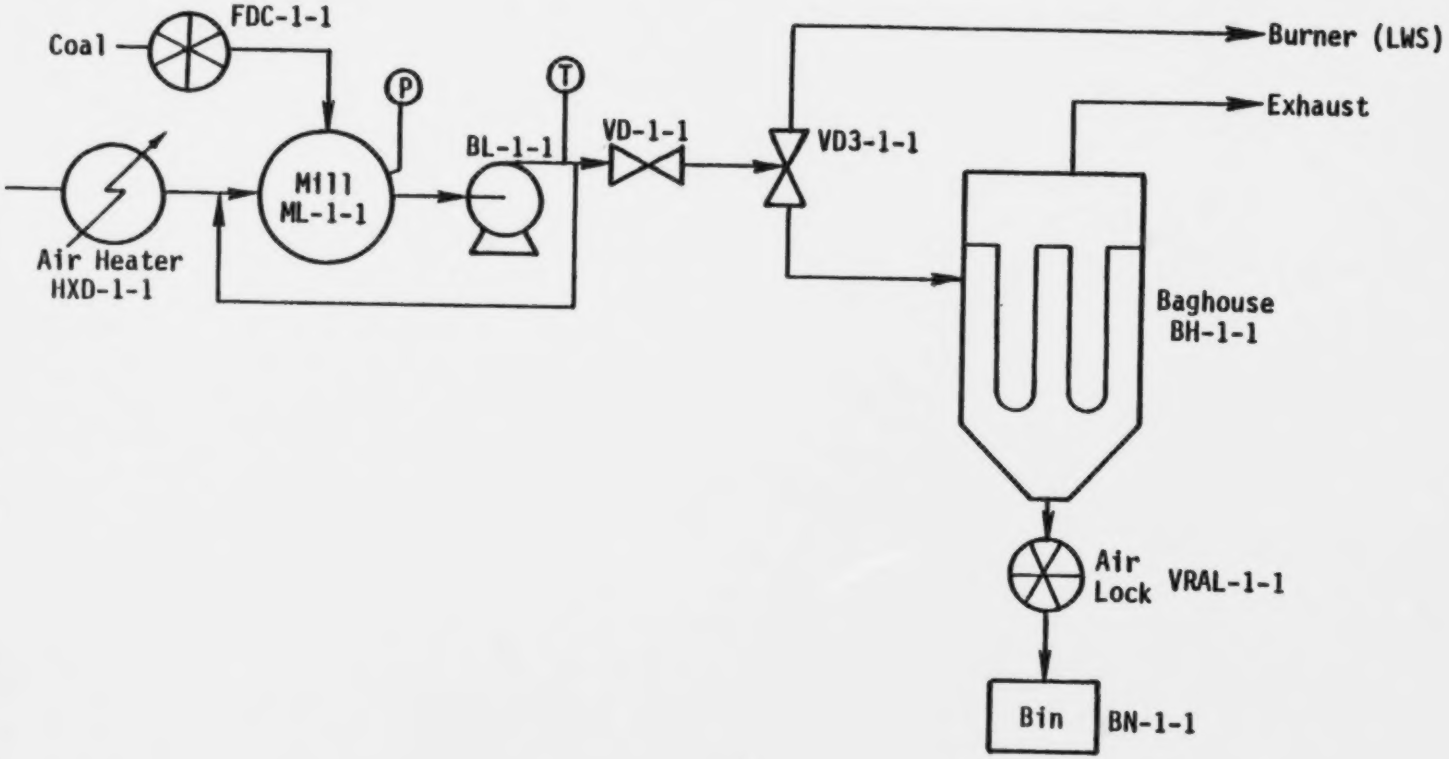
Coal
FDC-1-1
P
T
Air Heater
HXD-1-1
Mill
ML-1-1
BL-1-1
VD-1-1
VD3-1-1
Burner (LWS)
Exhaust
Baghouse
BH-1-1
Air
Lock
VRAL-1-1
Bin
BN-1-1

Figure 7-8. BSF - System 1.1 - Batch Pulverized Coal Production System - Version 1.0.

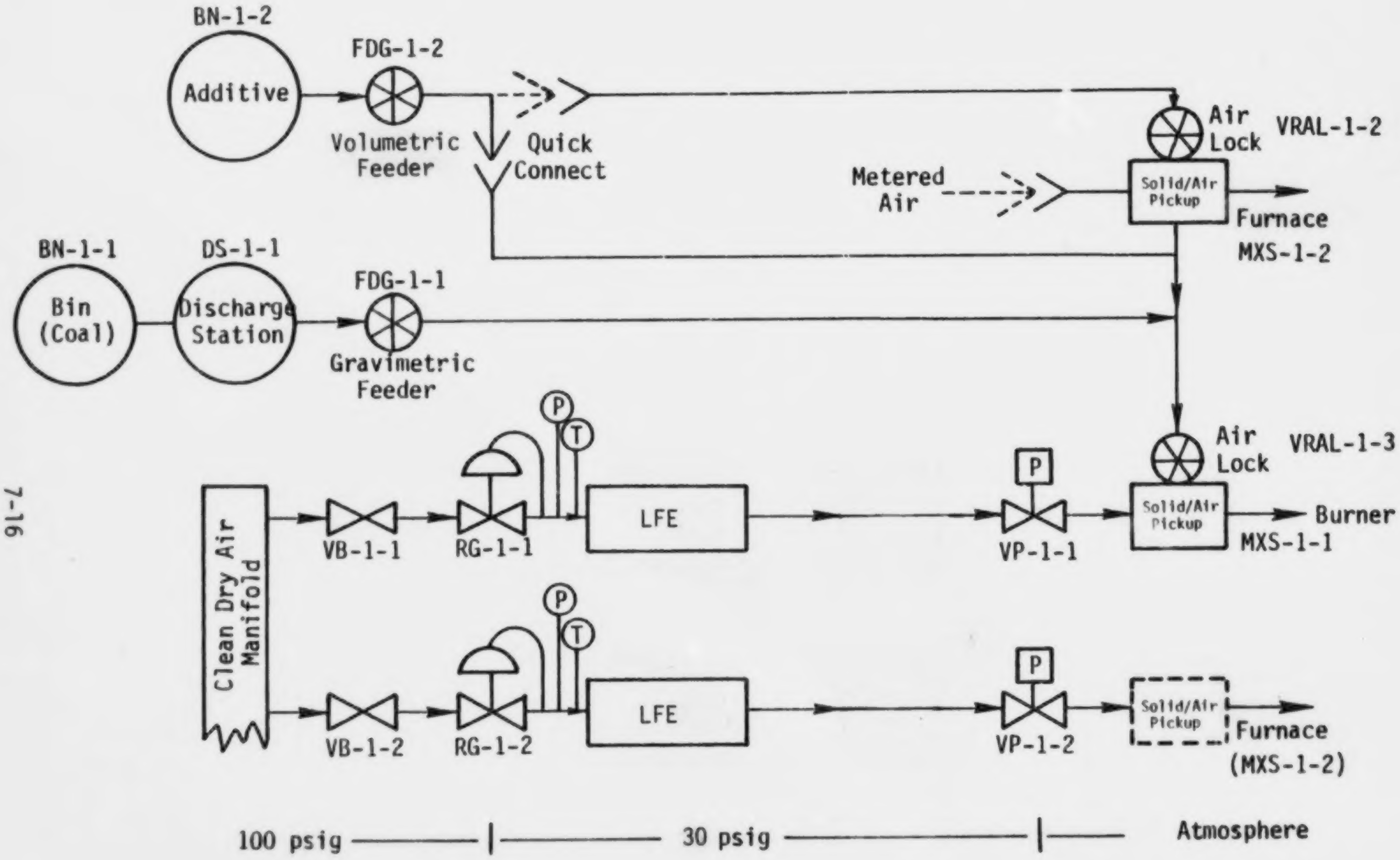
BN-1-2
Additive
FDG-1-2
Volumetric Feeder
Quick Connect
Air Lock
VRAL-1-2
Metered Air
Solid/Air Pickup
Furnace
MXS-1-2
BN-1-1
Bin (Coal)
DS-1-1
Discharge Station
FDG-1-1
Gravimetric Feeder
P
T
Air Lock
VRAL-1-3
Clean Dry Air Manifold
VB-1-1
RG-1-1
LFE
P
VP-1-1
Solid/Air Pickup
Burner
MXS-1-1
P
T
VB-1-2
RG-1-2
LFE
P
VP-1-2
Solid/Air Pickup
Furnace
(MXS-1-2)
100 psig
30 psig
Atmosphere

Figure 7-9. BSF - System 1.2 (with 2.1) - Coal and Solid Additive System.

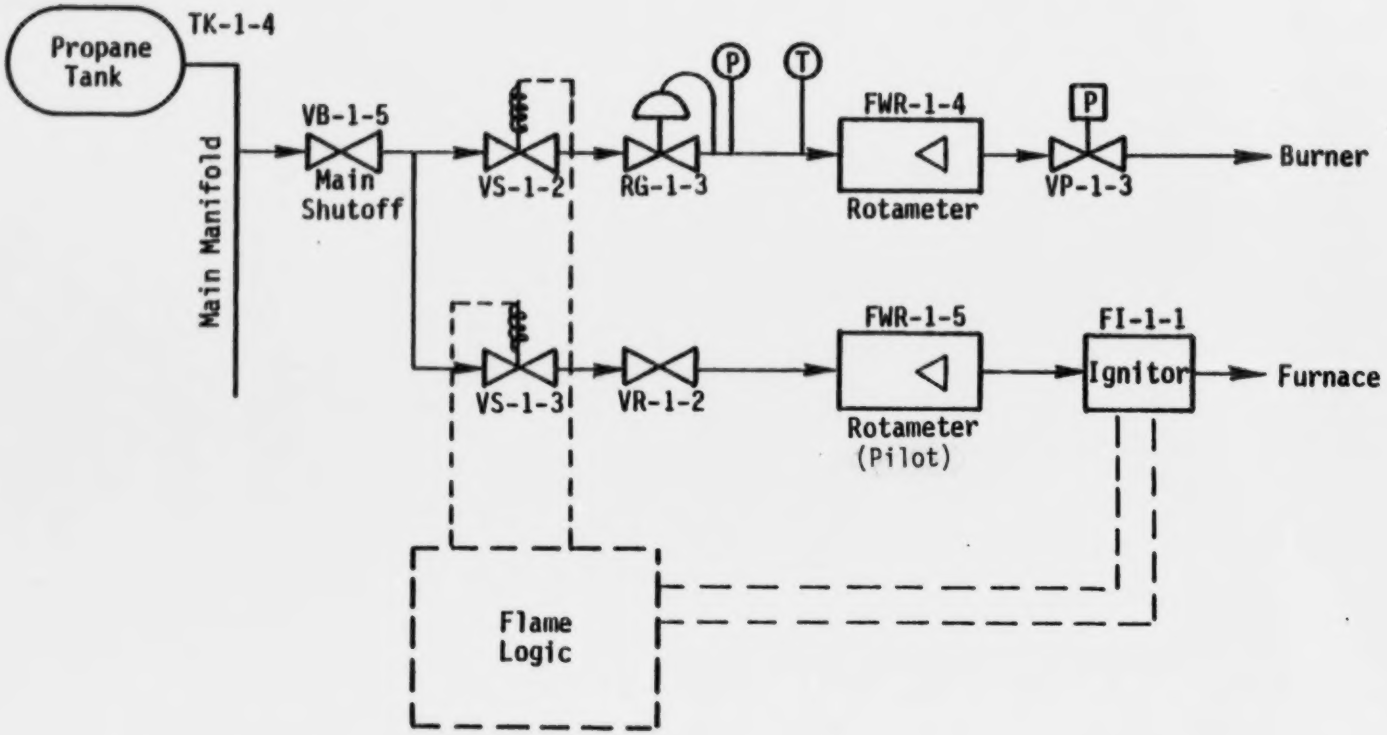
Propane Tank
TK-1-4
Main Manifold
VB-1-5
Main Shutoff
VS-1-2
RG-1-3
P
T
FWR-1-4
Rotameter
P
VP-1-3
Burner
VS-1-3
VR-1-2
FWR-1-5
Rotameter (Pilot)
FI-1-1
Ignitor
Furnace
Flame Logic

Figure 7-10. BSF - Gas Fuel Delivery - Metering System.

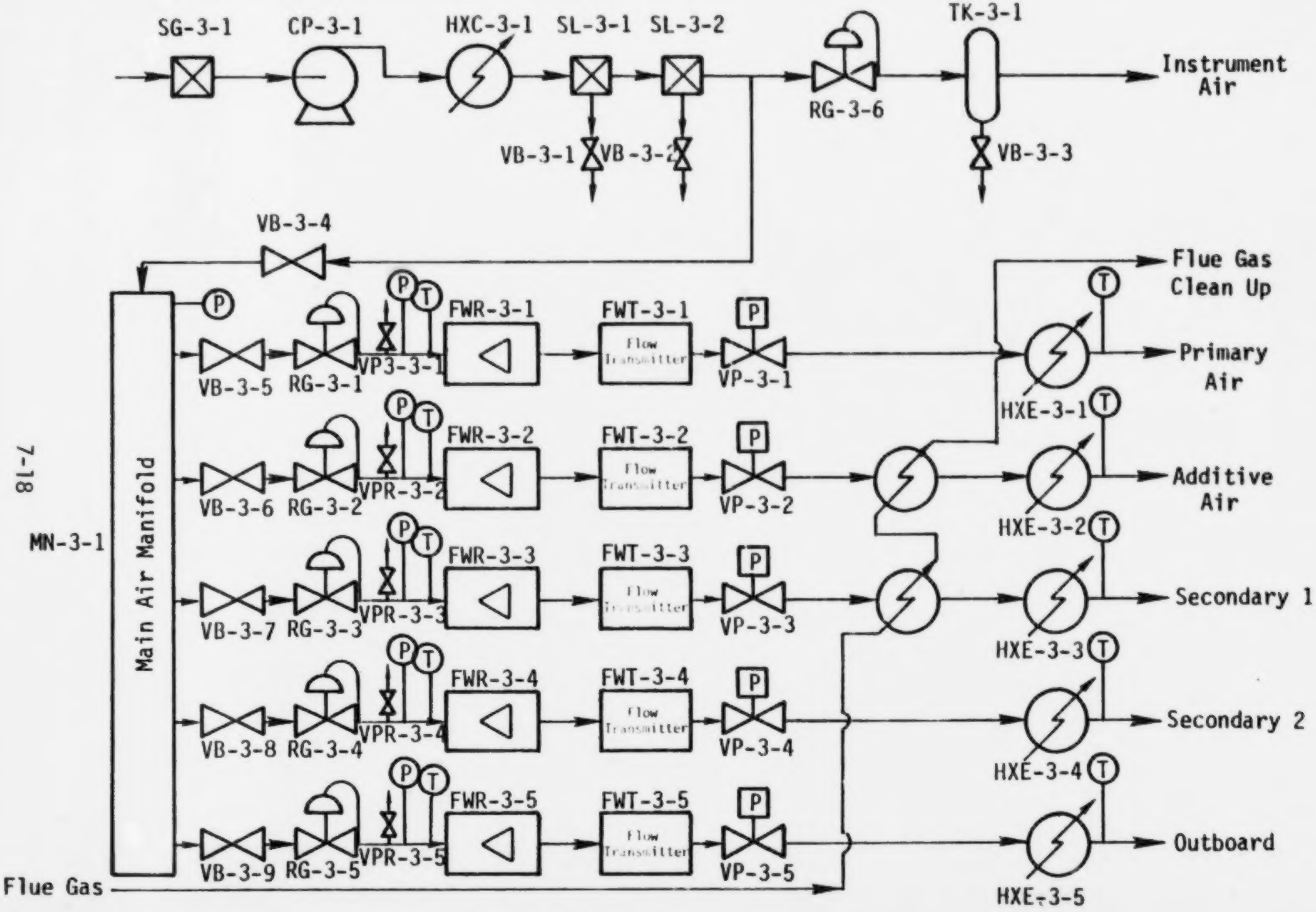
SG-3-1
CP-3-1
HXC-3-1
SL-3-1
SL-3-2
RG-3-6
TK-3-1
Instrument Air
VB-3-1
VB-3-2
VB-3-3
VB-3-4
Flue Gas Clean Up
P
T
FWR-3-1
FWT-3-1
Flow Transmitter
VP-3-1
Primary Air
VB-3-5
RG-3-1
VP3-3-1
HXE-3-1
FWR-3-2
FWT-3-2
VP-3-2
Additive Air
VB-3-6
RG-3-2
VPR-3-2
HXE-3-2
MN-3-1
Main Air Manifold
FWR-3-3
FWT-3-3
VP-3-3
Secondary 1
VB-3-7
RG-3-3
VPR-3-3
HXE-3-3
FWR-3-4
FWT-3-4
VP-3-4
Secondary 2
VB-3-8
RG-3-4
VPR-3-4
HXE-3-4
FWR-3-5
FWT-3-5
VP-3-5
Outboard
Flue Gas
VB-3-9
RG-3-5
VPR-3-5
HXE-3-5

Figure 7-11. BSF - Air Supply - Metering.

- Control
- Preheat

A compressor was chosen in preference to a blower to supply the combustion air because a high pressure (100 psig) air system has numerous advantages over a low-pressure system, namely:

- Improved control of individual streams resulting in negligible interaction between the various flow streams;
- Improved overall accuracy due to generally leak-free piping systems;
- "Linear" regulating valves can be used to take advantage of the high allowable pressure drop.

Five individually controlled and metered combustion air streams supply primary, additive transport, two main and one staging air streams. The capacities of each stream were selected to optimize metering accuracy. Table 7-2 lists their design capacities.

The choice of flowmeter is governed by accuracy, stability, turn-down (linearity), signal type and cost. For the flow rates of interest, the selected laminar flow elements are superior to rotameters and venturi/orifice meters. Venturi/orifice meters exhibit non-linear flow rate versus pressure drop characteristics and these have narrow ranges of acceptable performance. Rotameters for these flow rates are expensive and cannot be easily adapted for automatic data acquisition.

Laminar flow elements are stable and exhibit linear flow versus pressure drop across the element. Pressure drop signals can be indicated visually with inclined manometers for enhanced resolution and can also be converted to electronic signals using pressure transducers.

In each stream a pressure regulator and a metering valve control the airflow rate and maintain a constant operating pressure at the laminar flow element in order to minimize error introduced by nonideal pressure corrections.

The five airstreams are heated separately after metering. Separate heating has the following advantages:

- Independent temperature set points;

- Preheaters can be located near the furnace to minimize heat loss and insulation requirements;
- The need for larger pipes to accommodate the higher volumetric flow rates (of heated air) is minimized.

The designed maximum preheat temperature for the combustion airstreams is 900^{0}F. Five recuperative-type heaters, in conjunction with five independently controlled propane burners, were used to control the final air temperatures.

7.3.1.7 Burner

The furnace was equipped with a versatile distributed mixing burner modeled after the EPA prototype burner. The burner is shown schematically in Figure 7-12. Two secondary air streams are supplied to the burner. The secondary air swirl can be controlled by modifying the swirl and axial air flow rates. The burner has four external staging air ports supplied with separately metered tertiary air. The tertiary air injection velocity was modified by changing the air injector size. The burner was designed to fire coal or propane. Three fuel injectors were supplied: two coal injectors to supply the fuel in an axial core or radially spread by a divergent in the nozzle, and a propane injector. The furnace temperature was generally maintained by propane firing overnight and on weekends.

7.3.1.8 Furnace

The furnace system includes the components that confine the combustion process and the combustion products from the burner to the stack. The design simulates the time/temperature and velocity characteristics of coal-fired boilers and consists of the following function components:

- Radiant Combustion Zone
- Post-Flame Cavity
- Convective Heat Exchange Sections - Primary, Secondary and Reheat Superheaters
- Economizers and Air Heaters.

A summary of the BSF design specifications is shown in Table 7-3.

The design variables of the radiant combustion zone to be considered were:

- Geometry

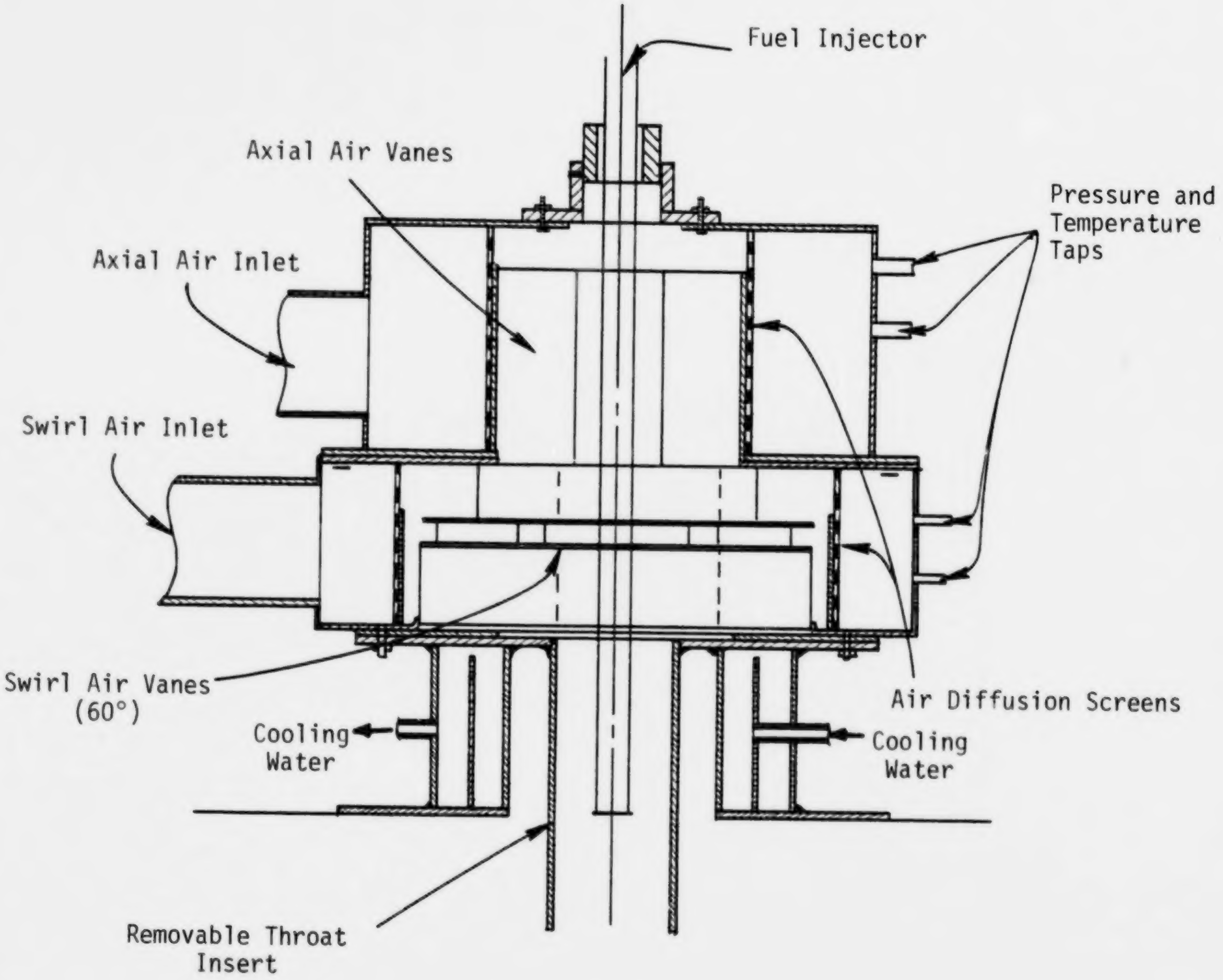
Fuel Injector
Axial Air Vanes
Pressure and Temperature Taps
Axial Air Inlet
Swirl Air Inlet
Swirl Air Vanes (60°)
Air Diffusion Screens
Cooling Water
Cooling Water
Removable Throat Insert

Figure 7-12. Distributed Mixing Burner Schematic, B.S.F. (Tertiary Air Ports Not Shown).

Table 7-3.

I. RADIANT SECTION DESIGN SPECIFICATIONS

GENERAL	
Internal Dimensions	24" ID x 93" Long
External Dimensions	36" OD x 96" Long
Orientation	Horizontal
Max. Designed Gas Temp	3200 ^{O}F
Furnace Volume	24·35 cu. ft.
Internal Surface Area	54·98 sq. ft.
No. Of Modules	4: One (1) Burner Module Two (2) Regular Modules One (1) Exhaust Module
Wall Construction	- Adiabatic Modules and Exhaust Module Consist of 4 Wall Layers: (inside to outside) 2½" B&W Mix 48C (or similar) 2" 3000^{O}F Insulation Cylinder 1½" Castablock Insulation 1/8" Carbon Steel Casing - High Quench Modules Consist Of 2 Wall Layers: 3" B&W Mix 48C (or similar) 1/8" Carbon Steel Casing
Residence Time @ 1 x 10^6 BTU/HR, $SR_T=1{\cdot}2$. Tmean = 2800^{O}F	1·2 Seconds
Total Port Area/%	177 sq. in./ 2.24%

Table 7-3 (Con't.).

I. RADIANT SECTION DESIGN SPECIFICATIONS (cont)

ADIABATIC MODULES (4 each 24" long)	
Wall Construction	- 2½" B&W Cast Mix 48-C $16\cdot5\ \frac{\text{BTU}}{\text{hr}\cdot\text{ft}^2\cdot{}^{\text{O}}\text{F/in}}$ - 2" 3000$^{\text{O}}$F Insulating Cylinder 2·0 " - 1½" Castablock 1·5 " - 1/8" Steel Casing - -
Overall Conduction Heat Transfer Coef. Estimate	0·43 $\frac{\text{BTU}}{\text{hr}\cdot\text{ft}^2\cdot{}^{\text{O}}\text{F}}$
Estimated Heat Loss At Mean Gas T=2800$^{\text{O}}$F	1170 $\frac{\text{BTU}}{\text{hr. ft}^2}$
Estimated Total Heat Loss At Mean Gas T=2800 $^{\text{O}}$F	16,100 $\frac{\text{BTU}}{\text{hr}}$ Per Module
% Loss of Input (1 x 10^6 Btu/Hr, Tair=600 $^{\text{O}}$F)	1·4 % Per Module
Active Cooling	External to Shell; 1" Wide x 1/8" Deep Water-cooled Passages; 6" Centers
Type of Ports	- (1) Observation = 4"x5" Diverge to 4"x11" - (4) Access = 1½"x5" - (2) Thermocouple = ¼"ID - (2) Slag = 2" ID
Estimated Weight	800 lb per Module

Table 7-3 (Con't.).

II. POST FLAME SECTION DESIGN SPECIFICATIONS

GENERAL	
Internal Dimensions	LEG #1 : 9"x9" Section x 10'0" LEG #2 : 9"x9" Section x 7'4" LEG #3 : 9"x9" Section x 15'0"
External Dimensions	LEG #1 : 15"x15" Section x 10'0" LEG #2 : 15'x15" Section x 7'4" LEG #3 : 15"x15" Section x 15'0"
Total Volume	18·19 cu. ft
Flow Area	81 sq. in (0·5625 sq. ft.)
Internal Surface Area	97 sq. ft.
External Surface Area	162 sq. ft.
Orientation	LEG #1 : Vertical Up LEG #2 : Horizontal Across LEG #3 : Vertical Down
Design Temp	Inlet 2900 $^{\circ}$F Maximum Outlet 2200 $^{\circ}$F Maximum
Overall Conduction Heat Transfer Coef.	0·667 $\frac{\text{BTU}}{\text{hr}\cdot\text{ft}^2\cdot\text{F}}$
Heat Loss Estimate	1700 $\frac{\text{BTU}}{\text{ft}^2\cdot\text{hr}}$
Total Heat Loss Estimate	166,000 $\frac{\text{BTU}}{\text{hr}}$
% Loss of Input	10·2 %
Wall Construction	- 3" 3000 $^{\circ}$F Insulating Board $\frac{\text{BTU}}{\text{hr}\cdot\text{ft}^2\cdot{}^{\circ}\text{F/in}}$ - 1/8" Thick Steel Casing
Res Time @ 1x10^6 $\frac{\text{BTU}}{\text{hr}}$ SR_T= 1·20, Tmean = 2550 $^{\circ}$F	- 0·9 Seconds
Gas Velocity	35 ft/sec
Estimated Weight	1800 lb

Table 7-3 (Con't.).

III. SUPERHEATER/REHEATER DESIGN SPECIFICATIONS

GENERAL	SUPERHEATER	REHEATER
Internal Dimension	8"x8" Section x 14'0"	8"x7" Section x 14'0"
External Dimension	14"x16" Section x 14'0"	14"x15" Section x 14'0"
Total Volume	6·22 cu. ft	5·44 cu. ft
Internal Surface Area	37·3 sq. ft	35·0 sq. ft
External Surface Area	70·0 sq. ft	67·7 sq. ft
Orientation	Horizontal	Horizontal
Design Gas Temp	2200 °F - 1500 °F	1500 °F - 850 °F
Wall Construction	3" Thick 2600 °F-Insulation Board	3" Thick 2600 °F In First Module. 3" Cast-block in Second Module.
Modules	(2) Adaptor=1'Long (2) Regular=6'Long	(2) Adaptor = 1' Long (2) Regular = 6' Long
Nominal Conduction Heat Transfer Coef	0·67 $\frac{BTU}{hr \cdot ft^2 \cdot {}^\circ F}$	0·67 $\frac{BTU}{hr \cdot ft^2 \cdot {}^\circ F}$
Estimated Heat Loss	1180 $\frac{BTU}{hr \cdot ft^2}$	704 $\frac{BTU}{hr \cdot ft^2}$
Estimated Residence Time	0·34 Second	0·37 Second
Estimated Weight	900 lb.	350 lb.

Table 7-3 (Con't.).

III. SUPERHEATER/REHEATER DESIGN SPECIFICATIONS (Cont.)

ACTIVE HEAT TRANSFER TUBE BUNDLES		
	SUPERHEATER	REHEATER
Tube Arrangement	Cross Flow Banks	Cross Flow Banks
Tubing Size	3/8"	3/8"
Wall Thickness	0·035"	0·035"
Tubing Spacing Perpendicular To Flow	2·0"	2·0"
Parallel to Flow	0·85"	0.85"
No of Rows	148	148
Tube Length Per Row	31"	27"
Total Length	382 ft	333 ft
Total Exchange Surface Area	37.5 sq. ft	32.7 sq. ft
Estimated Heat Transfer Coef	7·1 $\frac{\text{BTU}}{\text{hr}\cdot\text{ft}^2\cdot{}^{\circ}\text{F}}$	7·1 $\frac{\text{BTU}}{\text{hr}\cdot\text{ft}^2\cdot{}^{\circ}\text{F}}$
Estimated Heat Extraction Rate	472,000 $\frac{\text{BTU}}{\text{hr}}$	250,400 $\frac{\text{BTU}}{\text{hr}}$
X-Section Area of Tube	11·6 sq. in	10·1 sq. in
Free Flow Area (gas side)	52·4 sq. in	38·9 sq. in.
% Tube Area	18·2 %	20·6 %
Gas Velocity	41 ft/sec	39 ft/sec
Estimated Resid. Time	0·34 sec	0·37 sec

Table 7-3 (Con't.).

IV. AIR HEATER DESIGN SPECIFICATIONS

GENERAL	
Internal Dimensions	8" x 6" Section x 14'0"
External Dimensions	14"x14" Section x 14'0"
Total Volume	4.67 cu ft
Internal Surface Area	32.7 sq. ft
External Surface Area	65.3 sq. ft
Orientation	Horizontal
Design Gas Temp	850 °F - 250 °F
Wall Construction	3" Thick Castablock
Module:	(2) Adaptor = 1' Long (2) Regular = 6' Long
Nominal Conduction Heat Transfer Coef	$0.50 \frac{\text{BTU}}{\text{hr}\cdot\text{ft}^2\cdot{}^{\circ}\text{F}}$
Estimated Heat Loss	$235 \frac{\text{BTU}}{\text{hr}\cdot\text{ft}^2}$
Estimated Total Conduction Heat Loss	7,700 Btu/hr
Estimated Residence Time	0.58 Second
Estimated Weight	800 lb

Table 7-3 (Con't.).

IV. AIR HEATER DESIGN SPECIFICATIONS (cont)

ACTIVE HEAT TRANSFER TUBE BUNDLES	
Tube Arrangement	Cross Flow Banks
Tube Size	3/8"
Wall Thickness	0.035"
Tube Spacing Perpendicular To Flow	2·0"
Parallel To Flow	0.85"
No Of Rows	148
Length Per Row	23"
Total Tube Length	284
Total Tube Surface Area	27.8 sq. ft.
Estimated Heat Transfer Coef.	7·1 $\frac{\text{BTU}}{\text{hr} \cdot \text{ft}^2 \cdot {}^{\circ}\text{F}}$
Estimated Heat Extractions Rate	109,000 $\frac{\text{BTU}}{\text{hr}}$
X-Section Area Of Tube	8.6 sq. in
Free Flow Area	27.4 sq. in.
% Tube Area	23.9 %
Gas Velocity	34 ft/sec
Estimated Residence Time	0·58 Second

- Orientation
- Residence Time
- Thermal Environment

In field practice the pulverized coal enters the boiler cavity via an array of several burners. Dependent on the burner and boiler arrangement, the coal flame emerges with a unique flow pattern. With the exception of tangential and cyclone firing, the flame usually starts with axisymmetry and maintains this symmetry for a short period (less than 1 second). For simplicity in analysis and modeling, a cylindrical chamber is selected to simulate the radiant combustion zone. At 24 inches ID and 6 feet in length, the chamber has the following characteristics when fired at 1 x 10^6 Btu/hr:

- Residence Time = approximately 1-2 seconds
- Volumetric Heat Release Rate = 39.8 x 10^3 Btu/hr-ft^3
- Surface Area Heat Release Rate = 19.9 x 10^3 Btu/hr-ft^2

As shown in Figure 7-13, the basic 8-feet long horizontal chamber consists of three 2-feet long modules and one 2-feet long exhaust module. The radiant furnace length can be altered by addition or removal of modules. A combination of adiabatic modules and various cooling tubes will allow the furnace thermal environment to be varied over a wide range. Conceptual designs for the adiabatic module are shown in Figure 7-14. The external walls are cooled by water tubes. Measurement of water flow rates and temperatures will enable a heat balance computation to be made for the radiant furnace. The water-cooled surfaces are also less hazardous for operators.

The adiabatic modules consist of a high density catable refractory lining 2½ inches thick which is capable of withstanding the high temperature corrosive and abrasive particulate-laden combustion products. A vacuum-formed cylinder two inches thick made of B & W Kao-fibre insulation minimized the heat loss. A layer of insulblock fills the space between the Kao-fibre cylinder (33 inches OD) and the outer water-cooled steel shell (nominal 36 inch diameter).

The post flame cavity was required for two major reasons:

- It provides a reaction volume similar to the space above the active burner zone in a boiler;

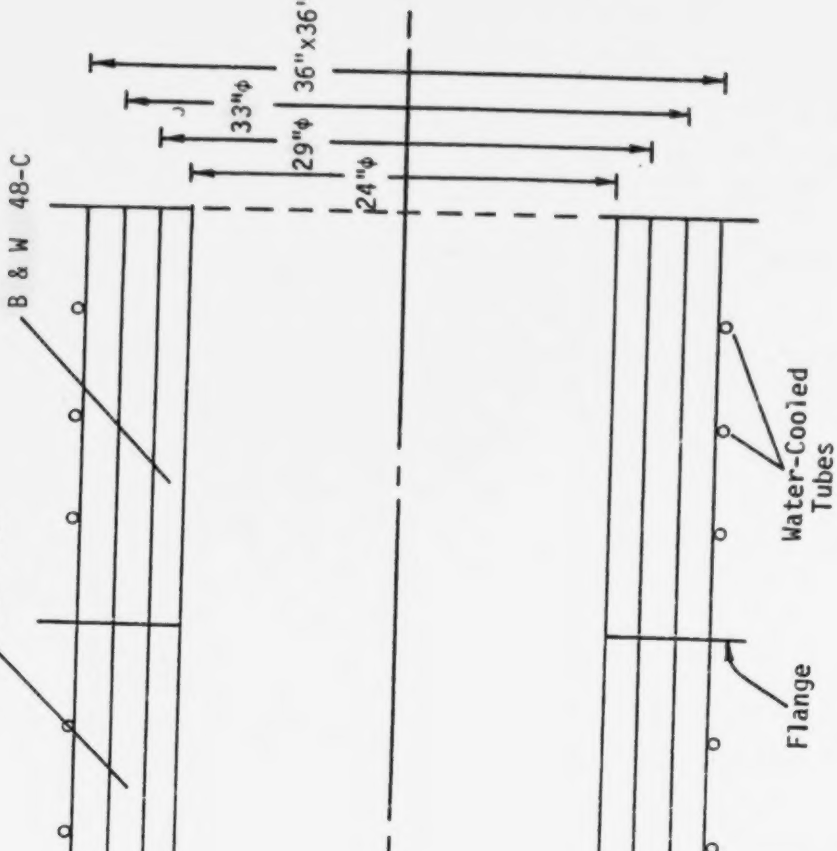
B & W 48-C
Kao-Fiber
Insulblock
36"x36"
33"φ
29"φ
24"φ
Water-Cooled Tubes
Flange

Figure 7-13. BSF - Radiant Section, Side Cross Section.

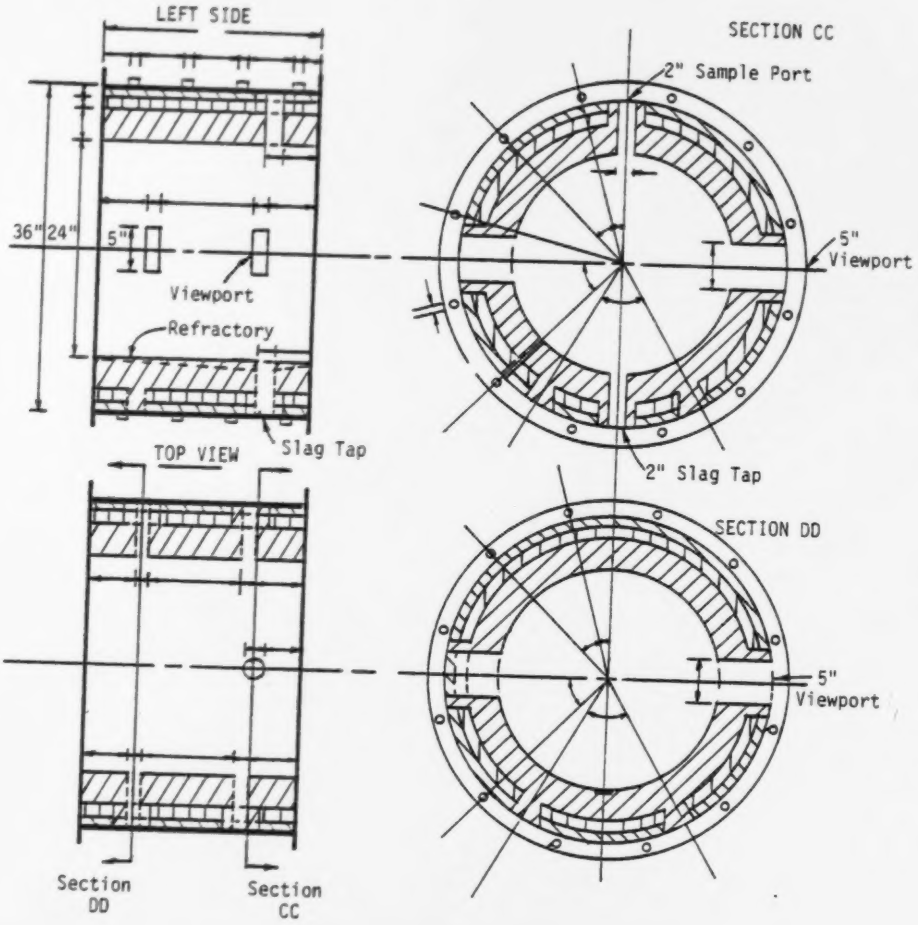
LEFT SIDE
SECTION CC
2" Sample Port
36"
24"
5"
5"
Viewport
Viewport
Refractory
Slag Tap
TOP VIEW
2" Slag Tap
SECTION DD
5"
Viewport
Section
DD
Section
CC

Figure 7-14. BSF - Radiant Adiabatic Furnace Module.

- It creates a region where the bulk gas velocity is similar to that of the gases leaving the active burner zone, hence, simulating bottom ash deposition.

Approximate calculations based upon designs of five field boiler units indicate that the median vertical bulk gas velocity is 32 ft/sec, with a residence time of approximately one second. Simulating these conditions in a 1×10^6 Btu/hr furnace requires a duct about 32 feet long with a flow cross section of 9" x 9". The section was lined with a 3-inch thick layer of Kao-fibre 3000 insulation board. Gas temperatures leaving the post-flame section can be controlled by inserting water-cooled tube modules along the inside wall. Figure 7-15 shows the concept of the post-flame section.

The average characteristics of superheaters in commercial boilers are:

- Velocity = 50-75 ft/sec
- Temperature = 2500^0F to 850^0F
- Vertically-arranged steam tubes of approximately 2-inch diameter.

In the Boiler Simulator Furnace design, a horizontal duct 14 feet long of inlet cross section 8" x 8" and with active convective heat transfer tubes will simulate the primary superheaters. The reheat superheater is similar in design, but has an 8" x 7" internal flow section. A schematic is shown in Figure 7-16. In these sections, controlled heat extraction tailors the designed temperature history for both homogeneous and heterogeneous reactions.

Particulate deposition on the tube surface depends on these variables:

- gas phase particulate loading;
- tube orientation;
- tube geometry: diameter;
- approach velocity;
- tube metal temperature;
- tube-to-tube distance.

In industrial and utility boilers, superheater steam is produced and results in certain gas and metal temperatures unique to the particular boiler. Since

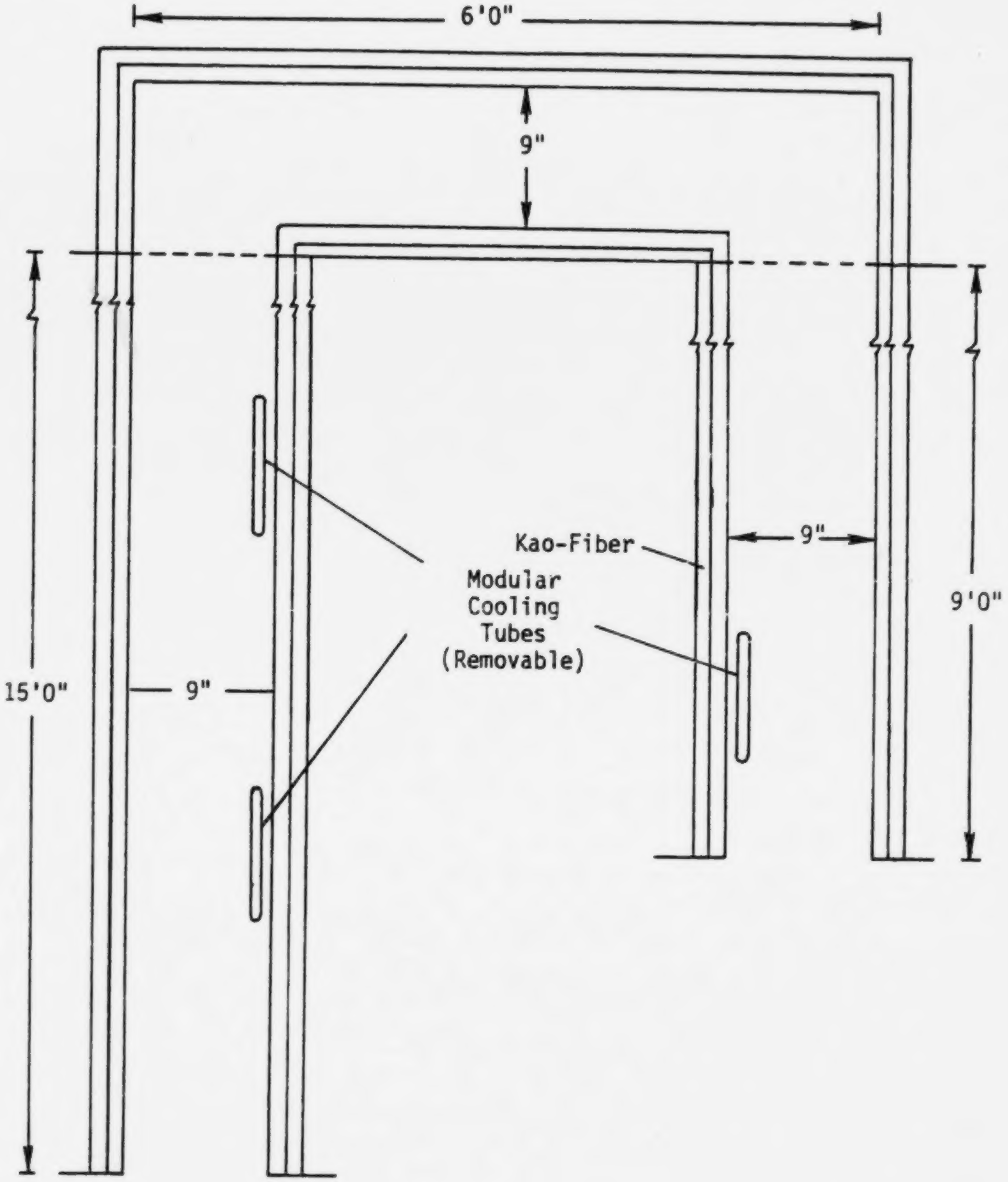
6'0"
9"
Kao-Fiber
9"
Modular
Cooling
Tubes
(Removable)
9'0"
15'0"
9"

Figure 7-15. BSF - Post Flame Cavity - Concept.

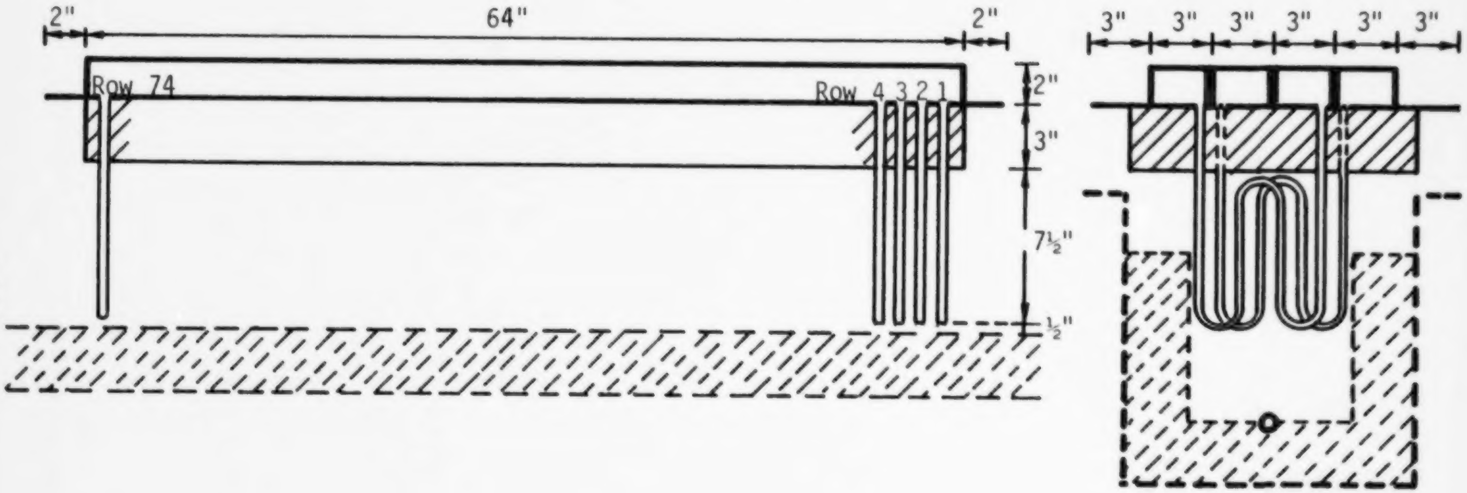
2"
64"
2"
Row 74
Row 4 3 2 1
2"
3"
7½"
½"
3"
3"
3"
3"
3"
3"

Figure 7-16. BSF - Convective Air Cooled Superheater Module.

steam presents additional operating complexity, air will be used as the coolant. In the convective section, two types of heat exchange modules will be used, namely: heat extraction modules and particulate deposition modules.

Four modules of air-cooled tube heat exchanges (as shown in Figure 7-16) will be used to control the gas phase temperature. The coolant tubes will be arranged at 90^0 to the direction of gas flow to simulate boiler tubes. Varying the coolant flow rates will control the rate of heat removal. These modules, lined with a 3-inch thick layer of Kao-fibre insulation, will reduce the rate of uncontrolled heat loss.

The economizer and air heater sections differ from the superheaters in their operating temperatures and construction. The coolant can be air-supplied from either the metered combustion airstreams or the blower-supplied ambient air, dependent on whether the preheated combustion air can produce satisfactory temperature history in the combustion products.

Two heat exchange modules will simulate the economizer and air heater. They will be formed from stainless steel with a 3-inch outer layer of insulating material. Arrangement of cooling tubes and test-section tubes will be identical to those in the superheater sections.

The heat extraction system has two functions:

- It provides proper thermal environment for the reactive combustion products;
- It maintains equipment integrity.

As a general principle, uncontrolled heat loss will be minimized and when heat is removed, sufficient instrumentation will quantify the rate of heat loss.

The furnace shell is cooled by a closed-loop system which is illustrated in Figure 7-17. Cooling on the furnace shell stabilizes heat loss to the air and minimizes burn hazards to workers. The furnace time temperature profile was modified by placing four water cooled rods into the radiant furnace. Heat extraction was controlled by the exposed cooling surface in the radiant furnace.

7.3.1.9 Clean Up

The BSF will be used to study the effect of combustion conditions on pollution control; therefore, the system includes special provision to investigate various clean up systems.

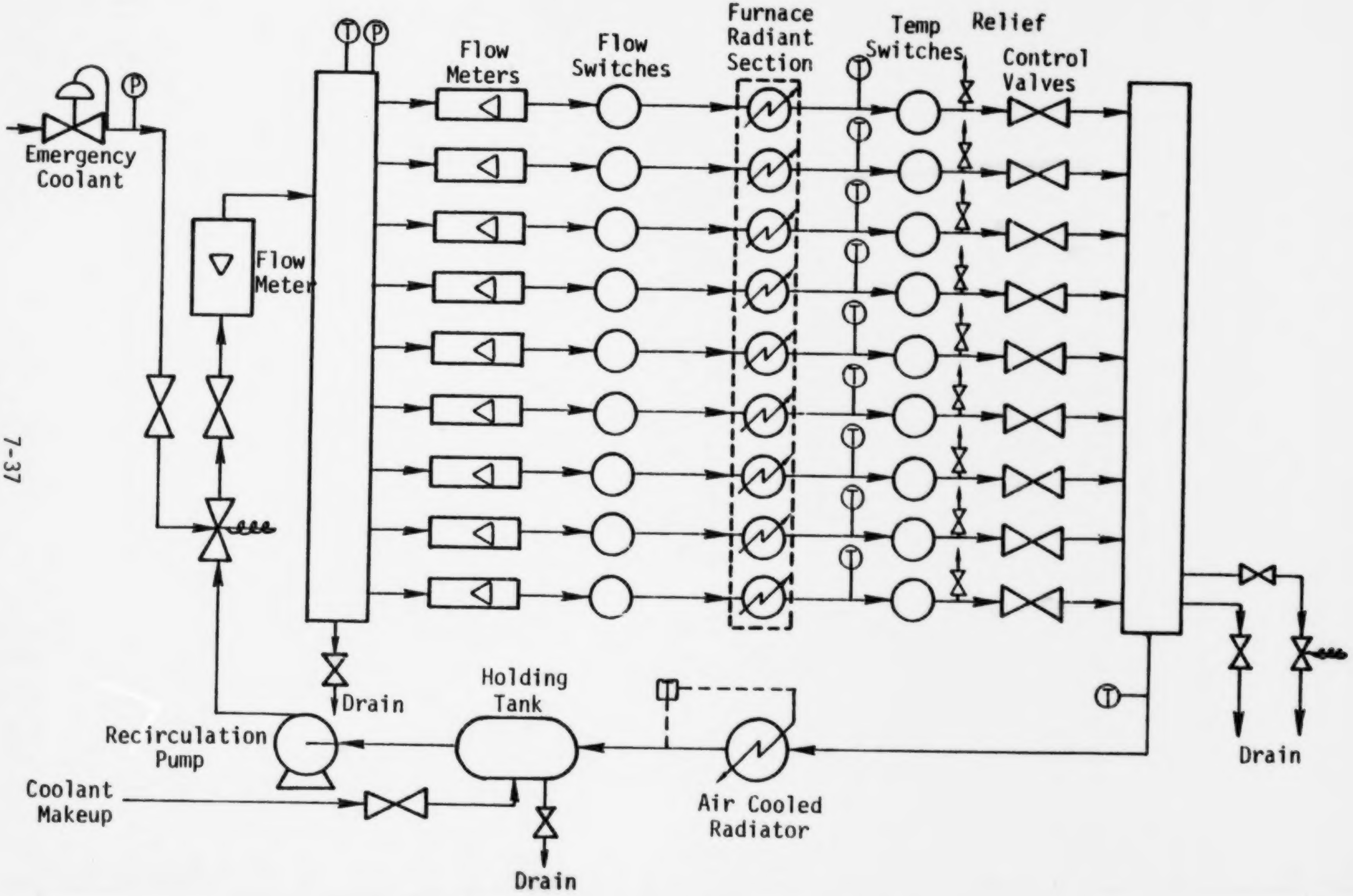
Emergency Coolant
P
Flow Meter
T
P
Flow Meters
Flow Switches
Furnace Radiant Section
T
Temp Switches
Relief
Control Valves
Drain
Holding Tank
Recirculation Pump
Coolant Makeup
Drain
Air Cooled Radiator
T
Drain

Figure 7-17. BSF - Furnace Heat Extraction Control System.

A typical bituminous coal will produce around 8 lbs/hr of ash. This will increase as high ash coals or solid additives are used. A bag filter unit separates the fly ash from the exhaust gas. Normally, an air-cooled heat exchanger will cool the stack gas to the bag operation temperature. Dilution cooling is cumbersome and introduces additional measurement problems when gas samples from the baghouse are of interest. In special cases, high temperature operation with the baghouse is needed for research objectives. Therefore, a baghouse capable of withstanding high temperatures was used.

Deposition of bottom ash/slag cannot be prevented. It is planned that two modes of clean up will be employed. The first will be manual removal of the ash deposits. The second will be by promoting formation of running slag which will flow towards the burner and out of the furnace via taps.

Operational experience with the baghouse and with bottom ash deposits and slagging problems is discussed in Section 7.3.2.

7.3.1.10 Data Acquisition

The Boiler Simulator is a complex system with numerous variables such as:

- Input - fuel/air flow rates and temperatures, coolant rates and temperatures;
- Output - gas product concentrations, opacity, particulate loading and size distributions;
- System - temperatures, ancilliary equipment operation information;
- Computed - pollutant formation rates, mass and energy balance, bulk velocities and residence times.

It is impracticable for the operator to monitor and record all information in a timely manner. Use of a well-integrated data acquisition system will enhance the experimentation efforts and improve data accuracy.

A simple model of a data acquisition system is shown in Figure 7-18. The key functional equipments are identified by the block diagram. This scheme permits information updates at regular time intervals. The controller (computer) detects alarm conditions, such as deviation of operating variables from setpoints, and alerts the operator. This will free the operator to perform other duties without compromise to data accuracy or equipment integrity. The

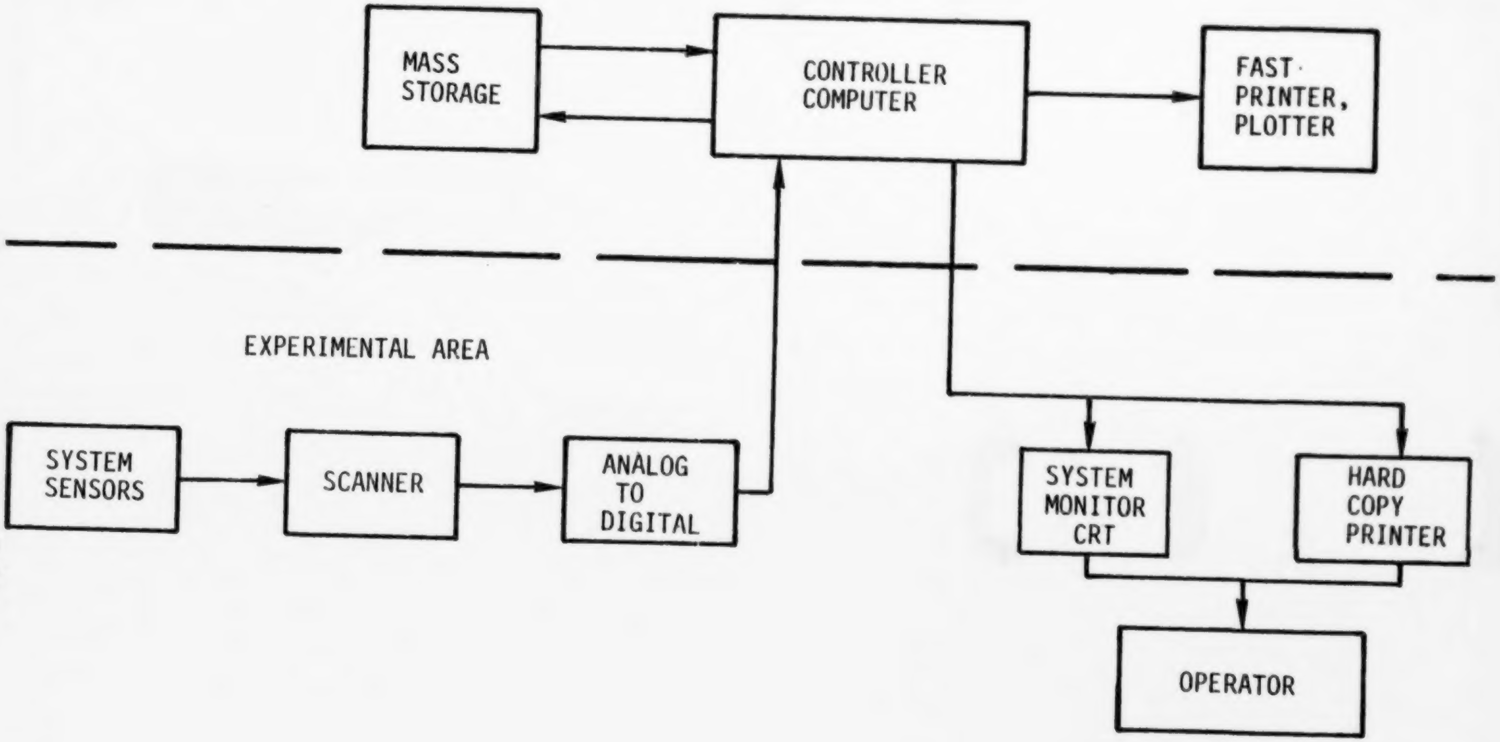
MASS STORAGE
CONTROLLER COMPUTER
FAST PRINTER, PLOTTER
EXPERIMENTAL AREA
SYSTEM SENSORS
SCANNER
ANALOG TO DIGITAL
SYSTEM MONITOR CRT
HARD COPY PRINTER
OPERATOR

Figure 7-18. BSF - Data Acquisition System Scheme.

computation power of the controller can be utilized to analyze the data and provide real-time information about overall system performance. All this will allow the operator to better assess the experimental process and take appropriate actions to accomplish experimental goals.

7.3.2 Operation Experience

The following is a brief recounting of operational problems encountered during startup, shakedown and initial experimental operation of the BSF facility. It is hoped that review of these problems may help others avoid some of the problems attendant to assembly of such a system. It should be realized that by its very nature, the BSF has all the hardware and control aspects of a full size boiler with the addition of a full complement of sampling, and analytical instruments, and a data acquisition system.

The problems encountered in operating the facility fell into two categories: minor problems which, while of nuisance value in time and trouble, did not jeopardize operational performance or delay conduct of experiments with the facility. On the other hand, the major problems either were of high nuisance value in wasted time or expense, or, without timely correction, would severely delay conduct of the experiments or not allow attainment of proper experimental conditions.

7.3.2.1 Minor Problem Areas

Laminar Air Flowmeters

The five air lines are regulated to 2 atm pressure upstream of the final air operated needle valves. Laminar flow elements are located in this constant pressure segment of each line.

The differential pressure across each element is read out on oil-filled, slant, draft gauges in the control room. The manufacturer's original data was used to establish the baseline airflow conditions during the shakedown runs. The use of the oxygen meter in the flue duct allows calculation of the mass balance as a check on the set flow rates. Several runs showed lack of mass balance, a discrepancy of around 15 percent. The flow elements were removed and found to be partially obstructed by debris common to newly assembled piping systems; rust flakes, teflon tape sealant scraps, etc. The elements were easily cleaned and re-installed, but mass balance was still not achieved. Upon checking with the manufacturer, it was found that their original calibration calculations and resulting data were in error. After receipt of new curves, subsequent mass balance runs achieved closure well within 1 percent total error. No further problems have been encountered with the flow measuring system.

Air Preheaters

Just prior to furnace entry, each air line passes through a propane fired preheater. The preheaters were fabricated by a local vendor to specification. During shakedown runs several preheaters developed leaks in the air annulus end closure nearest the propane burner. The cause was poor welding workmanship during manufacture. To prevent program delays each heater was rewelded on site in the suspect area, and returned to service. No further problems are anticipated.

Baghouse

The baghouse is a tall slender rectangular box with a very high surface to volume ratio. External natural convection cooling of the stainless steel walls depressed internal flue gas temperatures below the dew point, with consequent caking on the bags producing a high pressure drop. The addition of 3" cellulose insulating panels to the entire outside surface eliminated the cooling effect, raising the internal temperature so normal operation was restored. The baghouse has operated reliably ever since modification was made.

Coal Nozzle and Delivery Train

During early shakedown runs on pulverized coal, the NO_x levels were higher than predicted for the distributed mixing burner. Various combinations of primary, secondary and swirl air did not produce significant improvement. Visual inspection indicated the high divergence angle of the coal nozzle defeated the distributed mixing potential of the burner. In addition, the three supports for the central conical plug destroyed the annular fuel injection pattern, resulting in three distinct jets. A new nozzle assembly was designed and fabricated which featured a reduced injection angle and support by a central pintle shaft. This design also allowed external adjustment of the fuel injection gap to maintain correct injection velocities independent of furnace firing rate.

Concurrent with this development, it was observed that transport air velocities around 50 ft/sec were marginal in preventing pulverized fuel deposition in fittings of the delivery train. Screwed on pipe fittings of larger diameter were replaced by smaller solder fittings for interior smoothness and the entire delivery system was operated at greater than 50 ft/sec transport velocity. Satisfactory operation with characteristic low NO_x readings was obtained after a nominal period of tune up adjustment and minor modificatons. One important lesson was gained as a result of this modification: burners of this small scale require precision instrument design and fabrication techniques to insure proper operation; attention to machining dimension tolerance and aerodynamics aspects are foremost considerations.

Sorbent Feeder

The sorbent feeder is of the twin screw type driven by a variable speed servo motor. Volumetric flow rate is precisely controlled by state-of-the-art, digital electronics. During the first sorbent injection trials, uneven sorbent mass flow rates were experienced with both sorbent types (carbonate and hydroxide). A variation of ±10 percent during a ten minute run duration was not uncommon. Some improvement was gained by adding another set of stirring paddles to the hopper agitator, and providing air jets to prevent sorbent material from caking on the feed screws. These measures did not completely solve the problem. As a final precaution, all sorbent material is transferred to airtight drums on delivery. Further, dessicant bags cover the drum free surface and prevent moisture pickup when the lid is off. Daily cleaning and refilling of the hopper with fresh sorbent and frequent calibration of the delivery system became established procedures. The sorbent feed system has performed satisfactorily since these measures were adopted.

7.3.2.2 Major Problems

Convecture Section - Superheater

When the coal-fired shakedown runs began the furnace interior was free of ash, having been run on propane only for all curing and initial testing. The first evidence of ash buildup and blockage occurred at the entrance of the superheater convective pass. Two factors contributed: first, the large number of tubes in this section made close spacing necessary thus allowing ash bridging, and second, this convective section is located immediately downstream of a 90^0 turn enhancing turbulence levels so turbulent ash transport to wall and tube surfaces is augmented.

Confirming data related to high heat transfer suggested that removal of some of the cooling tubes was a solution. This section was modified by deleting 2/3 of the original heat transfer tubing. Satisfactory operation has been achieved, but this is still the most sensitive ash deposition section and requires regular cleaning.

Pulverized Coal Feeder

A loss in weight feeder was chosen for the fuel delivery system because of the required precision and need for unattended operation while performing the experiments. The unit features twin feed screws, DC servo-motor drive controlled by a state-of-the-art digital electronics system.

Upon initial calibration and use during the shakedown runs erratic fuel delivery was observed while in the "mass flow" mode (closed loop operation). It was determined at this time that the cause was the high turndown ratio at our operating point. The vendor would not divulge their machine sizing criteria to us during the purchase activity, and as a result they sent a machine capable of delivering 750 lb/hr when our nominal flow would be approximately 100 lb/hr. New feed screws and gear box were subsequently sent and installed, producing a 200 lb/hr maximum flow rate.

On additional testing, operation was still erratic, with addition of a new feature--flooding. The new feed screws and housing, although compatible parts according to the vendor, produced a radial gap that let an uncontrolled amount of fuel flow every time the hopper was refilled. This was particularly troublesome during an experimental run where fuel-rich conditions occurred for several minutes on hopper refill command. This problem was rectified by installing polyurethane sleeves inside the housing so that the radial gap was eliminated.

The vendor also indicated wind disturbance was involved in erratic scale operation. Wind shielding panels were erected but no improvement was noted. During the period of these troubles experimental operations continued by running the feeder in the (open loop) constant volume rate mode. This gave satisfactory results because of uniform fuel density.

The one remaining factor that effects accuracy of a loss in weight feeder are pressure differences between hopper inlet and feed screw outlet. Because of the necessity to measure all air entering the furnace the outlet of the feeder is enclosed within the shroud feeding the aspirated coal into the delivery line. Furnace pressure fluctuations are thus transmitted to the outlet of the feeder. The pulsations generated cause uneven coal delivery which are similar to that caused by wind. A third gearbox with an extremely high gear ratio was installed to alleviate this problem, but was only partially successful. The only satisfactory, complete solution is to replumb the entire delivery system to incorporate a rotary airlock which would isolate the feeder from the furnace fuel transport line. Since minimal satisfactory operation of this feeder is obtained in the open loop, volumetric mode, no additional changes have been made or are contemplated on the feeder system.

Furnace Slagging/Fouling

The immediate flame zone walls are well-insulated to attain surface temperatures approaching gas temperature. This is to simulate the radiation self-absorption of a large boiler flame that is not present in the small scale device. As a consequence the wall temperatures generally exceed the ash fusion temperatures, producing copious quantities of slag. This was anticipated by including three 4-inch diameter openings in the flame zone bottom. However, the slag accumulated so rapidly in early runs with sorbent additive that the slag solidified in the openings, rendering them unusable.

The furnace also experienced severe ash/slag buildup in the post-flame zone which was not refractory-lined. The worst slag buildup was at the 90° turn from the flame zone to the vertical post-flame zones (see Figure 7-19). This is also the point of a cross-section area contraction from over 3 ft^2 to .56 ft^2. Slag that formed in this vertical section, and to some extent in the horizontal crossover section, tended to flux with the high temperature insulating board, erroding the board and causing a gradual loss of the wall. Several attempts were made to "overfire" the furnace overnight, while on propane, in order to melt out the accumulated slag. After several attempts it was determined that the insulating board was being gradually consumed by the interaction with molten slag.

These two related problems demanded attention so that present and future experiments would not be jeopardized by the continued unscheduled shutdowns

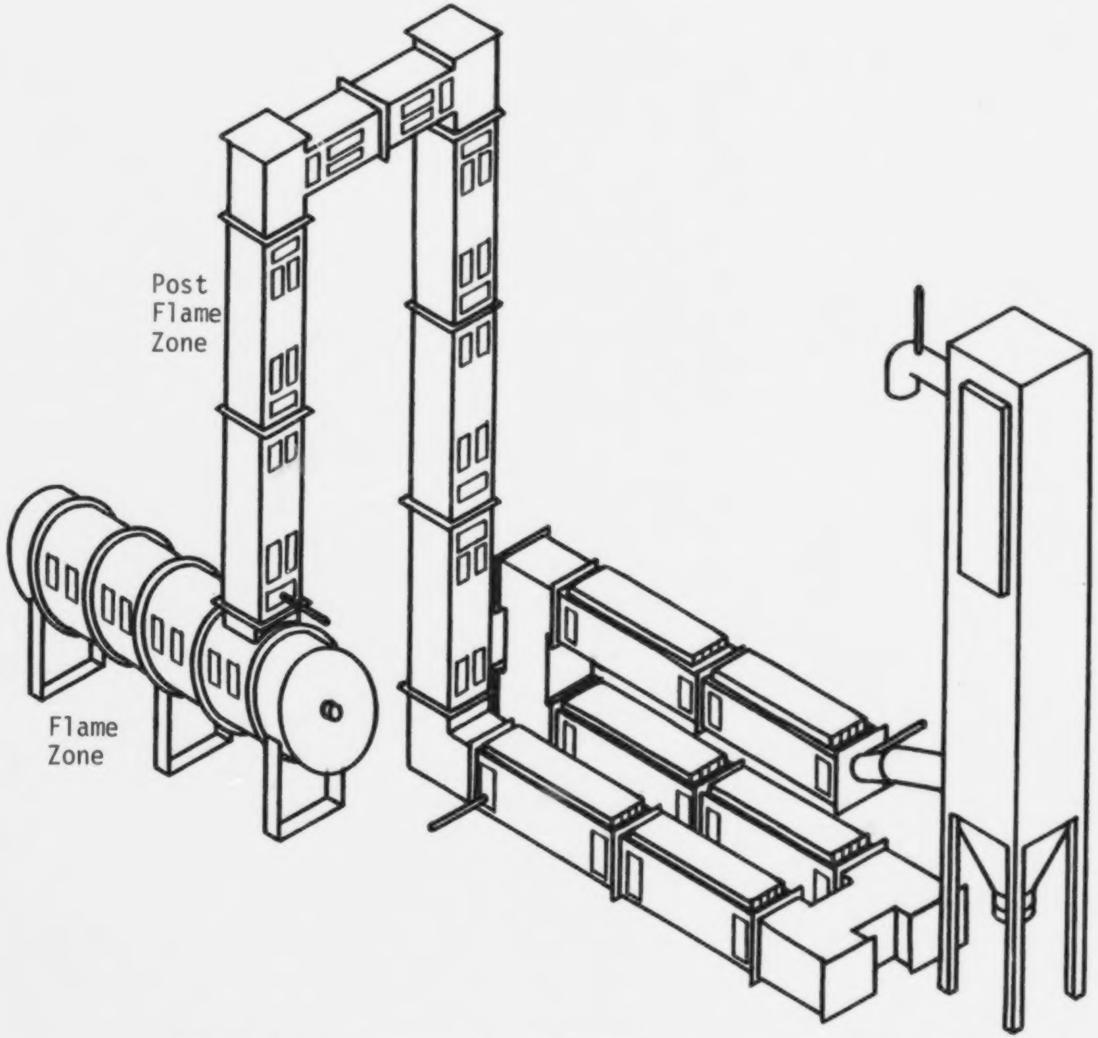
Post
Flame
Zone
Flame
Zone

Figure 7-19. Boiler Simulator Furnace - Original Configuration.

caused by flow blockage, lost insulation board, and extensive slag accumulation in the flame zone.

A two-phase repair plan was approved which would yield immediate relief for continued experiments and give time to implement construction of components for the final solution. The first phase featured:

- Addition of a large slag removal door in the flame zone end.
- Enlargement of the post-flame zone entrance section to 1.5 ft^2 by construction of a new section.
- Addition of a refractory-lined 4-foot-long post flame section with sufficient ports for sampling, external staging air and sorbent injection.

These modifications are pictured in Figure 7-20 and were installed on the furnace in August, 1981.

The second phase would be constructed so as to be installed after completion of the external staging experiments (Series A-2). Most units made in Phase I furnace reconstruction would become part of the final configuration, which features:

- Downfired flame zone for flame symmetry at low flow rates and freedom from slag.
- 100 percent refractory lining - flame and post flame zone.
- Slag drawer at end of downfired zone.
- Gradual cross-section area change from flame zone to superheater section entrance.
- Numerous ports for staging air, FGR, sorbent addition, gas sampling, and solid sampling with new IFRF probe.
- Ports at each corner for on-line soot blowing if required.

The second phase modifications were added starting 10 October 1981; the furnace was restarted after the end of this reporting period. The final configuration is shown in Figure 7-21 while the comparison of original furnace cross-section area with the new configuration is shown as Figure 7-22. The furnace temperature/time profile was documented and showed that a return to the 1 MBtu/hr nominal load produced the desired flame and post-flame residence times.

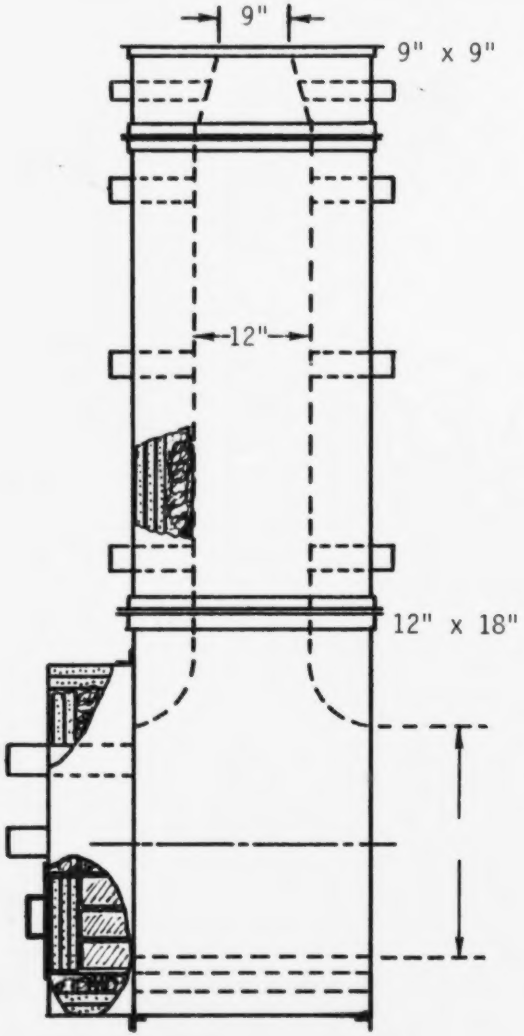
9"
9" x 9"
12"
12" x 18"

Figure 7-20. Modified Post Flame Cavity - As of August 22, 1981.

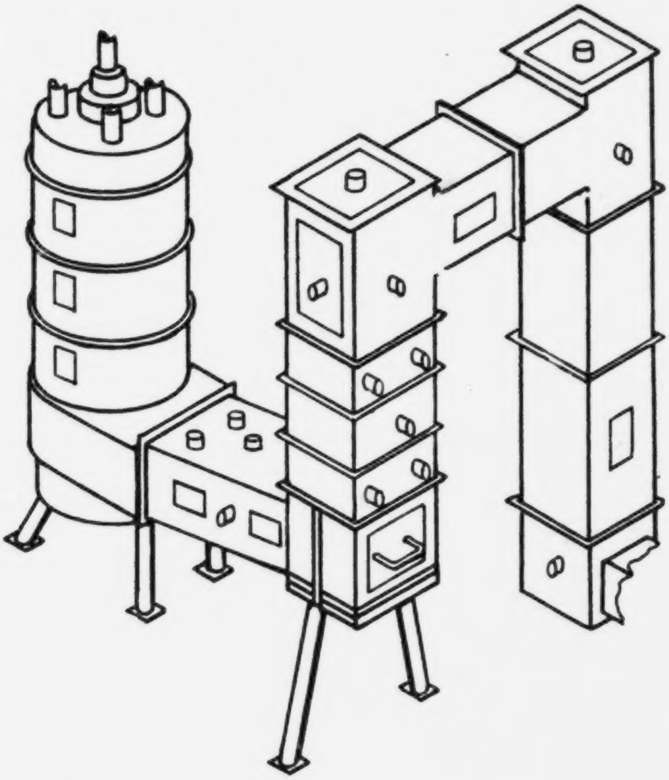

Figure 7-21. BSF - Downfired Configuration as of Late October, 1981.

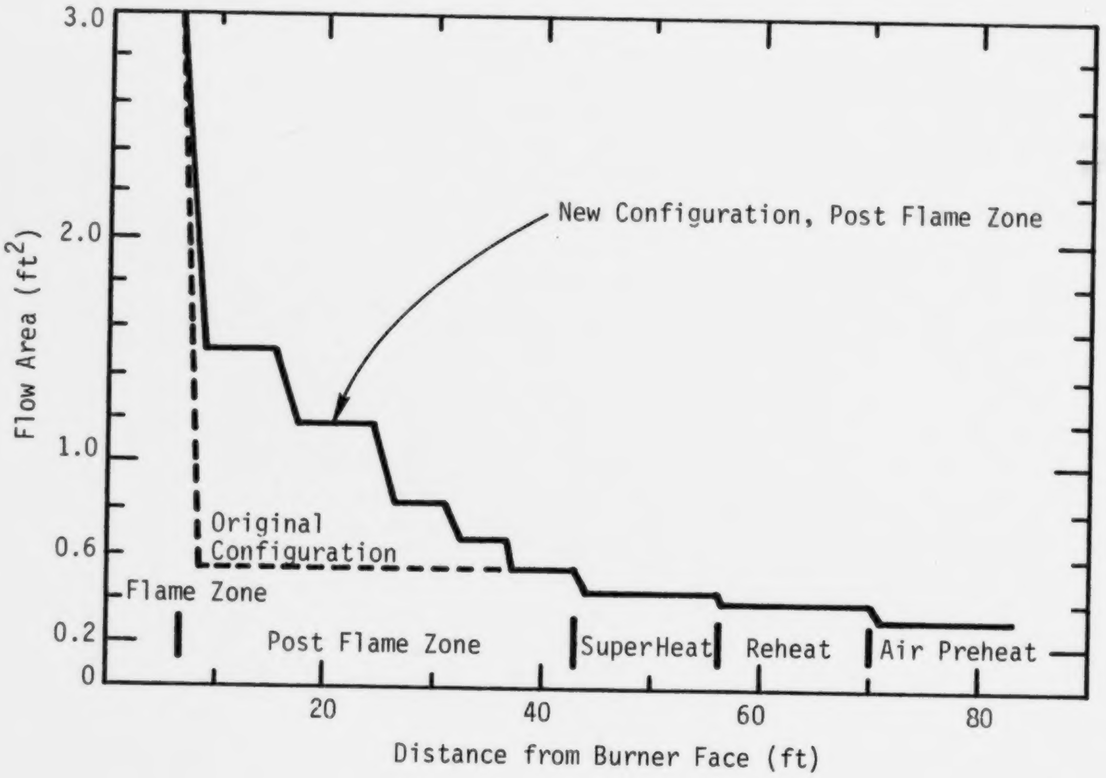

Figure 7-22. BSF Cross Sectional Flow Area Versus Axial Distance.

8.0 MEASUREMENT SYSTEMS

The analytical requirements of this project were extensive and necessitated the development of several new capacities at EER. Required capabilities included:

- The ability to acquire representative samples, both gas and solid, from furnace locations including the flame and stack.
- Routine continuous monitoring of gas phase species concentrations including: O_2, CO_2, CO, NO, NO_2 and SO_2.
- The analysis of input and output solids characteristics including: the C, H, N, S, and ash content of coal, ash, char and sorbent samples; the size distribution and surface area of both reacted and unreacted sorbents; and the mineral content and composition of sorbent, ash, and coal samples.
- The analysis of gaseous sulfur species other than SO_2, including H_2S, COS, CS_2 and thiophene.
- The measurement of furnace wall and gas temperatures.

The sample extraction and conditioning system developed for these studies is discussed in Section 8.2. The gas phase analytical systems, both batch and continuous and the development of solids analysis methods are discussed in Sections 8.2 and 8.3, respectively. All of the measurements performed at EER are described. An outside laboratory was used for standard coal analysis (proximate, ultimate, heating value, ash composition, etc.).

8.1 Sample Extraction and Conditioning System

Gaseous samples were taken from the furnace for the continuous monitoring of O_2, CO_2, CO, NO_x and SO_2. A standard water cooled probe for sample extraction and an ice-bath condenser followed by a filter for water and particulate removal has been well tested and shown suitable for the sampling of O_2, CO_2, and NO_x. The measurement of sulfur species in combustion products containing active sorbents poses several special problems. Sulfur species are water soluble and highly reactive with calcium based sorbents. It is imperative that gas-solid contacting be minimized and contact between the gas and any condensed water be avoided. A phase "discrimination probe" for the measurement of sulfur species has been designed, constructed, and tested. The sulfur species samples is extracted from the main particle laden sample stream at right angles to the flow and at a relatively low velocity (see Figure 8-1). The gas sample is transported in a heated teflon line maintained above 115°C under vacuum to a heated filter followed by a permeation tube drier. The permeation tube drier selectively removes water vapor from the gas sample using dry air as the dry gas medium. The sample was then pressurized and delivered to the analytical system (see Figure 8-2).

The permeation drier was tested to assure that it did not pass SO_2, CO, CO_2, NO, or O_2 across the permeable membrane. The water removal efficiency of the drier was also demonstrated. Figure 8-3 compares SO_2 concentrations without water vapor and after water vapor had been added to the gas and then removed in the permeation drier.

The phase discrimination probe and the SO_2 sample conditioning system were tested in the argon furnace. SO_2 was added directly ahead of the phase discrimination probe while sorbent was added to the combustion air in pulses. The presence of solids (which had experienced the entire flame region and were therefore probably reactive) had little effect on the measured SO_2 concentration. The difference between SO_2 concentration with and without sorbent was less than 2 percent.

The main sample, extracted down the probe centerline, was conditioned for standard analysis of CO_2, O_2, CO, and NO_x by condensing the water in an iced cyclone and then filtering before delivery to the continuous instrumentation.

The sample system used in the Boiler Simulator Furnace Studies consisted of four phase discrimination probes. The four SO_2 sample streams shared a conditioning system (drier, filter, etc.) as did the main sample streams. The overall continuous sampling and analytical system used in the BSF studies is shown in Figure 8-4.

8.2 Gas Sample Analysis

The following section describes the instrumentation and measurements systems used for gas analysis during these experiments. The development of analytical capacities for sulfur compounds required a major effort and is the main

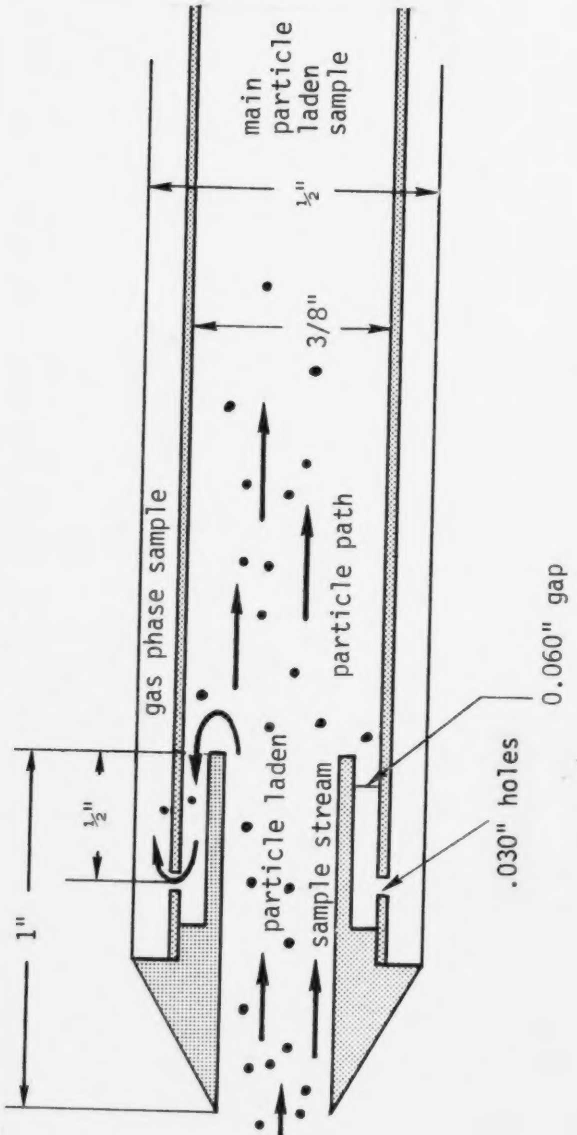

1"
½"
gas phase sample
particle laden
sample stream
particle path
3/8"
½"
main
particle
laden
sample
.030" holes
0.060" gap

Figure 8-1. Phase Discrimination Probe.

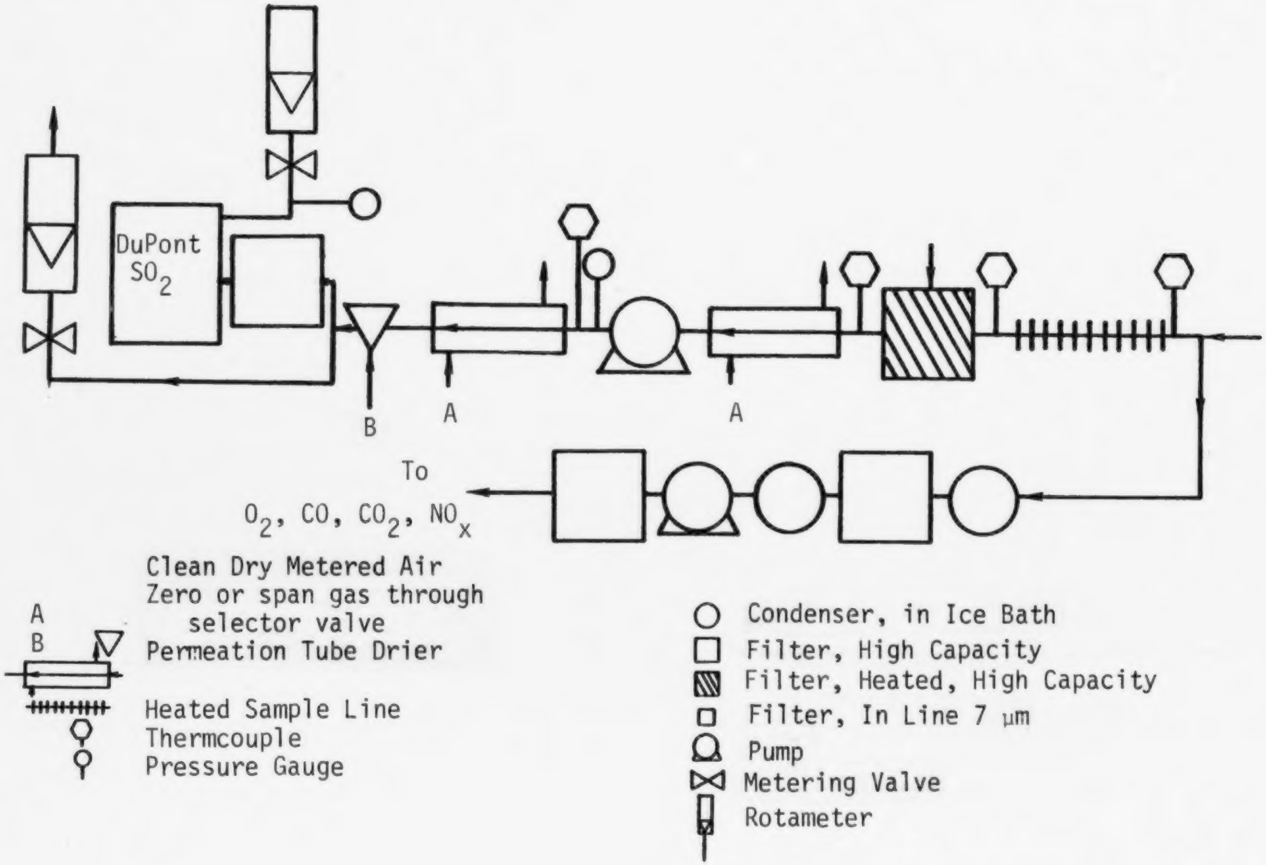
DuPont SO_2
B
A
A
To
O_2, CO, CO_2, NO_x
A Clean Dry Metered Air
B Zero or span gas through selector valve
Permeation Tube Drier
Heated Sample Line
Thermcouple
Pressure Gauge
Condenser, in Ice Bath
Filter, High Capacity
Filter, Heated, High Capacity
Filter, In Line 7 μm
Pump
Metering Valve
Rotameter

Figure 8-2. Gas Phase Sulfur Species Measurement System.

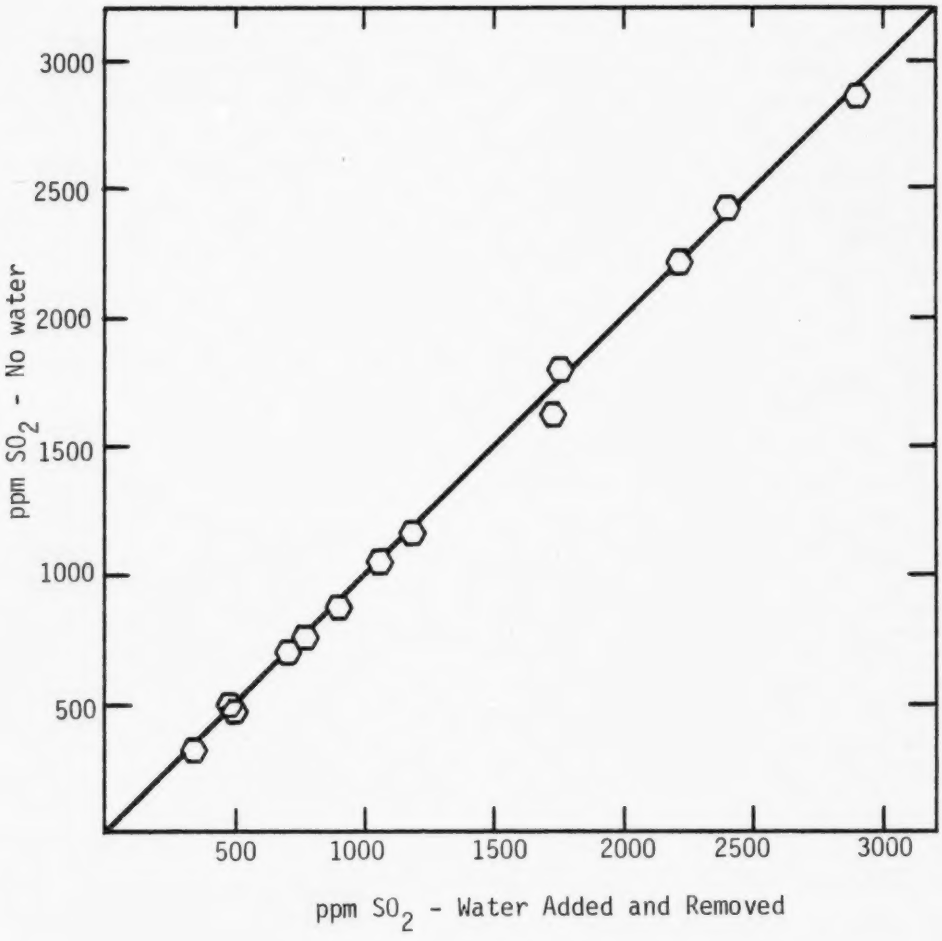

Figure 8-3. Verification of Permeation Tube Drier.

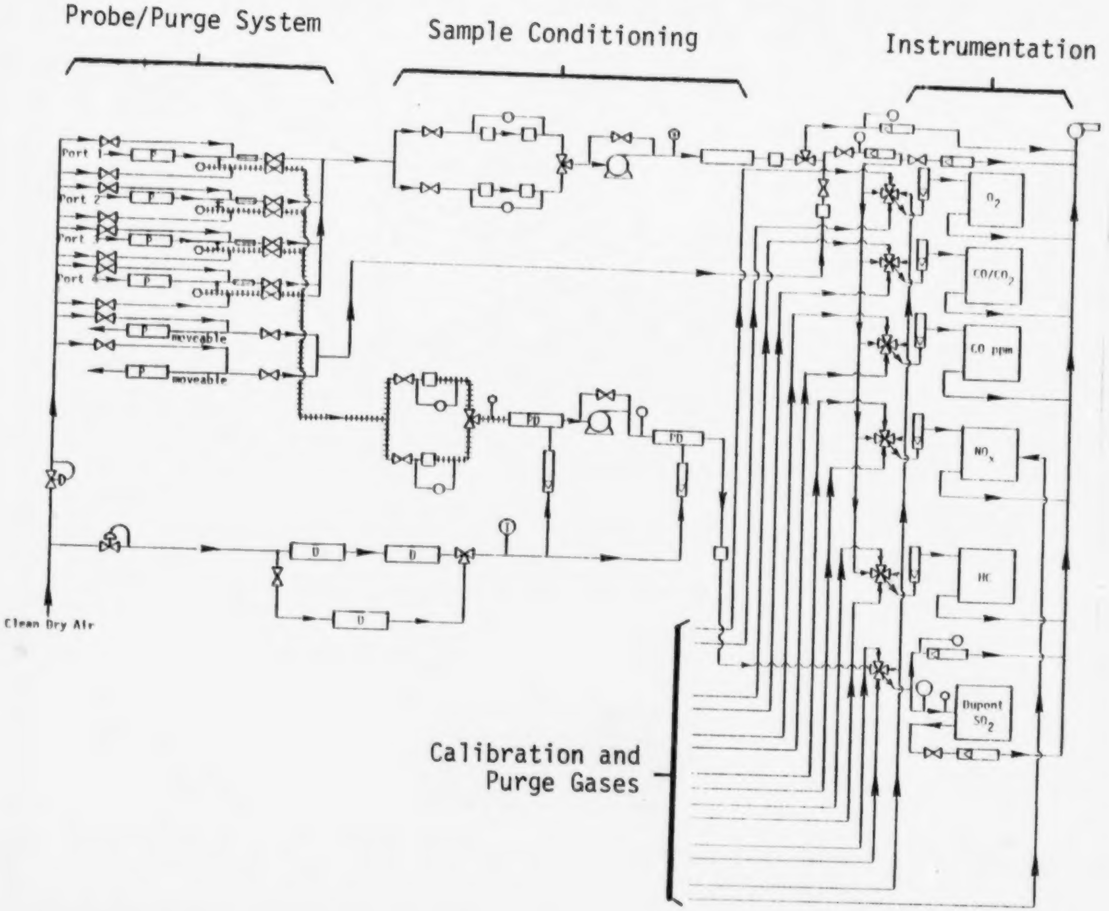
Probe/Purge System
Sample Conditioning
Instrumentation
Port 1
Port 2
Port 3
Port 4
P
moveable
moveable
D
FD
FD
O_2
CO/CO_2
CO ppm
NO_x
HC
Dupont SO_2
Clean Dry Air
Calibration and Purge Gases

Figure 8-4. BSF - Four-Probe Sample and Analytical System.

topic of discussion in the following sections. Continuous instrumentation, first standard systems for CO, O_2, CO_2 and NO_x, then SO_2 and H_2S are discussed in Section 8.2.1. The development of batch analysis methods for sulfur containing gases is described in Section 8.2.2.

8.2.1 Continuous Instrumentation

After the gas samples were extracted from the furnace and conditioned they were delivered to a set of continuous analytical instruments (Table 8-1). The instruments used were selected for reliability, ease of operation and cost. There is considerable experience at EER with standard CO, CO_2, O_2 and NO_x instrumentation. This experience was drawn on in selection and set up of the particular instrumentation with little effort spent on new developments.

The measurement of sulfur species is considerably more difficult, however, than the other measurements and required extensive work comparing instruments and developing sampling and analytical methods. The development and testing of methods for sulfur species analysis is discussed in the following sections.

Continuous measurement of SO_2 was made with a non-dispersive ultraviolet instrument manufactured by DuPont. SO_2 is measured by the difference in absorption of ultraviolet radiation by the sample gas at two wavelengths--a reference wavelength and at 320 nm which is absorbed by SO_2 specifically.

The NDUV instrument was chosen in preference to the pulsed fluroescent instrument made by Thermo Electron because of the linearity and stability of the DuPont and because there is no interference from water, CO_2 or O_2 as there is in the pulsed fluorescent instrument.

The DuPont instrument and sampling system were compared with EPA Method 7 SO_2 measurements under both cold and flame conditions. The agreement was good --see Figure 8-5--and was not a function of watervapor content or SO_2 concentration.

The DuPont instrument is suitable for measurement of SO_2 in combustion stack gases but aromatic and unsaturated hydrocarbons absorb U.V. light in the same wavelengths as SO_2; therefore, the DuPont cannot be used to directly measure SO_2 in fuel-rich combustion gases.

Table 8-1. Instrumentation for Continuous Measurements.

Species	Probe	Instrument	Range
O_2	WC, SR RD	Beckman 755 Paramagnetic	0-5, 0-10 0-25%
CO	WC, SR	Low-Anarad 500R NDIR	0-500 ppm
	RD	High-Anarad 600 NDIR	0-1, 0-10%
CO_2	WC, SR RD	Anarad 600 NDIR	0-20%
NO, NO_x	WC, WS RD	TECO 10R Chemiluminescent	0-5 ppm to 0-10,000 ppm
SO_2	SR PD	DuPont 400 Photometric	0-400 0-4000 ppm
H_2S	SR PD	Dilution with air Oxidation to SO_2 DuPont 400 Photometric	0-4000 ppm

WC - Water Cooled
WS - Water Spray
SR - Solid Rejection

RD - Refrigeration Dried
PD - Permapure Drier

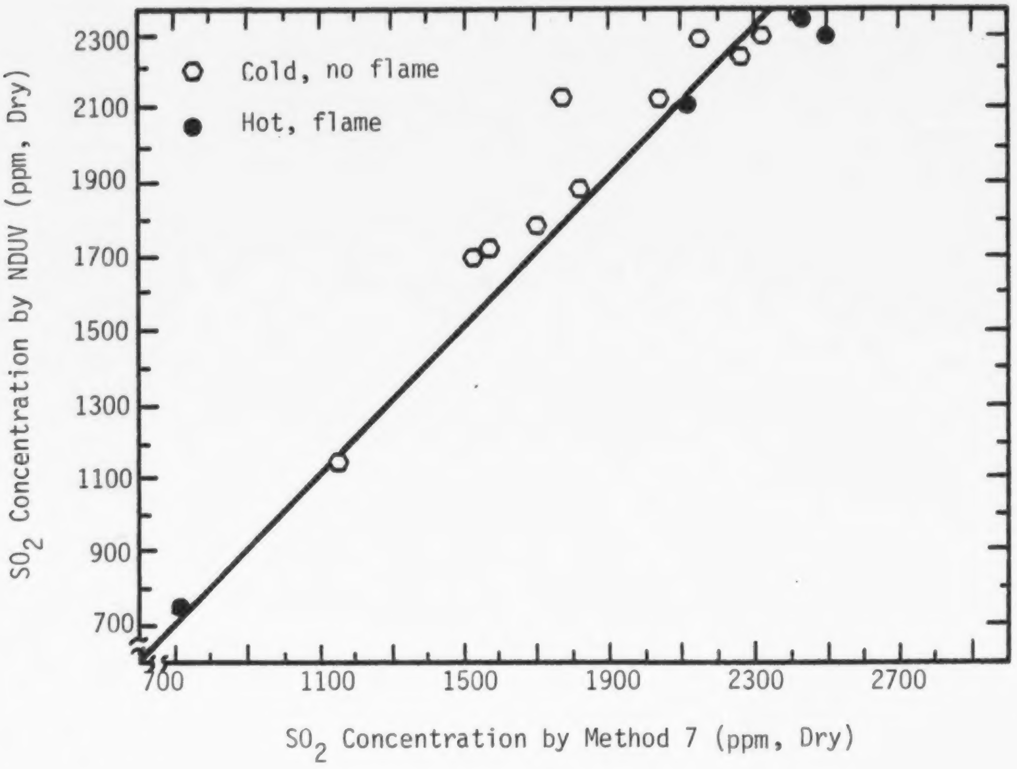

Figure 8-5. Comparison of SO_2 Analysis Methods: NDUV Versus Method 7.

Sulfur specie measurements in rich gases were made in two ways. On a continuous basis SO_2 and H_2S were measured using a catalytic converter system to oxidize the H_2S to SO_2. A batch analysis system using a GC equipped with a flame photometric detector was developed and is described in Section 8.2.2. The continuous system consisted of a dilution system to add O_2 to the sample, a heated catalytic converter and a SO_2 selective scrubber (see Figure 8-6).

H_2S was measured by diluting the sample with O_2, oxidizing the H_2S to SO_2 in the converter and measuring the resulting SO_2 concentration with the DuPont. SO_2 was measured as the difference between total SO_2 (all the sample gas through the converter) and H_2S (the sample was routed through the SO_2 scrubber before oxidizing). Figure 8-7 shows the agreement between measured SO_2 and expected (based on dilution) SO_2 concentrations for various SO_2 span gas/air mixtures.

The second method for measurement of sulfur species in a rich combustion gas was a batch method described in the following section.

8.2.2 Batch Sample Analysis

A gas chromatograph equipped with a sulfur specific flame photometric detector was used to measure sulfur species in the fuel rich gas samples. The GC system is by necessity a batch system; samples were taken in glass flasks and stored for subsequent analysis.

The gas chromatograph system is very complex and required a considerable effort in system set up, optimization, and calibration before measurements of real samples could be made.

The GC system used for these studies consists of a Perkin Elmer model Sigma 10 temperature programmable gas chromatograph equipped with a flame photometric detector and a gas sampling valve. An acetone washed porapac QS column 1/8' x 2 ft was used to separate the sulfur gases. The oven was temperature programmed to optimize separation and total analysis time. The system was tested with a mixture of sulfur species in air. Figure 8-8 shows the sample separation obtained with an actual sample, retention times, and optimized chromatographic conditions.

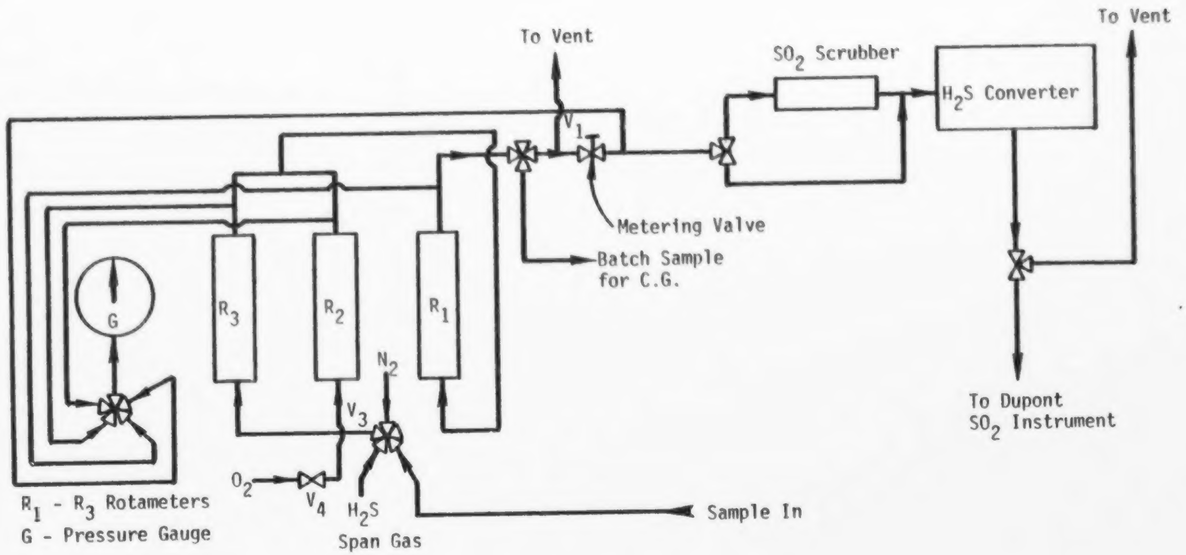

To Vent
V_1
SO_2 Scrubber
H_2S Converter
To Vent
Metering Valve
Batch Sample for C.G.
G
R_3
R_2
R_1
N_2
V_3
To Dupont SO_2 Instrument
O_2
V_4
H_2S Span Gas
Sample In
R_1 - R_3 Rotameters
G - Pressure Gauge

Figure 8-6. Sample Conditioning System for H_2S-Bearing Gases.

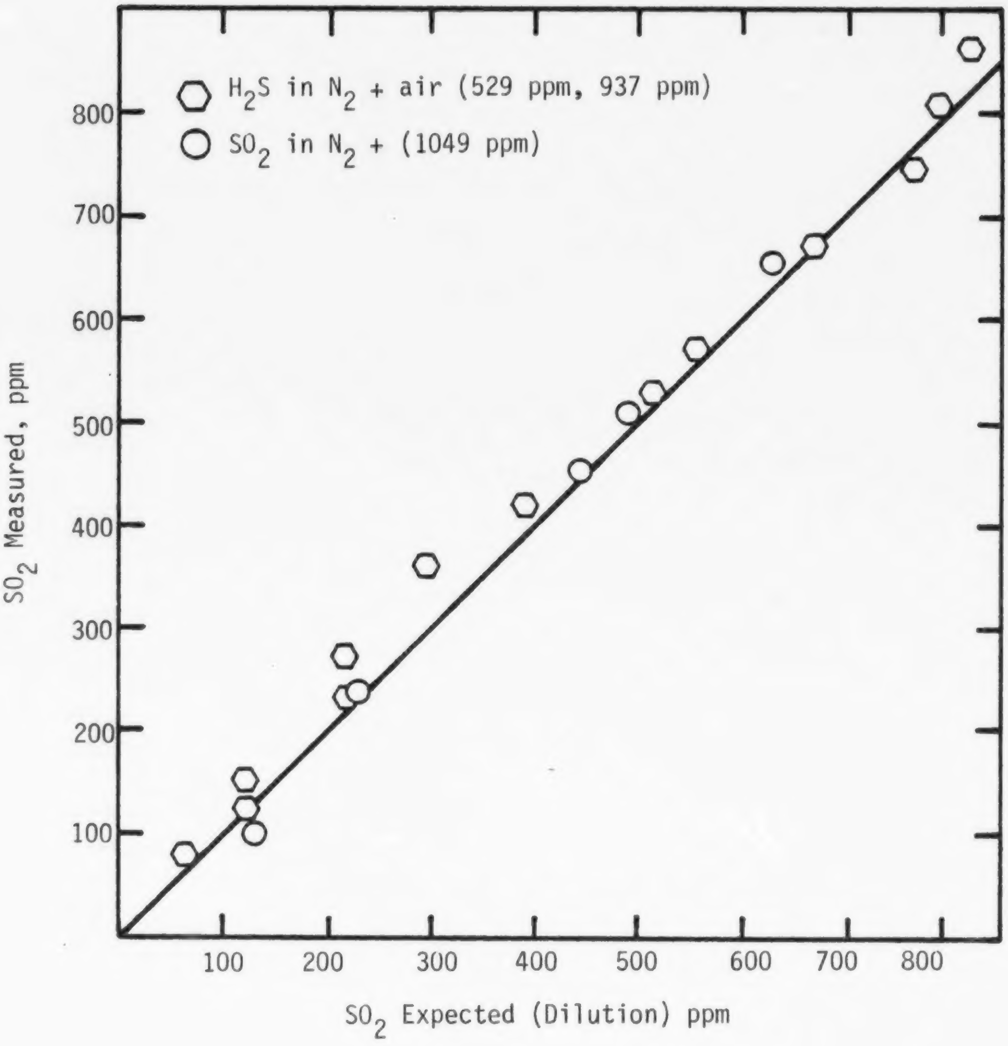

Figure 8-7. H_2S Measurement Verfication.

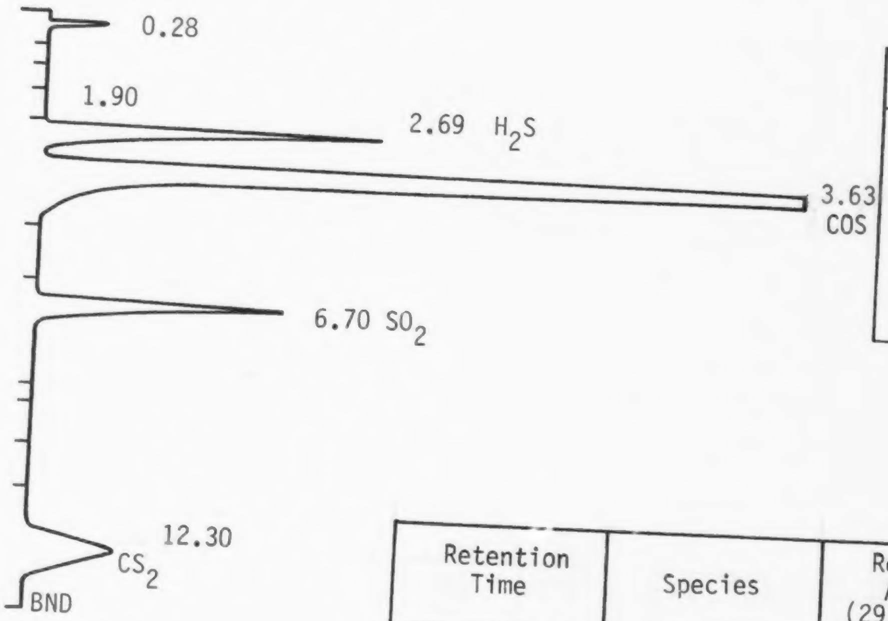

Chromatography Data
Pora pac QS, Acetone washed, 2' x 1/8" Teflon column; Temperature programmed He Carrier Gas at 30 cc/min

Retention Time	Species	Reduced Area (29.92" Hg)	ppm
2.69	H_2S	.896	16
3.63	COS	7.099	67
6.70	SO_2	.939	18
12.30	CS_2	.627	<1

Figure 8-8. Typical Gas Chromatogram of First-Stage Sample (Fuel Rich).

The flame photometric detector detects light emitted from sulfur as it is burned in a hydrogen/air flame. The detector response is approximately linear with the square of the mass flow rate of sulfur through the detector, but the response varies significantly among sulfur-containing compounds. Because the detector response is compound-dependent, calibration curves for each sulfur compound of interest had to be constructed. Furthermore, the gas chromotograph column-detector system was observed to absorb some sulfur at the beginning of test or calibration series if the system had not been exposed to sulfur-containing gases for several hours. This difficulty was overcome by injecting a standard gas mixture onto the column at least six times before sample gases were analyzed. The data shown in Figure 8-9 indicates that six injections of the gas mixture (H_2S was absorbed more than the other species) are sufficient to saturate the column before a test run.

The gas samples, either calibration gases or test samples, were injected under vacuum onto the GC column with a constant volume gas sample loop and sampling valve. The sample loop was evacuated, filled with sample, the sample pressure noted, and then the sample was injected onto the column (see Figure 8-10). The calibration standards were injected in the same manner as the test samples. The calibration curves were standardized to 29.92" Hg and the sample responses were corrected to the same basis.

The two H_2S/SO_2 measurements systems (GC and O_2 dilution and converter/scrubber system) were used to analyze several samples from the furnace and gave good agreement in most cases. A problem arose with the continuous H_2S system because a significant amount of the sulfur in the sample was unexpectedly COS, which is not quantitatively oxidized by the converter and therefore not measured with the continuous system. The converter could not be used to give data for a sulfur balance when significant amounts of sulfur were contained in the COS.

8.3 Solids Analysis

The measurement of physical and chemical characteristics of solid samples entering and withdrawn from the experimental systems was of key importance. Methods for the analysis of coal, ash, sorbent, and char samples were researched and developed. Some of the important characteristics of these solids (mineral composition of ashes, particle size distribution) were outside the range of

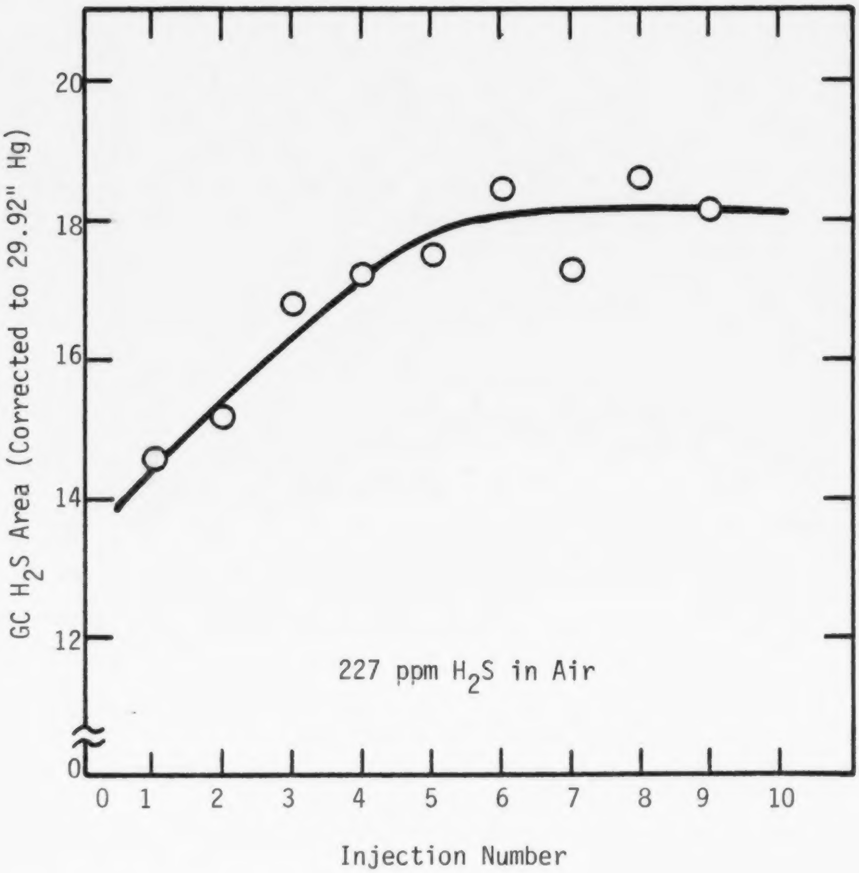

Figure 8-9. Retention of H_2S in GC System at Start-Up.

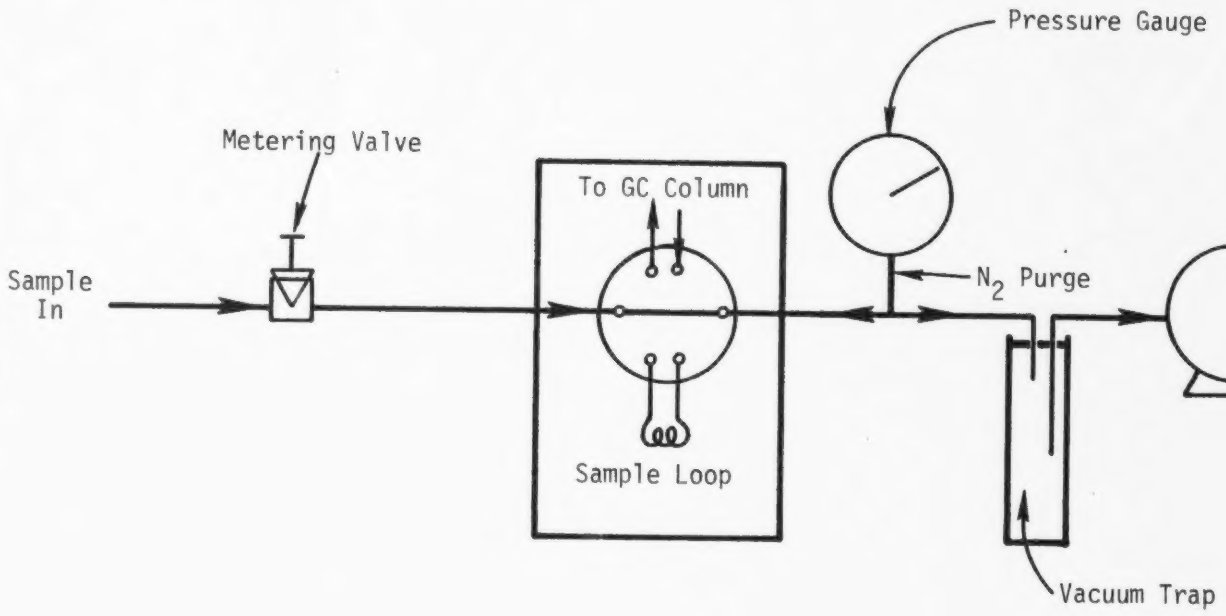
Pressure Gauge
Metering Valve
Pump
To GC Column
Sample In
N_2 Purge
Sample Loop
Vacuum Trap

Figure 8-10. Flow Diagram of GC Sampling System.

EER's analytical capabilities. These analyses, as mentioned ealier, were performed by an outside laboratory. In-house solids characterization abilities include: the measurement of carbon, hydrogen, nitrogen, sulfur, and oxygen (by difference) and ash content of coal or ash samples; the measurement of surface area of sorbent, coal, ash, or other particulate samples; the measurement of sulfur content of non-combustibles such as sorbent or ash samples.

Coal analysis for C, H, and N is done with a Perkin Elmer model 240 Elemental analyzer. The sulfur content of coal, ash and sorbents is measured using an instrument manufactured by LECO and will be discussed in some detail. Surface area is measured using an instrument manufactured by Quantachrome, Inc. and will also be described in detail.

The instrument used for measuring the sulfur content of solids was designed for combustible solids and had to be tested with sorbent and ash samples. This instrument burns the sample at high temperatures (>2400°F in an oxygen enriched atmosphere and measures the SO_2 evolved by light absorption in the infrared region. The instrument is equipped with an analytical balance and a microprocessor system which are used to convert the measured SO_2 content of the gases to equivalent weight percent of sulfur in the sample. Noncombustible solids, including calcium salts and coal ashes, require the use of a combustion accelerator to insure that all of the sulfur is evolved from the sample. Several combustion accelerators were tested, including V_2O_5, Al_2O_3, and MgO. V_2O_5 was the best for our applications.

Several standards were prepared to determine the accuracy of the methods developed. Calcium sulfate ($CaSO_4$), pure reagent grade, was mixed in known proportions (by mass) with pure, dry, unreacted calcium carbonate. The sulfur content of these standards was measured and compared to the expected sulfur content. These results are shown in Figure 8-11. There was good agreement between the measured and expected values of sulfur. Each point plotted is an average of at least six measurements. Blanks, containing pure $CaCO_3$ or $Ca(OH)_2$, were run before each measurement.

The surface area of the solid sorbent powders and of ash/sorbent samples from the furnace was determined by gas absorption using an instrument manufactured by Quantachrom, Inc. This instrument is based on the BET method, where

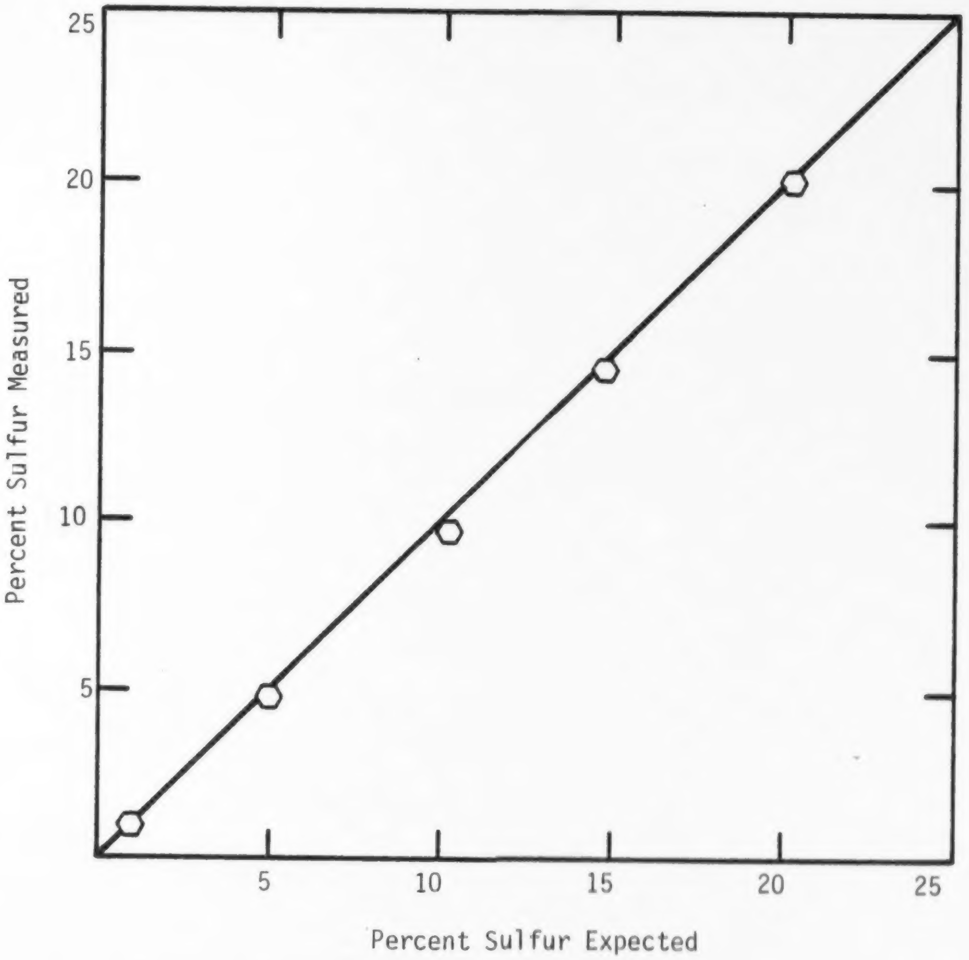

Figure 8-11. Calibration Curve for Known Sulfur Standards on LECO Analyzer.

surface area is related to the monolayer capacity of an adsorbent. The BET surface areas of porous and nonporous samples are conventionally determined from N_2 adsorption isotherms measured at $77^{o}K$. The instrument at EER is capable of doing single and multipoint BET surface area measurements with either N_2 or CO_2 as the adsorbate.

Sorbent or ash/sorbent sample surface areas are measured using a two point BET surface area with N_2 as the adsorbate gas. The two point method is sufficient because the solids behave in a very nearly ideal manner, and N_2 was used as the adsorbate because it is easier to use than CO_2 and to eliminate any possibility of a back reaction between CaO in the ash samples and CO_2 to form $CaCO_3$.

8.4 Temperature Measurement

The thermal environment experienced by the reacting coal/sorbent/sulfur group has a primary effect on the phenomenon observed including NO_x, SO_x and CO emissions as well as sulfur capture. Standard measurements of wall temperatures throughout the experimental systems were made with thermocouples embedded in the furnace walls (argon furnace) or projecting through the wall into the gas stream (BSF). Type S thermocouples with ceramic sheaths were used in the high temperature ($>2000^{o}F$) regions and type K thermocouples with stainless steel sheaths were used in the lower temperature regions.

Gas temperatures were measured with a ceramic shielded type S thermocouple in a suction pyrometer. The pyrometer was water cooled and equipped with an air driven asperator for suction. Figure 8-12 shows the pyrometer design.

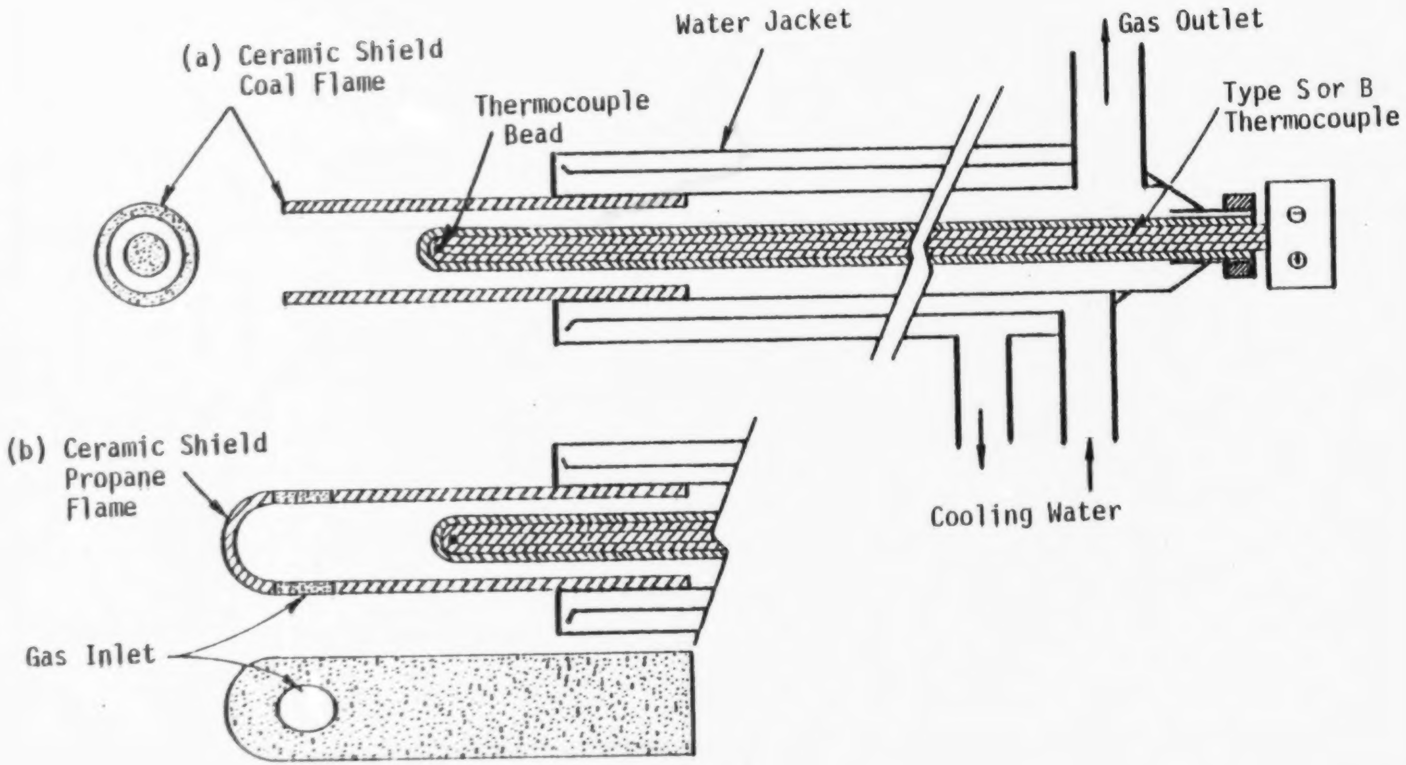
(a) Ceramic Shield
Coal Flame
Thermocouple
Bead
Water Jacket
Gas Outlet
Type S or B
Thermocouple
Cooling Water
(b) Ceramic Shield
Propane
Flame
Gas Inlet

Figure 8-12. Suction Pyrometer Schematic.

9.0 GAS-PHASE, PROGRAM-DEFINITION EXPERIMENTS

These experiments were designed to produce data defining the parameters which significantly affect the in-flame capture of sulfur by solid sorbents. The effects of various controllable combustion parameters were assessed using a sulfur-doped propane flame in a hot refractory-walled downfired furnace described in Section 7. The experiments were intended to establish which parameters were of interest and to define the experimental capabilities needed in the boiler simulator furnace.

The basic experimental scheme consisted of firing the furnace with propane/air at 50,000 Btu/hr using a diffusion burner. A sulfur additive, H_2S or SO_2, was metered into the burner either with the combustion air or the fuel as required by a specific experiment. Solid sorbent was injected at a known rate into the transport air; the sorbent type and feed rate was dictated by the experiment being performed. Specific alterations of the combustion conditions for each test are described below, along with the particular measurements required by each experiment.

9.1 Excess Air Experiments

The first set of experiments were done under excess air conditions with sorbent injected into the airstream of the diffusion burner. The parameters investigated included:

- Sorbent Effects
  - Composition
  - Particle size
  - Ca/S ratio
- Flame Effects
  - Excess air level
  - Furnace load
- Sulfur (Fuel) Effects
  - Sulfur species oxidation state
  - SO_2 concentration

Sorbent effects were assessed by injecting various sorbents including: 80 mesh limestone, <200 mesh limestone, <325 mesh lime $(CaOH)_2$, and mixtures of both lime and limestone with bentonite $(Al_2O_3\cdot</SiO\cdot H_2O)$. Figures 9-1, 9-2, and 9-3 show the effect of Ca/S on the sulfur capture for the three stones, 80 mesh $CaCO_3$, <200 mesh $CaCO_3$ and <325 mesh $Ca(OH)_2$. All of the data plotted were taken with SO_2 added at a firing rate of ~50,000 Btu/hr under excess air conditions, 4 - 8 percent O_2 in the flue. It is apparent that the finer particle sizes give better sulfur capture and that $Ca(OH)_2$ is a slightly better sorbent than $CaCO_3$. The best sulfur capture attained (for a "reasonable" Ca/S ratio of 4) was about 30 percent with the finely ground $Ca(OH)_2$ (see Figure 9-3).

The repeatability of the earliest experiments was poor; note the scatter in the data plotted in Figure 9-3. This scatter was probably due to uncontrolled fluxuations in solids feed rate. The solids feed system was improved by the addition of fluidizing air in the feed trough. This modification greatly reduced the scatter; the data plotted in Figure 9-4 were obtained on three different days under the same experimental conditions and show good coherence.

The effect of firing conditions on sulfur capture was assessed by firing under several furnace loads. The overall effect of furnace load was investigated by only changing the propane flow rate during an experiment while keeping all other parameters, air flow, solids feed, sulfur addition, sample location, etc. constant. This experiment gave data indicating (see Figures 9-5a, b) that furnace load has a significant effect on sulfur capture by both sorbents.

The method used to assess effect of load on sulfur capture resulted in a large variation in excess air level under the different firing conditions. In order to further define the load effect, and to eliminate the variation in excess air inherent in the approach described above, the effect of excess air on sulfur capture for two loads was determined. Figure 9-6 shows the data obtained at low furnace load (~32,000 Btu/hr). Under these firing conditions the excess air level had no apparent effect on sulfur capture. Figure 9-7 shows the data obtained by varying the excess air at medium furnace load (~48,000 Btu/hr). At this load air flow rate had a significant effect on sulfur capture. It is possible that this effect on sulfur capture is due to a change in furnace temperature (from the increased flow rate, decreased flame

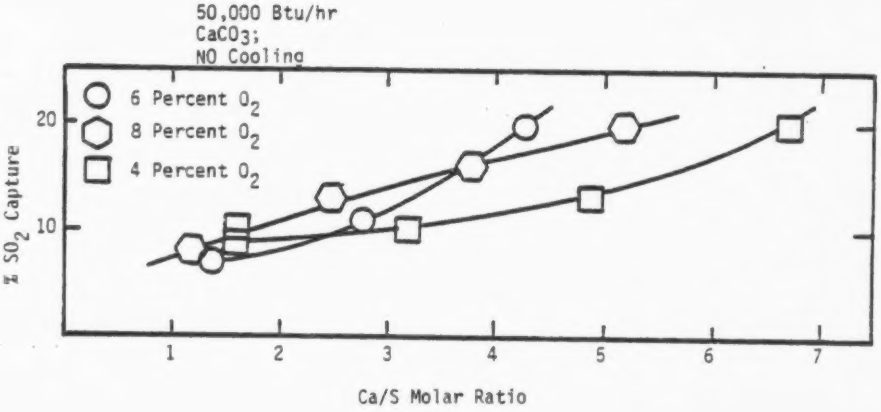

Figure 9-1. Effects of Sorbent Particle Size on Sulfur Capture, SO_2 as dopant, <80 mesh.

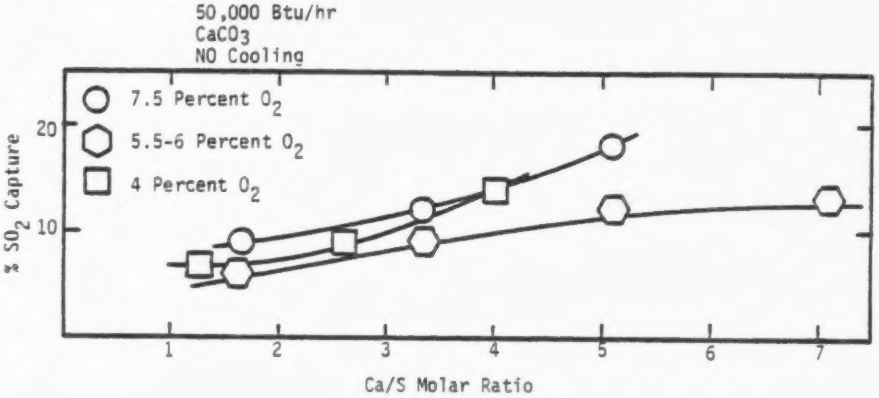

Figure 9-2. Effects of Sorbent Particle Size on Sulfur Capture, SO_2 as dopant, <200 mesh.

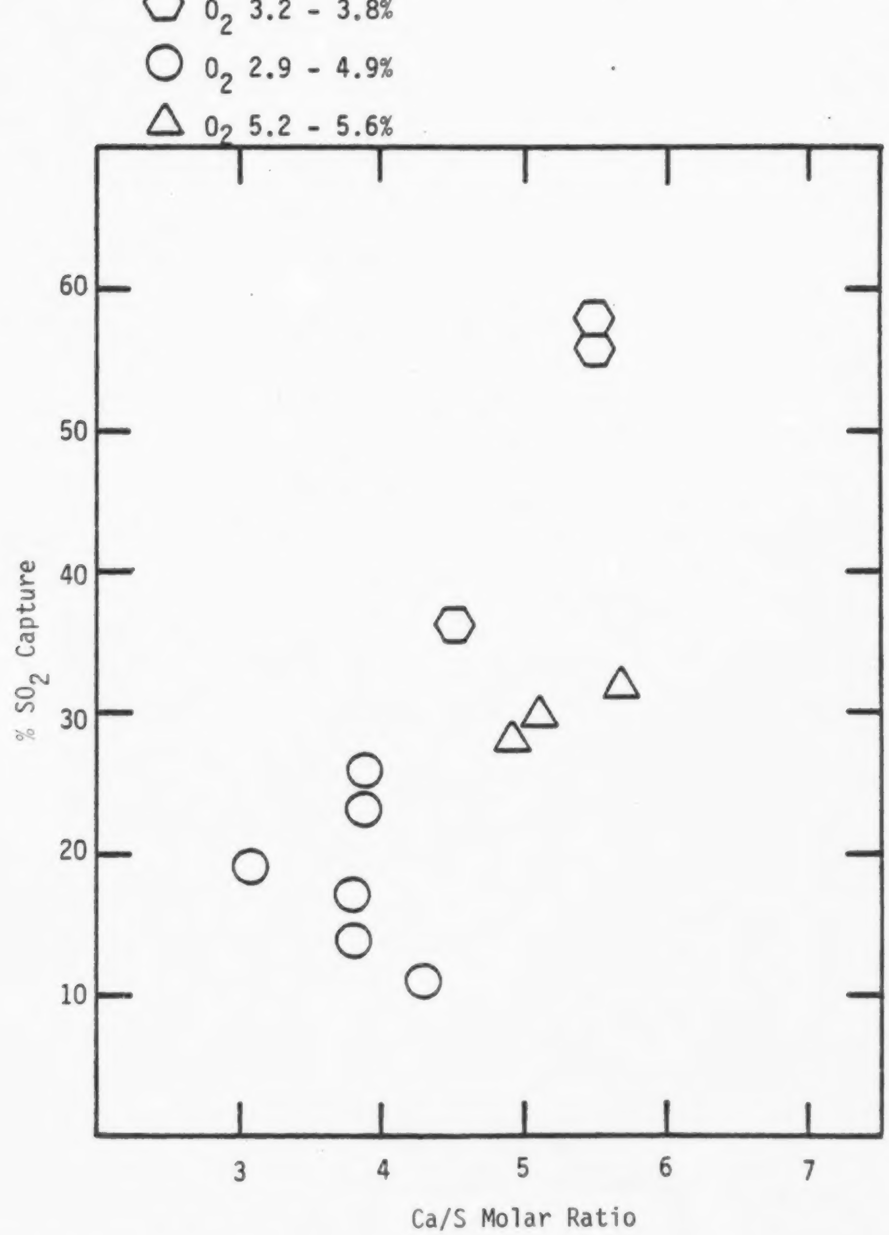

Figure 9-3. Effect of Ca/S Ratio on Sulfur Capture, ~46,000 Btu/hr, $Ca(OH)_2/Al_2O_3 \cdot 4SiO \cdot H_2O$, 50/50 Mix.

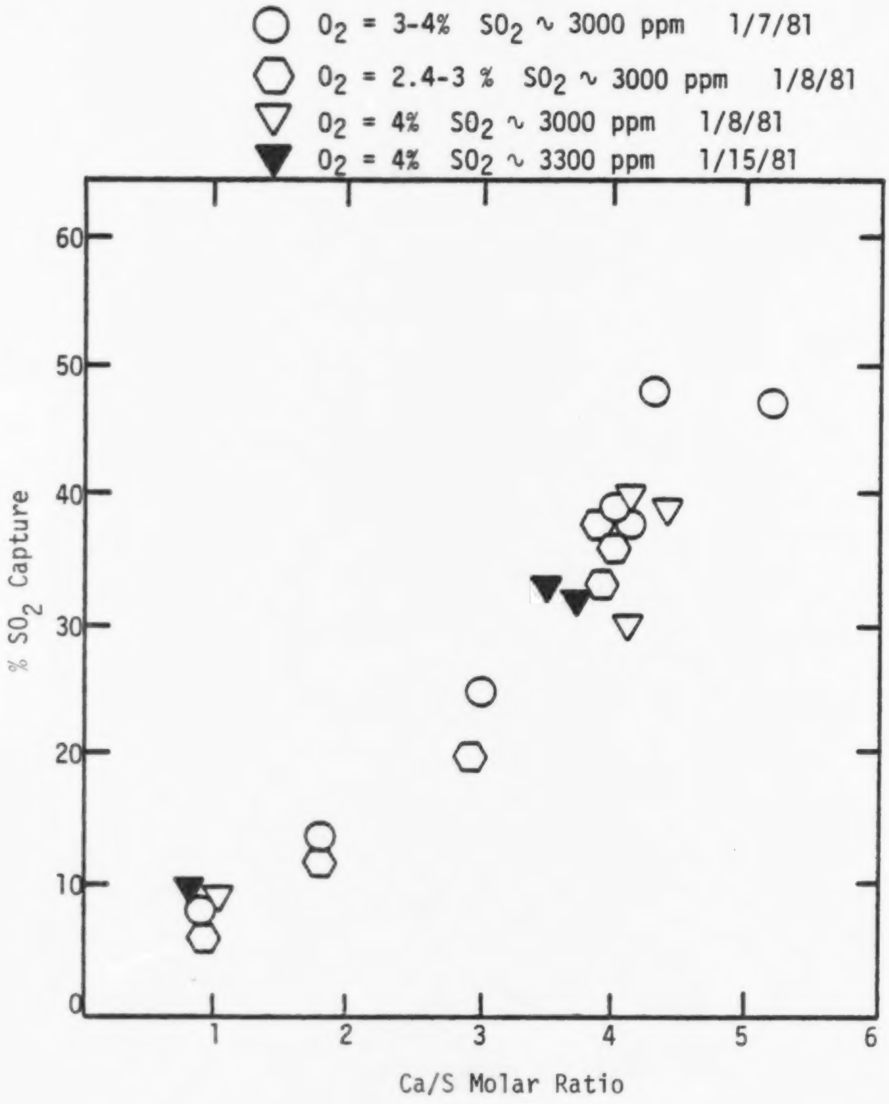

Figure 9-4. Effect of Ca/S on SO_2 Capture, 32,000 Btu/hr, P-Coal $Ca(OH)_2$.

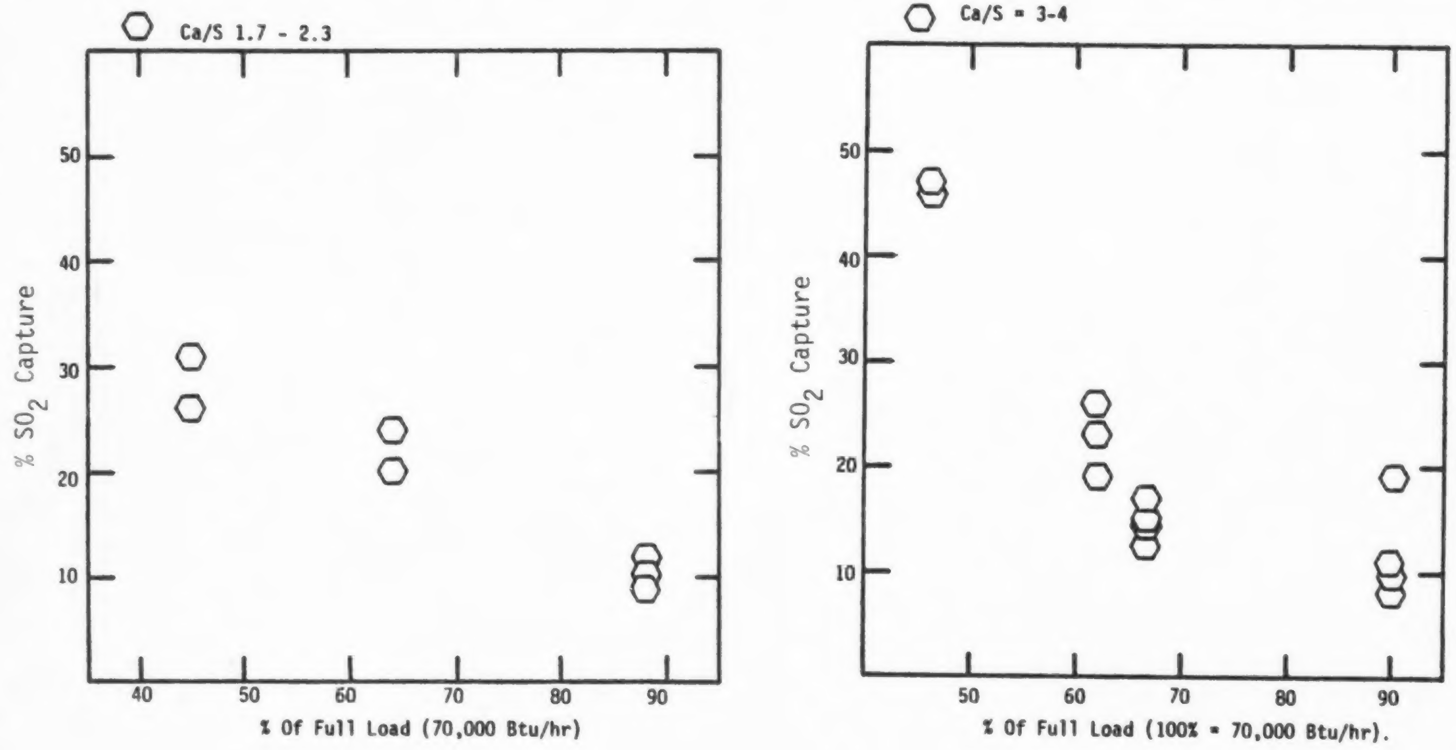

(a) $Ca(CO_3)$, SO_2 in ~4,000 ppm

(b) $Ca(OH)_2$

Figure 9-5. Effect of Furnace Load on Sulfur Capture.

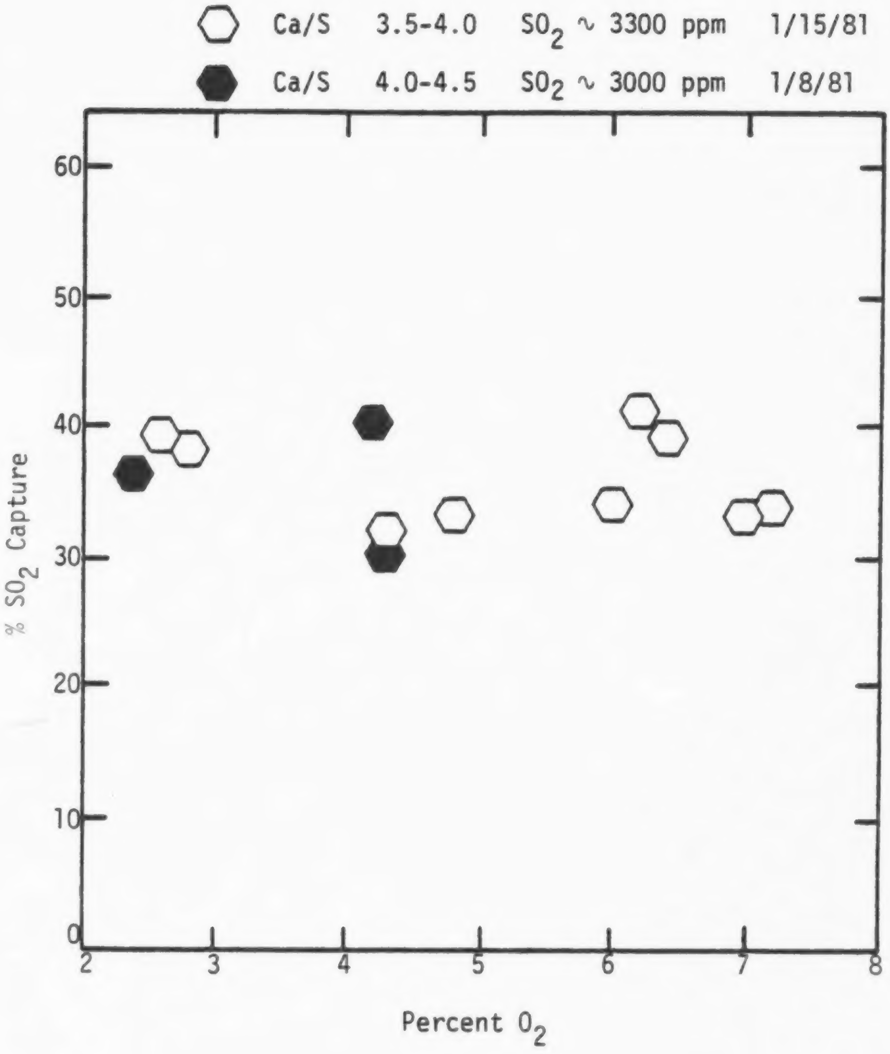

Figure 9-6. Effect of Excess Air on Sulfur Capture, 32,000 Btu/hr $Ca(OH)_2$.

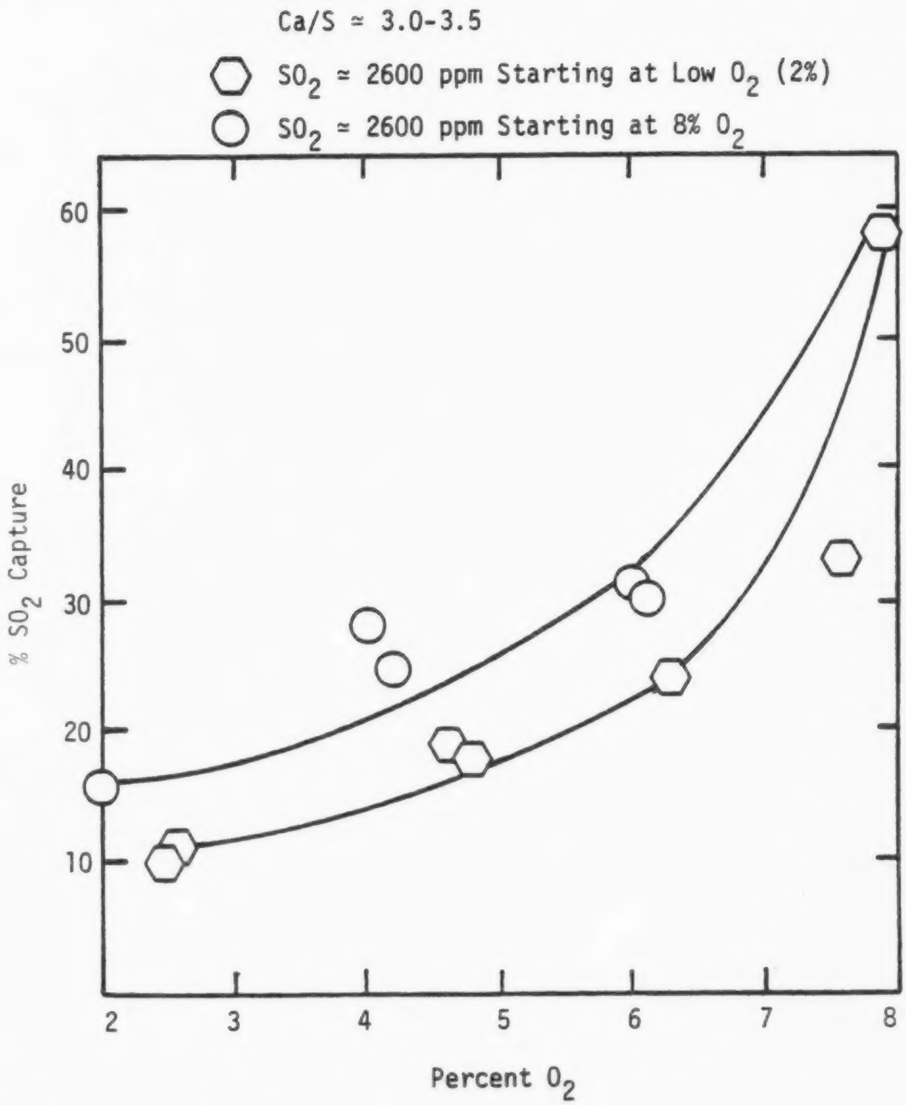

Figure 9-7. Effect of Excess Air on Capture, 48,000 Btu/hr, $Ca(OH)_2$.

temperature) rather than to increased oxygen availability. This explanation for the air effect is encouraged by the observed difference in the data taken while the air flow rate was increased (hot furnace at start) and the data taken while the air flow rate was decreased (cooler furnace at start).

The gas-phase experiments have indicated an effect on sulfur capture due to the flame. The cause of this effect is not rigorously defined but indications are that it is a time/temperature effect rather than an oxygen effect. More precise definition of this effect required a system with independently controllable temperature profiles and residence times; the Boiler Simulator Furnace is designed to be such a system.

Finally, under excess air conditions, the effect of various "fuel" parameters on sulfur capture was assessed. The effect of fuel sulfur type--oxidized or reduced--was determined by injecting either H_2S or SO_2 into the combustion air and measuring the sulfur capture at various excess air levels and constant calcium-to-sulfur ratio. The data plotted in Figure 9-8 show that, under excess air conditions, the input sulfur species oxidation state has no effect on sulfur capture.

The effect of fuel sulfur content on sulfur capture was investigated by varying the amount of SO_2 added to the combustion air. Figures 9-9 and 9-10 show curves constructed from data taken at various Ca/S ratios and various SO_2 concentrations but with constant firing rate and constant excess air. The data taken at the low load show a definite effect of SO_2 concentration on capture. The sulfur capture for a given calcium-to-sulfur ratio was higher for higher SO_2 concentration. The data taken at the medium load condition show the same effect but not as strongly.

Before staged combustion was initiated, the effect of sulfur "location" was determined. H_2S was added to both the combustion air and to the fuel for several firing conditions. There was no difference in the sulfur capture observed between the fuel additive and the air additive cases.

9.2 Staged Combustion

The effect of flame stoichiometry on sulfur solid-sorbent interaction was further investigated. Sulfur was added to the fuel was H_2S at the burner. Combustion was staged using a fuel-rich primary zone and adding second-stage

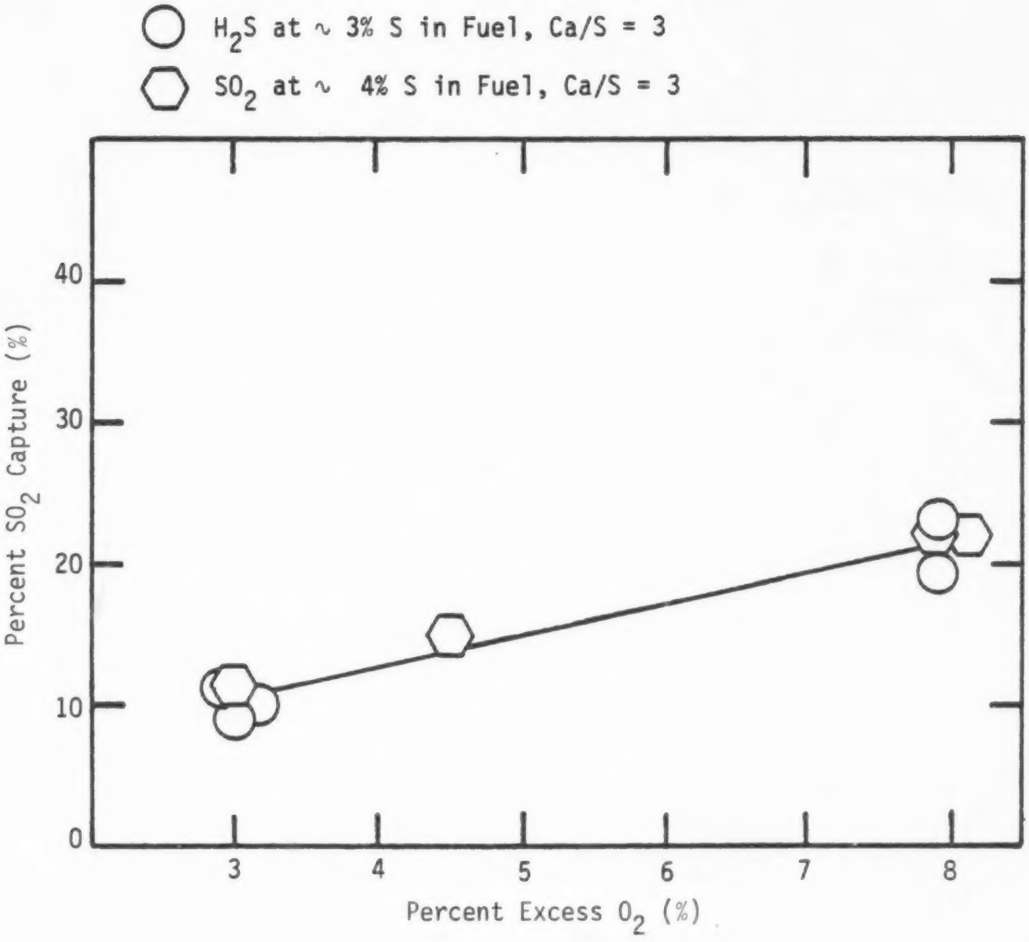

Figure 9-8. Effect of Input Sulfur on Sulfur Capture, Low Load (30,000 Btu/hr), $CaCO_3/Al_2O_3 \cdot 4SiO \cdot H_2O$ 50/50 Mix.

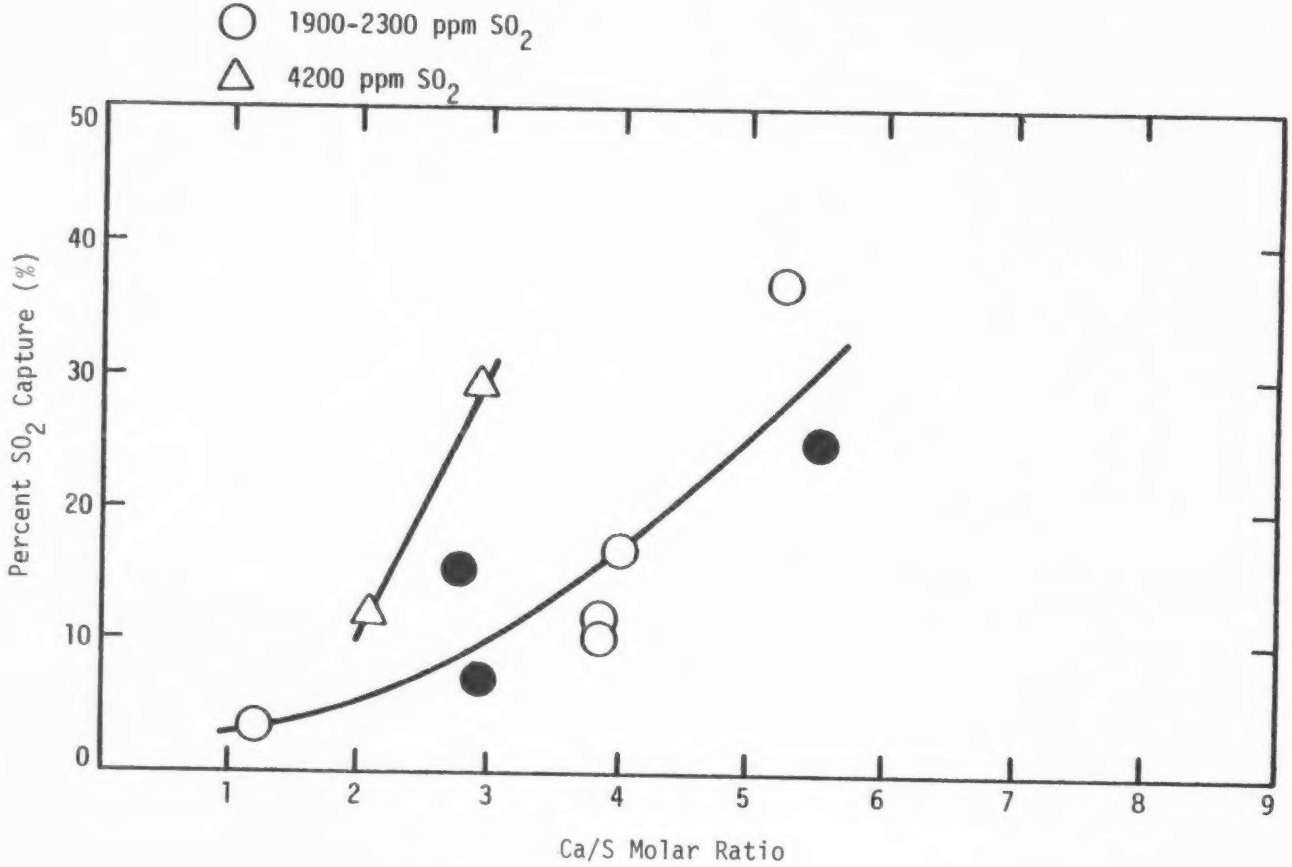

Figure 9-9. Effect of SO_2 Concentration on Sulfur Capture 4 Percent O_2, Propane at 32,000 Btu/hr, $Ca(OH)_2$.

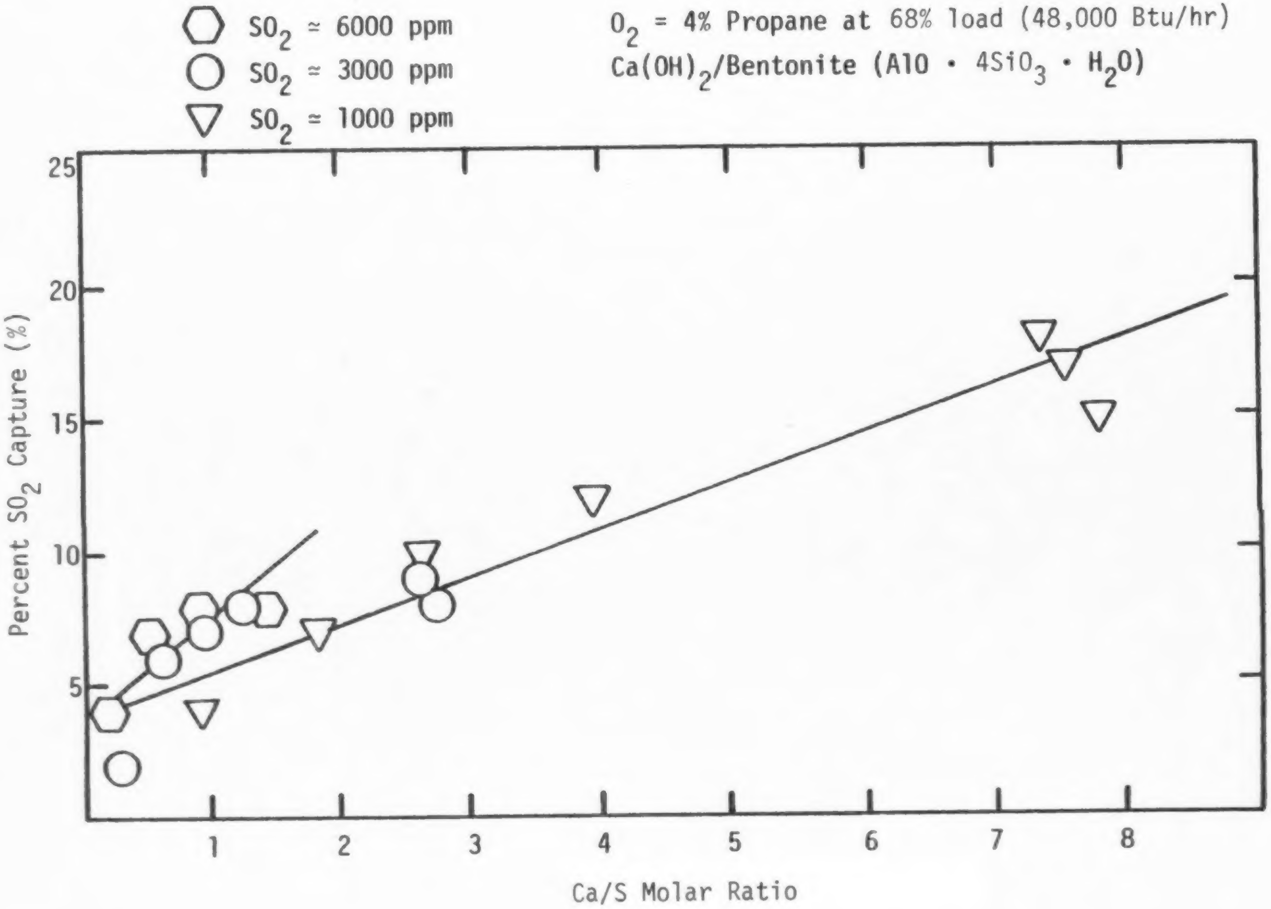

Figure 9-10. Effect of SO_2 Concentration on Sulfur Capture.

air to the furnace at a point approximately 45 inches below the burner. Primary zone stoichiometry was varied by changing the primary air flow rate. The overall stoichiometry was maintained at 4 percent excess O_2 in the flue.

The data plotted in Figure 9-11 indicate that primary zone stoichiometry had little effect on sulfur capture. The fuel-rich, reducing-atmosphere primary zone did increase sulfur capture slightly over excess air firing as can be seen from the data plotted in Figure 9-12. Staged combustion experiments were done with and without refractory choke separating the two combustion regions; the presence of this choke had little effect on sulfur capture (see Figure 9-13).

The effect of sorbent addition location upon sulfur capture was also investigated by adding the sorbent with the second-stage air. The addition of sorbent in the burnout zone, about 45 inches below the burner, gave a slight enhancement of sulfur capture (see Figure 9-14) even though the residence time of the solids in the furnace was less than half the solids residence time when added with the combustion air.

9.3 Sorbent Decomposition

Some investigation into the decomposition of sulfur containing solids was performed. The solids of interest, CaS and $CaSO_4$, are, respectively, the expected reaction products from fuel-rch and fuel-lean sorbent/sulfur doped flames.

Calcium sulfate was mixed 50/50 by mass with bentonite and added to the combustion air at the burner. SO_2 was measured at the furnace flue. The furnace was fired at 50,000 Btu/hr. Solid decomposition was calculated from the solid feed rate and the measured SO_2 concentration. The cacium sulfate did not decompose comletely when passed through the furnace. The greatest decomposition observed was 40 percent at 5 percent O_2 in the flue. Excess air rate had some effect on $CaSO_4$ decomposition. As can be seen from the data in Figure 9-15, increased excess air decreased $CaSO_4$ decomposition.

Calcium sulfide was also added to the furnace as a mixture (50/50 by weight) with bentonite. The experimental conditions were similar to those used for the $CaSO_4$ decomposition studies--excess air, 50,000 Btu/hr, solid added at the burner, SO_2 measured at the flue. Excess air level (for the

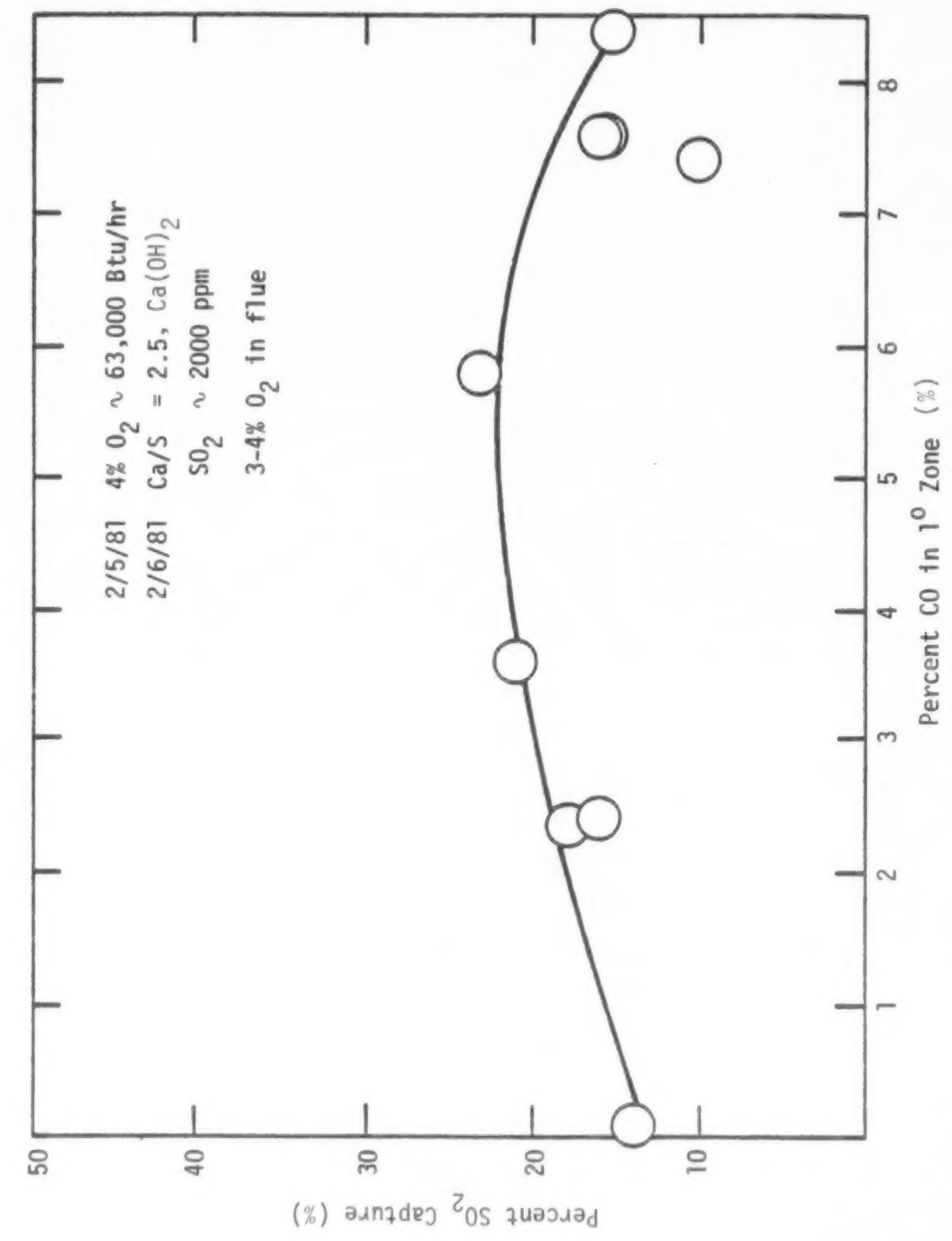

Figure 9-11. Effect of Primary Zone Stoichiometry on Sulfur Capture Staged Combustion.

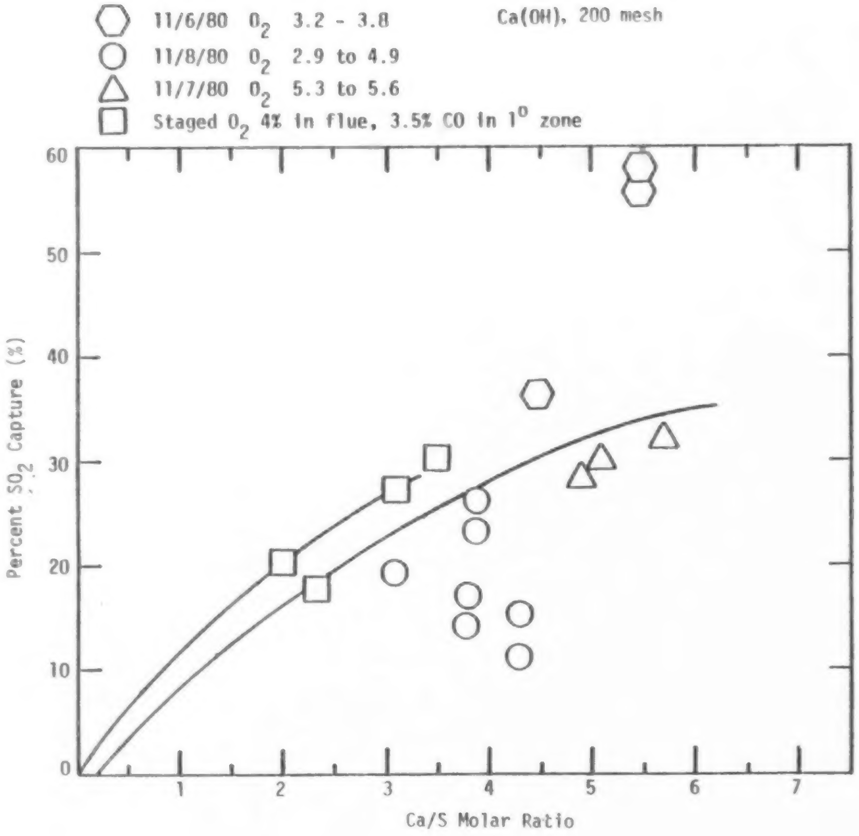

Figure 9-12. Effect of Staging on Sulfur Capture.

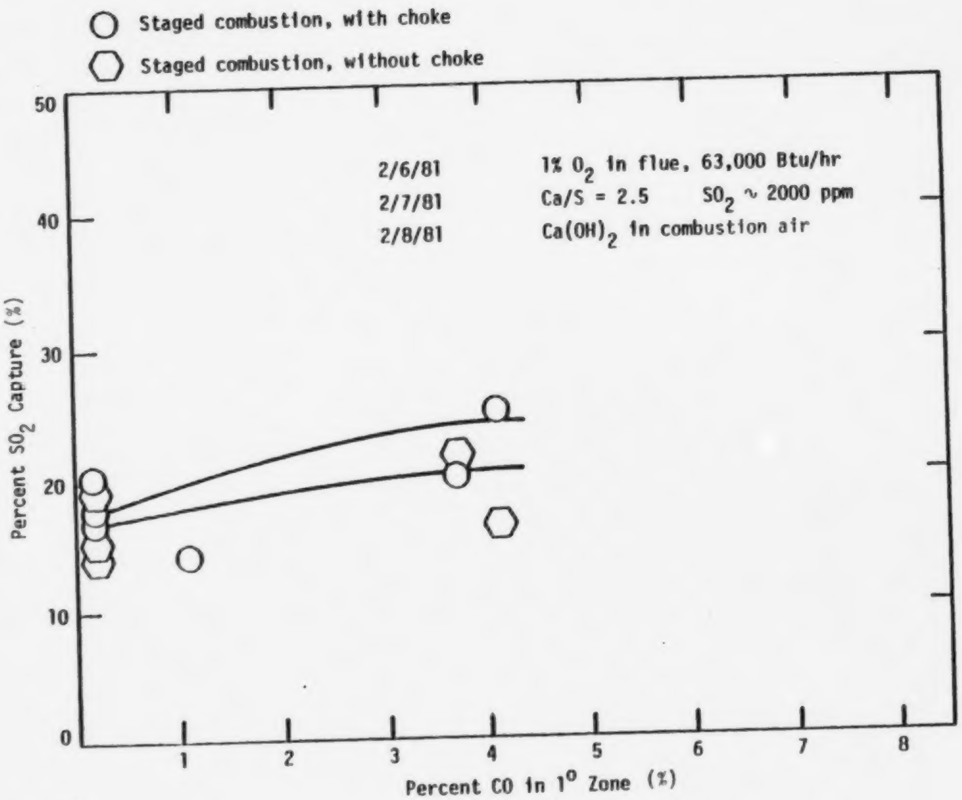

Figure 9-13. Effect of Choke on Sulfur Capture

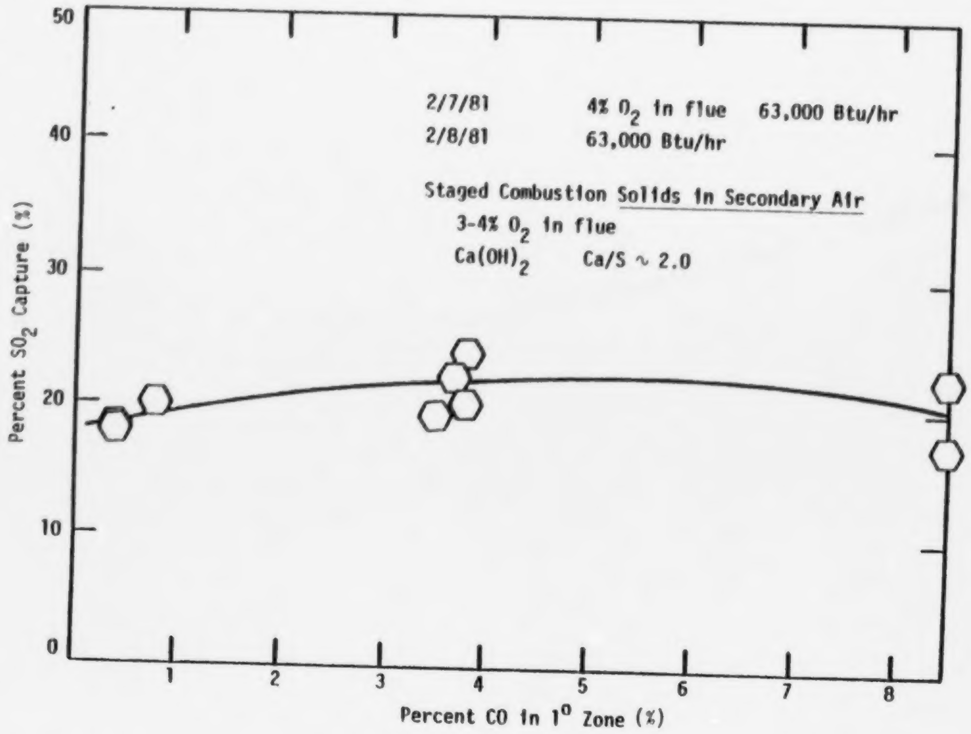

Figure 9-14. Effect of First Stage Stoichiometry on Sulfur Capture, Sorbent with Second Stage Air.

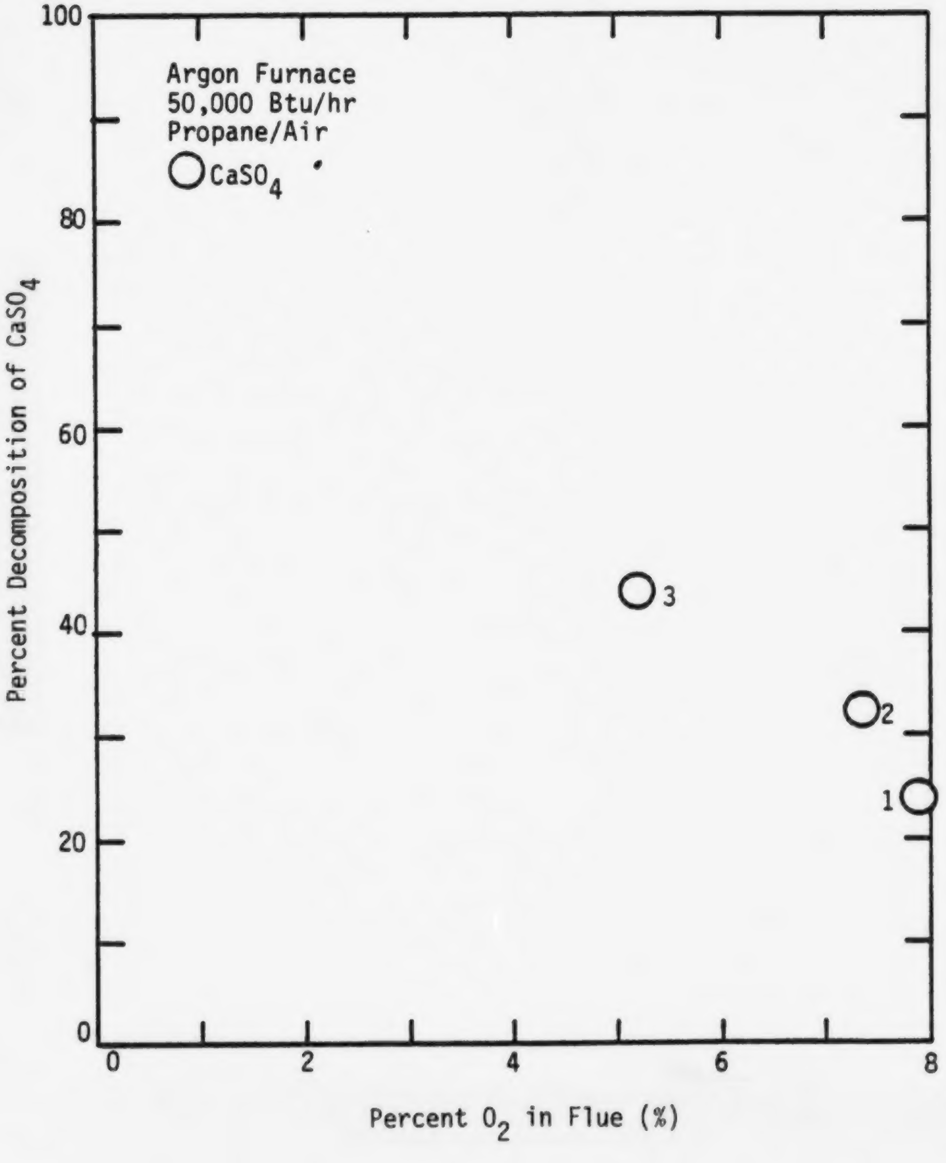

Figure 9-15. Effect of Excess Air on $CaSO_4$ Decomposition.

range investigated) had little effect on the decomposition of CaS in the furnace (see Figure 9-16).

Combustion air temperature had a slight effect on CaS decomposition (see Figure 9-17), CaS decomposition increased as air temperature increased.

The effect of SO_2 partial pressure was investigated by adding SO_2 to the combustion air, pulsing the CaS into the furnace at the burner and measuring the SO_2 concentration change at the flue. The SO_2 increase due to CaS addition was equal to the SO_2 measured for the same CaS feed rate without SO_2 added to the combustion air. This result indicates that SO_2 partial pressure has little effect on CaS decomposition under these conditions.

Water was added to the furnace at the burner during one of the CaS decomposition experiments. CaS decomposition was highest with water addition (70 percent decomposition) even though the furnace flue temperature dropped from 585 to 480^{o}F. This increased decomposition may have been due to a direct reaction between the solid CaS and water droplets right at the flame front. (CaS decomposes on contact with water.)

9.4 Equilibrium Considerations

Figures 9-18 and 9-19 show typical results of equilibrium sulfur species distribution calculations for propane/air/SO_2/$CaCO_3$ mixtures of various temperatures. Figure 9-18 shows fuel-lean distributions, and Figure 9-19 shows fuel-rich conditions. These calculations were also performed for several coals with similar results (see Figures 9-20, 9-21). the equilibrium calculations indicate that solid sulfur containing compounds are expected to decompose at flame temperatures, $CaSO_4$ being stable to temperatures around 2000^{o}F at SR=1.1 and CaS being stable up to 2700 at SR = .75.

The temperatures at which 50 percent of the sulfur may be found in the condensed phase at equilibrium for several coals and for propane are plotted against stoichiometric ratio in Figure 9-22. These results indicate that the solid phase is more stable under fuel-rich conditions.

Caution should be exercised in the interpretation of these results as equilibrium calculations do not adequately reflect the chemical kinetics actually occurring in a flame. The sharp drop in decomposition temperautre at SR = 1.0 may be a product of the rapid change in oxygen availability around

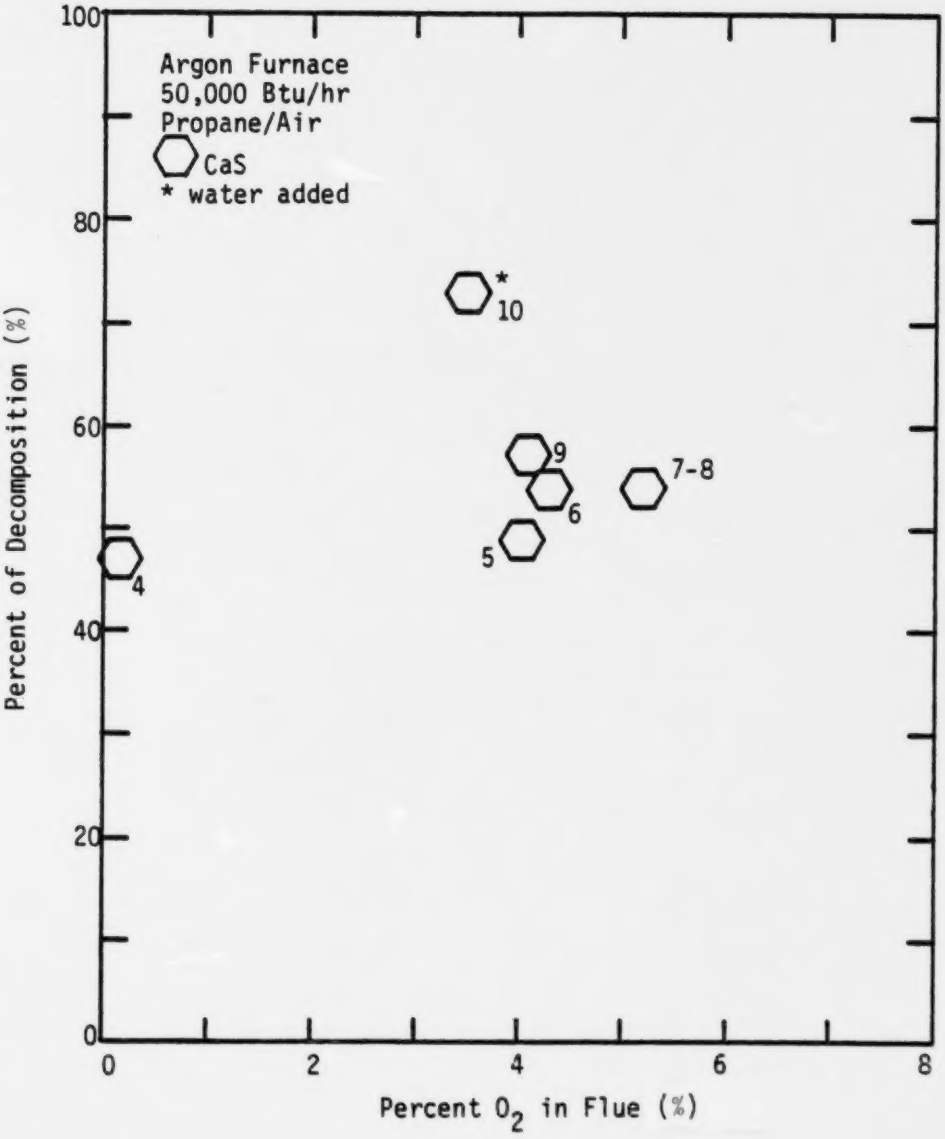

Figure 9-16. Effect of Excess Air On CaS Decomposition.

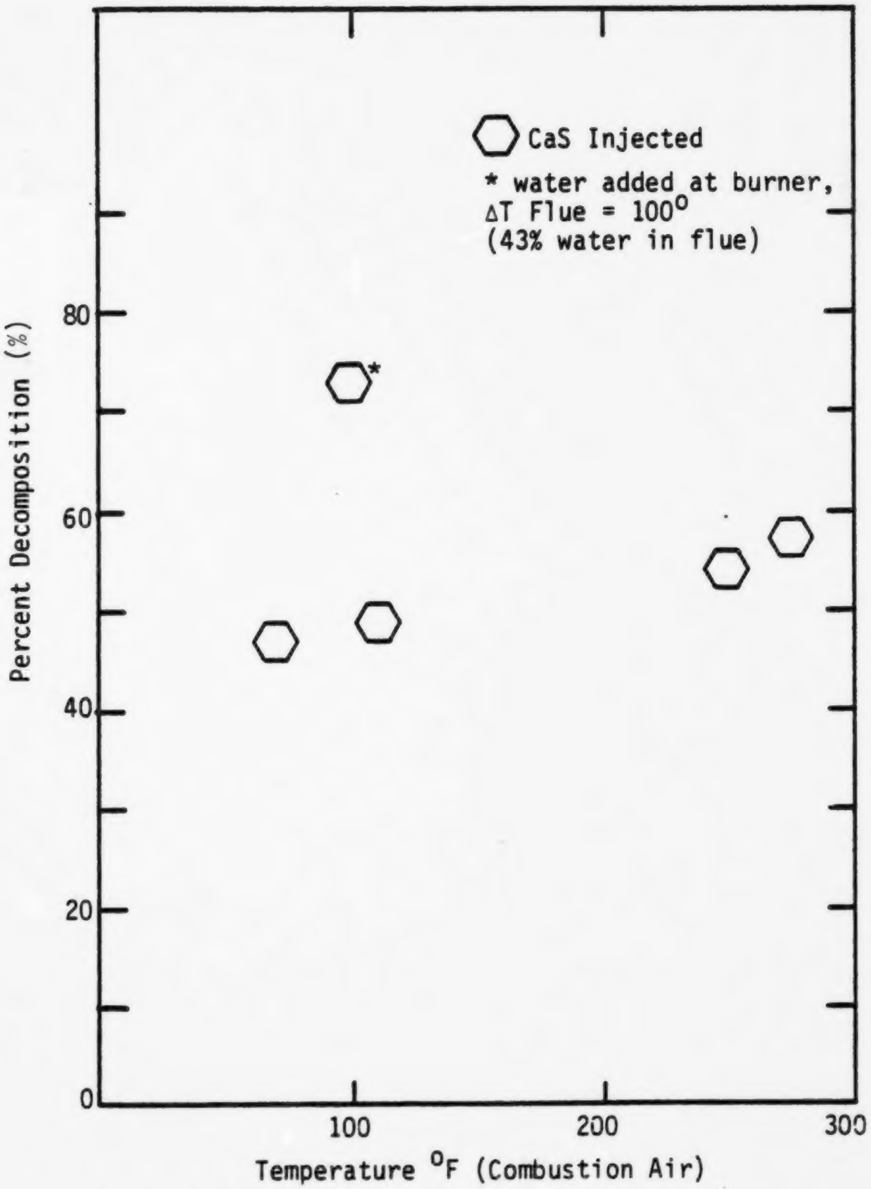

Figure 9-17. Effect of Air Preheat on CaS Decomposition, 50,000 Btu/hr.

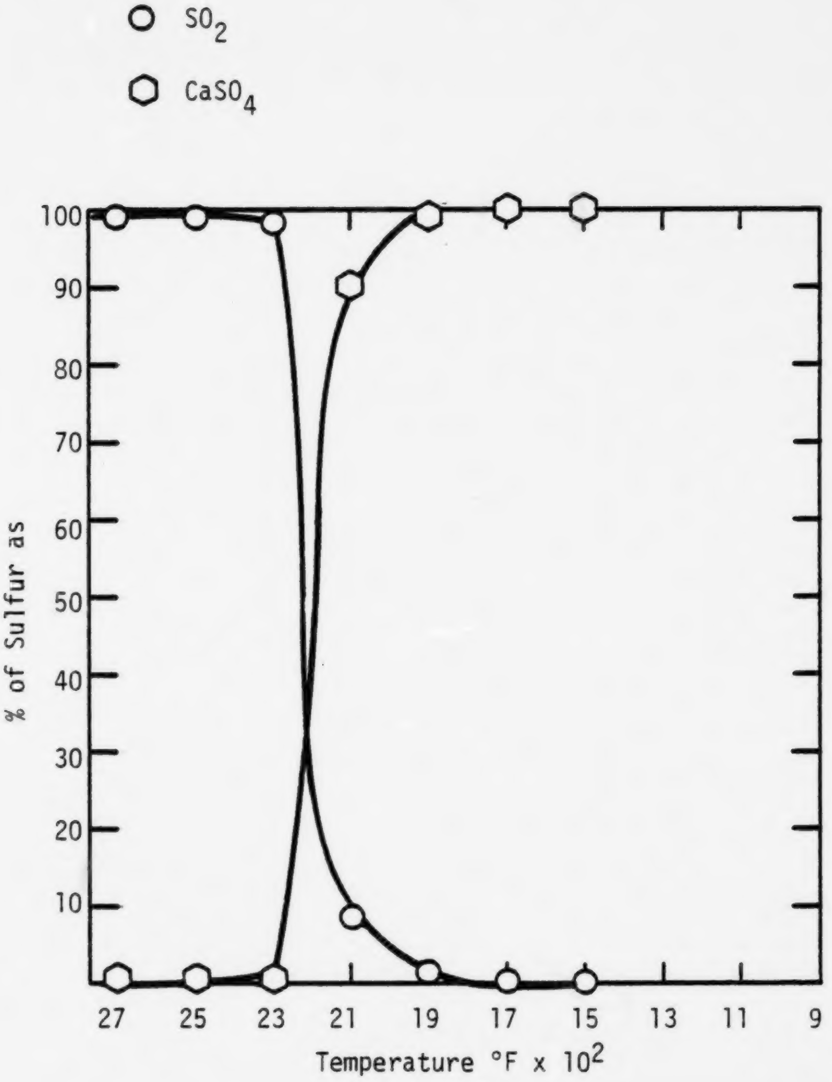

Figure 9-18. Equilibrium Sulfur Species Distribution, Fuel Lean Propane + H_2S + $CaCO_3$, SR = 1.20.

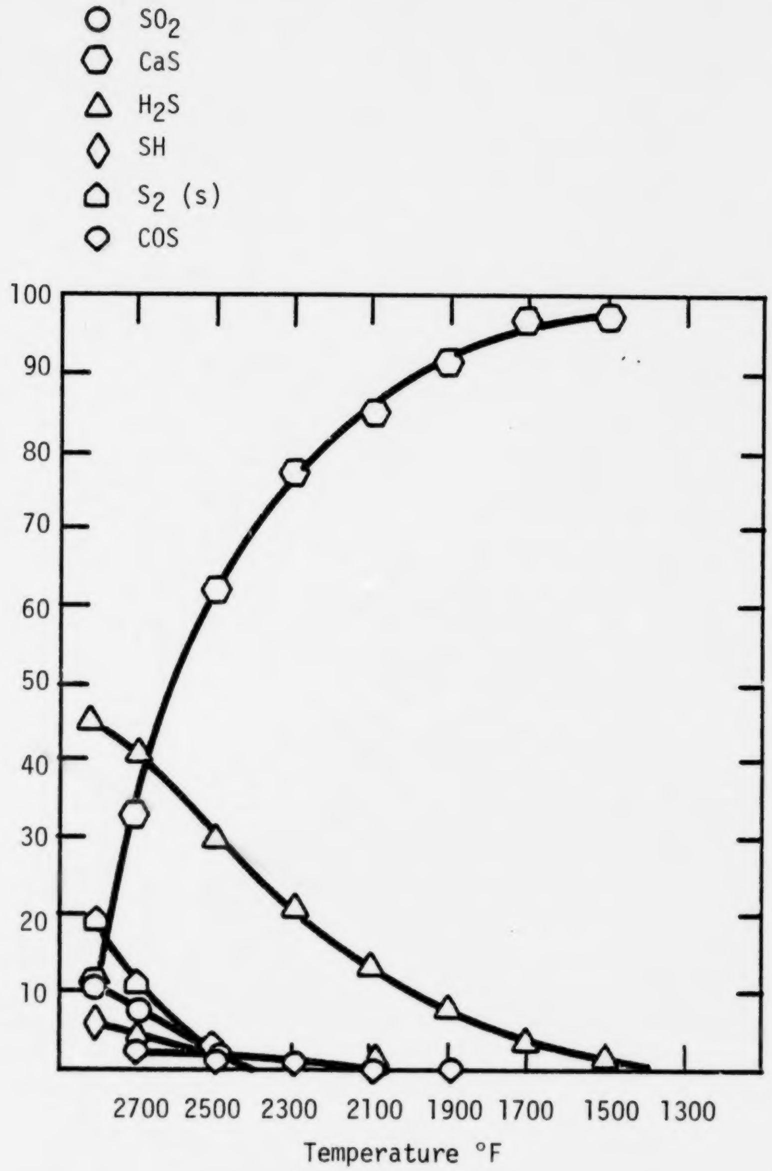

Figure 9-19. Equilibrium Sulfur Species Distribution, Fuel-Rich Propane - H_2S + $CaCO_3$, SR = 0.60.

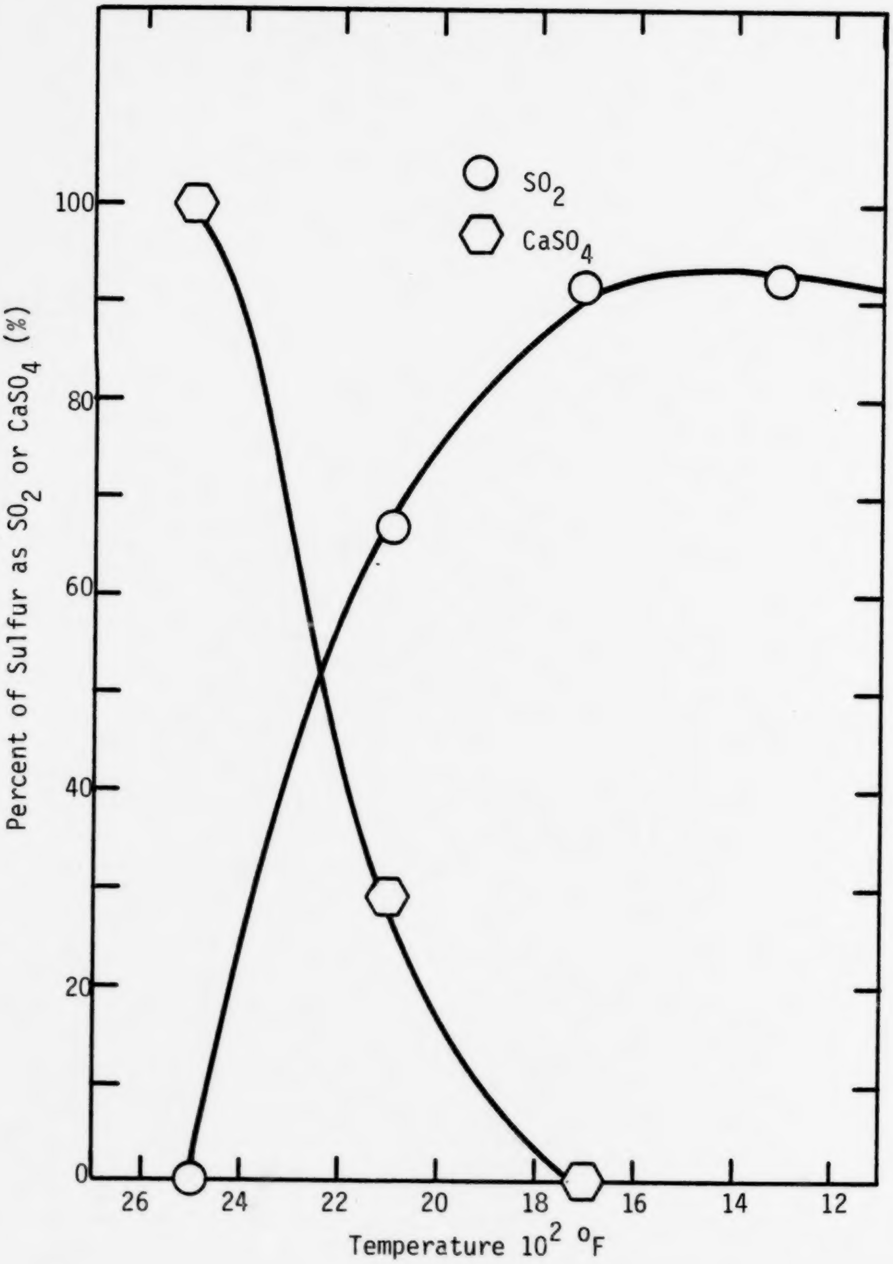

Figure 9-20. Equilibrium Calculations for Fuel Lean Sulfur Species Distribution, Lignite Coal + $CaCO_3$, Ca/S = 1.6, SR = 1.25.

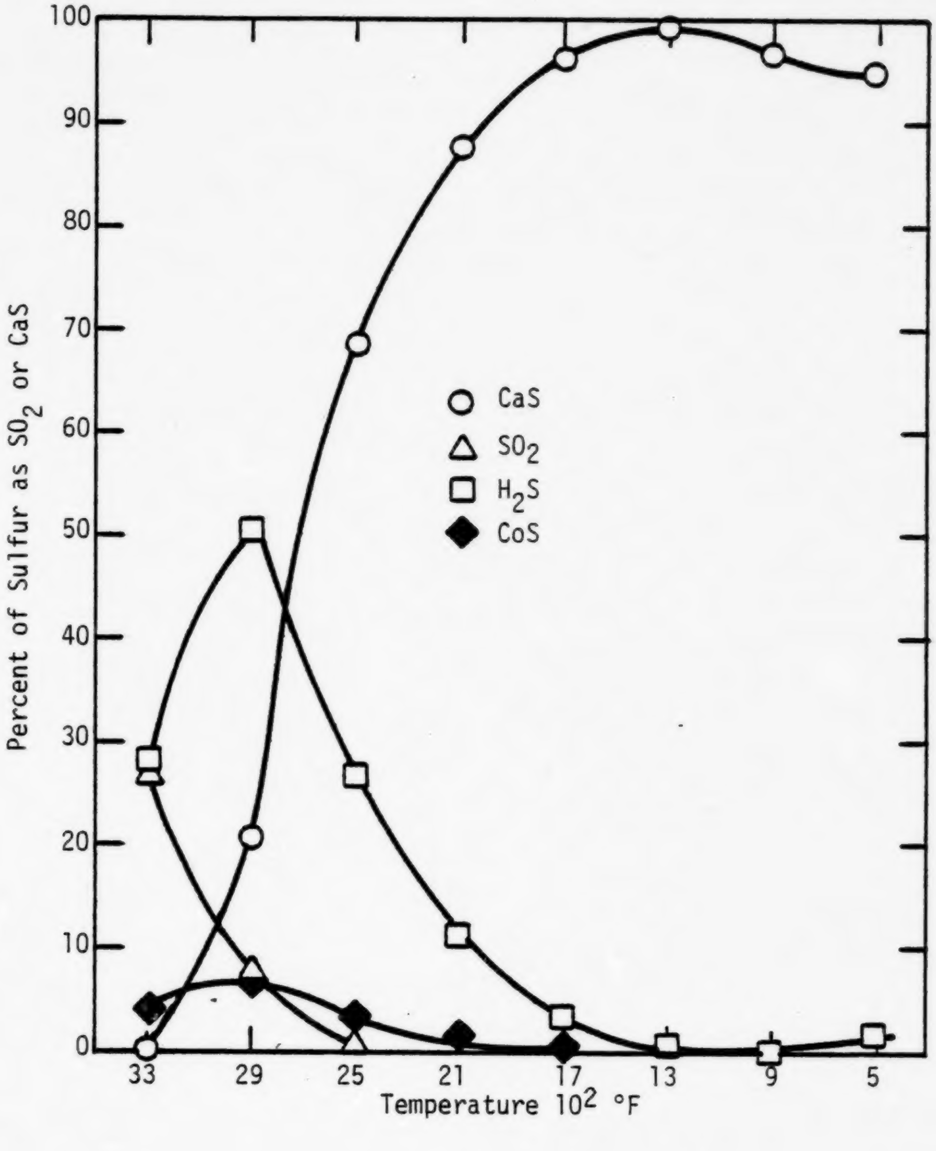

Figure 9-21. Equilibrium calculation for fuel-rich sulfur species distribution, lignite coal SR_1 =.50.

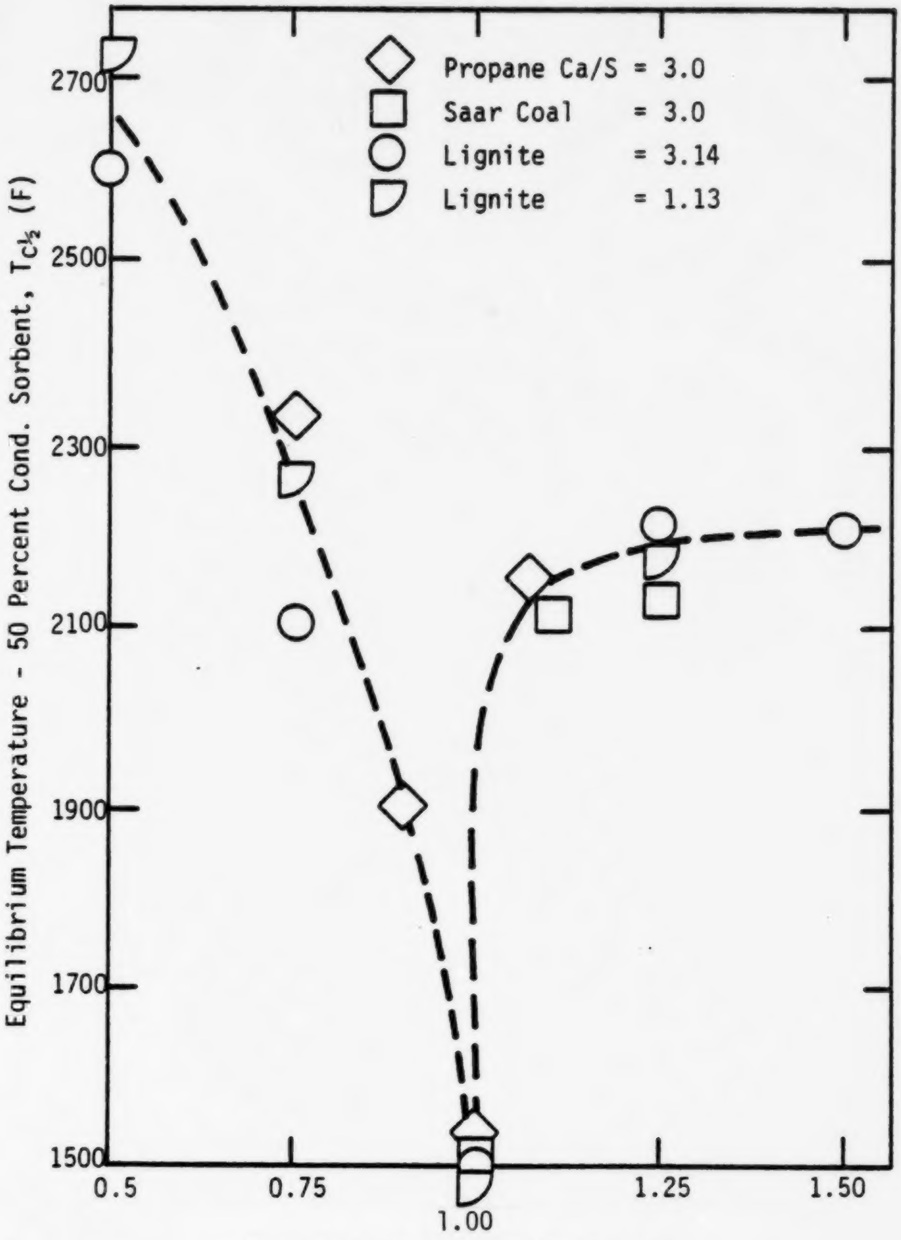

Figure 9-22. Equilibrium Temperature for 50 Percent Condensed Sulfur (CaS or $CaSO_4$) as a Function of Overall Fuel/Air Stoichiometry.

SR = 1.0 and may not reflect any condition which may actually be encountered in a flame.

9.5 Comparison With Available Models

The interpretation of the sulfur sorbent interaction data gathered in the gas-phase experiments may be aided by establishing a model of the observed results. The most appropriate existing model has been suggested by Coutant et al as an interpretation of results obtained in a similar experiment at the Battelle Columbus laboratories.

The experiments performed at Battelle were characterized by a mean reaction temperature (Tm) and residue time (t). The empirical model that resulted from their experiment is, on a molar basis:

$$\frac{SO_3 \text{ pickup}}{CaO} = .170\ SO_2{}^{.48}\ (i-e^{-kt}) \qquad (1)$$

where $k = \alpha - B/Tm;$ (2)

k was deduced from regression of the data.

This correlation was applied to some of the data obtained in the argon furnace. The normal operating conditions of the furnace gave residence times and mean temperatures (1-2 sec and 2200-2600^{0}F, respectively) which, when used in the rate expression, reduces the $(i-e^{-kt})$ term in Equation 1 to 1.0 essentially eliminating the time temperature dependence of the rate equation. Therefore, Equation 1 was reduced to, in terms of sulfur capture:

$$\text{Percent capture (sulfur)} = .170\ SO_2{}^{\frac{1}{2}}\ \frac{Ca}{S} \qquad (3)$$

This model of sulfur capture, with capture as a function of Ca/S ratio and SO_2 concentration only, was applied to some of the data obtained in our experiments with the argon furnace. The comparison of observed capture with predicted capture (from Equation 3) is shown in Figure 9-23. The straight line is the capture predicted from Battelle's model. The best capture data asymptotically approach the capture predicted by Battelle's model.

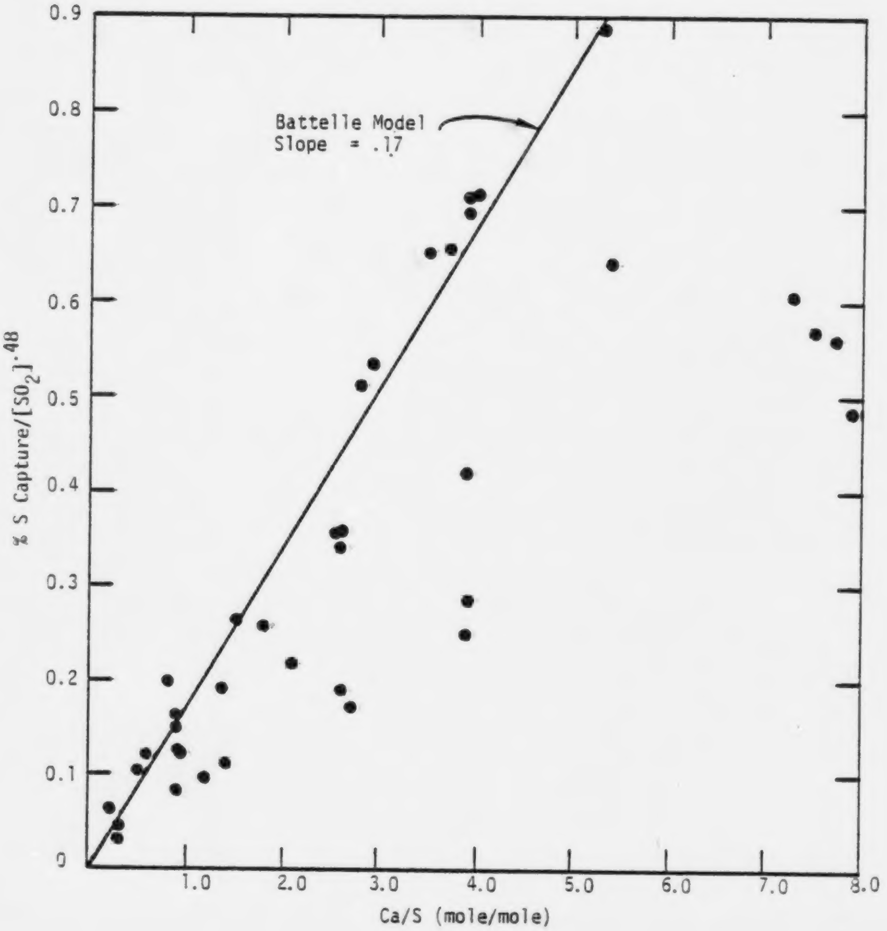

Figure 9-23. Percent Sulfur Capture, Normalized by SO_2 Concentration as a Function of Calcium-to-Sulfur Ratio. Argon Furnace Fired with Propane and Air.

10.0 PULVERIZED COAL FIRED EXPERIMENTS

The effect of sorbent injection on SO_2 emissions from several small scale coal fired furnaces was investigated. This section describes results obtained in three different facilities. Section 10.1 describes preliminary experiments performed in two facilities fired at 70,000 and 100,000 Btu/hr. The results from these experiments were used to plan the more extensive work in the Boiler Simulator Furnace. Section 10.2 contains the results and a discussion of the experiments performed in the Boiler Simulator Furnace.

10.1 Pulverized Coal Fired Experiments, Small Scale Furnaces, Preliminary Results

The effect of dry sorbent injection on SO_2 emissions from several coals has been investigated in two different small scale facilities. Preliminary investigations were performed in the small tunnel furnace (described in Section 7.1.2) and in the small convective furnace (described in Section 7.1.3). The experiments performed in these furnaces were exploratory in nature and were performed while the BSF was being built. The results were used to direct the investigation planned for the larger and more versatile BSF. No specific conclusions could be drawn from these studies.

10.1.1 Inherent-Capture Studies

During the NO_x fuel screening studies portion of this contract routine measurements of SO_2 emissions for the various coals were made. SO_2 emissions from the coals burned were seldom as great as would be measured for 100 percent conversion of the fuel sulfur. Figure 10-1 shows the sulfur retention (inherent capture) of the various coals as a function of coal sulfur content. There is no direct correlation between fuel sulfur and sulfur retention for the coals burned. An attempt was made to correlate the inherent-capture data with the coal ash content, including calcium, magnesium and iron content with little success. Gronhovd (ref 9) has developed a correlation of ash composition with sulfur retention for several North Dakota lignites from in-stack SO_2 measurements. This correlation:

$$\text{Percent of input sulfur emitted} = 110.0 - 12.7\,\frac{CaO}{Al_2O_3} - 48.1\,\frac{Na_2O}{SiO_2}$$

has been applied to experimental data obtained by Brown et al. (ref 10) in a pilot-scale research boiler at CCRL with good results. However, this correlation

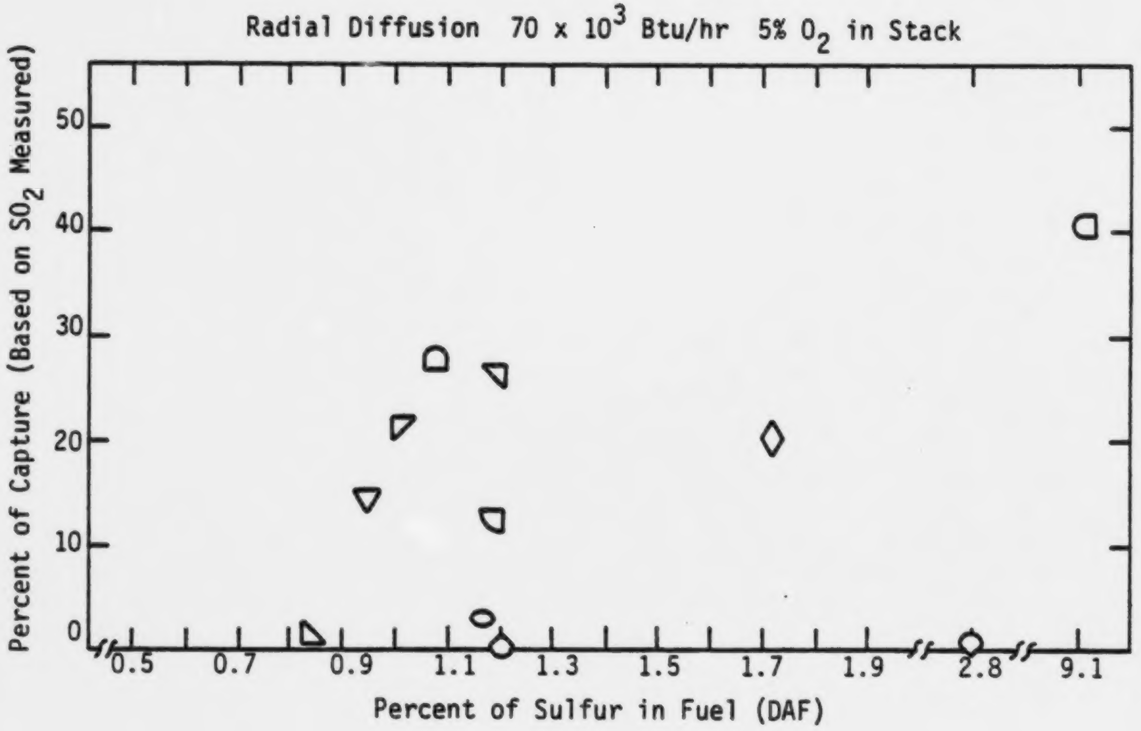

Figure 10-1. Inherent Capture as a Function of Sulfur Content.

appear to be inapplicable to the variety of coals burned in the Argon furnace (see Table 10-1). The only coal which exhibited inherent capture similar to that predicted was the Texas lignite.

10.1.2 Sorbent Addition Studies

The effect of limestone addition on the SO_2 emissions of two coals was investigated. The two coals, Utah 1 and a German brown coal designated KH5, were pulverized with limestone. Both coals were burned in two furnaces (described in Section 7), the Argon furnace and a furnace with a cooled convective section following the radiant section. SO_2 in the flue was measured at various excess air levels and ash samples were taken from the flue of the second furnace after the convective section. The sulfur content of ash samples from the convective furnace was measured. The sulfur content of each coal was measured after pulverization. This measured sulfur concentration was used to predict the SO_2 emissions from combustion by assuming that all the sulfur was converted to SO_2. The expected SO_2 level was 625 ppm for both coals. Figure 10-2 shows a comparison of the SO_2 measured (in the furnace with the convective sections) with the expected SO_2, calculated from the Utah coal sulfur content. The open symbols are for the ratio of SO_2measured to SO_2 expected, the closed symbols include the sulfur content of the ash (as equivalent SO_2 concentration) in the SO_2-measured to SO_2-expected ratio. Theoretically, the ratio of SO_2 measured, including the ash sulfur content, to SO_2 expected is 1.0; therefore, the closer the ratio to 1.0 the better the sulfur mass balance; sulfur mass balances for conditions where ash samples were taken were accaptable. Comparison of the data in Figure 10-2 for coal with and without added calcium indicates that the added calcium results in a decrease in SO_2 in the gas-phase and an increased retention of sulfur in the solid (reflected in a large difference in total S measured and SO_2 measured), especially at high excess air levels.

The data in Figure 10-3 show the ratio of SO_2 measured when firing coal with sorbent added to SO_2 measured when firing coal without sorbent addition as a function of excess air level (or percent O_2 in the flue) for the Argon furnace fired at two loads. (A ratio of SO_2 with Ca/SO_2 without Ca of 1.0 implies no sulfur capture, while a ratio of 0.50 implies fifty percent capture, etc.). Both coals gave better sulfur capture at lower loads.

Table 10-1. Inherent Capture Data

Coal	Symbol	% Capture	% Sulfur	% Calcium	% Iron	Predicted Capture
Rosa	∩	28	1.04			
Hardin	◹	26	1.04			
Farmington	◸	22	1.03	.66	.60	0
Shell, Texas	◡	12	1.02	1.70	.63	7
Colstrip	▽	14	0.63	.89	.10	1
Utah II	◺	2	.76	.33	.24	0
Gauley Eagle, W.Va.	⬭	3	.84			
Cadiz, Ohio	ᗡ	41	7.40	.02	2.92	0
Elkay	◇	1	2.47			
German Brown	☒	19	0.51	1.08	.55	9

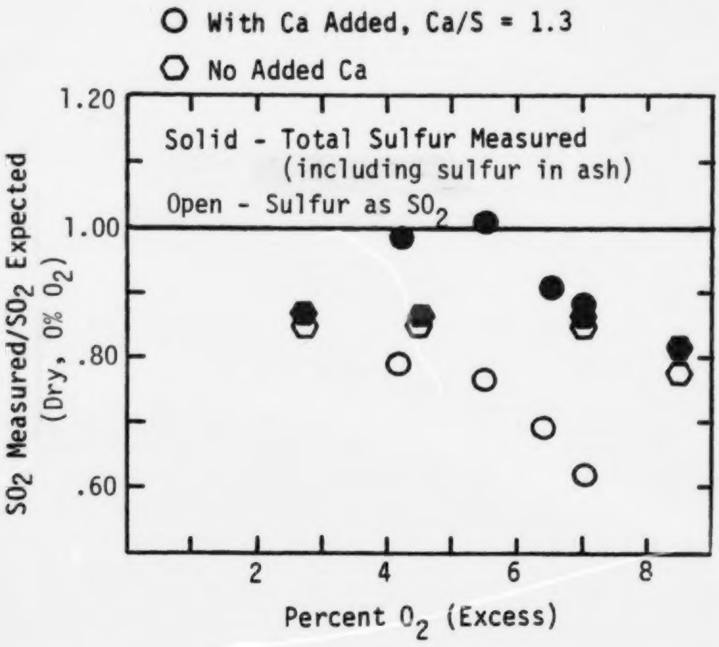

High Firing
Sulfur Balance/Capture
Convective Furnace 70,000 Btu/hr
Utah 1 Coal

Figure 10-2. Sulfur Balance, Convective Furnace.

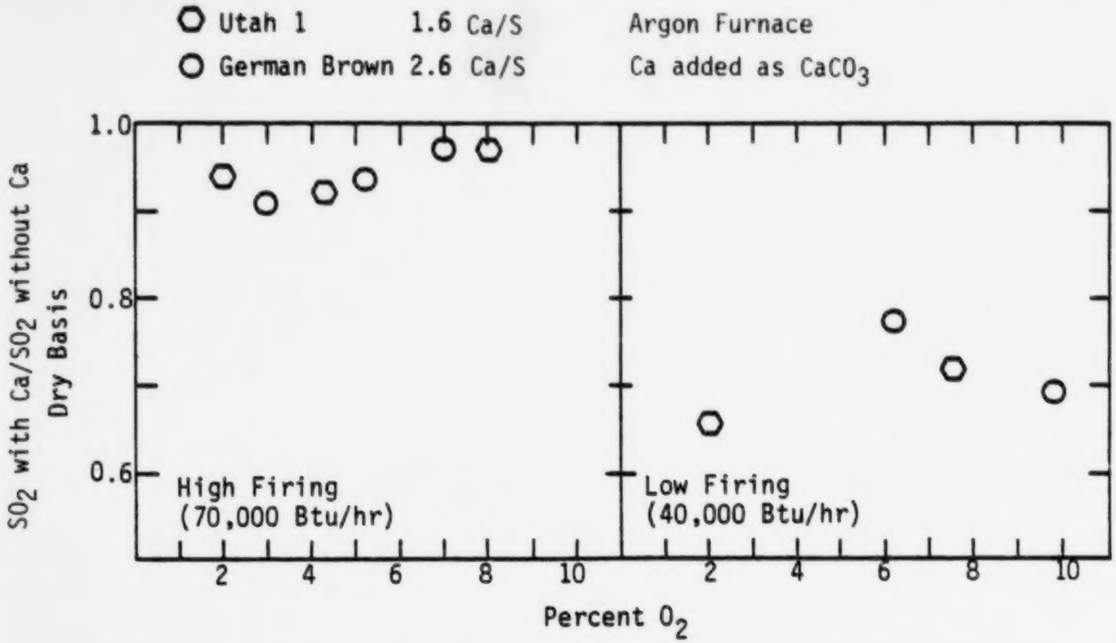

Figure 10-3. Effect of Load on Sulfur Capture.

10.2 Boiler Simulator Furnace Results

Three sections of the planned work in the boiler similator furnace have been completed. The first set of results were obtained during the facility shakedown, and were used to make decisions about the burner, sorbent and load to be used for the combustion parameter screening studies (Series A). The preliminary results are discussed in Section 10.2.1 and the results from the combustion parameter screening studies are discussed in Sections 10.2.2 and 10.2.3.

10.2.1 BSF Preliminary and Shakedown Results

Because the Boiler Simulator Furnace was a new facility, designed with some unique features, a considerable period of time was spent characterizing the furnace and its auxiliary systems. The facility shakedown testing and experiments were also used to select the baseline conditions for the sulfur/sorbent interaction studies. The results of these preliminary studies are briefly discussed in the following section.

After an oxygen and carbon balance for the furnace fired with both propane and coal was established, the response of the furnace to a pulse of SO_2 (while fired on propane) was determined. SO_2 was injected with the combustion air at the burner. Figure 10-4 shows the level of SO_2 measured at the three sample ports (#1 at the exit of the radiant furnace, #2 at the exit of the post flame cavity, and #3 at the exit at the convective sections). It appeared that the furnace responds in a manner characteristic of a plug flow system, but that there was some SO_2 retention in the furnace. (The maximum SO_2 measured for a pulse decreased through the furnace even though the SO_2 injection level was constant.)

The apparent SO_2 profile through the furnace was further characterized for both propane/SO_2 and coal fired conditions. Figures 10-5 and 10-6 show the SO_2 profiles measured in the BSF at several conditions and on several dates.

The general effect of load and radiant zone cooling on furnace time temperature profile and sulfur capture using Indiana coal and calcium hydroxide as a sorbent are shown in Figures 10-7, 10-8, and 10-9. Figure 10-10 shows the effect of flame shape (changed by changing the coal injector geometry) on capture, again Indiana coal fired with $Ca(OH)_2$ as the sorbent. The flame shape experiment

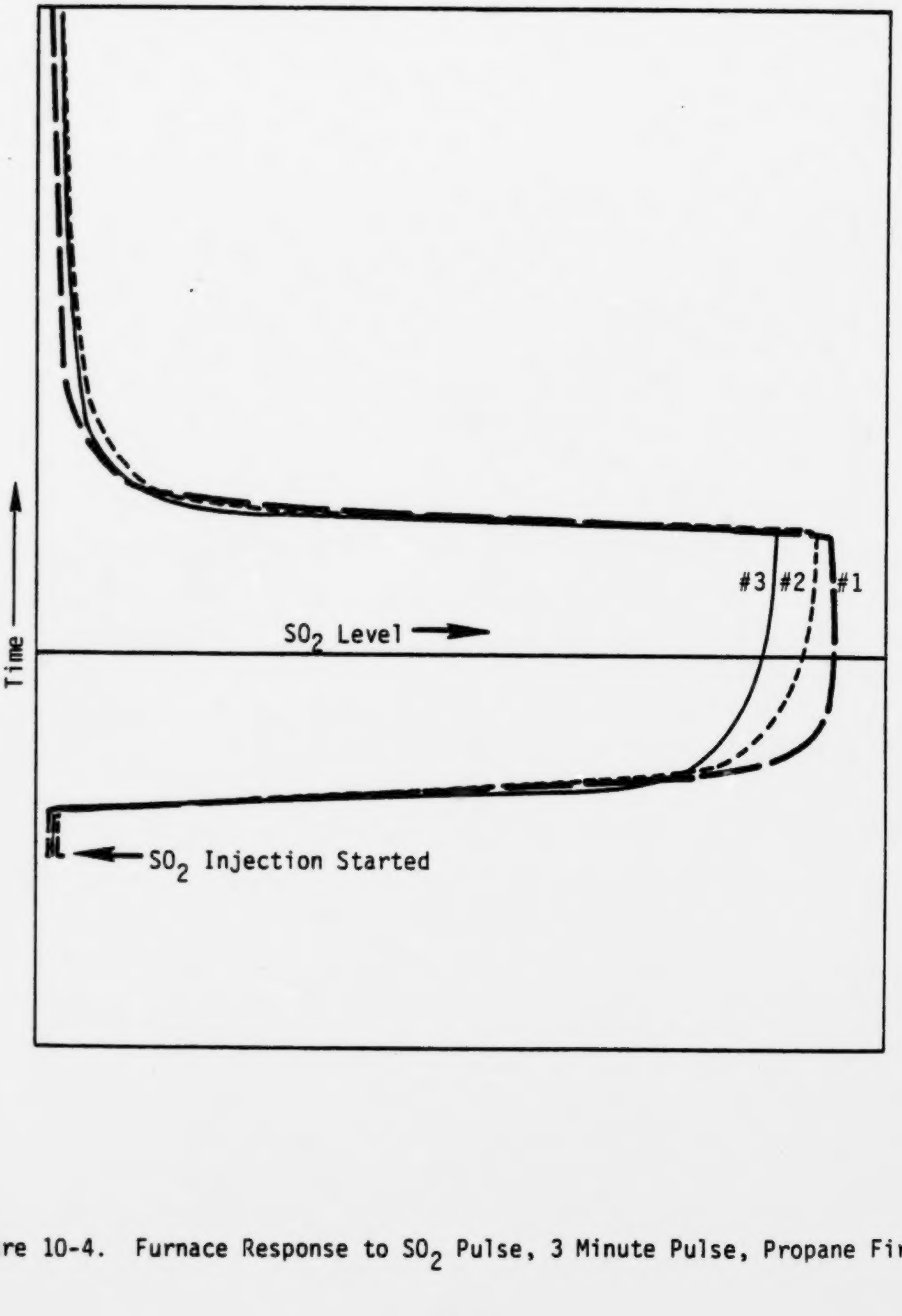

Figure 10-4. Furnace Response to SO_2 Pulse, 3 Minute Pulse, Propane Fired.

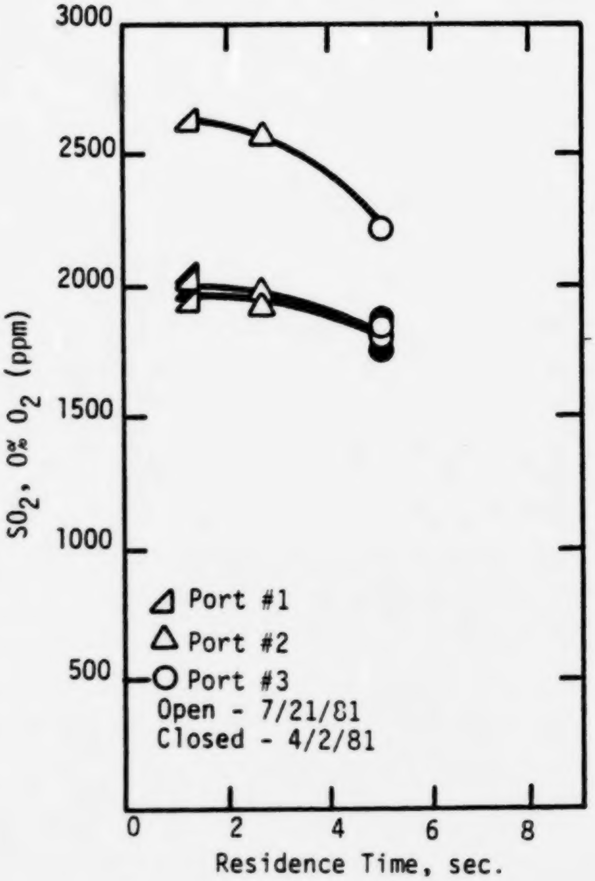

Figure 10-5. Baseline SO_2 Profile Through BSF, Propane + SO_2 Fired.

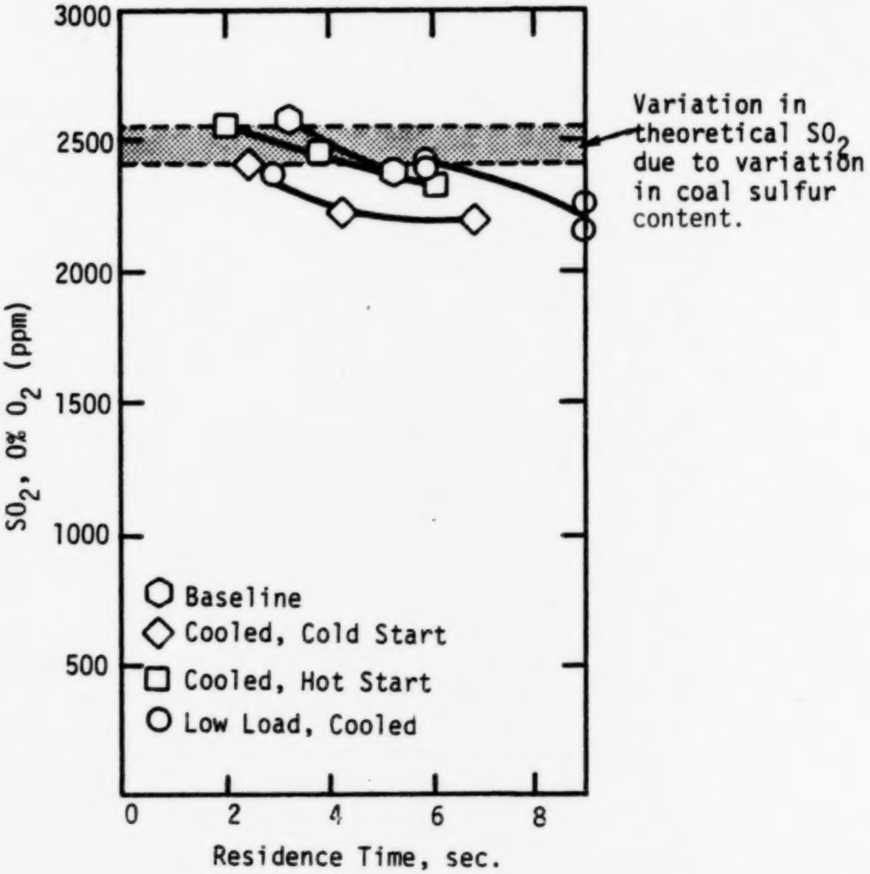

Figure 10-6. Baseline SO_2 Profile Through BSF, Indiana Coal Fired.

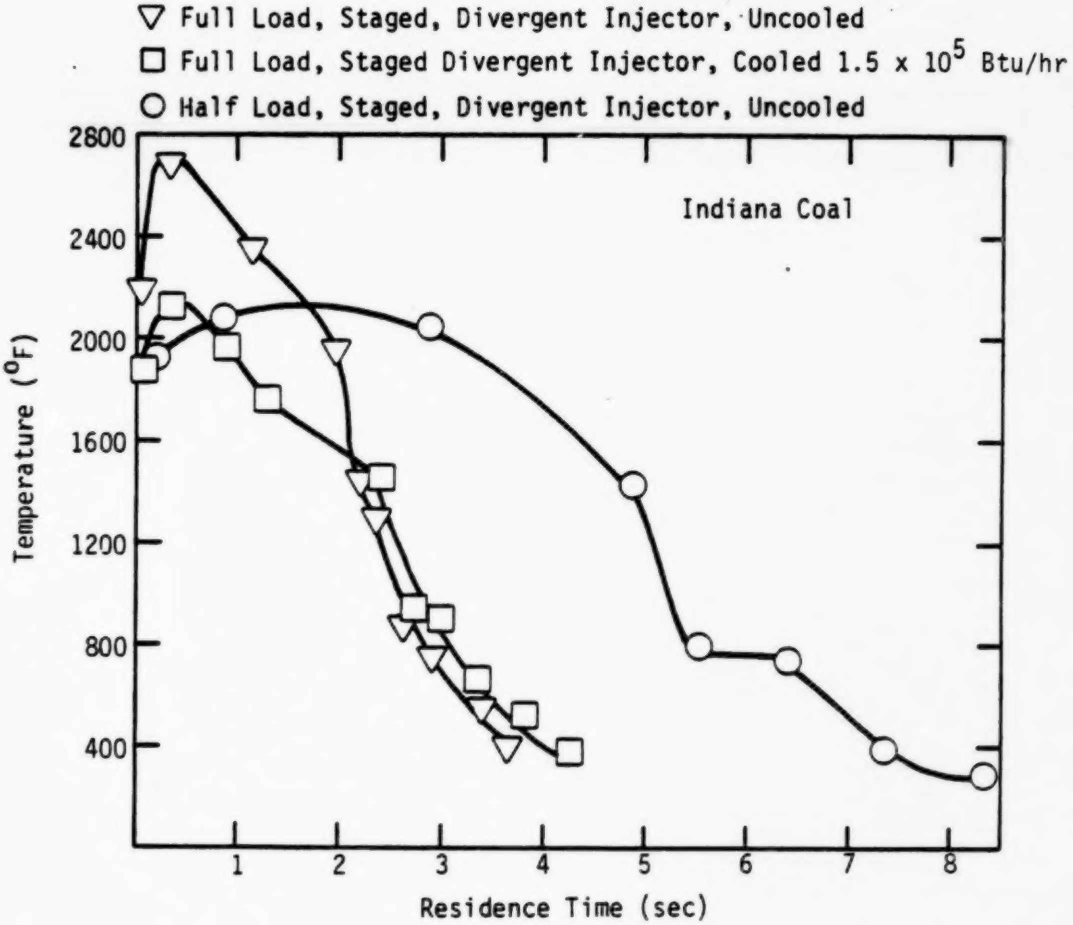

Figure 10-7. Effect of Cooling and Load on Time/Temperature Profile of BSF.

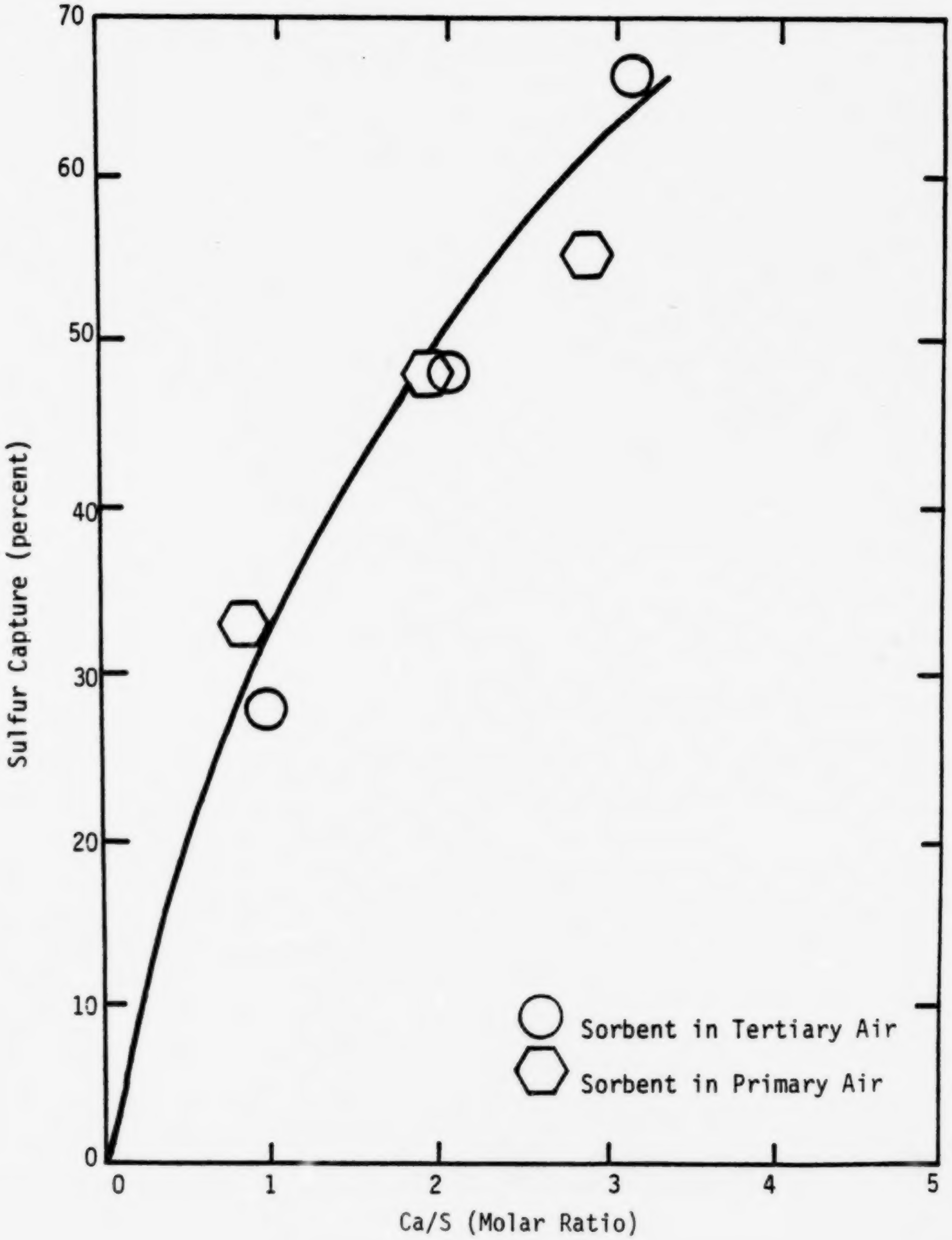

Figure 10-8. Sulfur Capture With 15 Percent Heat Extraction by Probes in Initial Post-Flame Zone. Firing Rate 1 MBtu/hr. Calcium Hydroxide Sorbent.

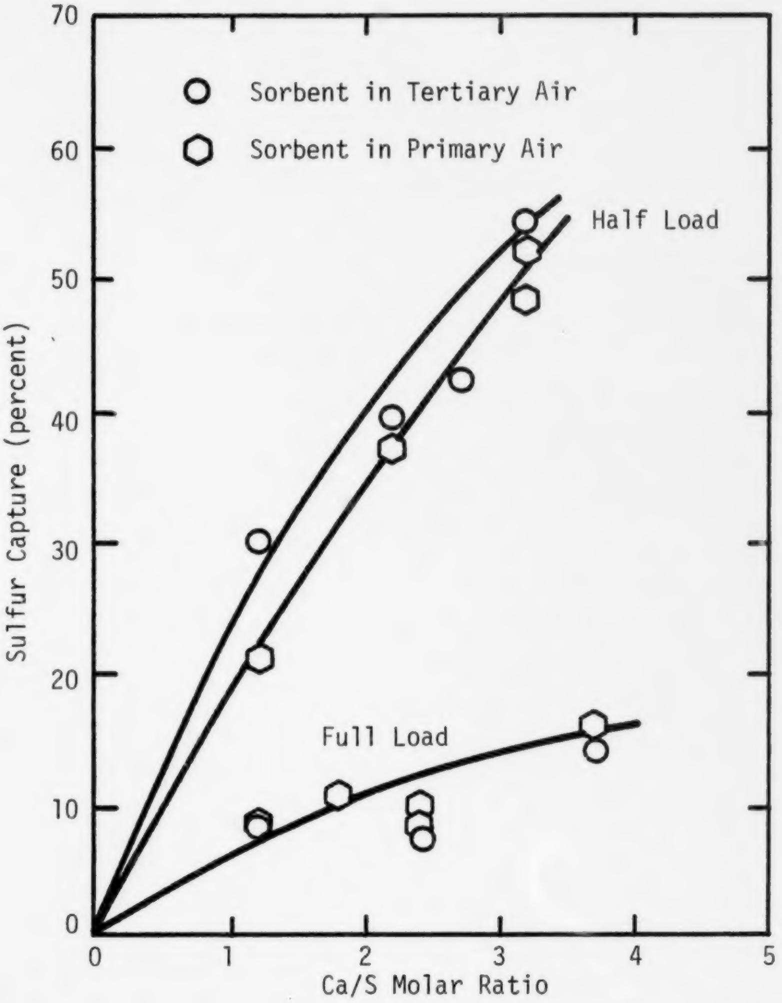

Figure 10-9. Sulfur Capture as a Function of Calcium Additive/Sulfur Ratio with Firing Rate (Load) as a Parameter. Indiana Coal, 2.56 Percent Sulfur, Full Load is 0.95 MBtu/hr, Calcium Hydroxide Sorbent.

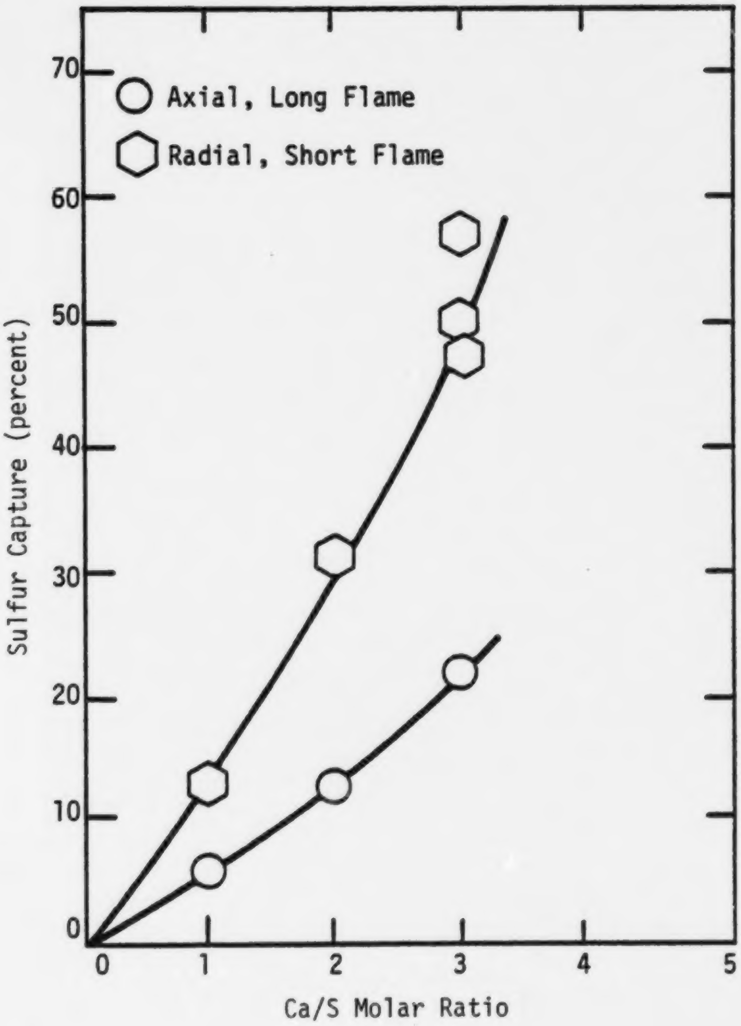

Figure 10-10. Effect of Flame Shape on Sulfur Capture. 1×10^6 Btu/hr, Cold Start, Uncooled, $CaCO_3$ in Tertiary Air, $SR_B = 0.75$, $SR_T = 1.25$.

was performed in the furnace during a heat-up cycle, which is why the captures are higher than the usual full load uncooled cases.

Sulfur capture was very low for full load uncooled condition and for the long, axial, flame. The low load case gave (as expected) a very long residence time. In order to have a baseline case with significant sulfur capture and reasonable residence times, the following conditions were selected for a baseline in the parameter screening studies:

Fuel: Indiana 2 coal (2.4% S)
Load: 0.8×10^6 Btu/hr
SR_P: 0.2
SR_B: 0.6
SR_T: 1.2
Cooling: 0.1×10^6 Btu/hr at radiant furnace
Sorbent: $CaCO_3$, Vicron 45-3 injected with tertiary air
Tertiary air: Medium velocity (50 ft/sec)

The problem of the SO_2 baseline through the furnace persisted. There was a pronounced decrease in the SO_2 measured at the exit of the convective section from the SO_2 measured at the exit of the radiant furnace; moreover, in the early shakedown tests this SO_2 profile became more pronounced as a series of tests progressed. Essentially, SO_2 baseline got worse as more sorbent was injected into the furnace. The data in Figure 10-11 shows the magnitude of the problem. The first set of symbols, ⬡, show the starting SO_2 profile and the SO_2 measured at each port when sorbent was injected at a rate equivalent to a Ca/S molar ratio of 1.1 (⬢). As expected, the SO_2 dropped throughout the furnace; however, when the sorbent was turned off the SO_2 did not increase back to the original level, but to a lower level (□). The baseline drift increased as more sorbent was injected into the furnace.

This baseline drift problem was minimized by minimizing sorbent injection times, but could not be eliminated. Figure 10-12 shows the baseline change

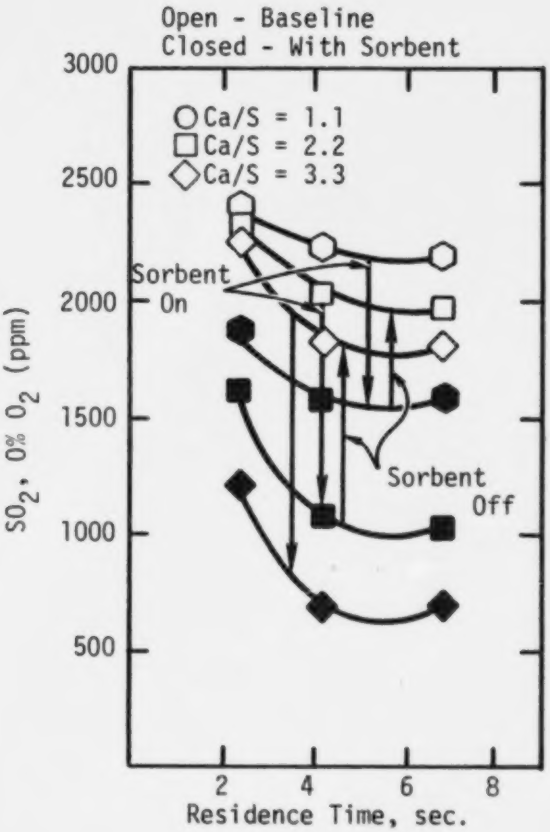

Figure 10-11. Baseline Drift, Furnace Shakedown Experiments, Base Case Conditions.

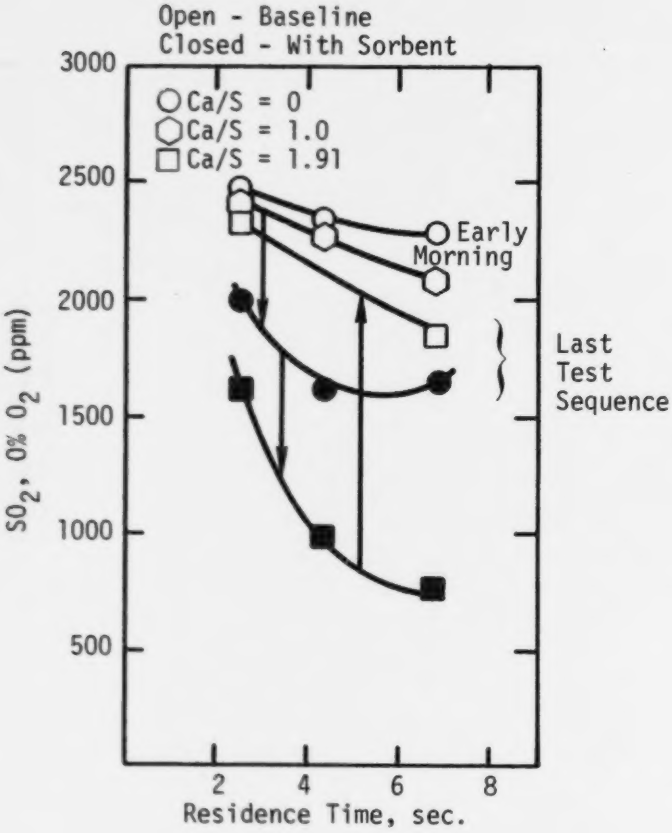

Figure 10-12. Baseline Drift, High T.A. Velocity Experiments.

for a set of experiments done in the parameter screening series. The baseline drift was smaller but still significant and is part of the reason for basing all of the sulfur capture values on measurements of SO_2 with and without sorbent for each sample port and condition.

10.2.2 Combustion Parameter Screening Studies - Internally Staged Conditions (Series A-1)

The purpose of Series A testing was to define the role of the combustion parameters in the effectiveness of limestone injection for SO_2 control. The excess air/DMB portion of this test series is described in the following section. As discussed in Section 6, the parameters which were studied included:

- Firing Rate
- Heat Extraction Rate
- Sorbent Location
- Overall Excess Air
- Burner Zone Stoichiometry
- Tertiary Air

Table 10-2 shows the completed test matrix for these studies. In every case the furnace was fired with Indiana 2 coal, injected with the divergent coal injector. The staging air was added through the four tertiary air ports at the furnace face. All of the tests were performed using a calcium carbonate sorbent, Vicron 45-3, which was fed independently (except for the sorbent milled with the coal case) with the twin screw sorbent feeder. The calcium to sulfur ratio was changed by changing the sorbent feed rate. At each test condition, samples were withdrawn at the end of the radiant zone, port flame cavity, and just prior to the baghouse.

For convenience, all of the experimental results are presented in terms of percent sulfur capture. The capture was calculated relative to the SO_2 emission from the furnace before sorbent addition for each data point. Thus, in general, each data point represents two SO_2 measurements, one with and one without limestone addition.

Table 10-2. Series A-1 Test Matrix Combustion Parameter Screening

ALL TESTS COMPLETED	SR_T	SR_B OR SR_1	TERT AIR VEL	FIRING RATE											
				800,000						500,000 Btu/hr					
				COAL-MILL		COAL-PA		T.A.		COAL-MILL		COAL-PA		T.A.	
				COOLING 0	COOLING 100K	COOLING 0	COOLING 100K	COOLING 0	COOLING 100K	COOLING 0	COOLING 100K	COOLING 0	COOLING 100K	COOLING 0	COOLING 100K
EXCESS AIR	1.2	1.1	M	E	E			E	○		E				
DISTRIBUTED MIXING BURNER STUDIES	1.2	0.6	M	E	E	○	○	○	●		E		○	○	○
		0.75						E	○						
		0.9			E			E	○						
	1.5	0.6	M						2						
	1.2	0.6	L						2						
			M						2						
			H						2						

*All tests are for at least two Ca/S ratios and 3 sample points.

○ - Original Test Matrix

2 - Added After DCD Review Meeting

E - Additional Tests Completed

The furnace shakedown studies, as discussed earlier, were used to choose appropriate firing conditions (load, residence time, coal nozzle), fuels, and sorbent for the parameter screening studies. Baseline time temperature profiles for the furnace were measured as was the baseline SO_2 concentration at several furnace locations for Indiana coal firing. There was a distinct SO_2 profile measured through the furnace as could be seen from the data in Figure 10-12. As discussed earlier, this baseline SO_2 profile was observed consistently throughout the test series. The total difference in SO_2 measured at the exit of the radiant zone and the exit of the baghouse (or, in later experiments, the exit of the convective sections) was influenced by the firing conditions and by earlier firing conditions. (Most notably, the amount of sorbent injected into the furnace immediately before.) This drift in SO_2 baseline is the motivation for basing sulfur capture values on SO_2 emissions just prior to the addition of sorbent for every case. Variations from standard conditions (defined in Section 10.2.1) are clearly noted on each of the figures.

10.2.2.1 Typical Emission Characteristics

Figure 10-13 shows the percent SO_2 capture as a function of calcium-to-sulfur ratio for the base case conditions. The data presented are for the entire duration of the test period, and they indicate the type of reproducibility that was achieved in this study. As expected, the percent capture increased approximately linearly with increasing calcium injection. All of the data shown in this figure were obtained at Port 3 (entrance to the baghouse) and they indicate that the overall sorbent utilization is approximately 20 percent.

Figure 10-14 shows cumulative sulfur capture through the combustion system at a calcium-to-sulfur ratio of 1.0. The figure is based on measured captures at three furnace locations and the residence times calculated for these locations. These data suggest that most of the sulfur capture in this case occurred within the radiant zone of the furnace (prior to two seconds residence time). Some capture occurred in the post-flame cavity (2-4 seconds); however, very little capture occurred in the convective sections (probably due to the low local temperatures). The temperatures shown are approximate wall temperatures at the end of each section (at the sample point).

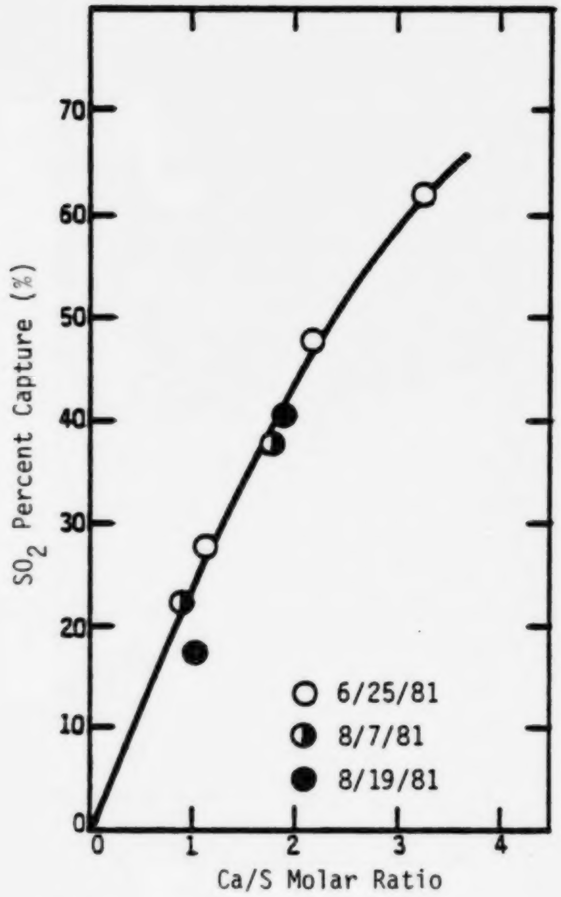

Date: As Shown	**Coal:** Indiana
Rate: 800,000 Btu/hr	Ca/S Mole Ratio: 2.5
Cooling: 100,000 Btu/hr	**Sample Port:** #3
SR_P: 0.2	**Sorbent:** $CaCO_3$, 45-3
SR_B: 0.6	**Injection Loc.:** Tertiary Air
SR_T: 1.2	

Figure 10-13. Sulfur Capture/Base Case Conditions.

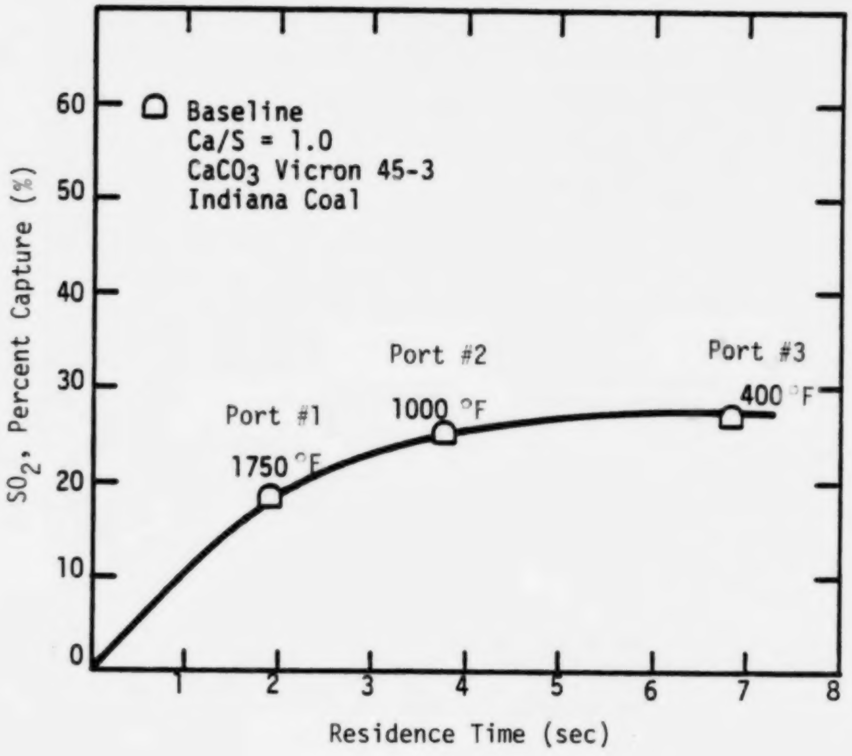

Figure 10-14. Sulfur Capture Through the Furnace, Base Conditions.

To further define the relative effectiveness of sorbent utilization in each combustion zone, all of the axial SO_2 profile data for this condition were converted to relative percentage capture. Relative sorbent utilization in each furnace zone was calculated from the SO_2 capture in each zone (calculated from the difference in concentration at the entrance of the zone and at the exit of the zone) and the calcium-to-sulfur ratio at the entrance of the zone (based on SO_2 at the entrance of the zone and available calcium at the entrance of the zone, calcium used in the previous zone (calculated from the capture in that zone) was assumed to be unavilable). For example, sorbent utilization in the post-flame zone was based on the SO_2 measured at the exit of the radiant furnace with sorbent and SO_2 at the exit of the post-flame zone with sorbent (giving sulfur capture in that zone) and a calcium-to-sulfur ratio calculated for the input (to the burner) calcium-to-sulfur ratio less the calcium used in the radiant zone (calculated from the capture in the radiant zone). Figure 10-15 summarizes these results in terms of the Ca/S ratio for the gases entering each of these sections. These results indicate that, in general, the flame zone utilization is slightly better than that in the post-flame cavity and that the sorbent effectiveness decreases with increasing Ca/S ratio. To further clairfy this effect, these data were replotted allowing for the 0.5 order dependence of the SO_2 concentration driving force (Coutant, et al., 1971). These results are shown in Figure 10-16, and they confirm that the apparent decrease in sorbent effectiveness at high sorbent loadings is largely due to the associated decrease in SO_2 concentration.

10.2.2.2 Influence of Heat Extraction Rate

The rate at which heat is extracted from the radiant zone of the system has a dramatic effect on sorbent utilization efficiency throughout the entire combustion process because the radiant zone environment controls the effectiveness of calcination (the loss of active surface through deadburning) and the kinetics of sulfation. Figure 10-17 summarizes the data obtained for various cooling loads at the base case condition and shows the effect of cooling on the furnace time/temperature profile. Increasing the radiant zone heat removal by 125,000 Btu/hr (15 percent of the total heat input) increased the SO_2 capture

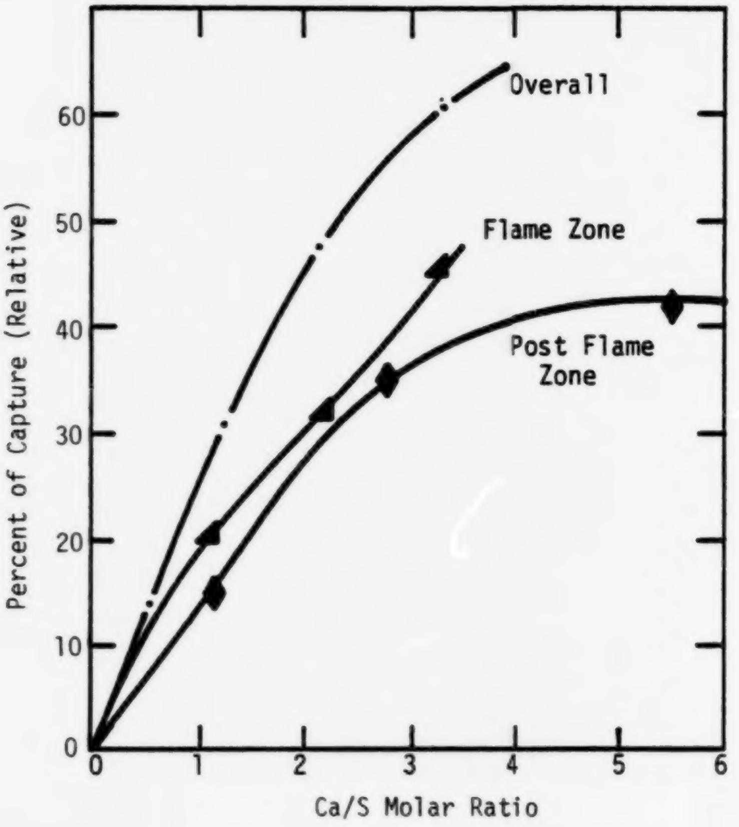

Figure 10-15. Relative SO_2 Capture for Added $CaCO_3$ and Individual Furnace Sections.

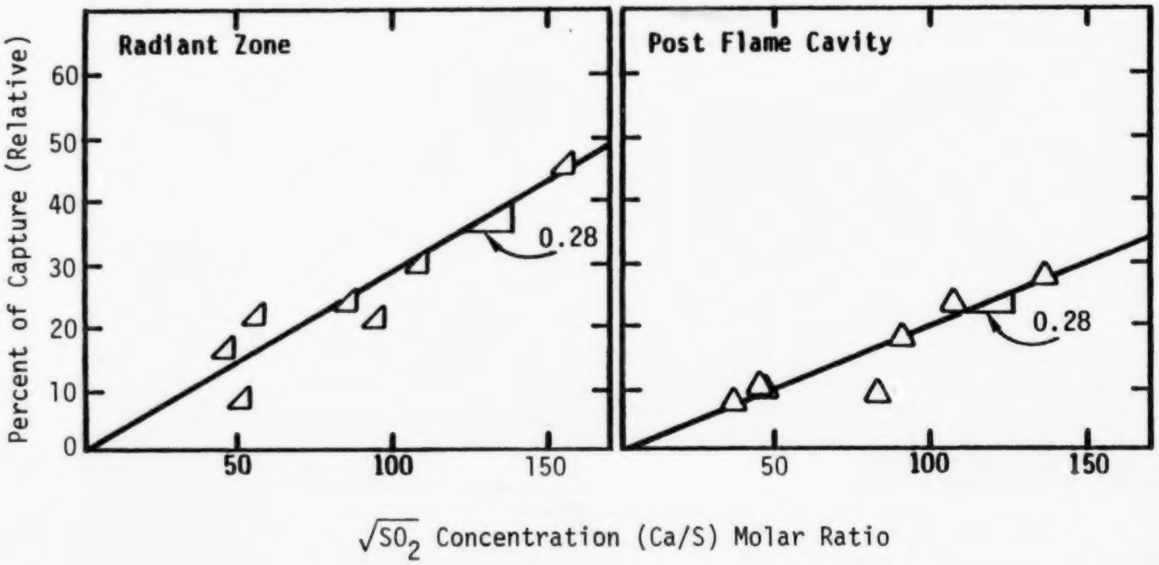

Figure 10-16. Correlation of Sulfur Capture - Base Case Conditions.

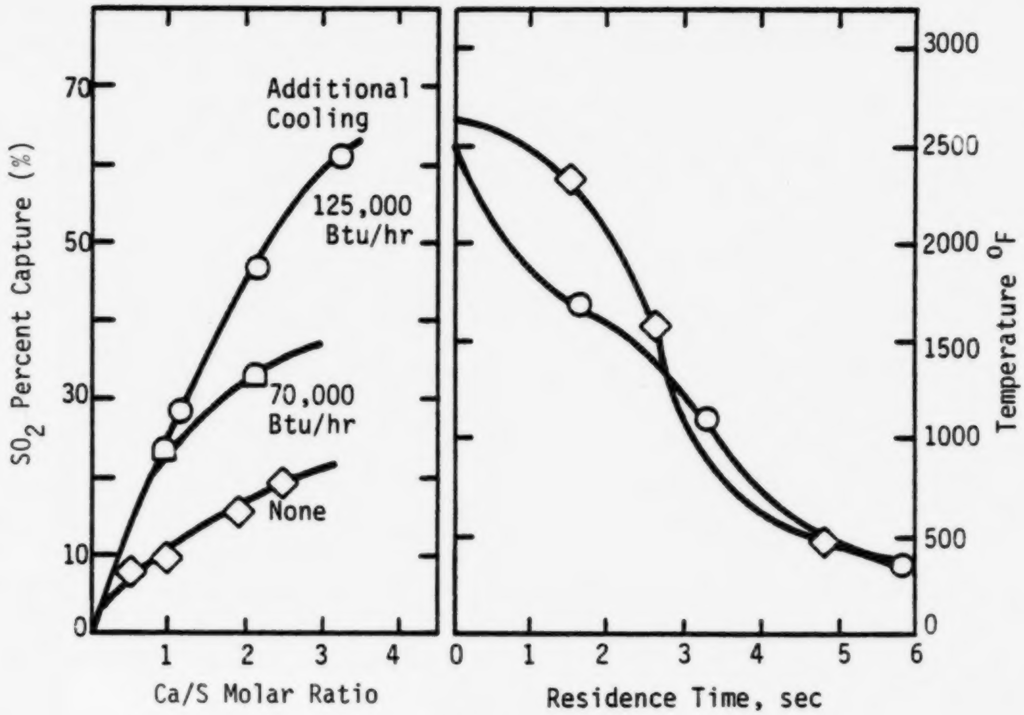

Date: 6/25, 7/1, 7/29/81
Rate: 800,000 Btu/hr
Cooling: As Shown
SR$_P$: 0.2
SR$_B$: 0.6
SR$_T$: 1.20

Coal: Indiana
Ca/S Mole Ratio:
Sample Port: #3
Sorbent: CaCO$_3$, 45-3
Injection Loc.: Tertiary Air

Figure 10-17. Influence of Heat Extraction Rate - Base Case Conditions.

by almost threefold. Cooling the radiant furnace also resulted in significantly lower temperatures in the first part of the furnace. Figures 10-18 and 10-19 summarize the influence of heat extraction rate at other conditions, including different sorbent locations (milled with the coal and injected into the primary air, low load [580,000 Btu/hr], and changed burner stoichiometry [SR_B = 0.75]). In all cases, increasing the radiant zone cooling by approximately 100,000 Btu/hr dramatically increased the effectiveness of the limestone sorbent.

Figure 10-20 shows the influence of heat extraction rate on the relative capture in each of the major furnace zones. Relative capture is calculated for the Ca/S ratio at the beginning of each furnace section. The Ca/S molar ratio was normalized by $\sqrt{SO_2}$ concentration to eliminate the driving force effect. It appears that the no-cooling case results in a material that is so inactive it is incapable of effectively capturing SO_2 even after the peak temperature zone. Figure 10-21 shows similar results for the low firing rate condition. In this case, cooling had little effect on the capture in the post-flame cavity, presumably because neither condition resulted in significant dead-burning in the flame zone, and because the residence time in the post-flame cavity was long enough that a slightly lower bulk-gas temperature (and hence reaction rate) did not significantly decrease relative capture. However, in contrast, the data from the radiant zone indicate that additional cooling significantly increased the flame zone capture as it did in the base case. The reason for this effect is not clear at the present.

10.2.2.3 Influence of Overall Excess Air

To establish the role of overall stoichiometry, the total air flow rate was increased from the base condition (SR_T = 1.2) to produce a 50 percent excess air case (SR_T = 1.5). The results from this experiment are shown in Figure 10-22. The data indicate that overall excess air had little effect on sulfur capture by limestone. A slight increase in sorbent effectiveness might have been expected based on the associated increase in tertiary air velocity and decrease in gas temperature; however, a decrease in sulfur capture due to reduced residence time and increased dilution may also have been expected. It appears that the effects cancelled each other.

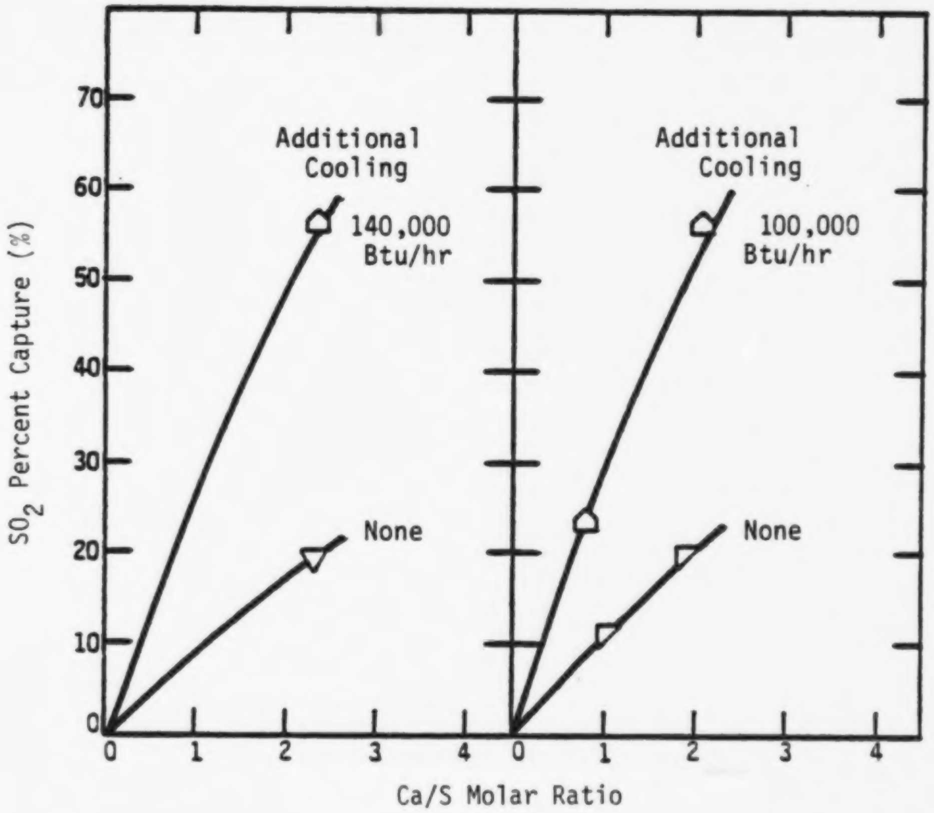

Date: 8/10, 8/21/81
Rate: 860,000 Btu/hr
Cooling: As Shown
SR_P: 0.2
SR_B: 0.6
SR_T: 1.2
Coal: Indiana
Ca/S Mole Ratio: As Shown
Sample Port: #3
Sorbent: $CaCO_3$, 45-3
Injection Loc.: Milled with Coal

Date: 7/29, 8/10/81
Rate: 750,000 Btu/hr
Cooling: As Shown
SR_P: 0.2
SR_B: 0.6
SR_T: 1.2
Coal: Indiana
Ca/S Mole Ratio: As Shown
Sample Port: #3
Sorbent: $CaCO_3$, 45-3
Injection Loc.: Primary Air

Figure 10-18. Importance of Heat Extraction with Alternate Sorbent Location.

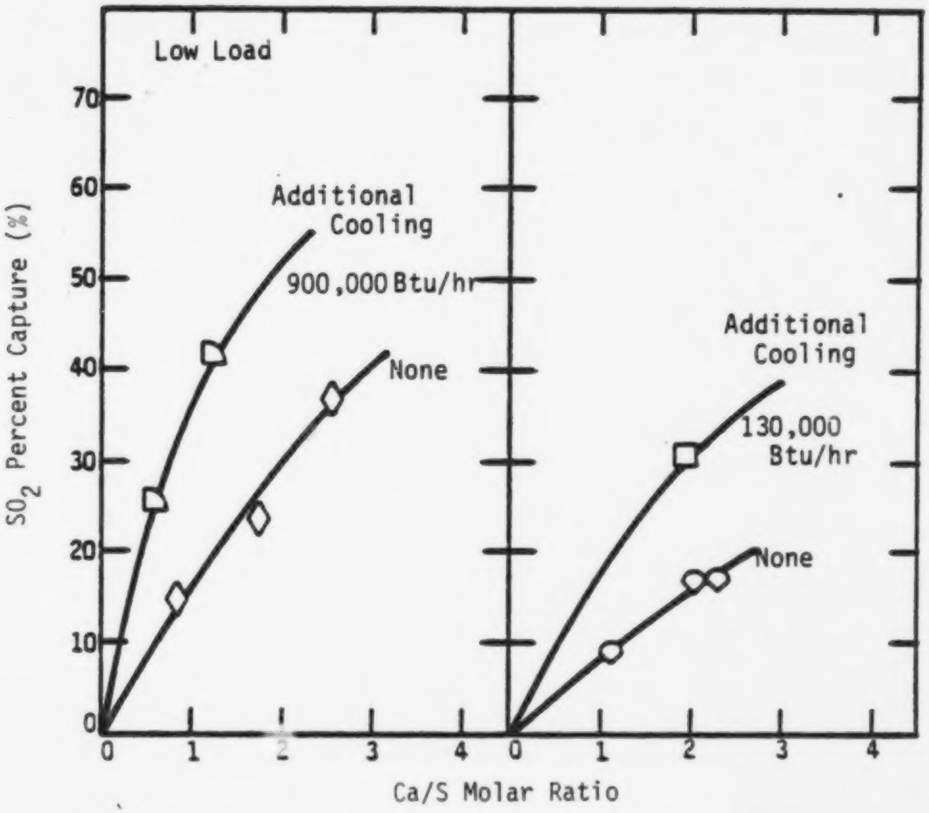

Date: 6/26, 7/14/81	**Date:** 7/7, 8/6/81
Rate: 580,000 Btu/hr	**Rate:** 800,000 Btu/hr
Cooling: As Shown	**Cooling:** As Shown
SR$_P$: 0.2	**SR$_P$:** 0.2
SR$_B$: 0.6	**SR$_B$:** 0.75
SR$_T$: 1.2	**SR$_T$:** 1.2
Coal: Indiana	**Coal:** Indiana
Ca/S Mole Ratio: As Shown	Ca/S Mole Ratio: As Shown
Sample Port: #3	**Sample Port:** #3
Sorbent: $CaCO_3$, 45-3	**Sorbent:** $CaCO_3$, 45-3
Injection Loc.: Tert. Air	**Injection Loc.:** Ter. Air

Figure 10-19. Additional Studies on Heat Extraction.

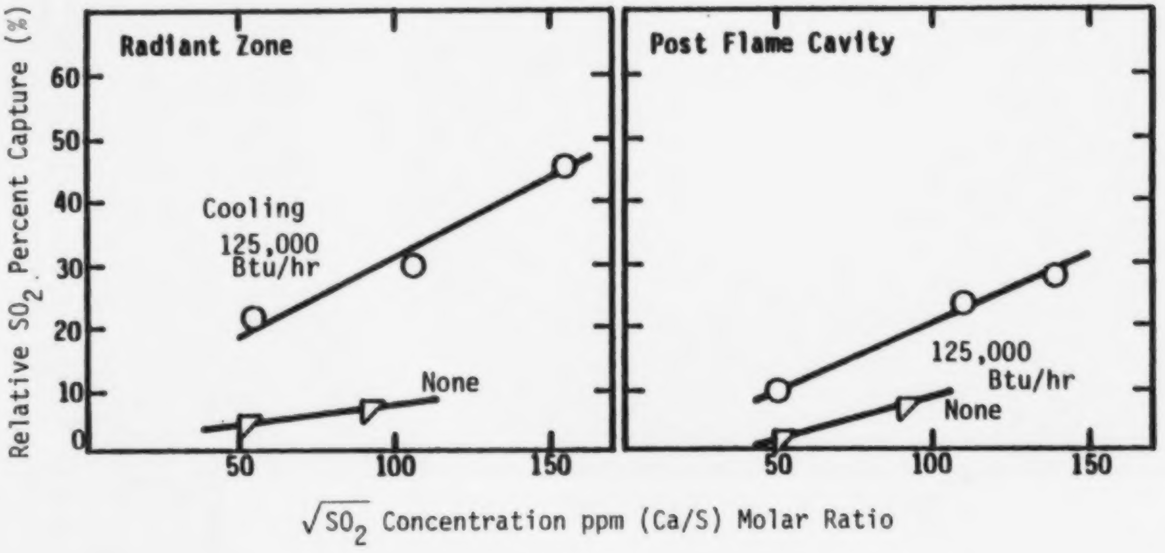

Figure 10-20. Effect of Heat Extraction on Zone Capture - Base Case Conditions.

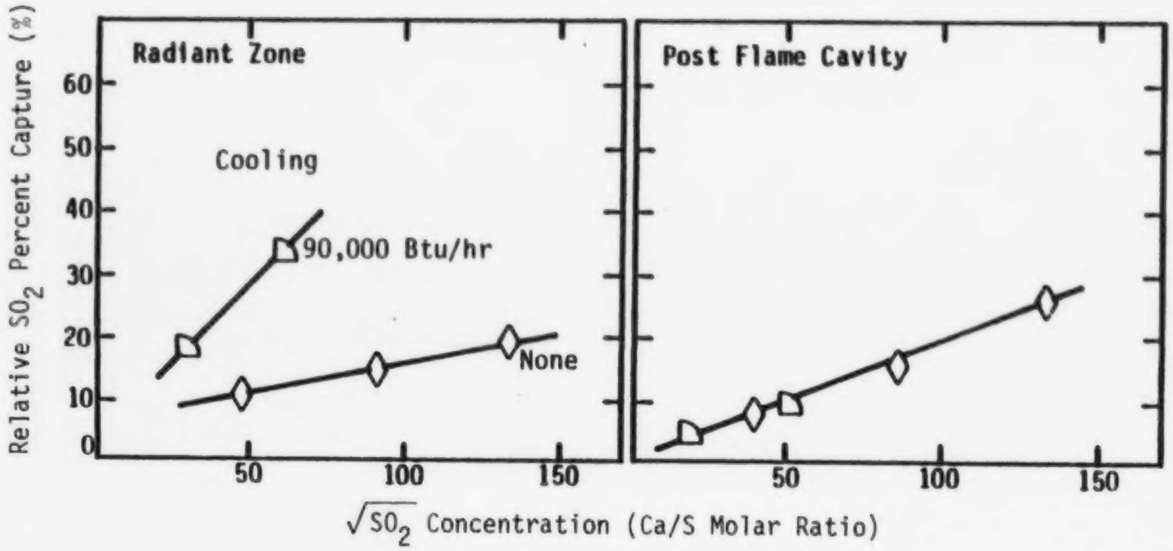

Figure 10-21. Effect of Heat Extraction on Zone Capture - Low Load.

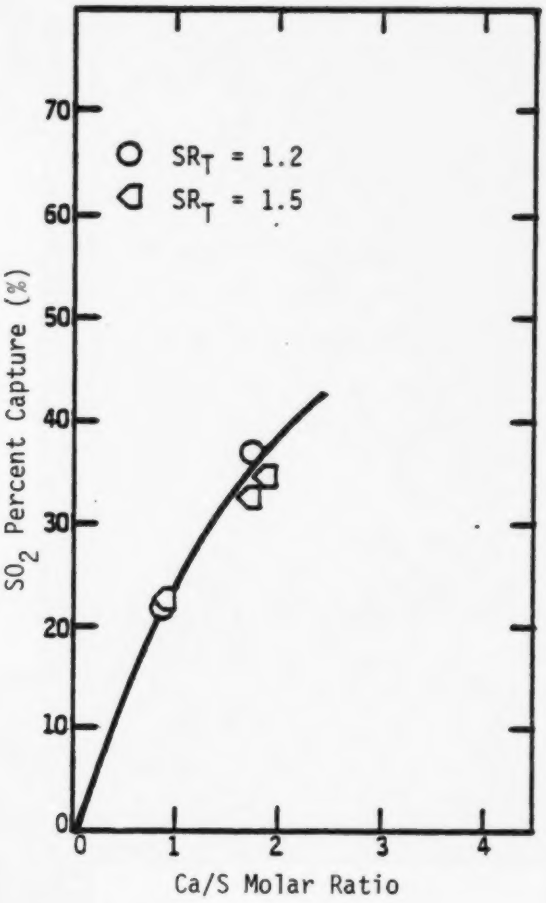

Date: 8/7/81
Rate: 840,000 Btu/hr
Cooling: 135,000 Btu/hr
SR_P: 0.2
SR_B: 0.6
SR_T: As Shown

Coal: Indiana
Ca/S Mole Ratio: As Shown
Sample Port: #3
Sorbent: $CaCO_3$, 45-3
Injection Loc.: Tertiary Air

Figure 10-22. Role of Overall Excess Air.

10.2.2.4 Influence of Burner Zone Stoichiometry

Figure 10-23 shows data for SO_2 capture after ports 2 and 3 (post-flame cavity and convective section) for a range of burner zone stoichiometries. These data were all obtained without additional cooling in the radiant zone. In general, the results indicate that the uncooled condition results in relatively poor capture and the capture appears to decrease significantly when the burner zone becomes excess air. Figure 10-24 summarizes data on the influence of burner zone stoichiometry for both the cooled and uncooled conditions. In general, there was a significant decrease in percentage capture above an SR_B of 1.0. This may be due to the very low tertiary air velocity associated with the excess air case. Because of the small amount of tertiary air under these conditions the sorbent may become entrained in the primary flame zone and severely deadburned, rather than being quickly carried beyond the initial, very hot, reaction zone. Figure 10-25 summarizes the effect of varying burner zone stoichiometry on the local capture in each of the major zones at the base case conditions. Again, this shows that at the excess air condition the sorbent is not reactive in either the flame zone or the post-flame cavity and this suggests that excessive deadburning has occurred.

10.2.2.5 Influence of Sorbent Location

Figures 10-26 and 10-27 summarize data taken on the influence of the sorbent injection location on sulfur capture. In these tests, the limestone was alternately injected with the tertiary air, with the coal and primary air, or premixed with the coal prior to the pulverizer. The data shown in Figure 10-26 indicate that under both full load and low load conditions the sorbent introduction method has essentially no effect on the sulfur capture. Figure 10-27a shows similar data for a sequence of uncooled tests and, as noted before, the overall capture is significantly reduced, but there appears to be little effect of injection mode. Figure 10-27b shows the only exception to this general trend. In this test series the burner zone stoichiometry was increased to give 10 percent excess air (SR_B = 1.1). In this case, introducing the limestone on the furnace axis with the coal produced significantly better capture than introducing it at a very low velocity through the tertiary air ports. These results

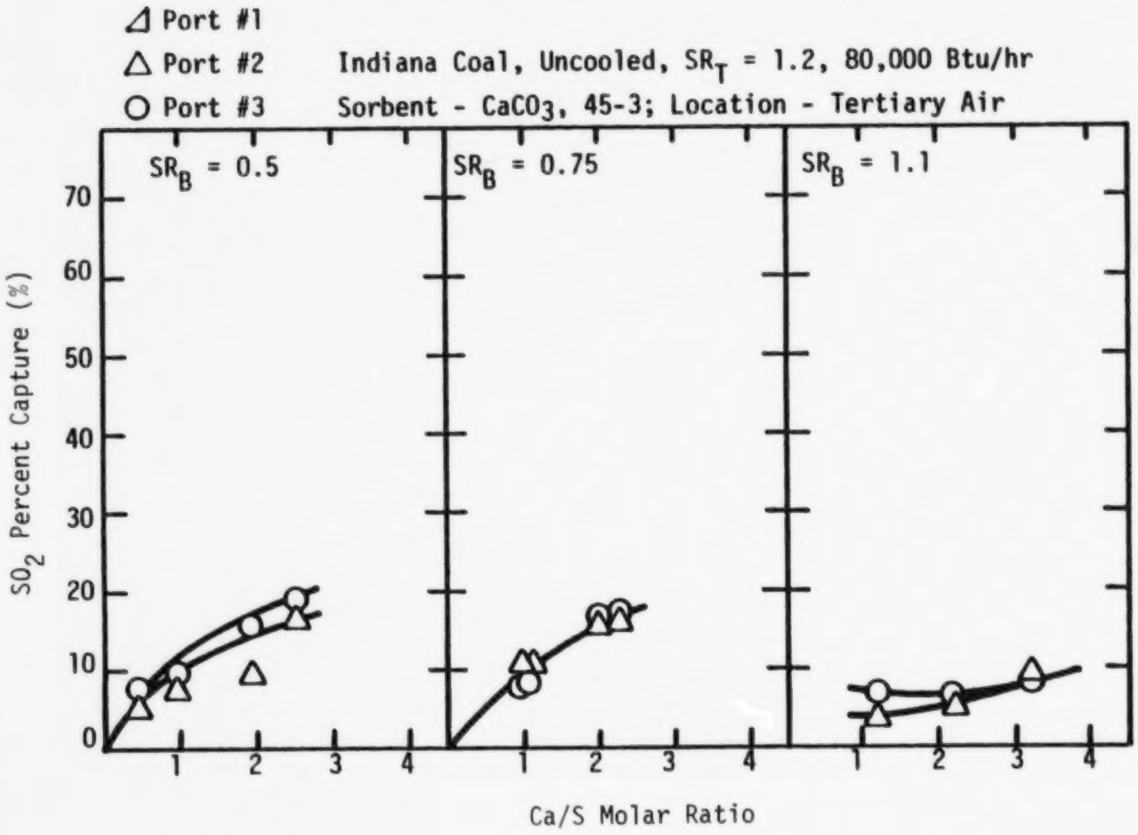

Figure 10-23. Influence of Burner Zone Stoichiometry - Uncooled.

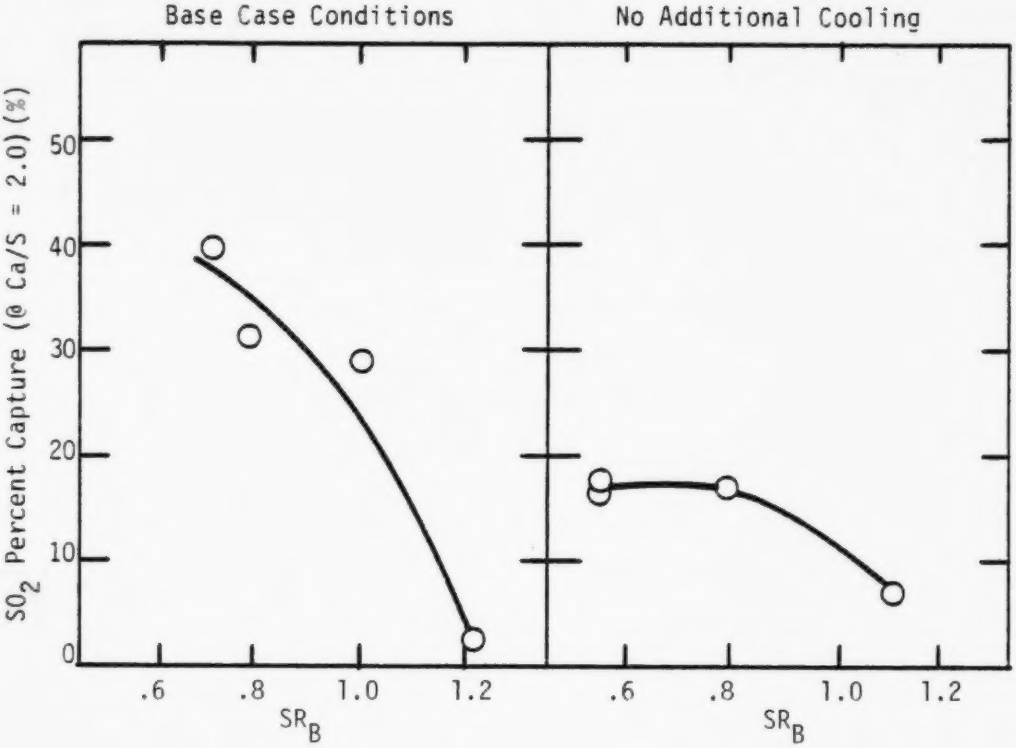

(a)

Date: 8/6, 8/7/81
Rate: 825,000 Btu/hr
Cooling: 130,000 Btu/hr
SR_P: 0.2
SR_B: As Shown
SR_T: 1.2
Coal: Indiana 2 (2.5%S)
Sample Port: #3
Sorbent: $CaCO_3$, 45-3
Injection Loc.: Tertiary Air
Calcium to Sulfur: 2.5

(b)

Date: 7/1, 7/2, 7/7/81
Rate: 830,000 Btu/hr
Cooling: None
SR_P: 0.2
SR_B: As Shown
SR_T: 1.2
Coal: Indiana 2 (2.5%S)
Sample Port: #3
Sorbent: $CaCO_3$, 45-3
Injection Loc.: Tertiary Air
Calcium to Sulfur: 2.5

Figure 10-24. Summary of Burner Zone Stoichiometry Results.

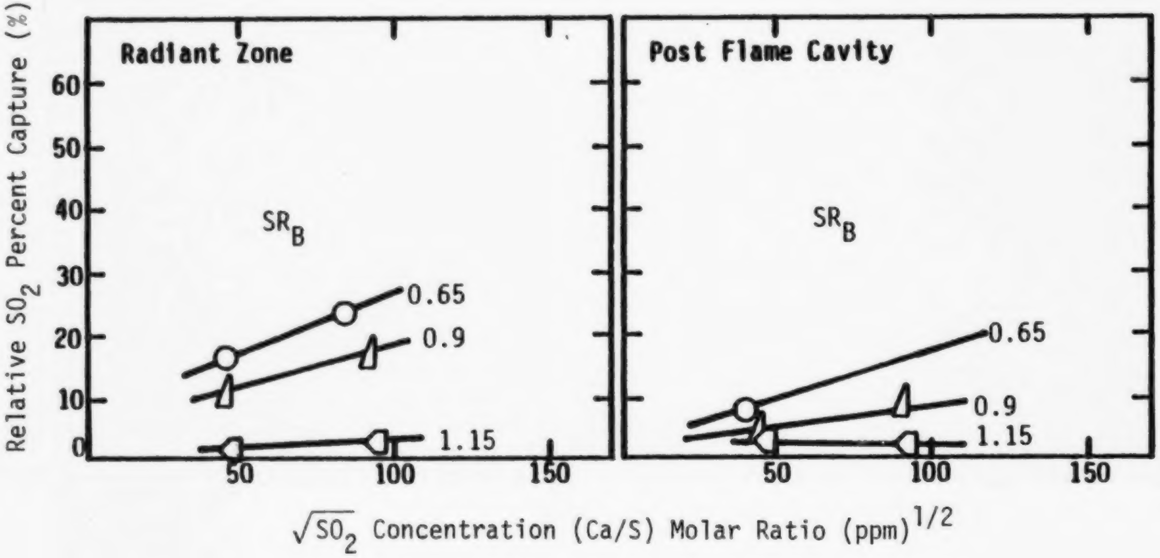

Figure 10-25. Effect of Burner Zone Stoichiometry on Zone Capture - Base Case Conditions.

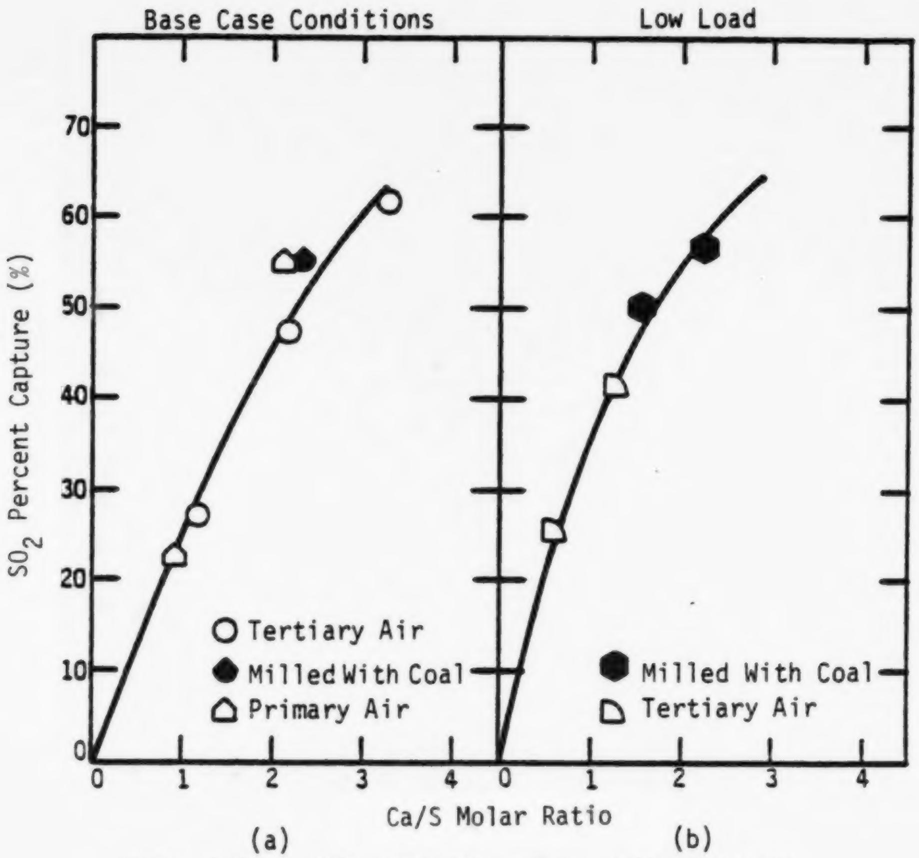

(a)

Date: 6/25, 7/29, 8/21/81
Rate: 800,000 Btu/hr
Cooling: 120,000 Btu/hr
SR_P: 0.2
SR_B: 0.6
SR_T: 1.2
Coal: Indiana
Ca/S Mole Ratio: As Shown
Sample Port: #3
Sorbent: $CaCO_3$, 45-3
Injection Loc.: As Shown

(b)

Date: 6/26, 8/14/81
Rate: 570,000 Btu/hr
Cooling: 70,000 Btu/hr
SR_P: 0.25
SR_B: 0.6
SR_T: 1.2
Coal: Indiana
Ca/S Mole Ratio: As Shown
Sample Port: #3
Sorbent: $CaCO_3$, 45-3
Injection Loc.: As Shown

Figure 10-26. Role of Sorbent Location.

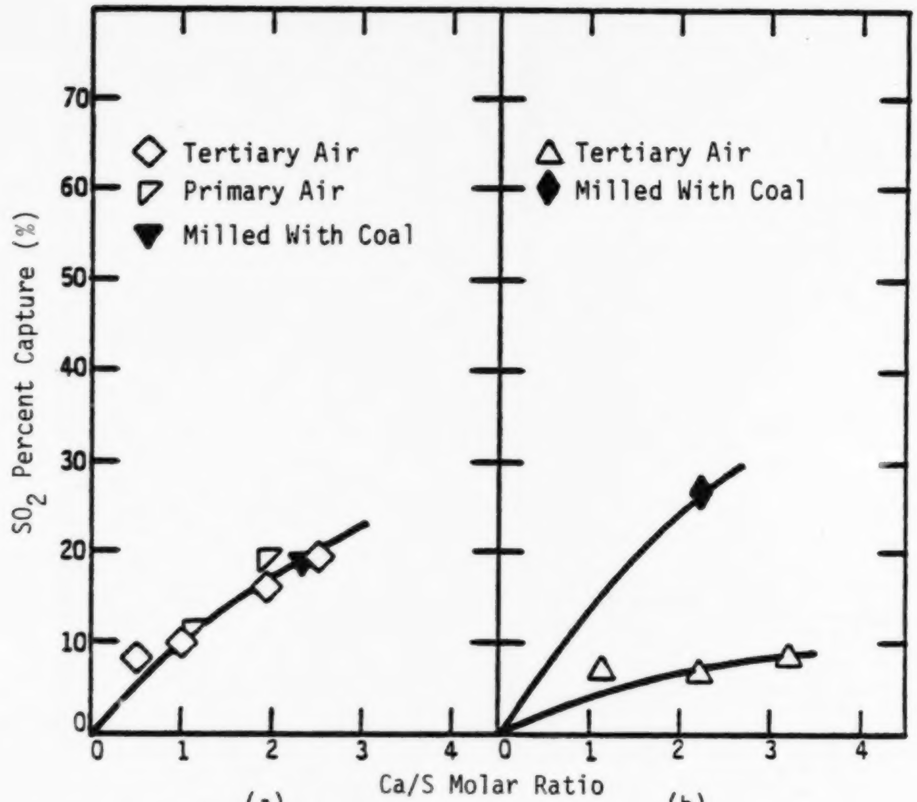

(a)

Date: 7/1, 8/10, 8/18/81
Rate: 800,000 Btu/hr
Cooling: None
SR$_P$: 0.2
SR$_B$: 0.6
SR$_T$: 1.2
Coal: Indiana
Ca/S Mole Ratio: As Shown
Sample Port: #3
Sorbent: CaCO$_3$, 45-3
Injection Loc.: As Shown

(b)

Date: 7/7, 8/18/81
Rate: 800,000 Btu/hr
Cooling: None
SR$_P$: 0.2
SR$_B$: 1.1
SR$_T$: 1.2
Coal: Indiana
Ca/S Mole Ratio: As Shown
Sample Port: #3
Sorbent: CaCO$_3$, 45-3
Injection Loc.: As Shown

Figure 10-27. Influence of Sorbent Location - Uncooled Condition.

further suggest that the extremely poor performance observed at the excess air conditions are associated with flame aerodynamics and not local stoichiometry (oxygen availability).

10.2.2.5 Influence of Firing Rate

Figure 10-28 shows the effect of reducing the firing rate at the base case conditions from approximately 800,000 Btu/hr to 570,000 Btu/hr. This results in increased residence times within both the flame zone and the post-flame cavity. As the temperature profile in Figure 10-28 shows, it also somewhat decreases the maximum wall temperatures measured within all portions of the furnace. As expected, based on the previously discussed trends, decreasing the firing rate increases the percentage capture at a constant calcium-to-sulfur ratio. Figure 10-29 shows similar test results for a no-cooling condition and for the case where the sorbent was pre-mixed with the coal. Only the latter shows a surprising trend: no effect. The reason for this result is not clear at the present time; however, it may be because the thermal environment on the inside of the flame is changed far less by decreasing firing rate than that near the wall.

Figure 10-30 shows the effect of firing rate variations on differential capture and indicates the relative effectiveness of the limestone in the radiant zone and post-flame cavity for the base case conditions. Reducing the firing rate significantly increases the percentage capture in the radiant zone; however, it has essentially no effect on sorbent effectiveness in the post-flame cavity. This suggests that both conditions produce a material that is equally effective in the lower temperature regions. Apparently little deadburning is occurring under either of these combustion conditions.

10.2.2.7 Influence of Tertiary Air Velocity

Figure 10-31 shows the influence of tertiary air velocity. In these studies the diameter of the tertiary air ports was varied to identify the influence of jet velocity on sorbent utilization. The data indicate that the velocity could be decreased by about 50 percent from the standard case with little

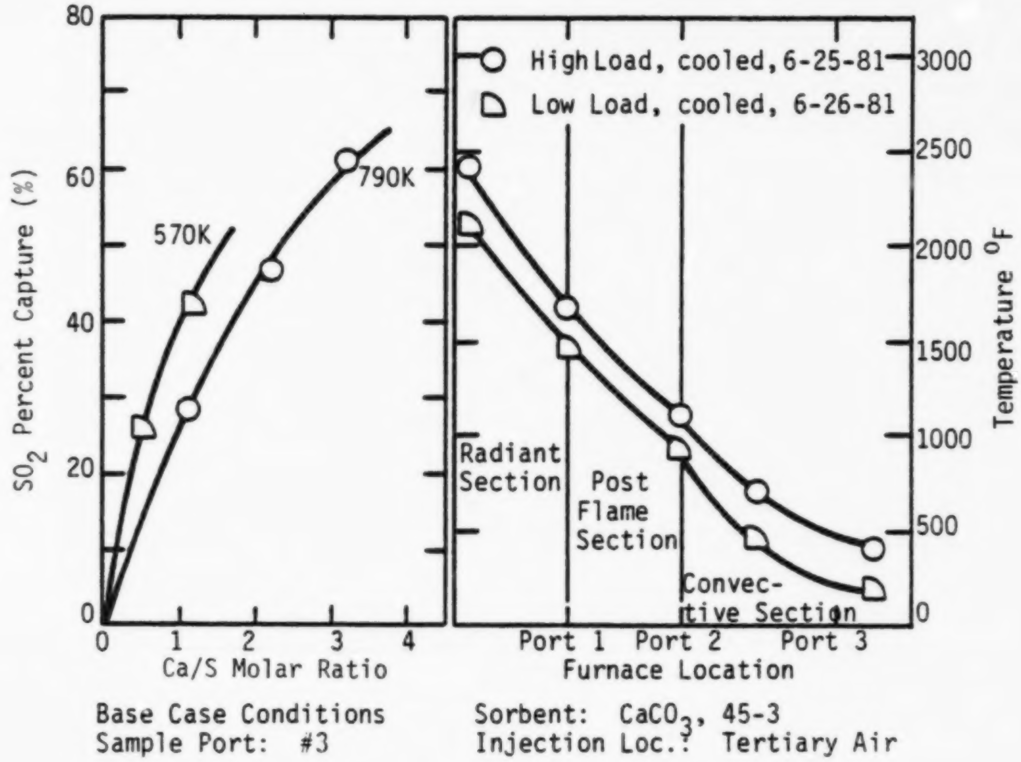

Figure 10-28. Influence of Firing Rate.

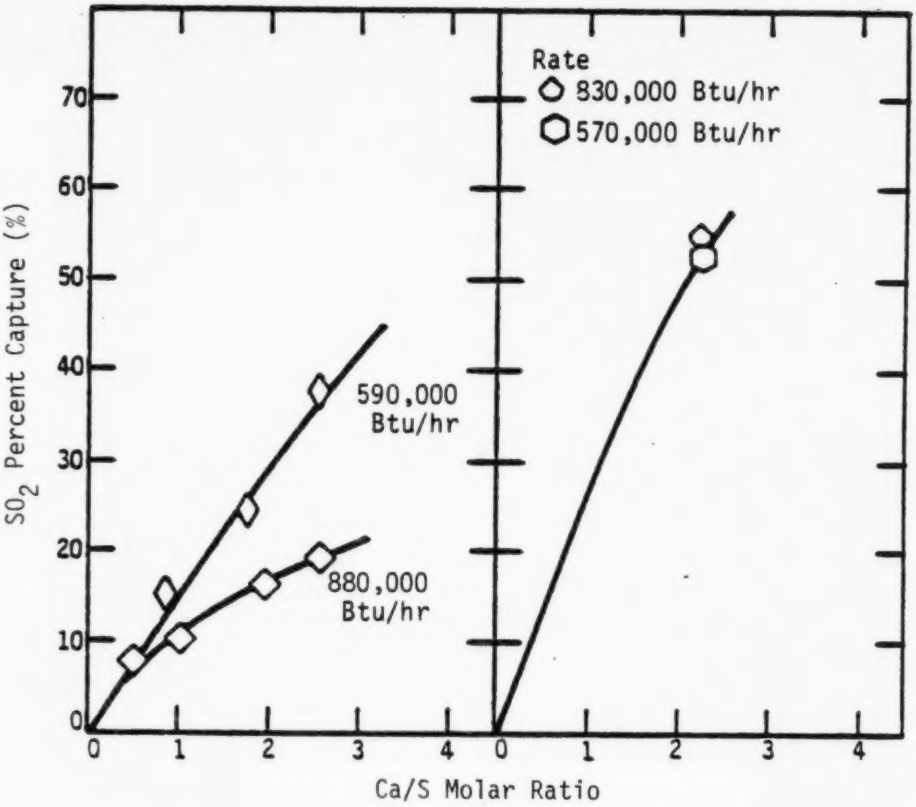

Date: 7/1/, 7/4/81
Rate: As Shown
Cooling: None
SR$_P$: 0.2
SR$_B$: 0.6
SR$_T$: 1.2
Coal: Indiana
Ca/S Mole Ratio: As Shown
Sample Port: #3
Sorbent: CaCO$_3$, 45-3
Injection Loc.: Tertiary Air

Date: 8/14, 8/21/81
Rate: As Shown
Cooling: 13%
SR$_P$: 0.2
SR$_B$: 0.6
SR$_T$: 1.2
Coal: Indiana
Ca/S Mole Ratio: As Shown
Sample Port: #3
Sorbent: CaCO$_3$, 45-3
Injection Loc.: Milled With Coal

Figure 10-29. Influence of Firing Rate - Alternate Conditions.

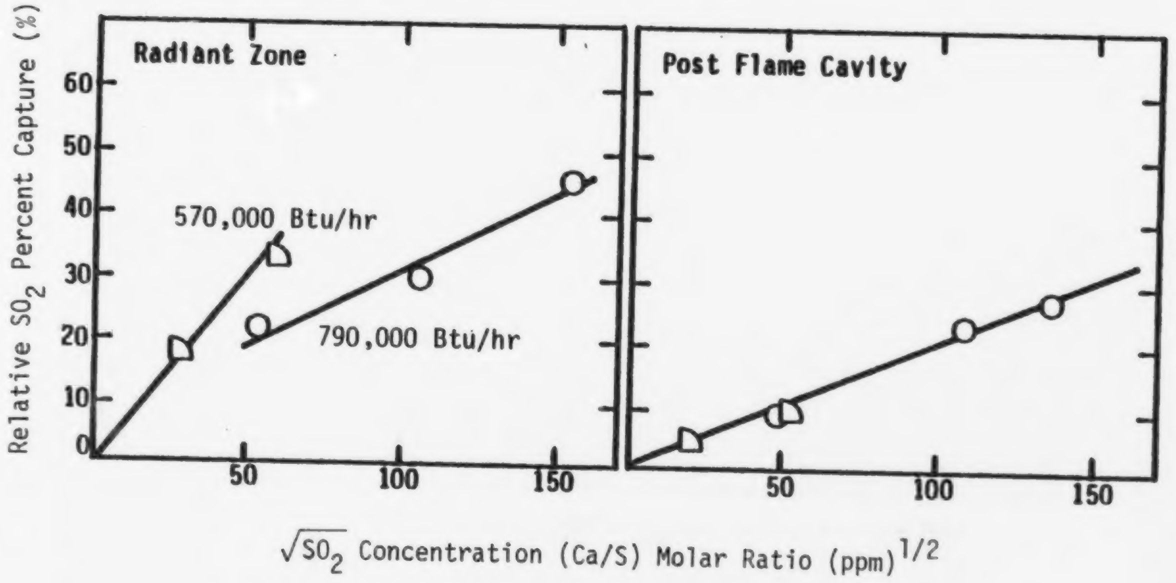

Figure 10-30. Effect of Firing Rate on Zone Capture.

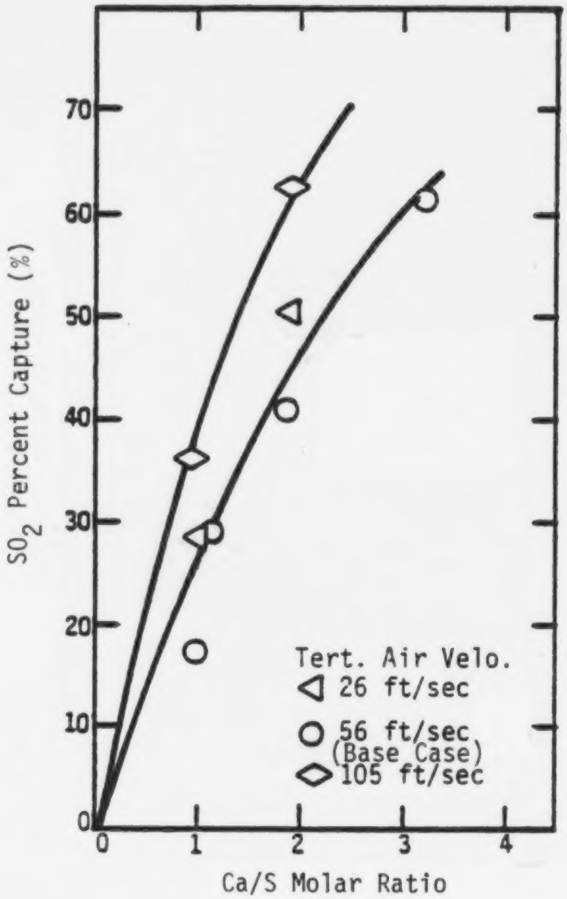

Date: 8/19, 8/20/81
Rate: 800,000 Btu/hr
Cooling: 110,000 Btu/hr
SR$_P$: 0.2
SR$_B$: 0.6
SR$_T$: 1.2

Coal: Indiana
Ca/S Mole Ratio: As Shown
Sample Port: #3
Sorbent: $CaCO_3$, 45-3
Injection Loc.: Tertiary Air
Other:

Figure 10-31. Effect of Tertiary Air Velocity - Base Case Conditions.

effect on the sulfur capture. However, increasing the velocity from the base case conditions significantly increased the sorbent effectiveness. Figure 10-32 shows the effect of tertiary air velocity on the relative zone capture. These results suggest that injecting the sorbent in a high velocity air jet increases the reactivity of the sorbent through the radiant and post flame regions. This increased reactivity may be due to decreased deadburning or to a high surface area produced by rapid calcination.

10.2.3 Combustion Parameter Screening Studies - Externally Staged Conditions (Series A-2)

The purpose of the external staging studies was to determine the effect of first stage (rich zone) stoichiometry on sulfur evolution from the coal and on sorbent utilization. The test matrix for these experiments was shown in Table 6-2. The parameters of interest included:

- Load
- Sorbent Injection Location
- Radiant Zone Cooling
- Fuel (propane versus Indiana coal)

The external staging experiments were performed by adding the fuel and part of the combustion air through the burner and adding the remaining combustion air at the entrance to the post flame section with separate air injectors so that the entire radiant zone was fired fuel rich. Figure 10-33 is a schematic detail of the radiant to post flame transition section in the BSF showing the sorbent and staging air injection locations.

Adding only part of the combustion air at the burner face had a profound impact on the time/temperature history of the sorbent and combustion gases. The data in Figure 10-34 show typical time/temperature profiles for two cases and demonstrates the impact of external staging on the furnace thermal profile. Adding only 60 percent of the combustion air at the burner face results in a lower radiant zone temperature and a much longer radiant zone residence time than when 114 percent of the theoretical combustion air is added at the burner face. The downstream air addition also causes increased post flame and convective section temperatures, because a significant portion of the fuel heat release is taking place in the second stage where burnout occurs.

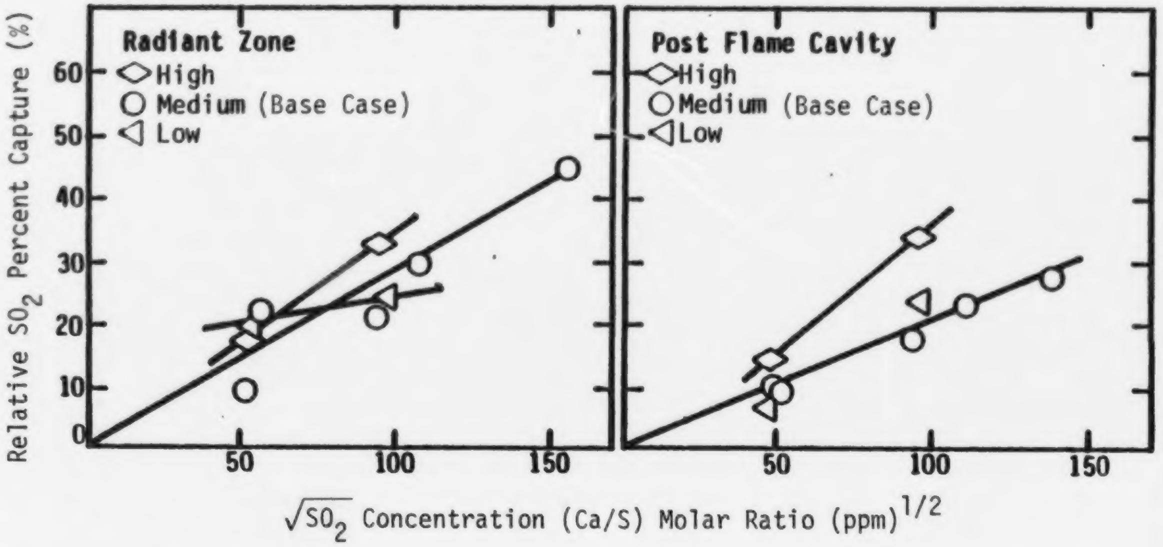

Figure 10-32. Effect of Tertiary Air Velocity on Zone Capture - Base Case Conditions.

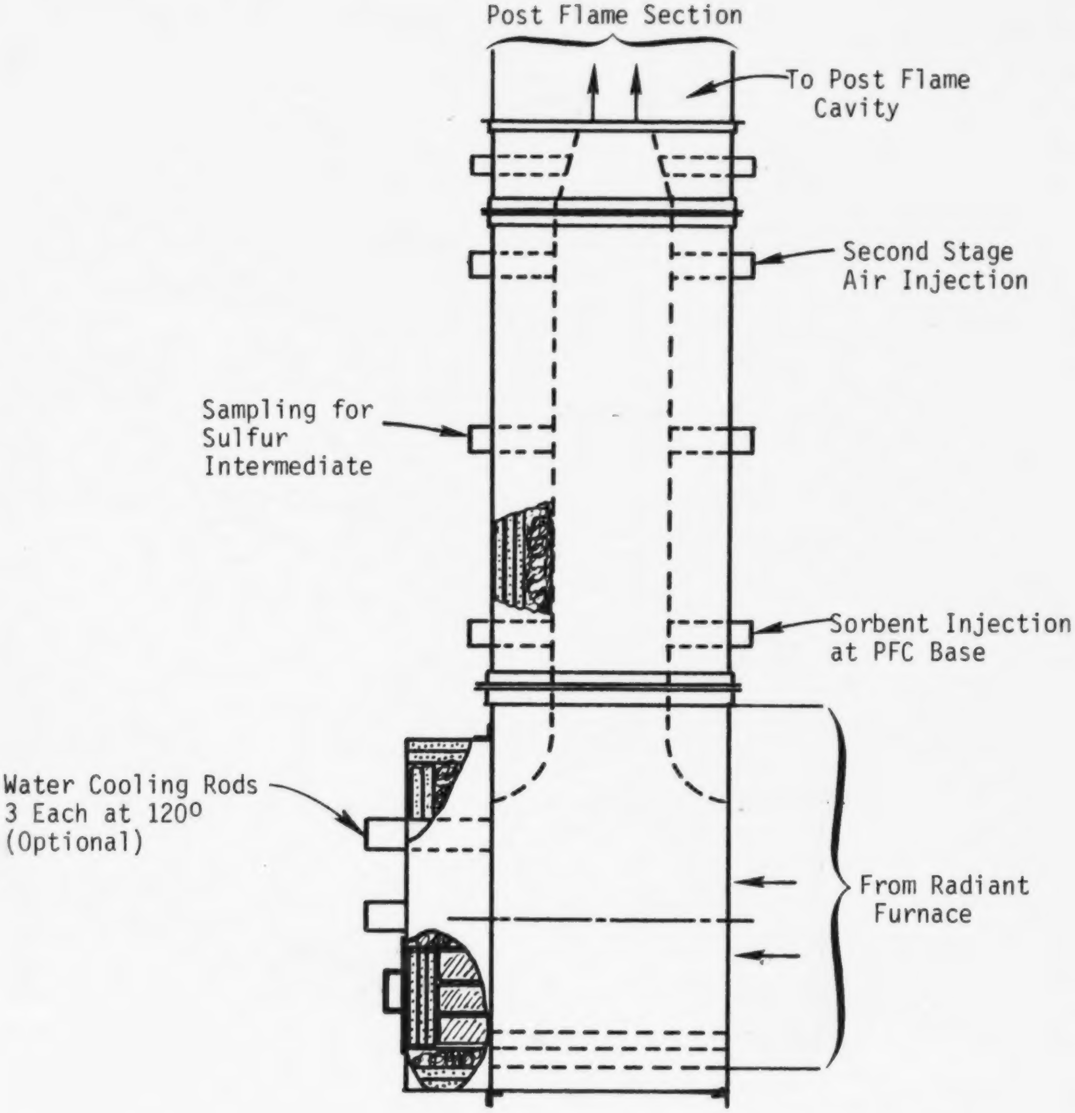
Post Flame Section
To Post Flame Cavity
Second Stage Air Injection
Sampling for Sulfur Intermediate
Sorbent Injection at PFC Base
Water Cooling Rods 3 Each at 120°
(Optional)
From Radiant Furnace

Figure 10-33. Detail of Boiler Simulator Furnace - External Staging Schematic.

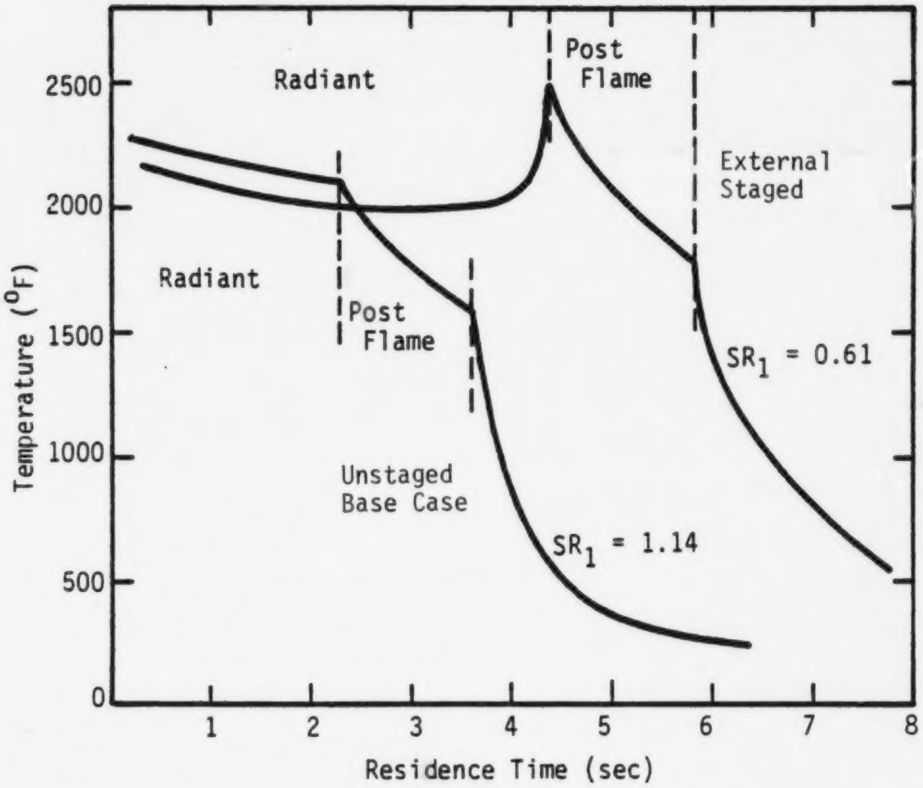

External Staging

Coal: Indiana
Rate: 800,000 Btu/hr
SR_1: Shown
SR_T: 1.15
Ca/S: ---

Sample Port: Shown
Sorbent: None
Injection Loc.: ---
Cooling: Yes

Figure 10-34. Impact of External Staging on Thermal Environment, BSF.

The first stage stoichiometry also affected the amount and form of sulfur found in the gas phase in the fuel rich zone. Figures 10-35, 10-36 and 10-37 show the total gaseous sulfur (based on the sum of the sulfur species measured and the theoretical gas phase sulfur) measured in the rich zone and the measured sulfur species distribution as a function of first zone stoichiometry. It is clear that both rich zone stoichiometry and thermal environment affect the gasification efficiency of the sulfur and the sulfur species distribution in the rich zone. The measured species distributions are non-equilibrium. Equilibrium calculations predict essentially all SO_2 under fuel lean conditions ($SR > 1.0$) and all H_2S under fuel rich conditions ($SR < 1.0$).

The gas phase sulfur species in the rich zone were measured by extracting a gas sample from the furnace, diluting the sample with pure oxygen and running the resulting mixture through the continuous H_2S converter discussed in Section 8. A batch sample of the diluted stream was taken in a glass sample bottle and injected into the sulfur - GC system (also discussed in Section 8). Originally, the GC samples were intended as back up for the continuous H_2S system, but when it was discovered that a significant amount of the sulfur in the rich zone was neither H_2S nor SO_2 (as predicted by the equilibrium calculations), the GC measurements of sulfur species became the primary sulfur measuring tool for the rich zone. It should be remembered throughout the following discussion that the GC measurements are difficult and that the batch sampling/dilution system imparts a significant sampling error to the results. More refined and reliable methods for the rich zone measurements are being developed.

The data in Figure 10-38 show the influence of first stage stoichiometry on sulfur capture and post flame cavity (pfc) temperature (wall temperature at the exit of the pfc). As was mentioned earlier, staging the combustion air changes the fuel heat release pattern and, therefore, the furnace temperature profile. The increased post flame cavity temperatures at low SR_1's were not surprising, but the observed decrease in sulfur capture was not expected. The drop in sorbent utilization at highly staged conditions may be due to sorbent deactivation by the second stage flame high regeneration (decomposition of reacted sorbent from CaS to CaO + SO_2), again because of the high second stage flame temperatures, or to the changed sulfur evolution pattern (large amounts of sulfur being evolved in the second stage) affecting sulfur capture.

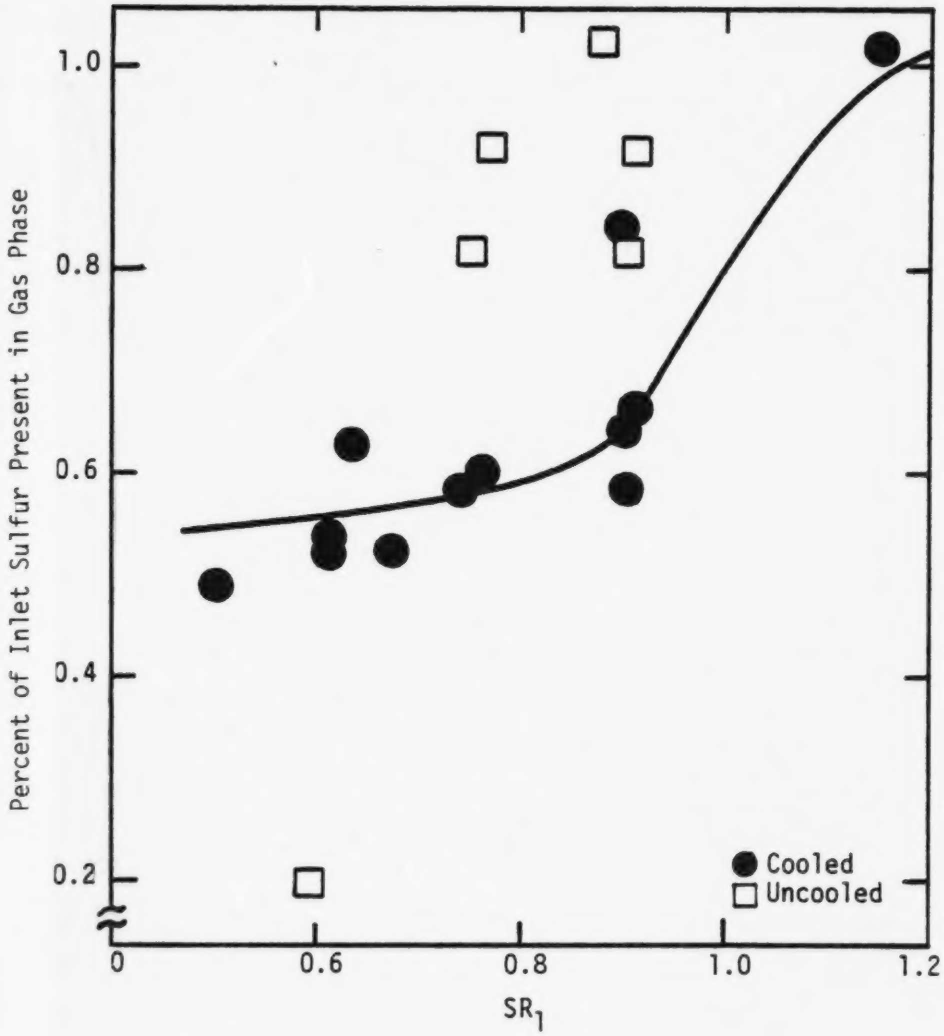

External Staging

Coal: Indiana
Rate: 800,000 Btu/hr
SR_1: Shown
SR_T: 1.2
Ca/S: ---

Sample Port: #1
Sorbent: None
Injection Location: ---
Cooling: Shown

Figure 10-35. Effect of First Stage Stoichiometry on Sulfur Evolution from Indiana Coal.

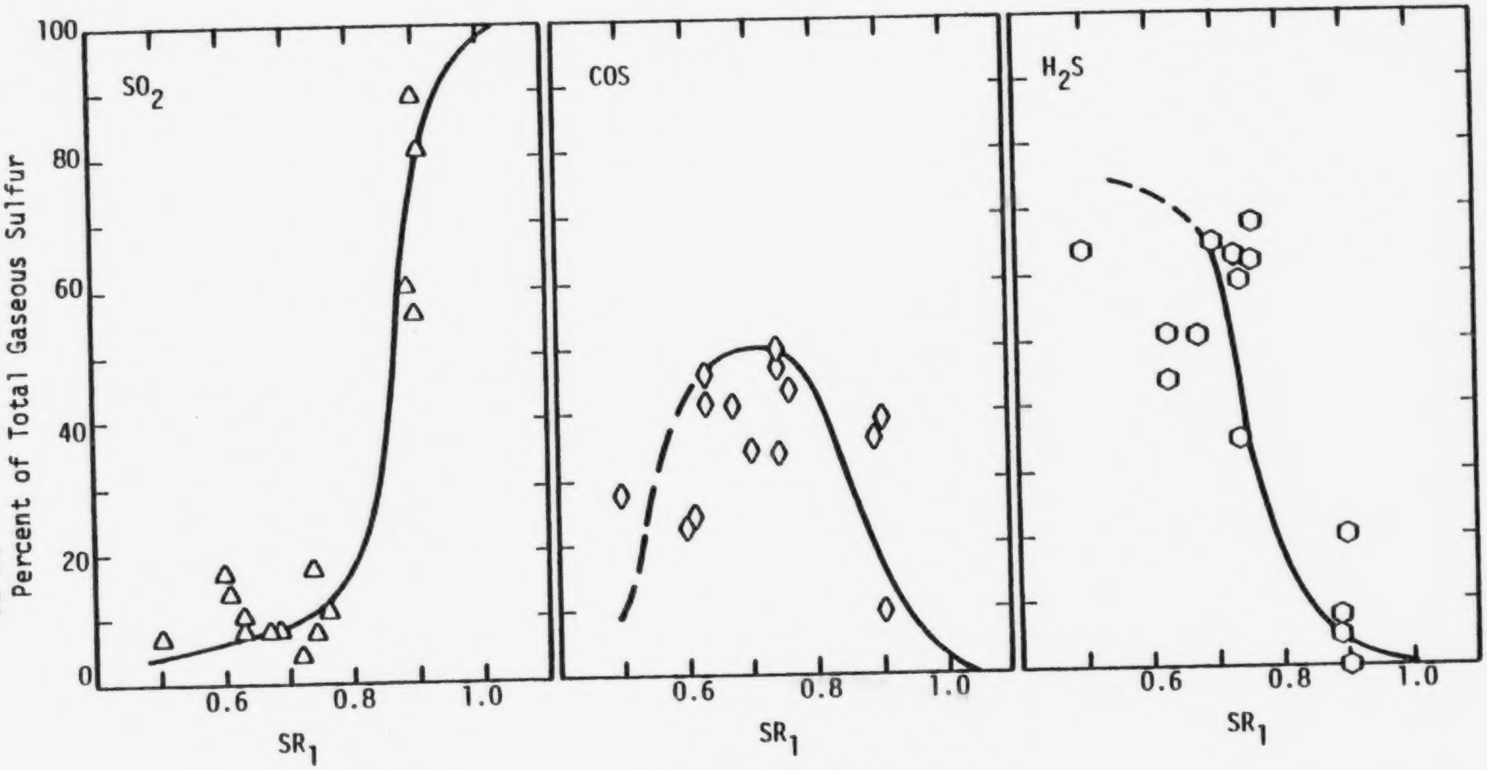

External Staging

Coal: Indiana
Rate: 800,000 Btu/hr
SR_1: Shown
SR_T: 1.2
Ca/S: ---

Sample Port: #1
Sorbent: None
Injection Location: ---
Cooling: Yes
2nd Stage Air: Trans Top

Figure 10-36. Effect of First Stage Stoichiometry on Sulfur Species Distribution, Cooled.

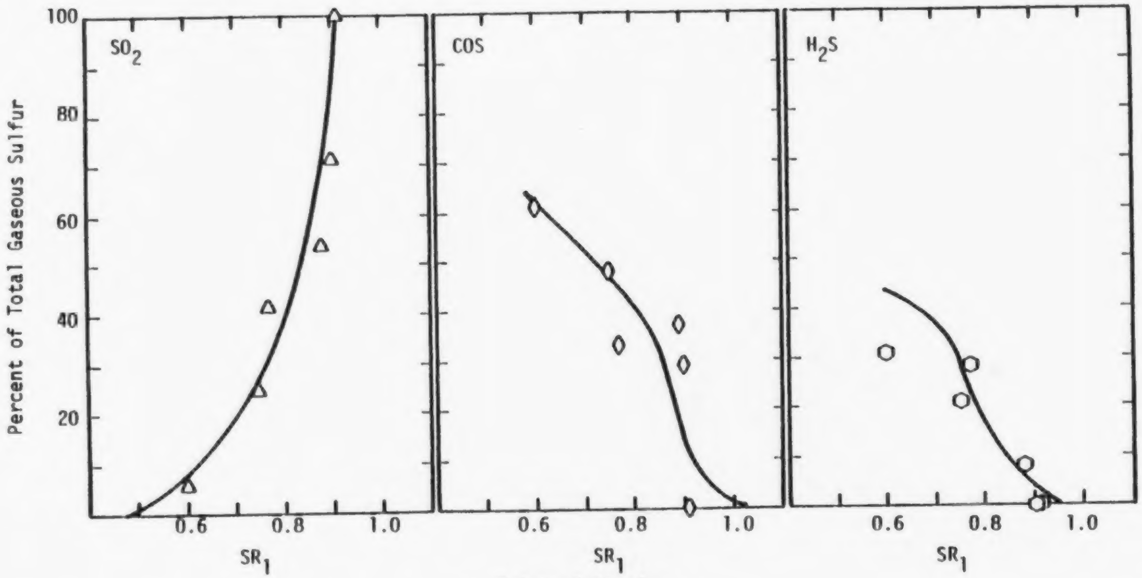

External Staging

Coal: Indiana
Rate: 800,000 Btu/hr
SR_1: Shown
SR_T: 1.2
Ca/S: ---

Sample Port: #1
Sorbent: None
Injection Location: ---
Cooling: No

Figure 10-37. Effect of First Stage Stoichiometry on Sulfur Species Distribution - Uncooled.

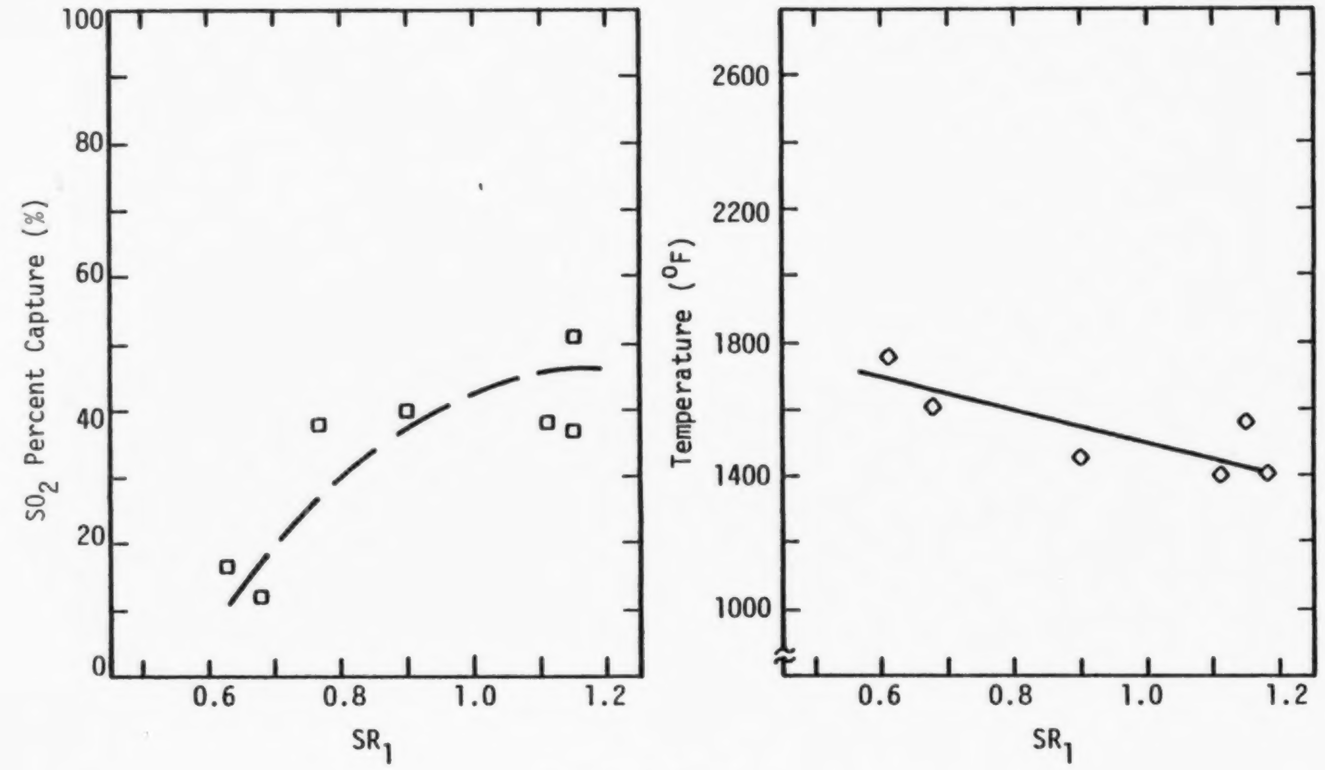

External Staging

Coal: Indiana
Rate: 800,000 Btu/hr
SR_1: Shown
SR_T: 1.2
Ca/S: 2.1

Sample Port: #3
Sorbent: $CaCO_3$, 45-3
Injection Location: Primary Air
Cooling: Yes
2nd Stage Air: Trans Top

Figure 10-38. Effect of First Stage Stoichiometry on Sulfur Capture and Post Flame Temperature.

The limited amount of data generated on individual sulfur species capture by sorbent in first stage is shown in Figure 10-39. The data can only be interpreted in a general manner (as they are based on very few measurements in a highly scattered data set) and indicate that no single species is more favorably captured.

The data in Figures 10-40, 10-41 and 10-42 show the effect of injecting the sorbent into the furnace in different manners on sorbent utilization. The data in Figure 10-40 can be used to compare the effectiveness of injecting the sorbent with the coal in the primary air and injecting the sorbent in an inert carrier gas (N_2) at the base of the post flame section. The results were somewhat surprising. We expected that injecting the sorbent at the base of the post flame cavity, before the staging air, would provide ideal conditions for a fast direction reaction between $CaCO_3$ and H_2S, which, in turn, would give high sorbent utilization. The sorbent utilization for this injection mode was significantly lower than for sorbent injection with the coal. There are several possible explanations for this, including: the reaction time was decreased because sorbent injected at the base of the post flame cavity, the injection mode (with N_2) gave poor mixing and/or poor calcination of the sorbent, or the sulfur had not yet evolved from the coal to react with the sorbent.

The data in Figure 10-40 can also be used to indicate the effect of cooling on sorbent utilization. When the sorbent was added with the coal, cooling the radiant section had only a slight impact on sorbent utilization, while in the internally staged (DMB) conditions cooling the radiant furnace dramatically increased sulfur capture.

The data shown in Figure 10-41 are used to compare the effectiveness of injecting the sorbent with the staging air instead of with the coal in the primary air. The observed sulfur capture was similar for the two injection modes. The decreased sorbent residence time in the staging air injection experiments did not decrease sulfur capture, perhaps because a significant portion of the coal sulfur is not available (in the gas phase) for capture until after the second stage flame.

The observation that sorbent injection into the staging air gave surprisingly high sulfur capture instigated an experiment where the sorbent was injected with air rather than nitrogen at the base of the post flame section.

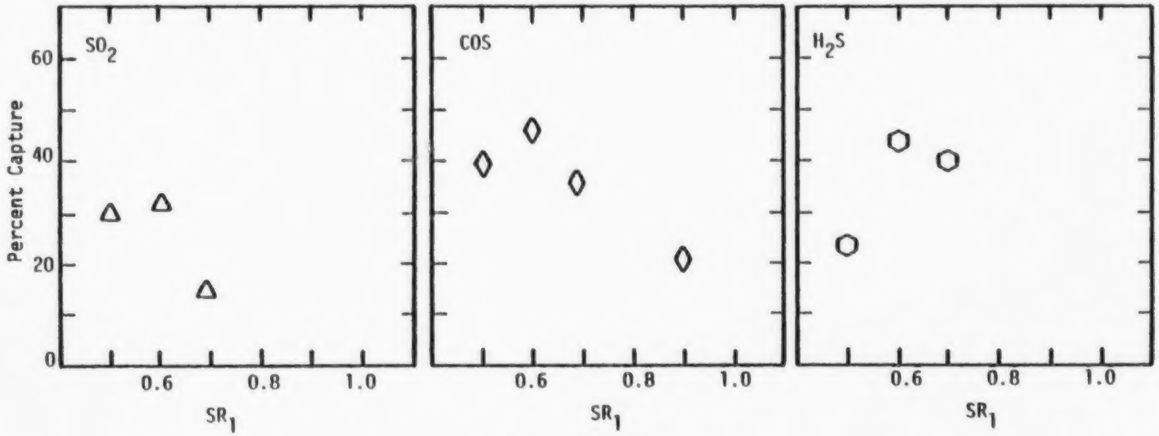

External Staging

Coal: Indiana
Rate: 800,000 Btu/hr
SR_1: Shown
SR_T: 1.2
Ca/S: 2.1

Sample Port: #1
Sorbent: $CaCO_3$, 45-3
Injection Location: Primary Air
Cooling: Yes
2nd Stage Air: Trans Top

Figure 10-39. Effect of First Stage Stoichiometry on Individual Sulfur Species Captures.

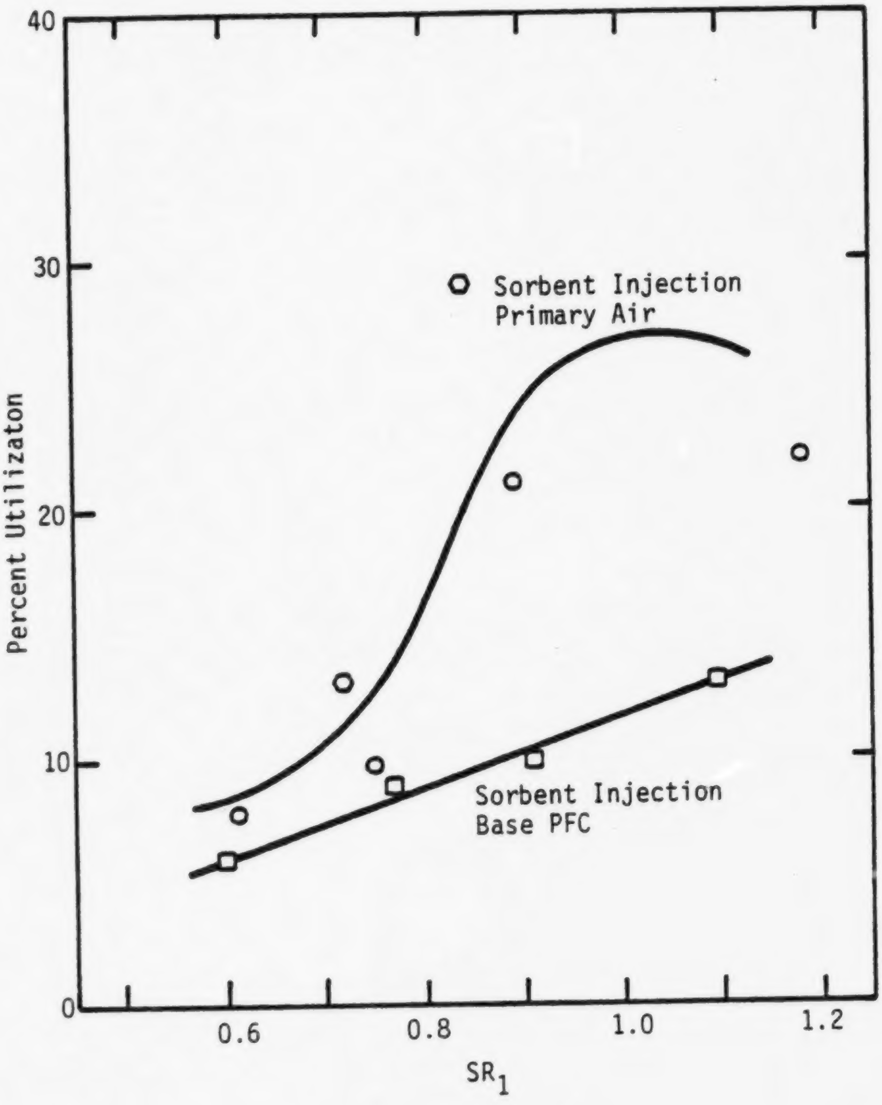

External Staging

Coal: Indiana
Rate: 800,000 Btu/hr
SR_1: Shown
SR_T: 1.2
Ca/S: 2.0 - 3.3

Sample Port: #3
Sorbent: $CaCO_3$, 45-3
Injection Loc.: Shown
Cooling: No
2nd Stage Air: Trans Top

Figure 10-40. Effect of Sorbent Injection Method on Sorbent Utilization.

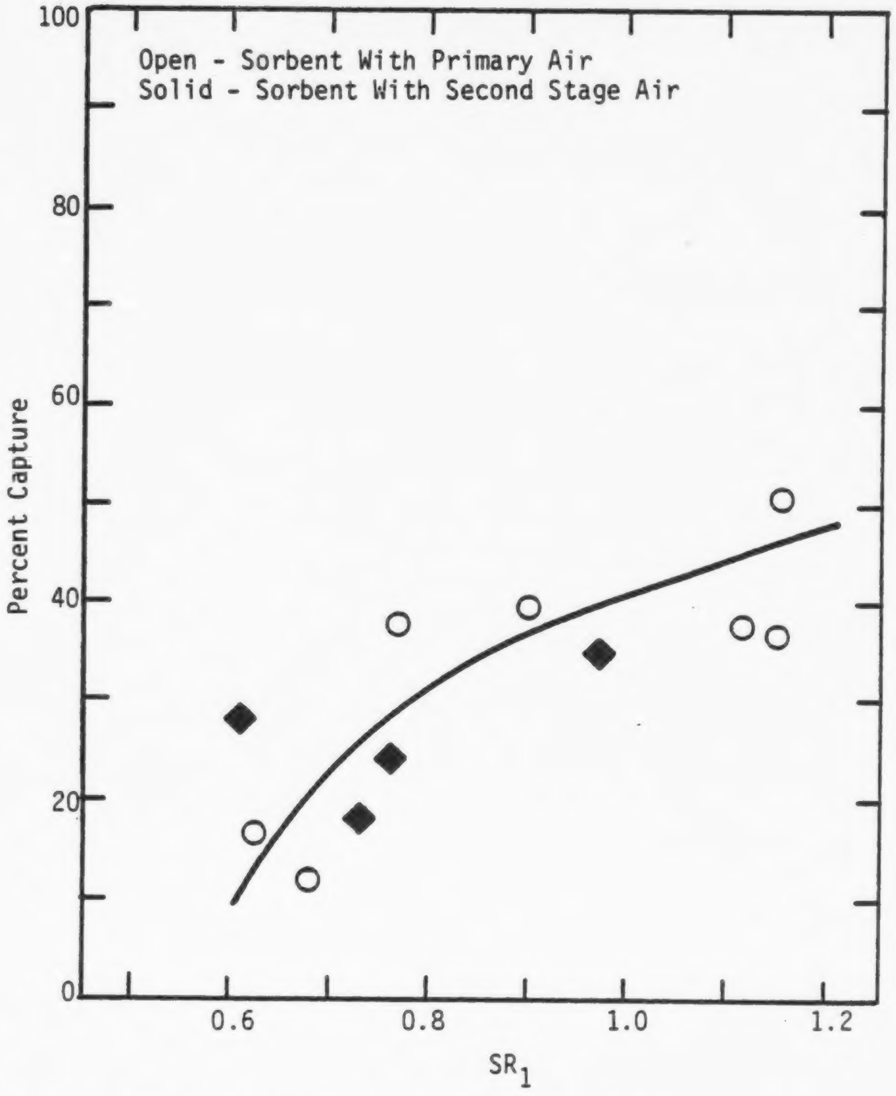

Coal: Indiana
Rate: 800,000 Btu/hr
SR_1: Shown
SR_T: 1.2

Ca/S: 2.1
Sample Port: #3
Sorbent: $CaCO_3$, 45-3

Figure 10-41. Effect of Sorbent Location on Sulfur Capture. Externally Staged, Cooled.

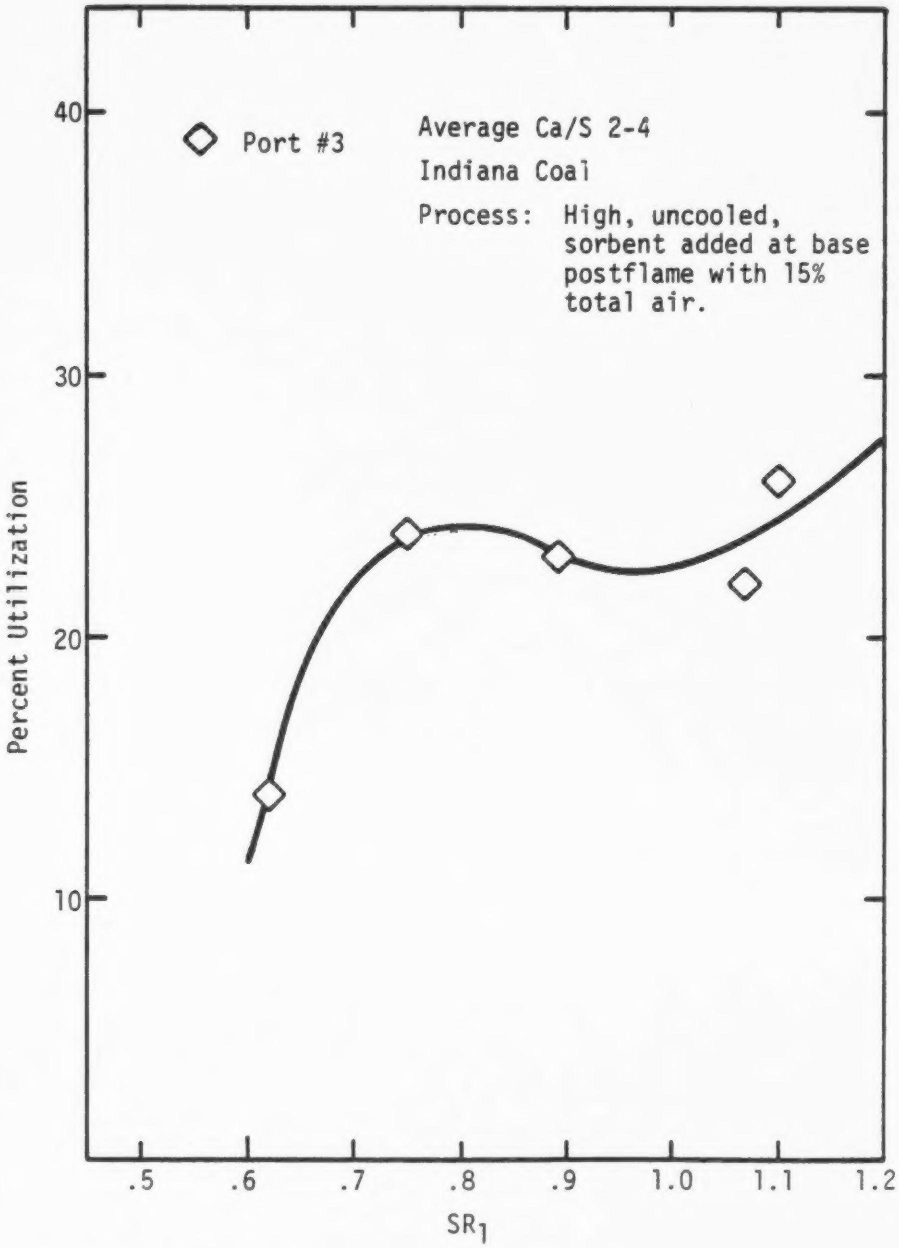

Figure 10-42. Effect of SR_1 on Sorbent Utilization, Sorbent Added With Air at Base of P.F.C.

Overall sorbent utilization is plotted as a function of first stage (not including the sorbent injection air) stoichiometry in Figure 10-42. At stoichiometries greater than 0.9 sorbent utilization for this injection mode are as high as when the sorbent was injected with the coal. Moreover, at lower rich zone stoichiometries sorbent utilization did not drop off as much as it did when injected with the coal. This difference may be the results of two factors: when the staging air is added in two portions the second stage flame and coal burnout region is "smeared", this smearing may result in a cooler second-stage, post flame cavity (reducing sulfur regeneration and/or sorbent deadburning). Also, the spread out char burnout may result in more of the coal sulfur being evolved where active sorbent is available.

Reducing the furnace load while firing with external staging reduced overall sorbent utilization as can be seen from the data plotted in Figure 10-43. Again, this result is different than that obtained under internally staged conditions. The reduction in sorbent utilization may be due to the lower sulfur availability (because of char sulfur retention) in the first stage.

The problem of char sulfur retention was further investigated by comparing sorbent utilization for coal fired conditions with sorbent utilization for propane doped with H_2S firing. Figure 10-44 shows data collected on sorbent utilization for propane + H_2S firing. The sorbent utilization does not drop at low first stage stoichiometries as it did in the coal fired experiments. Figure 10-45 shows the overall sorbent utilization for the propane fired condition compared with the most similar coal fired case. The data for the coal fired condition have been corrected to actual gas phase stoichiometry (since part of the fuel is still solid in the first stage) for comparison with the propane data.

The bench-scale studies of sorbent injection for SO_2 control are incomplete at this time. Experiments investigating the effect of sulfur capture under fuel-rich conditions in gas flames, further study of the effect of physical staging on sulfur capture for coal flames, further study of the effect of thermal environment on sulfur capture under fuel-rich and fuel-lean conditions, and investigation of the effect of fuel and sorbent type on sulfur capture are planned (as discussed in Chapter 6) and will be performed in the next year.

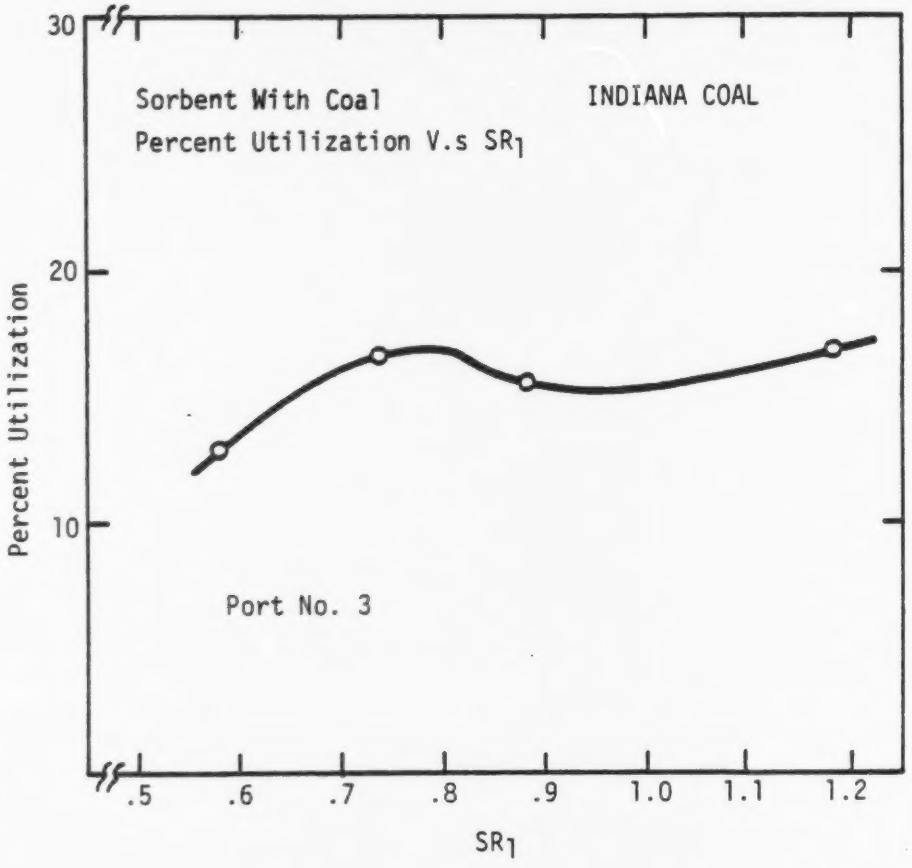

Figure 10-43. Effect of SR_1 on Sorbent Utilization Low Load, Uncooled.

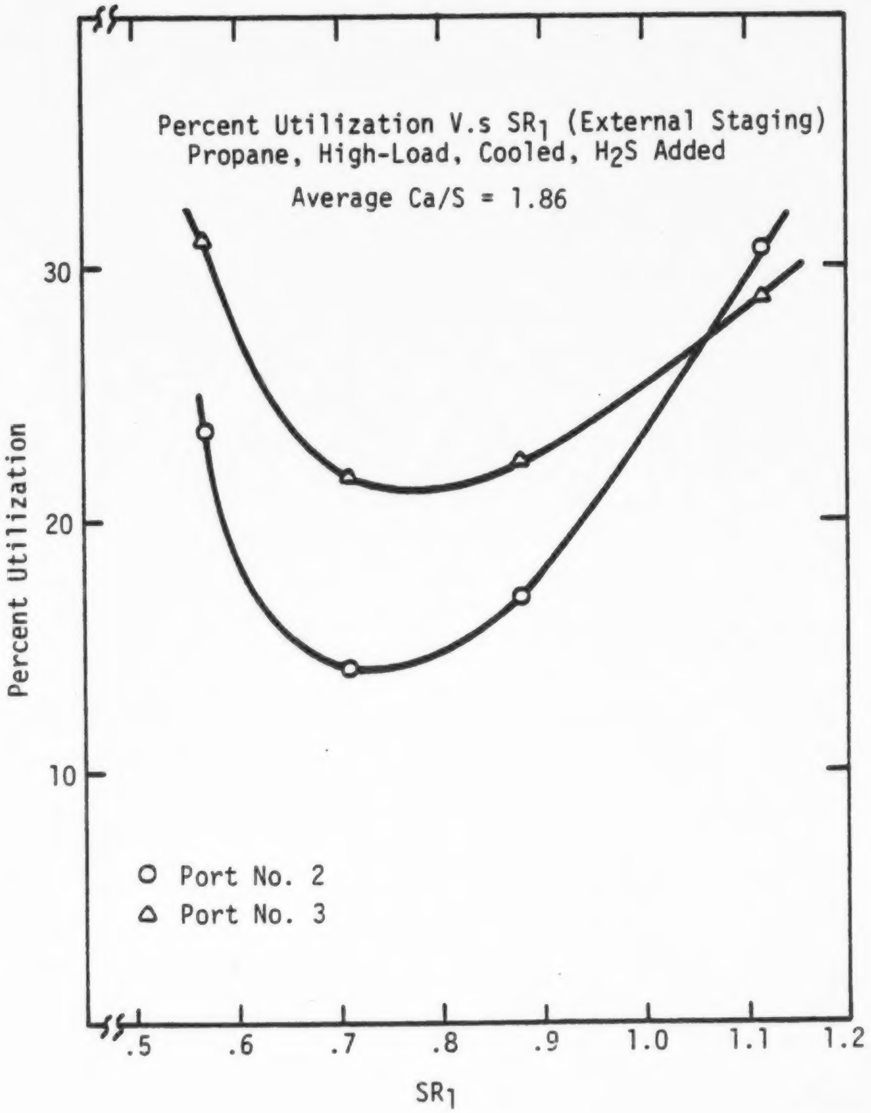

Figure 10-44. Effect of SR_1 on Sorbent Utilization for Propane Doped With H_2S (2500 ppm Equivalent Exhaust SO_2).

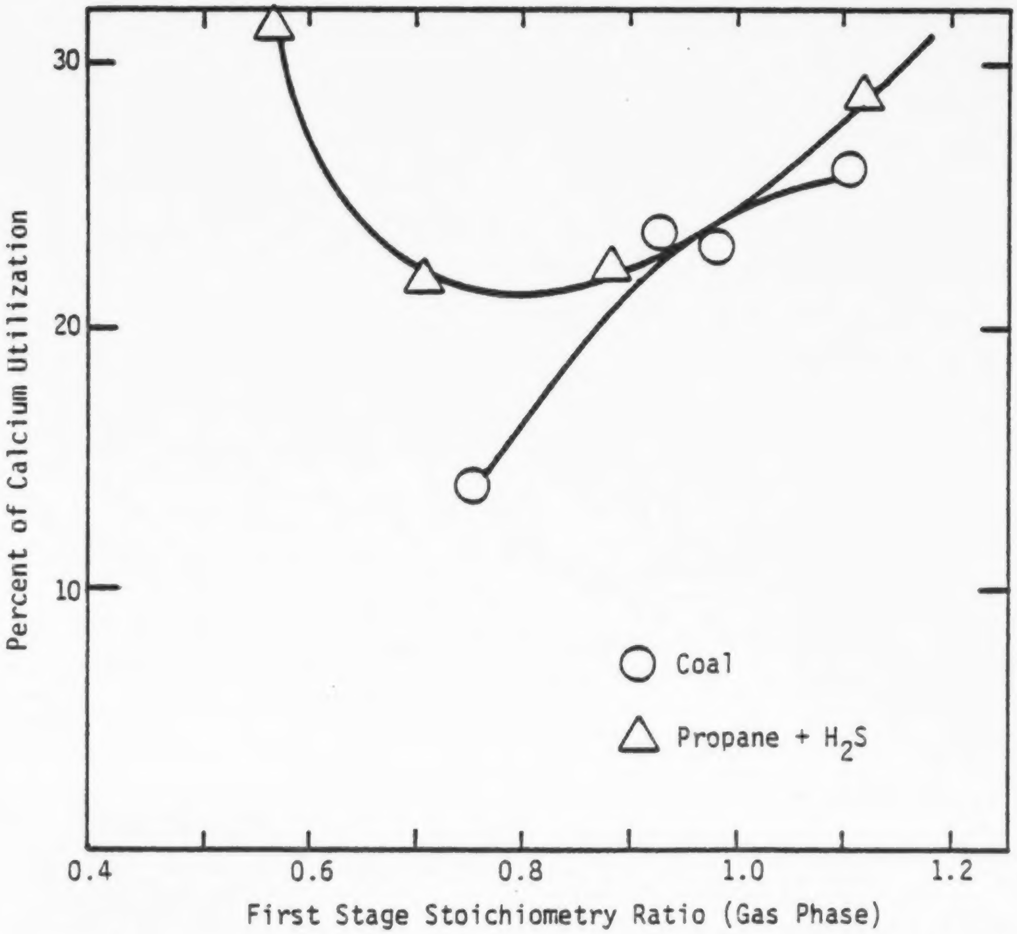

Figure 10-45. Capture and Retention of Sulfur Under External Staged Conditions for Coal and Propane Doped With H_2S, Sorbent Added With Air at Base of Post Flame Section, Uncooled.

11.0 CONCLUSION

This report covers progress achieved during the fourth contractural year of EPA Contract 68-02-2667. Current results of studies investigating the use of the direct injection of dry sorbents for SO_2 control are reviewed, experimental work at both pilot and bench-scale is presented, and the design, construction and testing of a new bench-scale facility for the study of sorbent injection for SO_2 control is discussed. Further experimental work at pilot and bench-scale, investigating both NO_x control and SO_2 control, is planned for the next contractural year.

11.1 Pilot-Scale Results, No_x and SO_x Control

Two low No_x distributed mixing type burners were tested in the large watertube simulator (LWS) to determine the effect of various operational and fuel related parameters on NO_x emissions. The results obtained with these burners in the LWS are compared with results obtained in other facilities in Figures 11-1, 11-2 and 11-3. In general, even though absolute levels of NO_x emissions were different in the different facilities the effect of burner zone stoichiometry (Figure 11-1), overall excess air (Figure 11-2), and load (Figure 11-3) are similar. The effect of these operating parameters was also independent of coal type although, again, the absolute levels of NO_x emissions were different for the different coals in the same facility (the LWS). In general, increased load, increased excess air and increased burner zone stoichiometry (decreased staging) all increased NO_x emissions for all the coals in the facilities compared. NO_x emission characterization of the EPA prototype distributed mixing burner was performed under EPA Contract 68-02-3921 and is described in detail in that report. In general, the effects of burner zone stoichiometry, excess air level and load on NO_x emissions were similar to those observed with the Steinmüller burner, again baseline NO_x emissions for the different coals were different and NO_x emission levels for the same coal were slightly different for the two burners.

In addition to the characterization of NO_x emissions a series of experiments was carried out with both burners to determine the potential for SO_2 removal by direct injection of calcium-based sorbents. These studies were carried out without modifying either burner and only at conditions which were

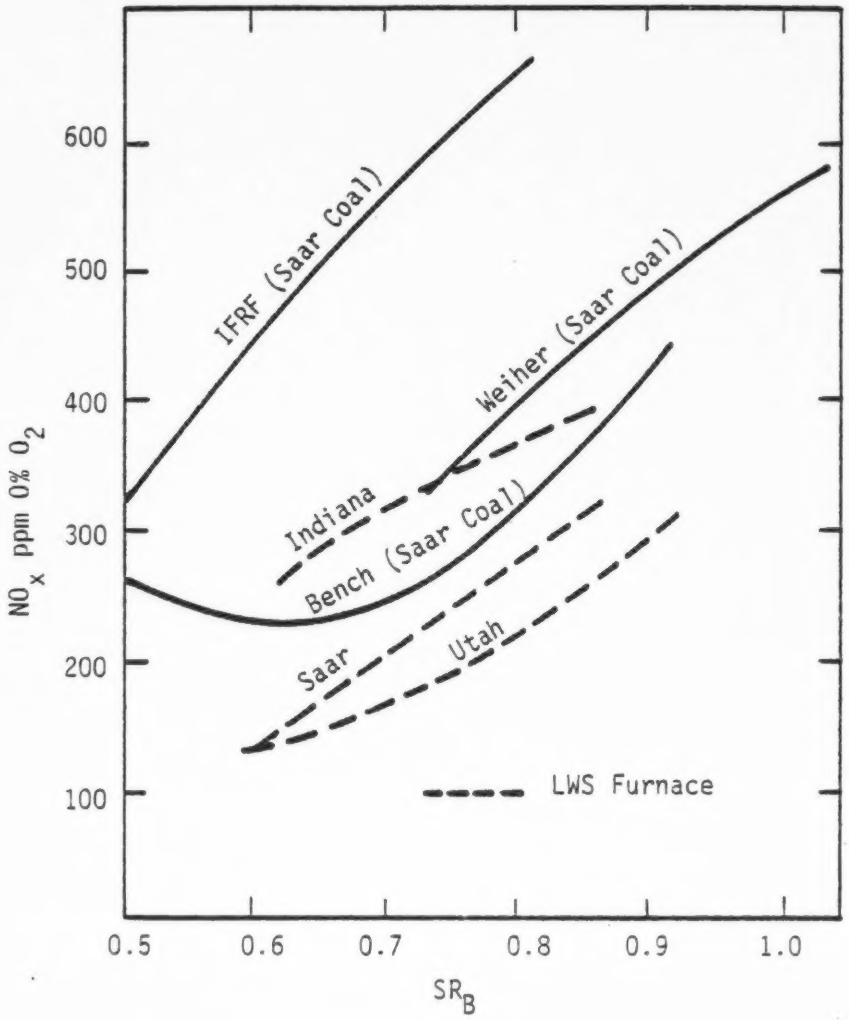

Figure 11-1. Effect of Burner Zone Stoichiometry on NO_x Emissions ~ Comparison of Data, Steinmüller Burner.

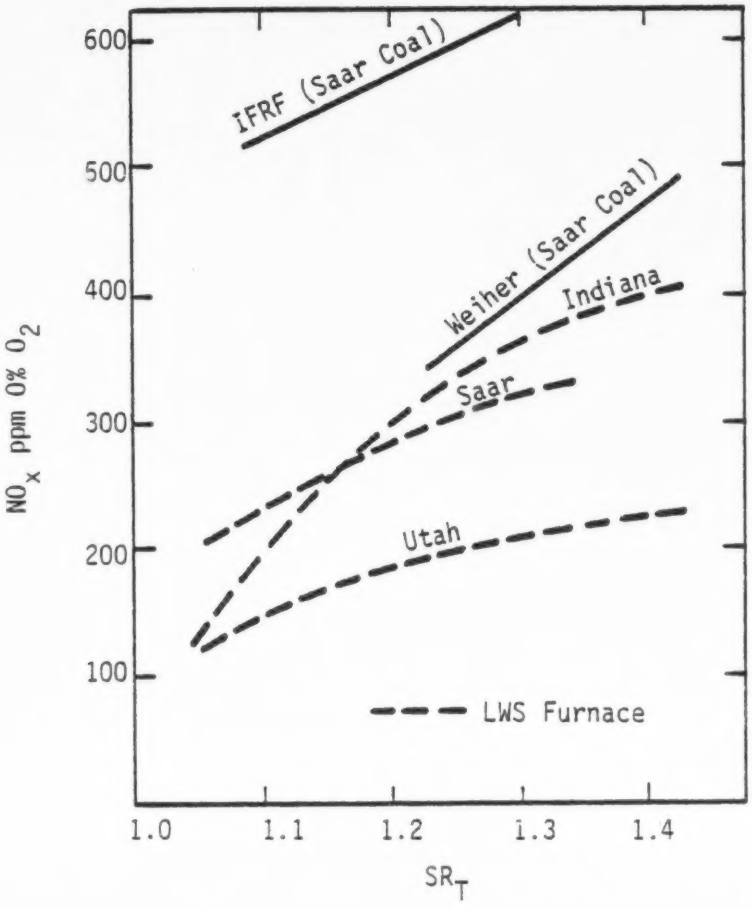

Figure 11-2. Effect of Excess Air on NO$_x$ Emissions - Comparison of Data, Steimuller Burner.

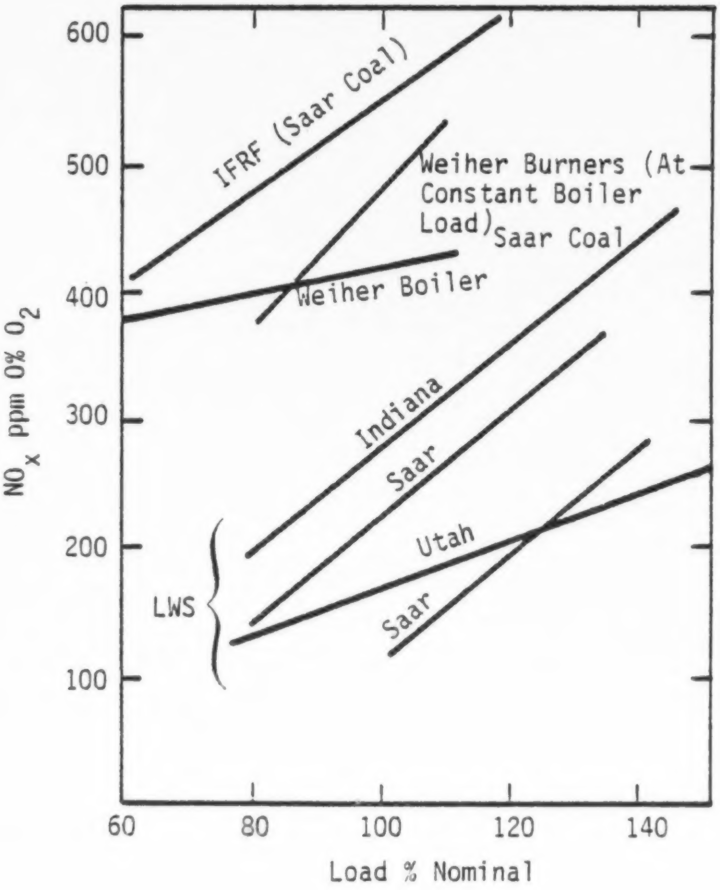

Figure 11-3. Effect of Load on NO$_x$ Emissions ~Comparison of Data, Steinmüller Burner.

optimized for NO_x emissions. No attempt was made to optimize the firing system for sulfur capture. Results of the sorbent injection tests in the two burners indicate that sorbent type ($Ca[OH]_2$ or $CaCO_3$) and injection location (with fuel or staging air) had small effects on the sulfur capture in either burner. The effect of sorbent location was more pronounced with the prototype burner and appears to be a result of changes in sorbent thermal history. The data also indicate that sulfur capture increases with coal sulfur content. The data in Figure 11-4 summarize results from studies with the EPA prototype and Steinmüller burners in several furnaces. Results from Steinmüller tests in the LWS and in the IFRF furnace are included along with data from the prototype burner. Comparing the prototype and Steinmüller LWS results using Indiana coal, it is seen that the prototype burner resulted in higher sulfur capture even though the burners were operated at comparable conditions. This is perhaps indicative of the influence of burner design conditions. The prototype-burner LWS results with Utah coal and the low sulfur coal IFRF test results show good general agreement. This indicates that burner effects may be unimportant for low sulfur coals; all of these results are from burners which were not optimized for SO_2 cpature, and therefore, should be treated with caution.

The good agreement between the LWS data for Indiana coal and the IFRF data with the high sulfur coal is somewhat surprising in light of the higher furnace temperature (1000°C vs 600°C in the LWS) employed at IFRF.

In general, the pilot-scale tests indicate the need for more definitive assessments of the parameters controlling SO_2 capture via dry sorbents. Specifically, studies should focus on the potential for application of this technology in field boilers, and the optimum burner design and operating parameters required to maximize sulfur capture without affecting NO_x emissions or boiler efficiency. Further studies of sorbent injection for SO_2 control are planned for several pilot-scale furnaces and using two burners in the next year as a continuation of the 2667 contract effort.

11.2 Bench-scale Results, Parametric Screening Studies of Sorbent Injection for SO Control

The bench-scale results indicate that thermal environment is the major furnace parameter affecting sulfur capture under fuel-lean conditions. Results summarized in Figure 11-5 show sulfur capture in the radiant and post-flame

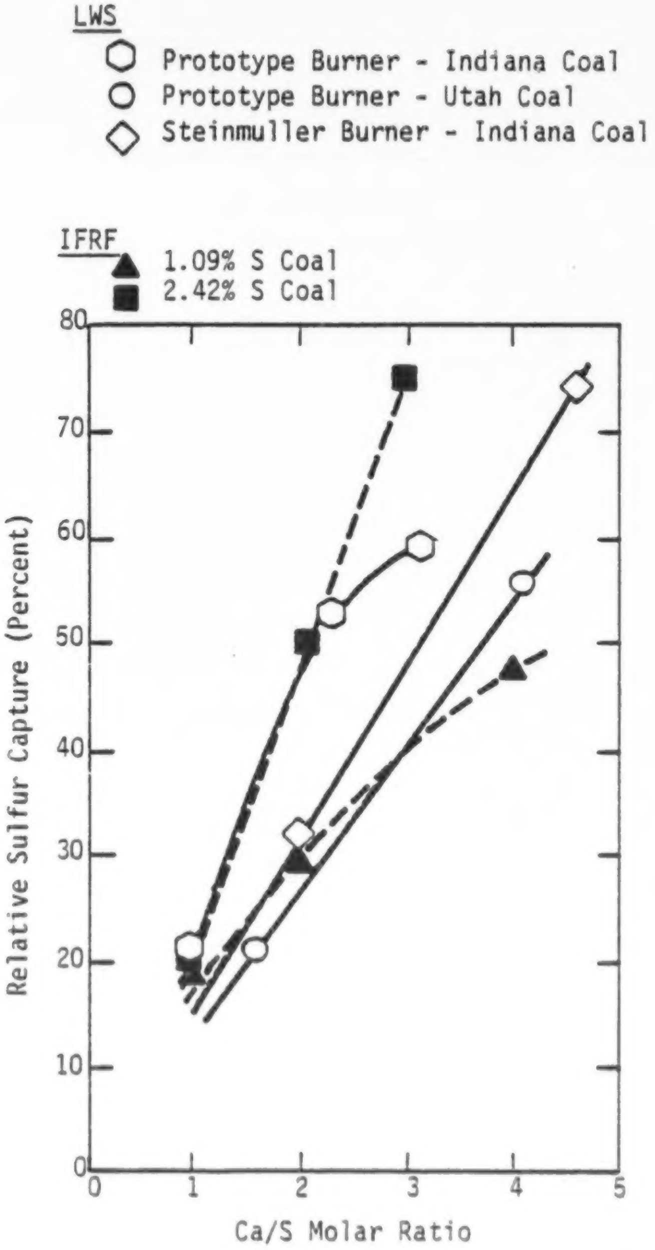

Figure 11-4. Comparison of Steinmuller and DMB Data - Limestone Injected in Tertiary Ports.

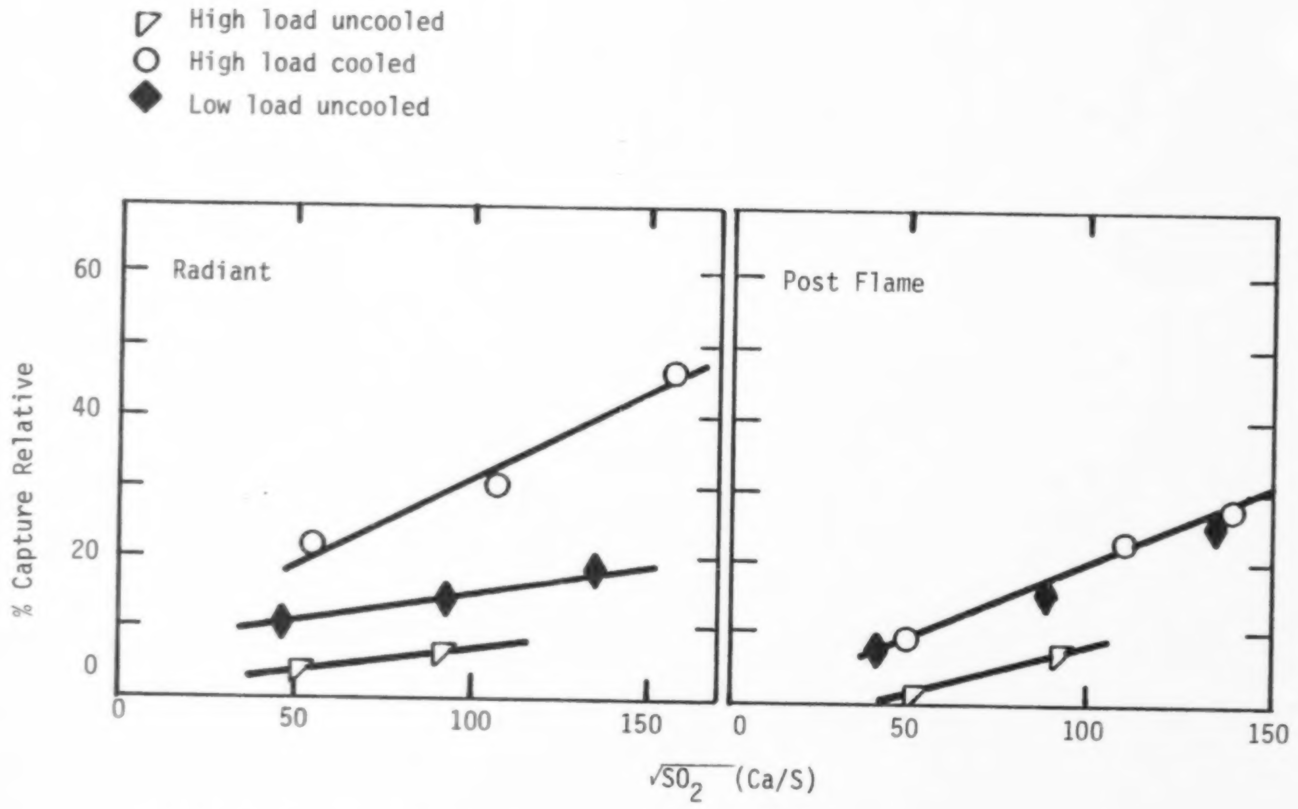

Figure 11-5. The Effect of Load and Radiant Zone Cooling on Sulfur Capture.

sections of the BSF as a function of Ca/S $\sqrt{SO_2}$ in each zone. Three conditions are shown: High firing rate, with and without radiant zone cooling; and low load without cooling. Reducing the firing rate reduced the temperatures and increased the residence times. Cooling the radiant zone decreased peak temperatures with little effect on the residence times. Radiant zone cooling dramatically increased capture, the low-load conditions gave relatively poor capture in the radiant zone, but both reduced-temperature cases (cooled and low-load) gave approximately the same capture in the post-flame section.

Sulfur capture under fuel-rich conditions was evaluated using both the Indiana coal and propane/H_2S as fuels. Sulfur capture appears to be proportional to sulfur species driving force to the 1/2-power. The increase in sulfur species concentration under fuel-rich conditions (due to reduced dilution) should benefit sulfur capture. Figure 11-6 summarizes data on the sulfur species distribution as a function of stoichiometric ratio based on equilibrium calculations (free energy minimization) and on actual experimental measurements of the gas phase near the end of the fuel-rich zone. The equilibrium calculations indicate that for stoichiometries below 0.95 H_2S is the only species of importance. However, data from propane/H_2S and Indiana coal measurements demonstrate that a wide spectrum of reduced sulfur species are present under these conditions. With the propane air flames, SO_2 was significantly more important at rich conditions than would have been anticipated from equilibrium calculations and both COS and CS_2 were non-negligible. The data in Figure 11-6b indicate that with the Indiana coal the gas phase species distribution was non-equilibrium and that a significant amount of coal sulfur remained in the solid phase. These results emphasize two problems associated with sulfur capture under fuel-rich conditions: SO_2 concentrations may be non-negligible and a large fraction of the sulfur may remain in the solid phase. Tests will be carried out in the next year with propane/H_2S in an attempt to separate the effects of sulfur evolution from the coal, and capture from the gas phase.

A further complication of the sulfur capture process under fuel-rich conditions is due to the impact of the physical staging method, used to obtain long residence times under fuel-rich conditions, on the thermal characteristics of the experimental system. The data presented in Figure 11-7 was obtained with

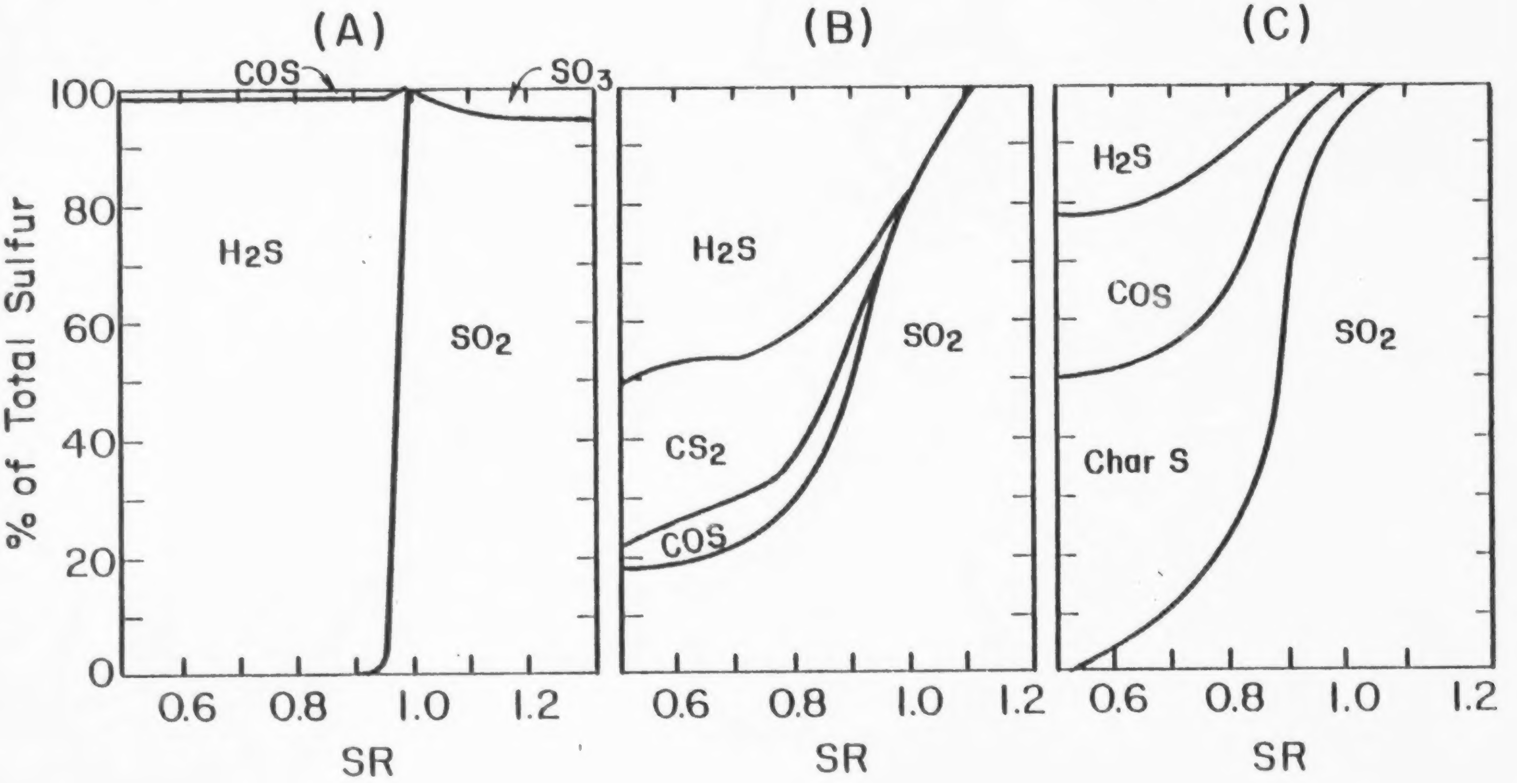

Figure 11-6. Effect of stoichiometry on sulfur species distribution. A, equilibrium calculations; B, propane and H_2S; C, Indiana coal.

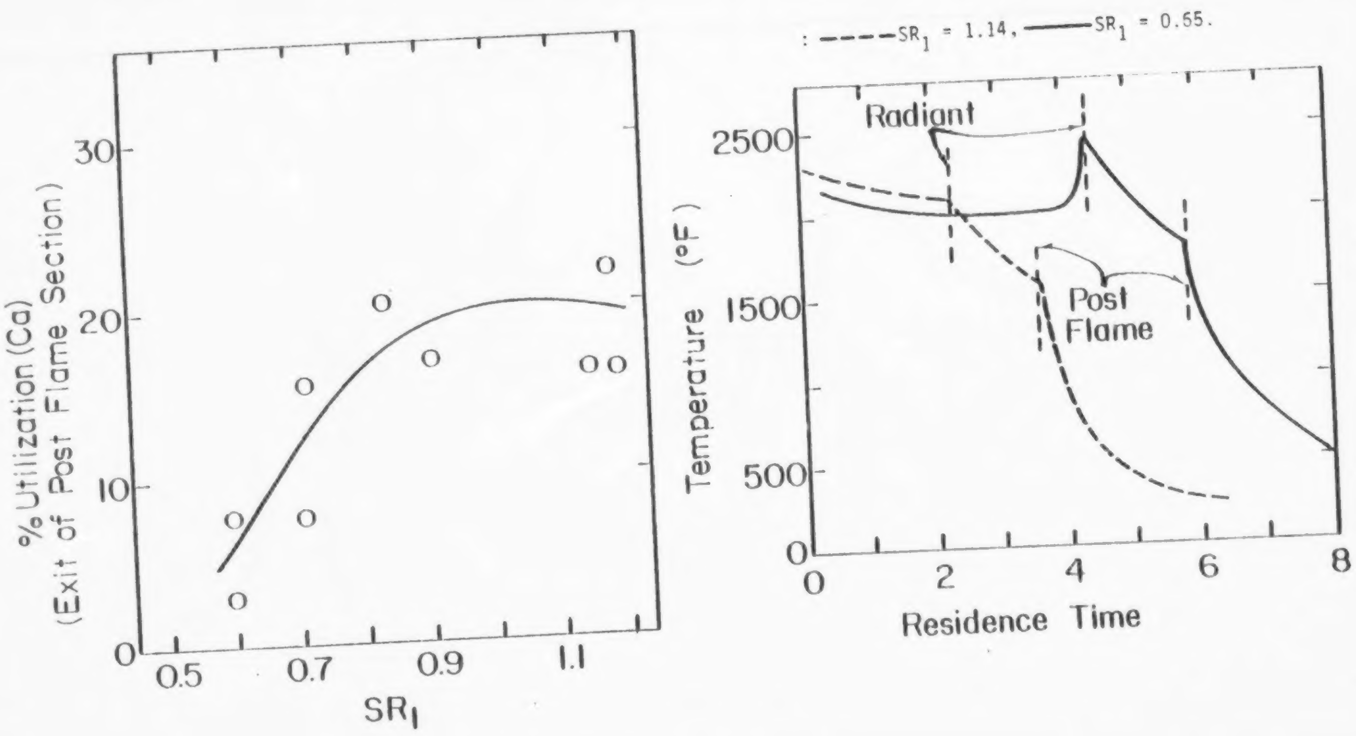

Figure 11-7. The effect of rich zone stoichiometry on sorbent utilization and thermal history, Indiana coal-fired.

Indiana coal. The temperature profiles were derived from wall and gas temperature measurements for calculated residence times. It can be seen that first stage stoichiometry had a dramatic effect on the thermal history of the reactants. Under rich conditions, the radiant zone temperatures are significantly reduced and the residence time is increased due to the decreased mass flow rate. The temperature at the entrance of the post-flame section, where the second-stage air is added, increases during burnout of the coal. The magnitude of this increase will depend on the primary-zone stoichiometry and on the inter-stage heat removal. As shown in Figure 11-7 the effect of first-stage stoichiometry on sorbent utilization for Indiana coal at rich zone stoichiometries greater than 0.7 was slight. However, captures decreased dramatically for fuel-rich stoichiometries less than 0.7. This is probably due to a combination of regeneration during burnout, a reduction in sulfur species driving force because of sulfur retention in the char and a decrease in the reaction rate because of the lower temperatures in the fuel-rich region.

12.0 REFERENCES

1. Whitten, C. M. and R. G. Hagstrom, "Pilot Plant Moving Grate Furnace Study of Limestone - Dolomite for Control of Sulfur Oxide in Combustion Flue Gas", Division of Process Control Engineering NAPCA, Contract PH-22-68-68, May 1969.

2. "Evaluation of Dry Alkalis for Removing Sulfur Dioxide from Boiler Flue Gases", Final Report, EPRI No. FP-207 (Research Project 491-1), 10/76.

3. Altig, R. C. and P. Sedor, "Additive Injection for Sulfur Dioxide Control-A Pilot-Plant Study", NAPCA, Babcock and Wilcox Report No. 5460, Contract PH86-67-127.

4. Gartrell, F. E., "Desulfurization of Stack Gas by Dry Limestone Injection," TVA, Vols. I, II, & III, EPA 650-2-73-019A, B, C; 8/73.

5. Hein, K. R. G. and W. Glasser, "The Application of Dry Additives on Reducing SO_2 Emission for Brown Coal-fired Boilers", Paper presented at the Lignite Conference, San Antonio, 6/71.

6. Flament, G. "The Simultaneous Reduction of NO_x and SO_x in Coal Flames by Direct Injection of Sorbents in a Staged Mixing Burner," International Flame Research Foundation Research Report Doc. No. G19/a/10, 9/81.

7. Folsom, B. A., L. P. Nelson, J. Vatsky, "The Development of a Low NO_x Distributed Mixing Burner for Pulverized Coal Boilers", IERL-RTP-1083, 10/80.

8. Reese, D. P., A. Abele, D. Zallen, "A Laboratory Method to Simulate Utility Boiler Fly Ash", EPRI Final Report Project 629-4, 12/80.

9. Brown, T. D., G. K. Lee, H. A. Banbrough, "Sulfur Neutralization by Lignite Ash: Pilot-scale Combustion Experiments", Journal of Engineering for Power, ASME Paper #78-WA/Fu-7, 6/79.

10. Gronhovd, H., P. H. Tufte, S. J. Selle, "Some Studies on Stack Emissions from Lignite-fired Power Plants", 1973 Lignite Symposium, Bismark, N.D.